University of Genoa

Design and Realization of Electronic Measurement Systems for Partial Discharge Monitoring on Electrical Equipment

By

Andrea Bruzzone

A thesis submitted for the degree of
Doctor of Philosophy in Science and Technology for Electronic and Telecommunication Engineering (Cycle XXXIII)
Curriculum: Electromagnetism, Electronics, Telecommunications

in the Faculty of Engineering
Department of naval, electric, electronic and telecommunications engineering

Tutors: Prof. Paolo Gastaldo
Coordinator of PhD Course: Prof. Mario Marchese

February 2021

Declaration of Authorship

I, Andrea Bruzzone, declare that this thesis, titled "*Design and Realization of Electronic Measurement Systems for Partial Discharge Monitoring on Electrical Equipment*", and the work presented in it are my own.

I confirm that:

- This work was done wholly or mainly while in candidature for a research degree at this University.
- Where any part of this thesis has previously been submitted for a degree or any other qualification at this University or any other institution, this has been clearly stated.
- Where I have consulted the published work of others, this is always clearly attributed.
- Where I have quoted from the work of others, the source is always given. With the exception of such quotations, this thesis is entirely my own work.
- I have acknowledged all main sources of help.
- Where the thesis is based on work done by myself jointly with others, I have made clear exactly what was done by others and what I have contributed myself.

Abstract

The monitoring of insulations that composing high voltage apparatus and electrical machines is a crucial aspect for a predictive maintenance program. The insulation system of an electrical machine is affected by partial discharges (PDs), phenomena that can lead to the breakdown in a certain time, with a consequent and significant economic loss. Partial discharges are identified as both the symptom and the cause of a deterioration of solid-type electrical insulators. Thus, it is necessary to adopt solutions for monitoring the insulation status. To do this, different techniques and devices can be adopted. During this research activity, two different systems have been developed at the circuit and layout level, which base their operation respectively on the conducted and on the irradiated measurement, in compliance with the provisions of current standards, if foreseen. The first system is based on the use of a classic signal conditioning chain in which gain value can be set through PC control, allowing the conducted measurement of partial discharges in two frequency bands, Low Frequency (LF) and High Frequency (HF). Based on these bands, the application of the system is diversified. In this case, the information obtained from the measurement can be analysed by an expert operator or processed by an intelligent system, obtaining in both cases information on the status of the machine under test. The second makes use of a UHF antenna built on PCB, which takes care of detecting the irradiated signal generated in the presence of discharge activity, which is then appropriately conditioned and processed by analog electronics, to then be acquired through a programmable logic, which interprets it and returns information on the status of the machine, which can also be checked by an expert user. The application of this system is linked to the type of insulation and the type of power supply adopted, which differentiate its characteristics. In both systems, the analysis of the measurement of partial discharges is suitable for the prevention of failures and the planning of suitable maintenance interventions.

Acknowledgements

This activity was made possible thanks to the joint work with many people that I would like to thank.

First of all, I thank my tutor, Professor Paolo Gastaldo, and professors Francesco Guastavino and Rodolfo Zunino for referring me to this activity.

Then the people with whom I worked closely, such as Federico Gallesi, Edoardo Ragusa, Christian Gianoglio, Eugenia Torello and Luca Briano.

Obviously, I have above all to thank the person who started the life path with me, right at the start of this research activity, my girlfriend, Silvia, who has always supported and advised me during these three years, in which we have also grown together as people.

And again my family, mum and dad, my grandmothers, my brother Stefano with Giulia, Clara, Tommy, Elena and Davide, as well as all the friends who have been close to me during this period.

To all these people my most loving thanks go.

Contents

List of Figures

List of Tables

1. Introduction

The electrical systems, supplied to medium (MV) and low voltage (LV), are composed of machines and electrical components, whose parts at different potentials are separated by insulation materials [1]. At working conditions, these insulations are subject to aging, due to a series of external factors such as: electrical, thermal, mechanical and environmental stresses. In these conditions, a disruptive discharge can be created between parts of the machine, which are no longer properly isolated. This can cause a malfunction of the machine, due to partial short circuit, and, in worst cases, it is possible to reach unexpected system shutdown, that can involve considerable economic loss. Consider, for example, an industrial plant in which there are electrical machines subject to failure of the insulation, in case of crash, all production is suspended, with serious economic damage. It is obviously that these types of apparatus are periodically checked, but it is also important to know when it is more appropriate to carry out the maintenance to limit the shutdown of a plant and consequently the costs and inconvenience. Furthermore, predicting an equipment failure is not possible by only making a priori considerations, in fact motors, generators or transformers, even if identical, can behave in a totally different way if subjected to different environmental conditions. For example, for a motor powered by an inverter, the occurrence of an insulation fault may be due to the electrical stress to which it is subject, which can be amplified by the accumulation of dirt due to the environment in which it is operating [2]. In this context, it is very important to design and realize an electronic measurement system able to show an appropriate view of the state of the device under test. So, it is also necessary to have an experienced diagnostics team or an intelligent and automatic system that alerts when there are critical issues in a machine, in order to perform an efficient predictive maintenance and to avoid sudden failures, and which is able not only to identify, which is the machine next to failure, but also the nature of the fault that will occur. In this way, it will be possible to provide maintenance with useful information on the health of the system, and then it will be possible to decide whether to intervene immediately on the machine nearing the fault, or whether it is possible to wait until a scheduled stop.

Therefore, in short, it is possible to define a partial discharge (PD) as an electrical discharge that occurs across a portion of the insulation between two conductors. PDs are the symptom and the cause of the deterioration of the insulation in the electrical machines and components. Moreover, discriminating different types of PD sources would provide an assessment on the severity of the damage of the insulation system [3].

In this mind, there are some different techniques and approaches to study the partial discharges phenomena. The literature provides several approaches to PDs monitoring. In general, monitoring first involves the acquisition of signals by conducted or irradiated sensors [4]. So, it is possible to have different electronics measurement systems to monitoring the PD activities, based on various approaches and electronic circuits, and to diagnose potential failure conditions.

1.1 Goals

In view of the above, the main purpose of this thesis is to design and realise different devices suitable for diagnostics in electrical machines, related to the activity of partial discharges. In order to do this, first, it was necessary to study the literature about partial discharges in general and the specific electronic circuits and techniques. Then, it was possible to design a more complex architecture, that would allow to fulfil all the specifications provided during the design stage and based on the reference standards. This thesis has the purpose to develop a traditional high performing and optimized measurement system based on conducted signals and a high sensitive measurement systems based on the irradiated ones, in such a way as to make them useful for predictive maintenance purposes being more performing with respect of measurement systems present in the market.

1.1.1 *Conducted PD Measurement System*

For the conducted system, it is expected that the development of a device is confirmed with the standards and instruments traditionally on the market, but at the same time has innovative and usually not present features, but also allows for comparable and possibly better performance. Furthermore, not only the problems due to the design

were taken into consideration, but also all the engineering aspects that allow to obtain a commercial product definitively, for example the packaging or the IP grade of protection and more.

Traditionally in the context of partial discharges, the measurement is of the conducted type. This implies the need to have available a connection to the power part of the device under test. Given the high voltages involved, about a few tens of kV, it is necessary to introduce suitable voltage divider systems, which allow the measurement to be carried out safely. The output signal from the divider must be suitably conditioned by a pre-existing impedance, but whose characteristics must obviously be taken into consideration in the design. The activity focused on the development of a signal conditioning chain, to then be able to digitize it, considering also previous studies carried out over the years, which did not lead to high performing results. On a structural level, a preamplifier should be placed near the sensor, in order to prevent the signal from being corrupted by ambient noise, which can interfere with the connections. The idea involves the use of two PCB, one near the measurement point, which is responsible to the signal conditioning, and a detached one, which manages the interface with the acquisition system and allows to provide some commands to the first one. The signal can be displayed on an oscilloscope or, interfacing with appropriate software, on specific graphics. Taking into consideration that this system is designed to be used in the industrial world, it must therefore have suitable packaging and connections.

1.1.2 *Irradiated PD Measurement System*

For the irradiated system, it is expected to develop a device based on what was designed by the spin-off *Diasol Srl* of the University of Genoa, namely the SolBox® project. It is a system that involves the use of an antenna built on PCB, a signal conditioning stage (filtering and amplification) followed by a signal preprocessing circuit, which is then processed by an embedded logic, in this case an FPGA. Based on this, the signal conditioning and preprocessing chain was totally redesigned, in order to obtain a definitive optimized and high performing version, while the section relating to logic was substantially maintained at the hardware level and revised at the

firmware level, even if this is not part of what has been analyzed in detail and realized in the context of this thesis. As for the conducted system, taking into consideration that this system is designed to be used in the industrial world, it must therefore have suitable packaging and connections, considering all engineering aspects.

About the positioning of the device and the type of application, within the scope of this thesis, different versions of the device under examination have been designed, also diversified according to the type of power supply of the electrical machine under test. However, all versions provide for counting the events associated with the discharge activity and activating various alarms (with light signals through the use of some LEDs) that indicate the exceeding of a threshold for a certain number of discharges in the unit of time. At the moment, this device is applicable to machines powered at low voltage (LV), with windings realized by means of enameled wires, for which it is important to check if discharges are present or not, without having information on their amplitude. However, the system is easily adaptable to other types of machines, where it is necessary to also evaluate the amplitude of the discharge signals.

2. Partial discharges

Partial discharges are identified as both the symptom and the cause of a deterioration of solid-type electrical insulators. To describe the phenomenon of partial discharges it is useful to first introduce the concept of "Total Discharge". It occurs when the insulation, between two parts at different potentials, gives way creating a low resistance conductive path. A short circuit is then created which causes a system breakdown. With a Partial Discharge, only part of the insulation is short-circuited, while the rest is still able to guarantee insulation. The discharges derive from local electric field concentrations and appear as current pulses with duration in the hundreds of nanoseconds or less, depending on the nature. Furthermore, discharge phenomena usually occur in the presence of emission of sounds, light and heat and are therefore generally very clear. Therefore, the PD measurement is an important task to diagnose potential failure conditions

2.1 PDs – Causes and phenomena

An electrical machine, even if subjected to partial discharges, will continue to operate correctly, until, in a more or less long time, it will incur a disruptive discharge, that is an electric discharge that occurs when the potential difference between two conductors generates an electric field so high as to overcome the dielectric strength of the insulation material, causing the system breakdown.

2.1.1 Partial Discharge Pulse

A partial discharge is identified as a pulse of current, very fast and which is characterized by a rise time that is up to ten times higher than the falling time. The impulse can be modeled with the following equation 2.1:

$$\mathbf{I} = \mathbf{I_0} \cdot \left(\mathbf{e^{-at}} - \mathbf{e^{-bt}}\right)$$

Where a is the time constant of the rising edge and b of the falling edge.

The pulse shape of discharge, associated with it, is shown in *Figure 2.1*.

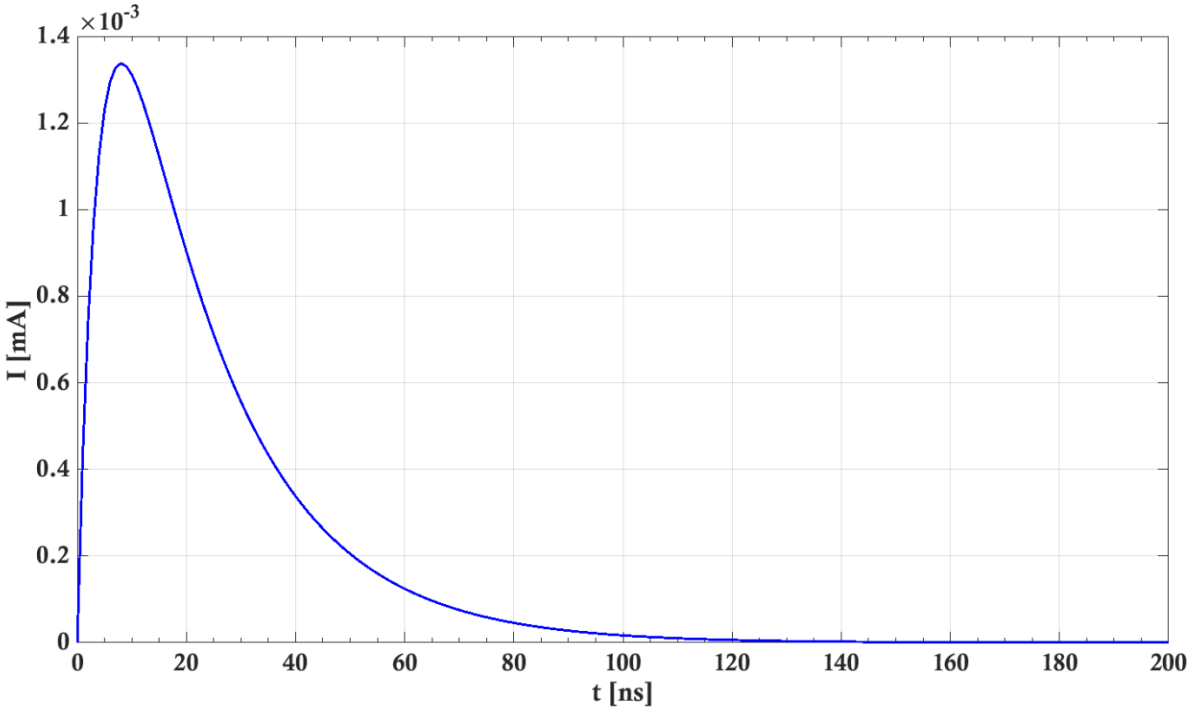

Figure 2.1: Partial Discharge Pulse Waveform

The amplitude of the curve is determined by the intensity of the discharge, while the duration depends on the morphological nature of the defect where the PD takes place and on the distance between the source of the discharge and the measurement system. Considering the conducted signals, the rise time is in the order of tens of ns while the fall time is in the order of hundreds of ns.
At the same time, a partial discharge can be properly observed in voltage, while the reference unit of charge is Coulomb [C], in these cases usually pC.

2.1.2 Causes and effects

Among the causes that lead to phenomena associated with the activity of PDs there is the local overheating due to the passage of current, which leads to damage to the insulating material, since carbon residues can be deposited on the surface, with the consequent resistivity reduction. At the same time, due to the lack of surface insulation due to humidity and the deposition of conductive dust over time, a small

electric arc can be generated (an electric discharge in the air that brings a very high power in a very short time) which leads to the formation of very active substances, such as ozone (O_3) and nitrogen oxides (NO_2). All these factors can accelerate the deterioration process of the insulating material, with an inevitable increase in the discharge activity which consequently increases the phenomena associated with it.

In this context, PDs occur due to defects in the insulation system and can therefore be used as an indicator of the presence of defects. At the same time, their occurrences also contribute to damage of the insulation itself. These defects may arise from problems in the production stage or from the normal aging of the equipment, as a result of mechanical, electrical, environmental or thermal stress. For example, considering MV transformers, with epoxy resin insulation, in the production phase, small voids can be created in the resin which can then lead to partial discharges during normal operation [5]. However, even if an almost perfect insulation system is created in the production phase, during operation, due to overheating, the material will become porous, and the problem will arise anyway. Furthermore, even contamination of surfaces by conductive dust alone can lead to partial discharges on the surface [2].

An example of degradation for conventional enamel, after electrical aging at 150°C, is shown in *Figure 2.2*.

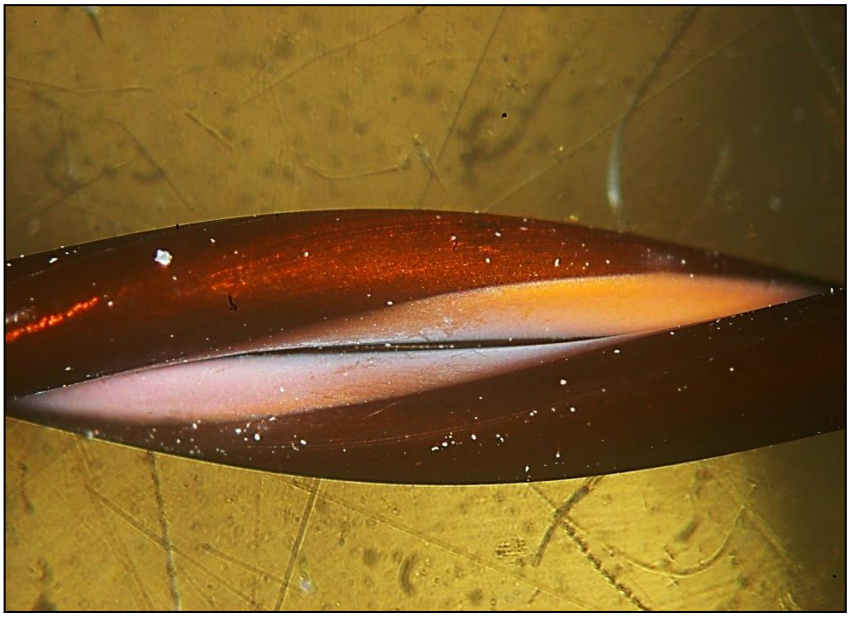

Figure 2.2: Degradation area for conventional enamel after electrical aging at 150°C

In the figure above it is possible to see the evident degradation, denoted by the lighter color of the material.

At this point it is important to pay attention to the distinction between machines operating in medium or low voltage, if the first can operate even for a long time in the presence of partial discharges, the second are not able to withstand them, within 10/100 working hours of the machine, it will reach breakdown conditions. The cause of this is to be found in the materials with which the insulations are made: in case of medium voltage, elements such as Mica are used, while in case of low voltage equipment only polymeric organic materials are used, which degrade quickly in presence of partial discharge. Furthermore, there are some materials, called self-restoring, which due to their chemical-physical characteristics are restored as soon as the discharge activity ends, this is the case of gas or liquid insulation systems. The solid materials are not self-restoring, and the discharge irreversibly damages the part of the involved insulation.

2.2 PDs Types

As mentioned above, defects in the insulation system can occur due to problems in the production or due to the natural aging of the equipment.

If the contamination of the insulation surfaces by conductive dusts is considered, this can lead to partial discharges on the surface [6]. Another possibility is that, during installation or transport, small cracks are created in the insulation system, which in turn can lead to discharges. A final example may concern the presence of a conductor termination with sharp edges or not properly rounded in gas. In these cases, the distribution of the electrical field results very divergent: this can lead to the so-called corona discharge activity [7].

As we have seen, various factors can be identified that lead to the occurrence of partial discharge activity phenomena, but at the same time, discharges can also be of different types based on their disparate nature. For this reason, two large subfamilies can be distinguished: internal and external discharges to the insulation system.

2.2.1 Internal PDs

Discharges due to defects in the solid insulation system are defined as internal discharges. The origin of these discharges is to be linked to the presence in the insulator of small cavities, called voids, which can be formed during the processing phases or arise as a result of mechanical, electrical, environmental or thermal stress. The physical phenomenon that causes a discharge is due to the presence in the insulator of materials with a minor dielectric constant, which occupy the cavities, usually air or other gases. This situation leads to the electric field concentrations in the defect: the electric field in the cavity is greater than that in the surrounding insulation leading to exceed electric strength in the void volume and the PD activity can take place. During the discharge activity two different situations may occur, based on the substances that are released. Since conductive carbon residues are released, the discharge activity may disappear in a short time. This is because the surface of the defect becomes conductive and there is no longer the difference in electric potential that is able to trigger new discharges. If the residues cannot render the void surface conductive, the PD activity will continue leading to the progressive surrounding material erosion.

Another example of internal discharge is associated with the phenomenon of treeing. It occurs due to local and intense electric fields inside the dielectric material, giving rise to micro-charges that branch on the insulation, hence the name treeing. On the occurrence of this phenomenon, in a short period of time, there may be a total discharge that will lead to the breakdown of the apparatus. In the following *Figures 2.3* and *2.4* it is possible to observe two examples of internal discharges. In the first figure is referenced to the schematization of an internal discharge with void, while in the second the real effects of the phenomenon of treeing.

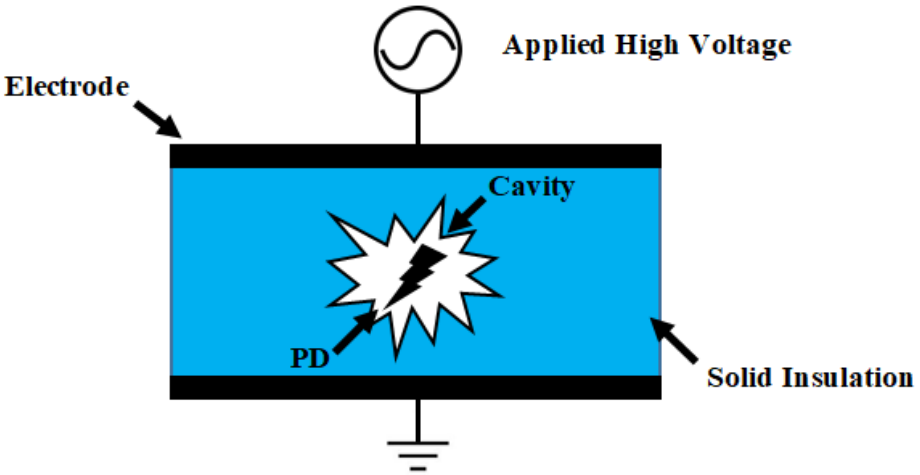

Figure 2.3: Schematization of a partial discharge in a cavity

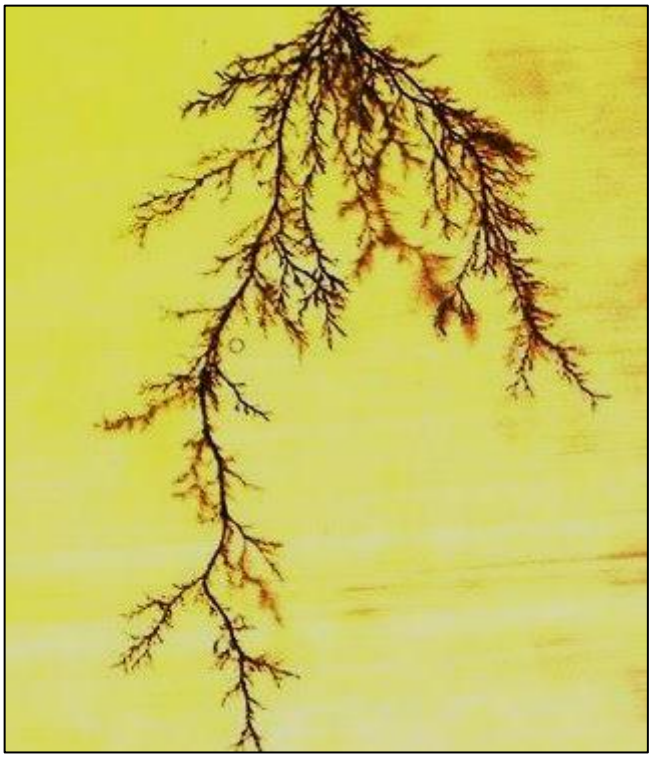

Figure 2.4: Real effect of treeing

2.2.2 External PDs

Partial external discharges are defined as those that occur on the surface of the insulation. A schematization is shown in *Figure 2.5*. This cause the release of ozone

(and other substances) into the air, in addition to possible surface tracing, by altering the characteristics of the insulation. All this, over time, can lead to the creation of zones with low resistance and consequent phenomena of total discharge. The cause of all this is linked to the electrical field components near and on the surface of the insulating materials.

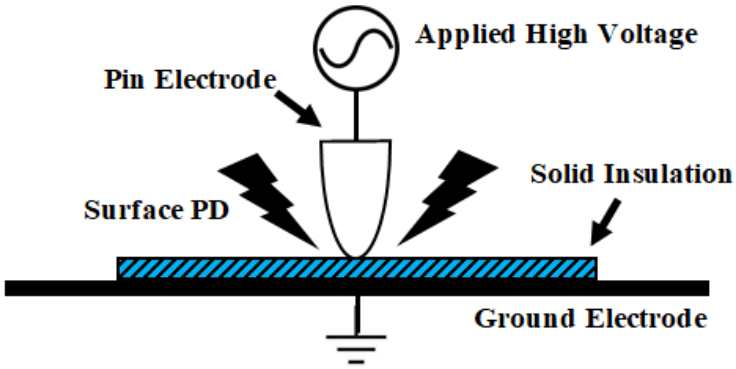

Figure 2.5: Schematization of a surface PD

The PD conditions, schematized in *Figure 2.6*, occur when the dielectric strength of the gas, near the insulating material surface, is locally exceeded. As with surface discharges, ozone is released into the air during discharge activity. In these cases, specific chemical reactions can lead to corrosion of metal surfaces and the formation of conductive deposits, which worsen the PD activity.

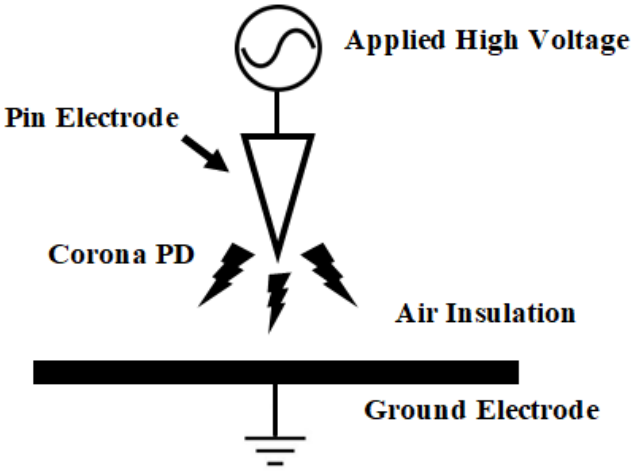

Figure 2.6: Schematization of a corona PD

2.3 Measurement Systems Techniques

The measurement of partial discharges is possible since, with each discharge, there is a charge transfer and therefore an impulsive current circulation in the insulation system, which generates a conducted or irradiated electromagnetic signal. To carry out the measurement it is possible to adopt, depending on the situation, different types of measurement systems. These include the coupling capacitor system, which must be positioned at the power supply terminals, the system that involves the use of UHF (Ultra High Frequency) antennas, placed near the equipment, or the system based on a particular transformer, called HFCT (High Frequency Current Transformer), which is positioned in correspondence with the earth connection of the plant on which the measurement is made. Three examples are shown in *Figures 2.7, 2.8* and *2.9*.

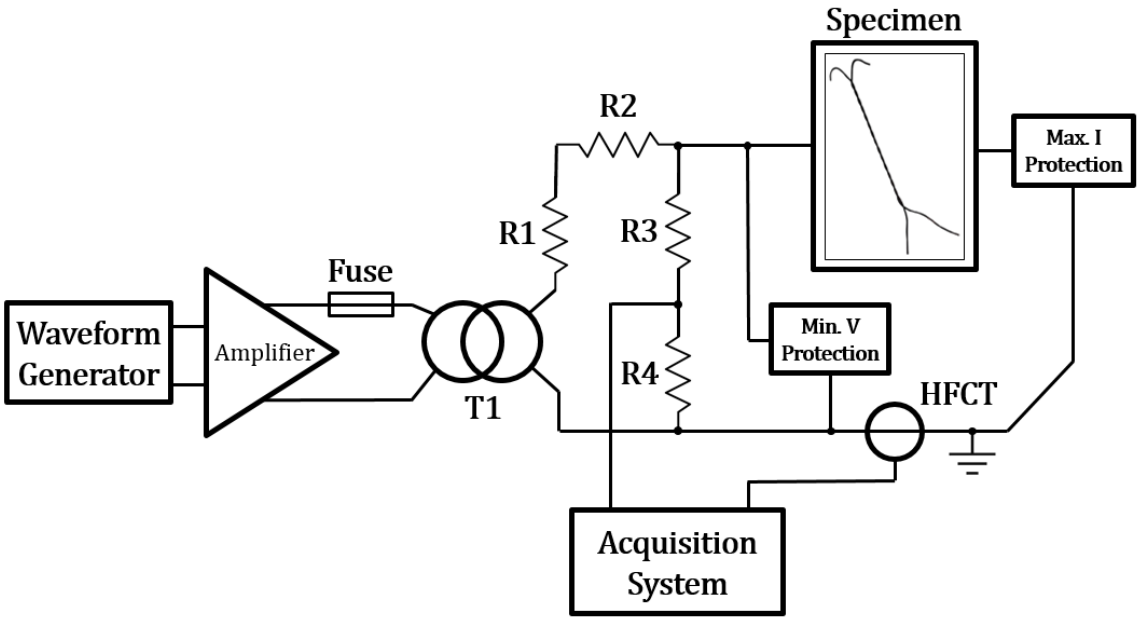

Figure 2.7: Example of setup circuit for HFCT PD Measurement System

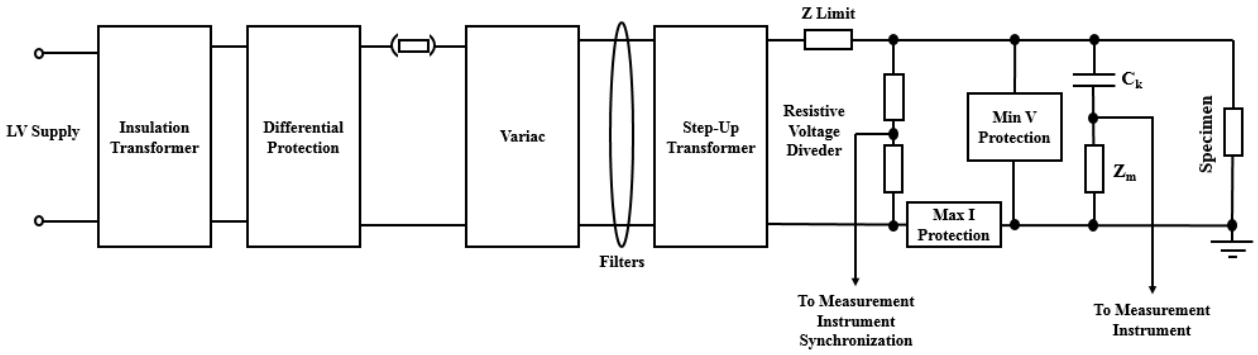

Figure 2.8: Example of setup circuit for Conducted PD Measurement System

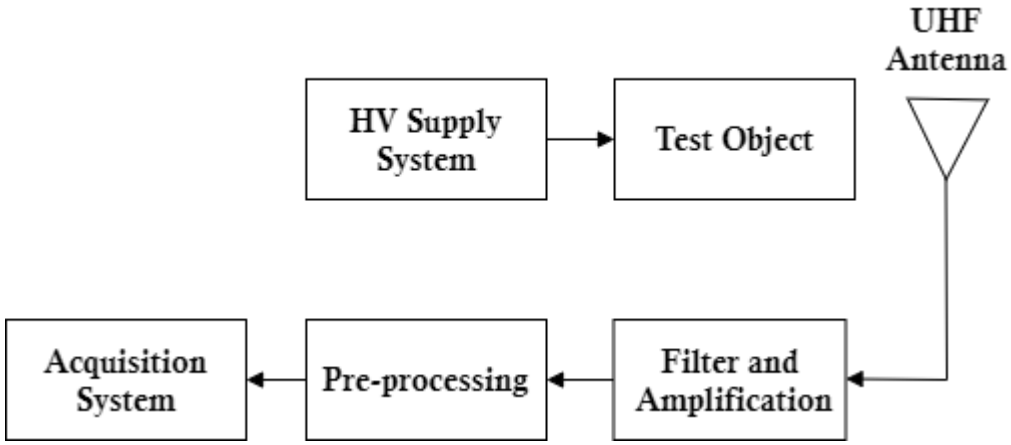

Figure 2.9: Example of generic setup circuit for Irradiated PD Measurement System

2.3.1 Typologies of machines under test

An electrical machine can be manufactured using different kinds of insulating systems depending mainly on the rated power and the rated voltage [13]. Considering low rated voltage amplitudes, for example, a stator winding can be manufactured using the Type I random wire wound structure [14], where only organic insulating materials are employed. These kinds of insulating systems, if subjected to partial discharge activity, fail in short time so that during the service low rated voltage machines must result as PD free. Type II form wound insulating systems [15], on the contrary, made using composite organic and inorganic materials can be subjected to a moderate PD action during the normal service.

PD measurements can be adopted in the case of both type I and type II insulating systems to obtain information about the actual insulating system conditions. In the case of low rated voltage generators, detection systems providing ON-OFF information about the presence or not of discharge activity can be sufficient giving action, if necessary, to immediate maintenance actions. In the case of high rated voltage amplitudes, PD measurements can also return information about the morphology of the insulating system defects and the evolution of the discharge phenomena so that condition-based maintenance protocols can be implemented. This is because, due to the insulation characteristics, it is not necessary to intervene promptly on the machine.

It is possible to give two more detailed examples of these different treatment based on the type of rotating machine under test, considering Low Voltage (LV) machines with enameled wires and Medium Voltage (MV) with taped strips. In this regard, LV is defined for voltage values $\leq$ 1000V rms in AC or $\leq$ 1.5kV in DC and for MV with voltage > 1kV and $\leq$ 30kV rms in AC or > 1.5kV and $\leq$ 35kV in DC. In the first case, the analysis of the measurement takes place by the presence or absence of discharges, because in case a PD activity is detected it is necessary to intervene as soon as possible. In the second case, however, the amplitudes of the discharges can be analyzed in detail and other information can be obtained to define the morphology of the involved defects.

2.3.2 *On-Line and Off-Line Measure*

Partial discharge measurements can be performed in two ways: with the system out of service (Off-Line) or with the system in normal operation (On-Line) [8]. There are no better measurement techniques than the others since the results provided by the two methods are in many aspects different each other. On the one hand, Off-Line measurements provide very detailed results, but need to be carried out with the system stopped, so the conditions of the equipment are not those of normal operation. The measurements performed on-line, on the other hand, refer to the actual operating conditions, but are less detailed and more difficult to interpret, due to noise and crosstalk phenomena. For equipment in service on plants, it is more useful to carry out

On-Line measurements, in order to obtain information on the health of the equipment without having to stop the plant and avoid economic losses. However, the measurement is not easy to carry out, first of all it is necessary to have a part of the circuit on board the machine for the measurement. In addition, the noise within the system will be high and, since the machine is connected to other equipment, it is possible that discharges from the latter are erroneously attributed to the machine under test. The PD detection system could include permanent connections to the machine power supply representing themselves sources of failures. Furthermore, in some cases, it is difficult to identify where the defect is localized.

Considering, for example, a wind power plant, it is clear that the On-Line measurements are better, since they allow to continuously monitor the actual conditions of the insulating system. At the same time, setting up a measurement system in a wind turbine is not easy and there are many external interferences.

On the other hand, Off-Line measurements can better highlight the cause of any anomalous trends, given the lower interference. In this way, only the specific machine under test is checked, so as to be able to discriminate the defects associated with it. For example, as regards the three-phase systems, only one phase is powered at a time, so that only the defects present in each single phase can be highlighted. Furthermore, with the machine disconnected, it is possible to measure the apparent charge of each discharge phenomenon, calibrating the system and having a reference regarding the amplitude of the discharge (putting in relation the amplitude of the discharge, as measured in mV, with the involved apparent charge), so as to have more information on the machine state.

Note how the measurement of partial discharges must be carried out following the IEC and IEEE Technical Specifications, which give information on the methods to be used for both Off-Line and On-Line measurements.

2.3.3 *Partial Discharge Analysis*

The reasons why the phenomenon of partial discharges occurs and what it can cause have already been defined. At the same time, it is evident how an extensive analysis is important for identifying defects in the insulation and performing prevention and diagnostics on electrical apparatuses. To do this, two different analysis are possible:

- PD Time Analysis
- PD Pattern Analysis [8]

In the case of temporal analysis, the discharges and their amplitudes over time are observed. Therefore, it is possible to evaluate how many pulses occur in a time interval, what amplitudes they have and if they exceed a certain threshold or what form they take and what are the rise and fall times. Basically, it is enough to have an appropriate conditioning system and an instrument on which to view the signals, usually a digital oscilloscope. An example of this type of time graph is shown in *Figure 2.10*, in which the signal relating to the PDs can be observed in the blue trace, while the red trace shows the reference sinusoid (in this case 50 Hz) of the applied voltage.

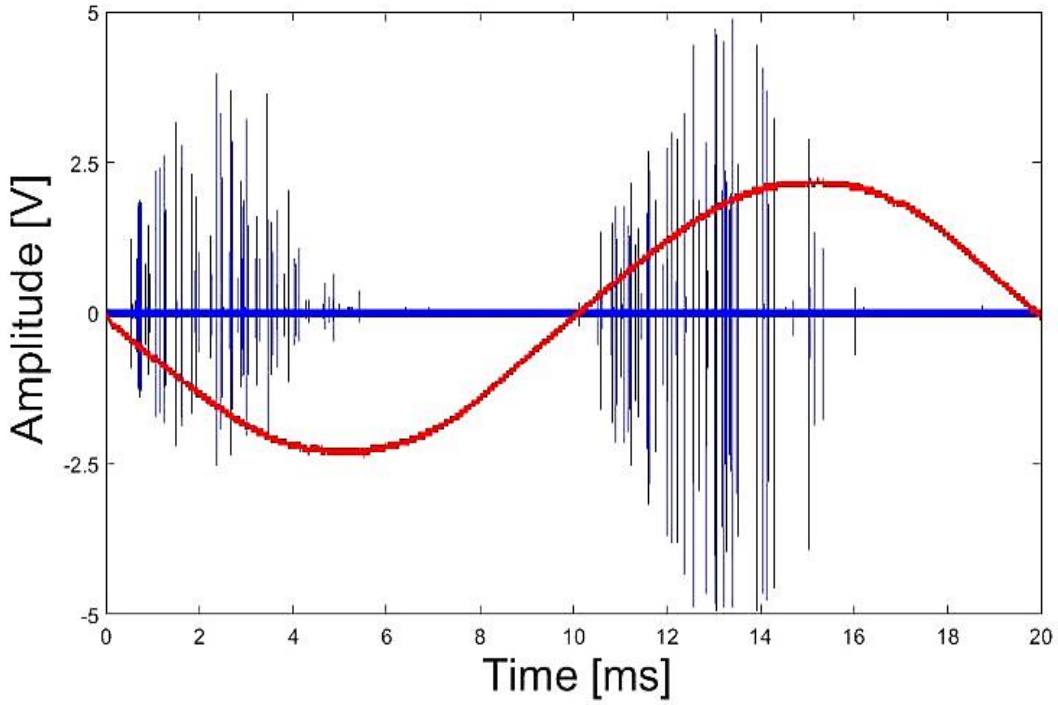

Figure 2.10: PD Time Analysis

As for the analysis through the PD patterns the question is more complex because, in addition to what is listed above, it is necessary to provide an appropriate PRPDA (Phase Resolver Partial Discharge Analyzer) digital systems. To create a PD Pattern, the partial discharges are recorded in a certain time interval and then they are related to the phase of the power supply voltage. The occurrence phase is shown on the abscissa axis, while the amplitude of the discharges themselves are shown on the

ordinates. The resulting graph therefore shows the number of partial discharges occurred in a certain number of cycles of the supply voltage and their concentration with respect to the phase. Using different colors depending on their concentration, a three-dimensional graph is obtained (an example is shown in *Figure 2.11*), containing numerous information, which allows an expert to identify the type of defect present in the insulation system. To obtain information on the type of defect it is necessary to measure not only the amplitude, but also the occurrence phase. With phase of occurrence the time instant in which the discharge takes place is meant with respect to the phase of supply voltage applied to the object under test: it is expressed in degrees. At the same time, it is necessary to provide a more complex architecture that also allows sampling and storing a good amount of data in memory. The data post elaboration allows to the PD pattern.

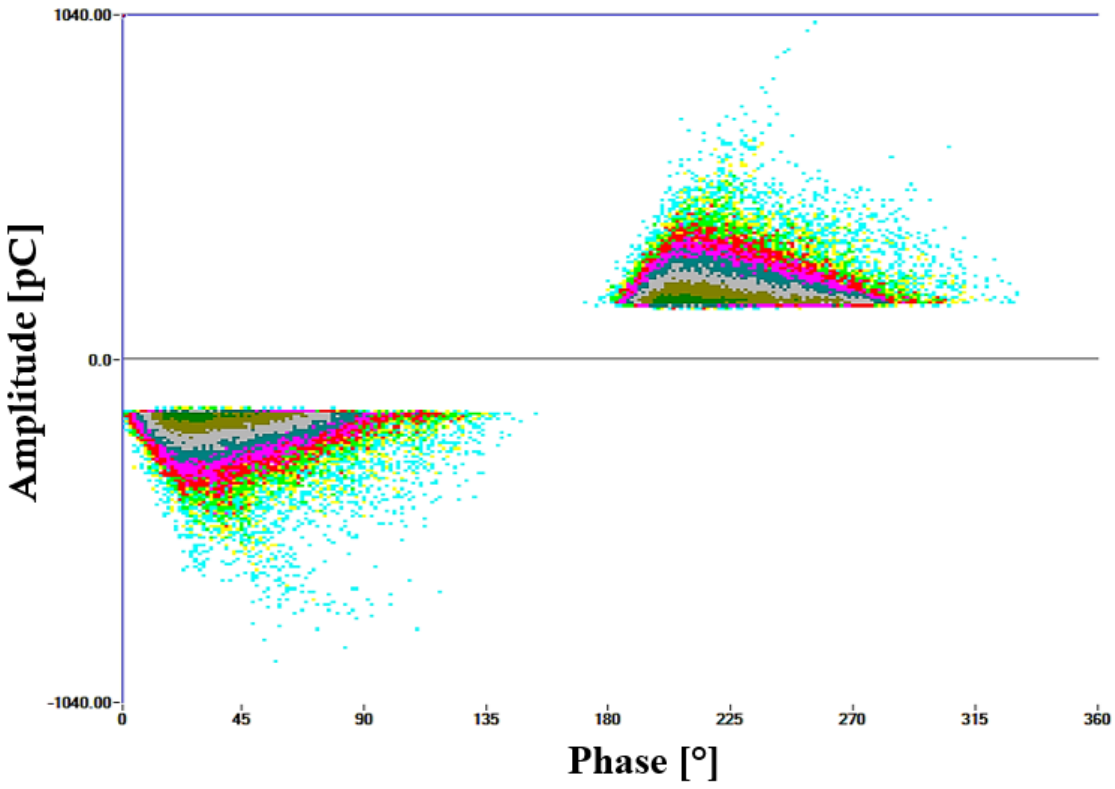

Figure 2.11: Example of a PD Pattern

Regardless of the characteristics of the two analyses, in both cases it is possible for an expert operator or an intelligent system to carry out the morphological identification

and diagnosis of the defects through an accurate examination of the graphs. As previously mentioned, in order to avoid unnecessary downtime of a system or sudden failures and to plan maintenance in a properly way, it would be necessary to use a predictive diagnostic, able both to identify which machine will be close to failure and to recognize the nature of a problem to which it will be subject. In this way it will be possible to provide useful information to the maintenance workers and therefore it will be possible to decide immediately if the apparatus needs to be stopped and repaired, avoiding further damage due to an untimely intervention. In order to perform an efficient scheduled maintenance and to avoid sudden failures, it would be necessary to have predictive diagnostics, which is able not only to identify, within the plant, which is the machine next to failure, but also the nature of the fault that will be verified. In this way, it will be possible to provide maintenance technicians with useful information on the health of the system to schedule the maintenance intervention. To implement a predictive diagnostic technology, it is helpful to analyze the obtained data, through methods that use Machine Learning [9], in addition to making use of assessments by expert operators. These techniques can make it possible to identify not only the machine that is about to be affected by an insulation defect, but also to characterize the defect type and its location.

2.3.4 Non-Electrical detection of PDs

There are some techniques of non-electrical detection of partial discharges, which aim at identifying the point in which the discharges occur, but do not give information on the amplitude of these. It can refer to changes due to chemical changes or variations in pressure of a gas, heat, sound or light and. In the practical side, only the last two have relevance.

For example, there are some systems that exploit the emission of sound for measurement, these are directional microphones that use piezoelectric sensors. The acquired signal is amplified and converted into frequencies so that it can be heard in the headphones by an expert operator [10]. The operator must be able to identify the origin of the discharge activity, by pointing the microphone towards the equipment under test. All this provide that the intensity of the sound is considerable and

consequently that the discharge activity is quite advanced, running the risk that the equipment is already about to be compromised. For reference, partial discharges of a few hundred pC can be detected by the human ear, but a lot depends on the background noise, which can compromise its audibility.

On the other hand, if the discharge activity is very high, a blue light can be observed with the naked eye around the point where they are occurring, as shown in *Figure 2.12*.

There are techniques [11] that involve photographic apparatuses or others that make use of photomultipliers, based on ultraviolet radiation generated by discharges. For example [12], the test object can be placed in a dark room. The camera lens is directed toward the test object, and the aperture is opened during all the time of application of the test voltage. In addition, the object under test is illuminated for a short time so to obtain a figure of partial discharges overlapped on it.

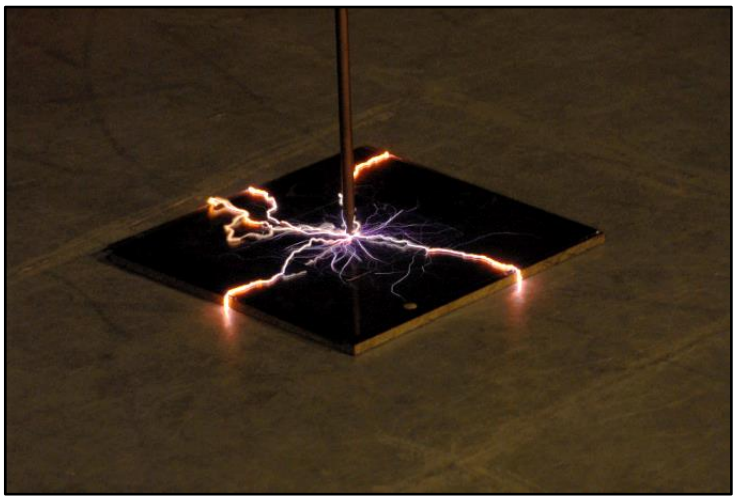

Figure 2.12: Partial discharge with light effect visible to the naked eye

2.4 IEC-60270 Standard

IEC-60270 Standard [16] applies to measurements of partial discharges that occur in electrical equipment, components or systems subjected to tests with alternating voltages up to 400 Hz or with DC voltage. It defines the terms used, the quantities to be measured, the measurement methods. It describes the test circuits, specifies calibration methods for the instrumentation and offers suggestions relating to the discrimination between partial discharges and external interference.

Furthermore, it defines a partial discharge as follows: *"Localized electrical discharge that only partially bridges the insulation between conductors and which can or cannot occur adjacent to a conductor".*

2.4.1 Apparent Charge

The standard defines a partial discharge pulse as that charge which, injected at the terminals of the object under test, for a short interval of time and within a specified test circuit, would give rise to the same reading on the measuring instrument of the partial discharge current pulse itself. Basically, apparent charge can be defined as the measurable charge associated with the discharge event, which causes a short current pulse at the terminals of the object under test, which will provide a certain reading on the measuring instrument. This discharge does not really represent the one involved at the location where the discharge occurs, which cannot be measured directly, but depending on the measurement circuit used it is possible to have more or less sensitivity. The response relative to the measurement circuit can be analyzed, using a current pulse of known amplitude and recording the value of the discharge pulse, usually expressed in pC, which has been read on the measuring instrument. In this way it is possible to perform a calibration and obtain comparable measurements.

2.4.2 Inception, extinction and test voltage

The International Electrotechnical Commission (IEC) - 60270 standard also defines two important parameters such as the inception and the extinction voltage. The first is defined as: "*Applied voltage at which repetitive partial discharges are first observed in the test object, when the voltage applied to the object is gradually increased from a lower value at which no partial discharges are observed.*"

Therefore, more simply, the inception voltage is defined as the minimum voltage that originates the discharge activity. On the other hand, it is defined as extinction voltage, that for which the discharge activity is interrupted. In particular, the standard defines it as: "*Applied voltage at which repetitive partial discharges cease to occur in the test object, when the voltage applied to the object is gradually decreased from a higher value at which PD pulse quantities are observed.*"

Furthermore, on the basis of the inception voltage, it is possible to define a further parameter of considerable relevance, namely the test voltage. It is defined as that value 1.1 times higher than the inception voltage, and which is to be used to power the machine under test during the measurement. Obviously, before supplying power, it is advisable to check specifications of the machine under test, to avoid exceeding the voltage level and risking permanently damaging the insulation.

2.4.3 Test Circuits

The standard sets up different test circuits according to the desired characteristics and the application. In *Figure 2.13* some test circuits are shown, indicated by the standard. In particular, in this case for the conducted system, reference was mainly made to the first of these (a). In the two diagrams the capacitance called C_K is a low inductance coupling capacitor, while Z_m is the measurement impedance, used to condition the signal in order to measure it with a measurement instrument (for example an oscilloscope). The difference between the two circuits is relevant to the sensitivity due to the position of the test object (usually named C_a). In fact, in the first circuit (a) only the recirculation current (in the coupling capacitor) is measured, consequently the discharge is partially measured here. In the second circuit (b), with the device in series with the measurement impedance, the current flowing inside can be measured instead, with an obvious increase in sensitivity. For safety reasons, the first solution is preferred, even if with less sensitivity. Considering the circuit (b), if the insulation of the system under test fails, there is a voltage drop between the terminals of the measurement impedance, and therefore of the measurement device, equal to the power supply voltage making the operator at a considerable risk. This does not happen in the first circuit, being the coupling capacitor in series with the measuring impedance. For this reason, the first circuit solution was chosen as part of the work carried out. Furthermore, remember that it is essential that all the components used for the realization of the measurement circuit have to be partial discharges free.

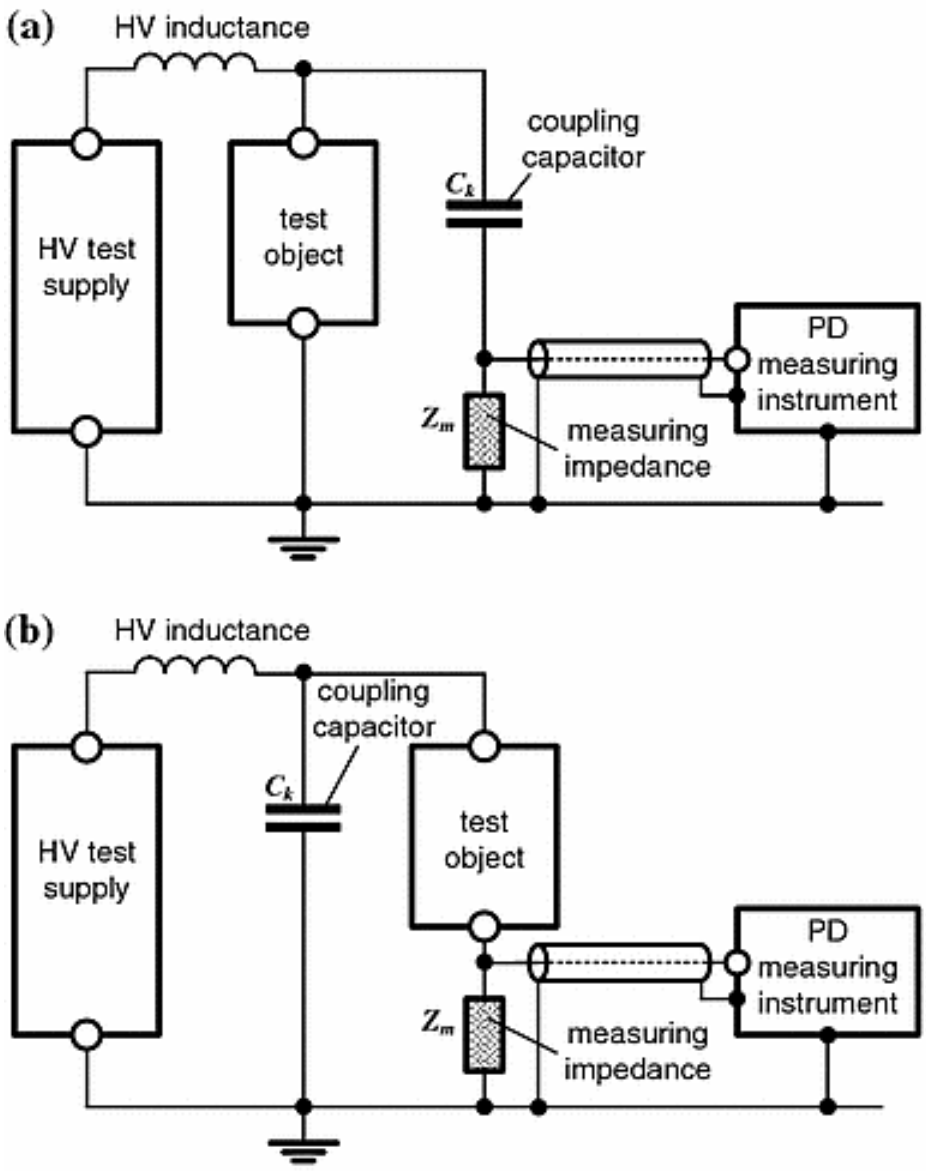

Figure 2.13: Two different test circuits reported in the IEC-60270 standard

2.4.4 Calibration

The purpose of calibration [16] is to verify that the measurement system is able to correctly measure the amplitude of a specified PD. The calibration of a measuring system is performed to determine the scale factor *k* for the measurement of the apparent charge. It must be performed whenever the object under test changes because it is associated with a different ability compared to other objects. Obviously, depending on the capacitance value, the test circuit is affected in a different way. Then

calibration will be performed with each new object under test unless tests are performed on a series of similar objects with capacitance values within ± 10% of the mean value. The calibration of a measuring system in the complete test circuit is performed by injecting short duration current pulses into the terminals of the object under test. A known charge value is associated with this pulse, which must comply with appropriate specifications in terms of performance, as referred to in the standard. Therefore, a calibrator must be able to generate a series of periodic pulses, which must be sized according to the charge to be injected. The repetition frequency of the pulses can be fixed or variable depending on what is desired, for example, twice the frequency of the test voltage. Between two consecutive pulses of the same polarity, it is necessary a minimum pulse resolution time T_r, that is in general inversely proportional to the bandwidth Δf of the measuring system. At the circuit level, in principle, a calibrator is composed of a square wave generator (U_0) followed by a series capacitor (C_0) and to show signal it is necessary an opportune conditioning with an impedance (R_m), as shown in *Figure 2.14*. From the IEC-60270 standard, the pulses must have a of rise less than 60 ns, instead there is no restriction for the falling time and the choice of components must comply with what has been said.

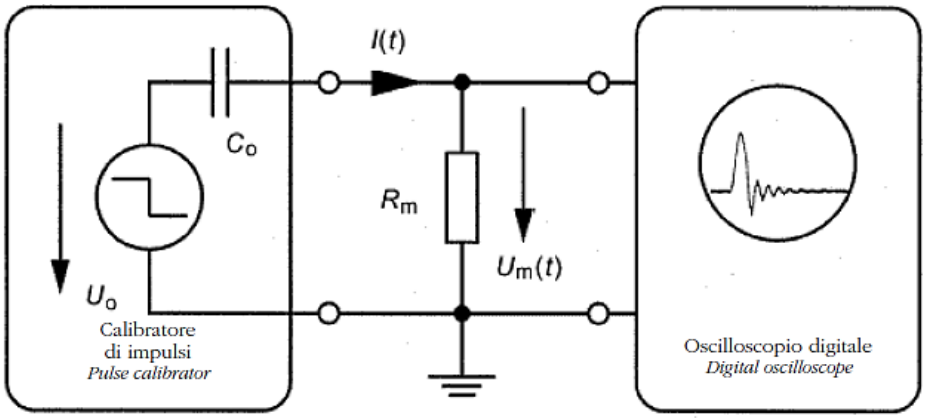

Figure 2.14: Circuit for displaying a direct calibration pulse

2.5 Measurement Sensors

The sensors for the measurement of partial discharges, adopted as part of this research activity, basically concerned:

- Measurement impedances and coupling capacitors
- Inductive sensors
- UHF Antennas

The first two types refer to the conducted measurement, while the last obviously to the irradiated one.

2.5.1 Measurement impedances and coupling capacitors

Within a well-defined measurement system, as shown in previous Figure 2.8, two elements of considerable importance are the measurement impedance and the coupling capacitor (see *Figure 2.15*). As regards the measurement impedance, it is an RLC, which allows to condition the impulse of the discharge to be able to measure it correctly, according to the prescriptions of the standard. This depends on the type of measurement to be made, there are versions for a measurement in Low Frequency (LF) and others for High Frequency (HF). An example of an adopted impedance for the LF version is shown in *Figure 2.16*, where in (a) the PCB layout is observed, while in (b) the final assembled version. For LF, means measurements performed according to the standard, up to 1MHz, while for HF means frequency band from 1MHz to 20MHz or higher, which falls outside the standard.

Figure 2.15: Coupling Capacitor

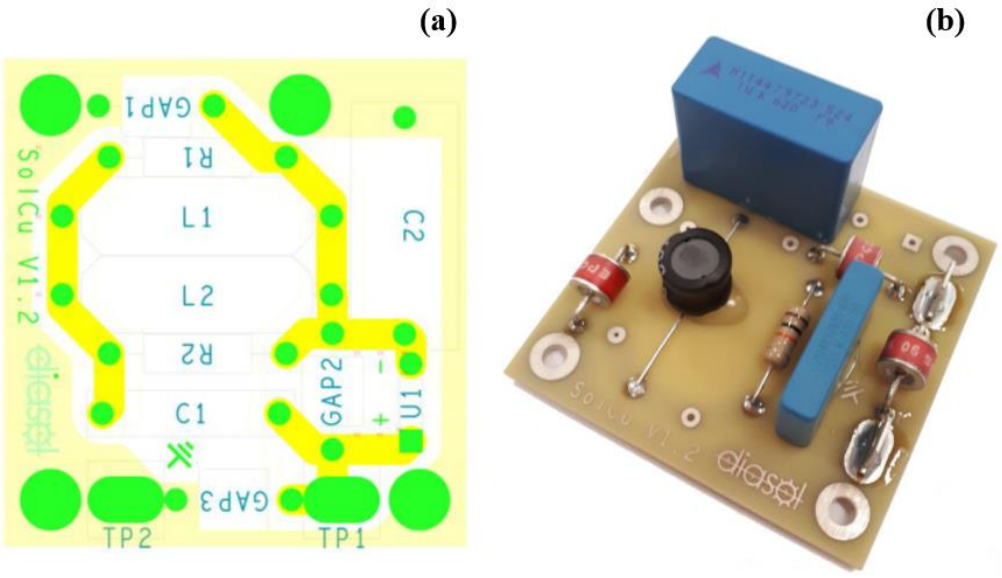

Figure 2.16: (a) PCB layout and (b) final version for LF Measurement Impedance

As mentioned, the use of an impedance requires to have a correct measurement, obviously this depends on the appropriate sizing of the components that constitute it, which was not the subject of this activity. For completeness, below, in *Figure 2.17* is shown an example of a real conditioned LF PD signal.

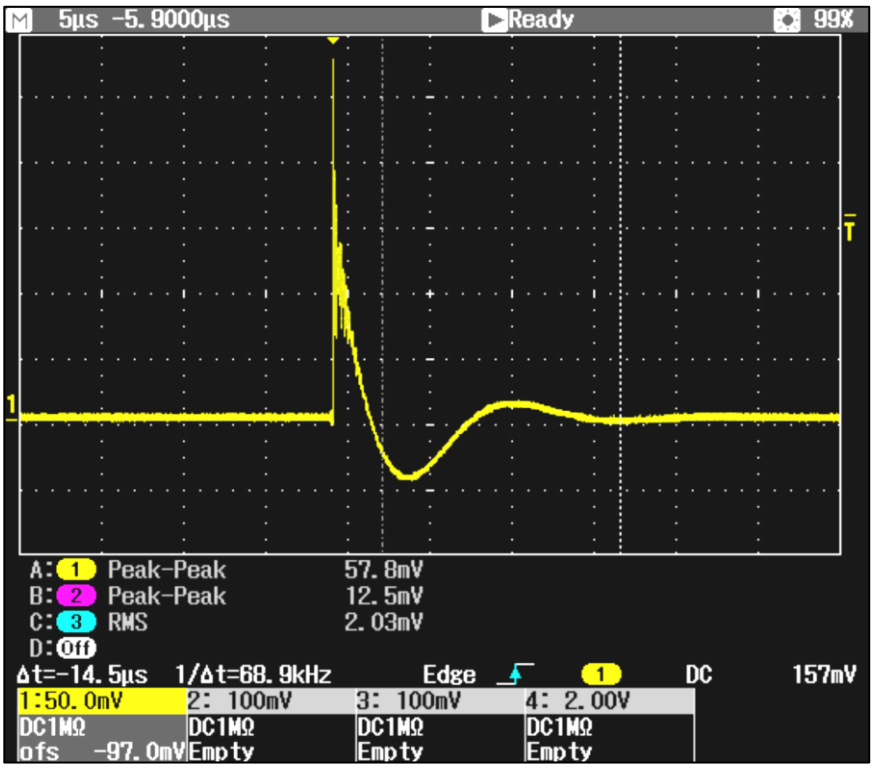

Figure 2.17: Conditioned LF PD signal

2.5.2 Inductive sensors

If it is necessary to perform measurements for which it is not possible to access the power parts, it is important to use inductive sensors, such as ferrites and HFCT. Thanks to these, it is enough to insert the power cable of the system to be measured inside a ferromagnetic material toroid, with which the sensor is made. The flow of a current pulse inside the power cable also induces one on the sensor windings, in order to carry out the measurement. An example of a clamped inductive sensor is shown below in *Figure 2.18*.

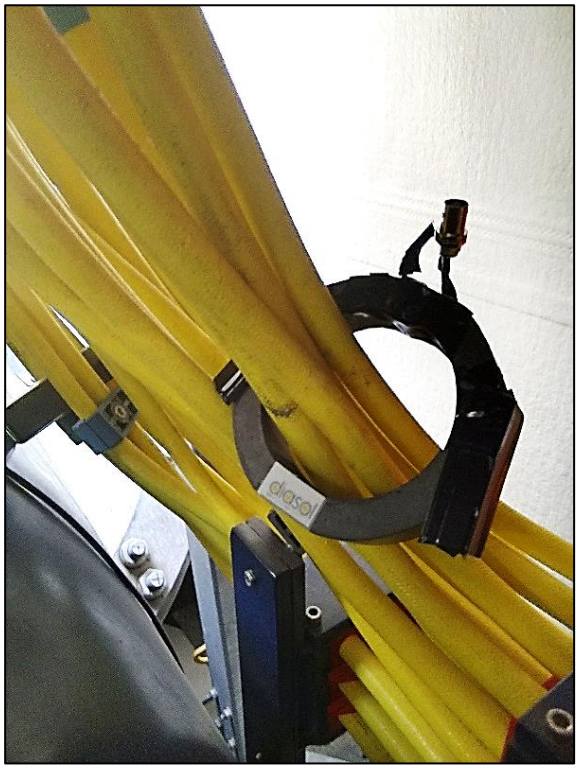

Figure 2.18: Clamped inductive sensor

A special feature is linked to the fact that with these sensors is not possible to carry out the calibration of the measuring system, and then correlate the amplitude of the discharge to the charge itself. They are however useful for carrying out measurements and checking for discharges all those times it is not possible to connect the measurement system to the power part. They are usually sized to have an output impedance of 50Ω, therefore the measurement system must take this into account in order to have a correct impedance adaptation, even if they are sized differently.

2.5.3 UHF Antennas

These are particular antennas, made to work Ultra High Frequency (UHF), which indicates the radiofrequency signals transmitted in the band ranging from 300 MHz to 3 GHz. There is the possibility of finding on the market already prefabricated antennas that differ for the band work or it is necessary to size and build ad hoc antennas. In the case of this research activity, a UHF antenna sized and built on PCB was adopted. It should be noted that the sizing did not specifically concern this research activity, but is the result of previous studies, even though the problem was nevertheless addressed and there were changes to its geometry. In *Figure 2.19*, one of the versions of the antenna used is shown.

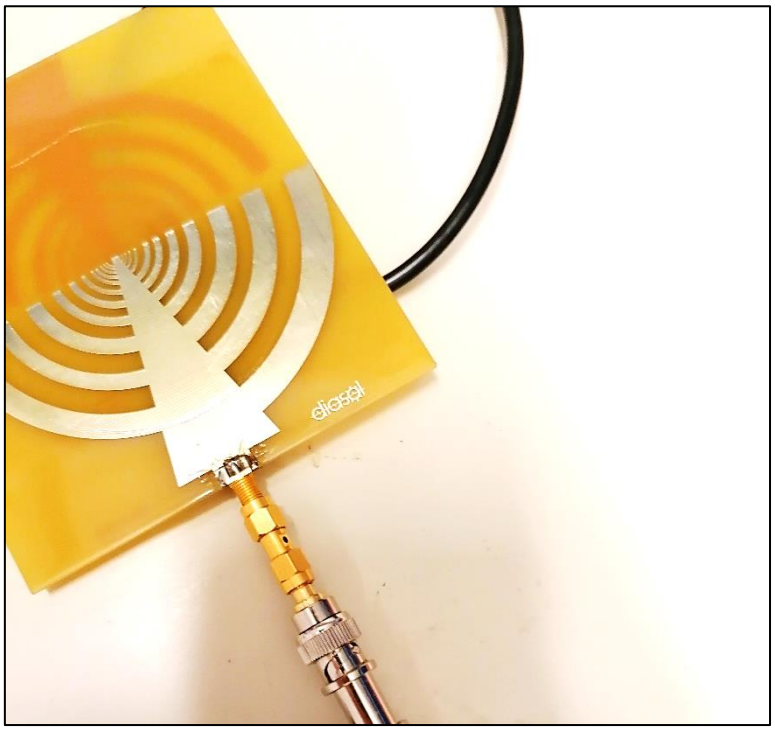

Figure 2.19: PCB UHF Antenna

3. Conducted PD measurement system

The conducted partial discharge measurement system, developed during this research activity, is organized according to the scheme shown in *Figure 3.1*. Basically, the system is based on two main boards, the filtering and amplification board and the control board, which deal with signal conditioning, and in addition an optional board that acts as a switch, if you want to make measurements on multiple devices (up to four). The boards in question all have a microcontroller on board, from the Microchip PIC family, and therefore require the development of appropriate firmware. A connection to a PC via USB is provided for the control and switch boards. Furthermore, an ad hoc communication protocol is provided for the communication between the two main boards. It should be borne in mind that, in part, these boards concerned previous study activities, which however highlighted problems and deficiencies in the section dedicated to the signal and which compromised its development. In this regard it was necessary to redesign some fundamental stages, including those of filtering, amplification and protection, at the circuit level and PCB layout. This has allowed the development of devices that work properly and are capable of being put on the market. Given the need to place the system in places that are often uncomfortable and not easily accessible, the system must be characterized by small dimensions, the least number of connections and flexibility. For example, in this mind, it is important to have a single line for supply voltage, measurement signal and command, to reduce a number of connections and to have flexibility.

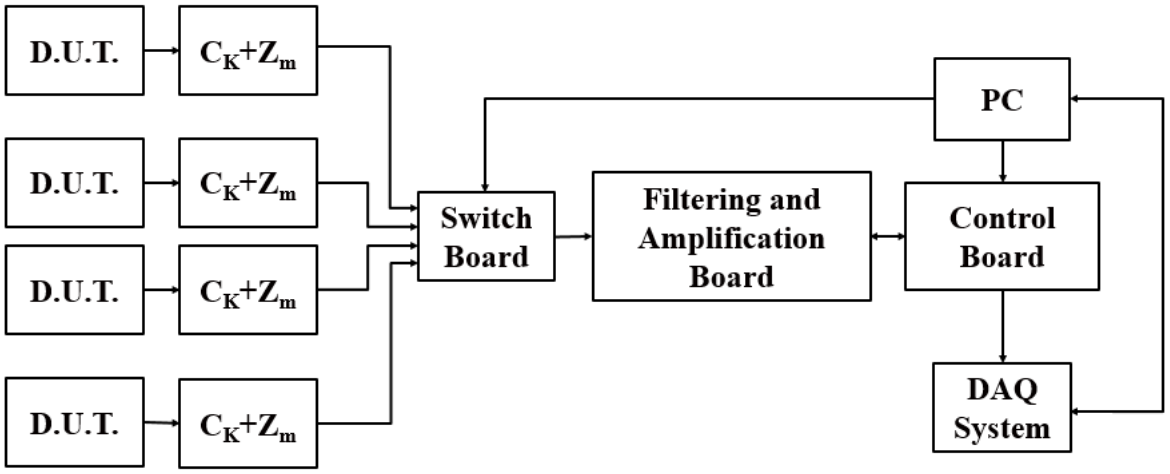

Figure 3.1: Block diagram of the conditioning and measuring system

The simplified behavior of the system is as follows: the control board receives a series of commands from the operator, through a PC connected via USB, which basically refer to the value to be set in the section with variable gain amplification. The control board decrypts what is received via USB and sends it to the signal conditioning board, which in turn decodes the signal and carries out what is required by the command.

3.1 Communication protocol

The need for a single line on which, in addition to the control signals, also the power supply and the measured signal, made it necessary to provide for the use of a custom protocol for communication. It takes place between the control board and the amplifier board, through an RG58 cable. Some pre-existing but far more complex protocols could have been evaluated. Since it is essentially not necessary to have complexity and in order to have a compact and low-cost device, it was chosen to define a simple custom protocol, which will be defined below.

3.1.1 Characteristics of the custom protocol adopted

The two main boards communicate with a protocol that has been suitably defined and managed through the microcontrollers mounted on them. This protocol has some fundamental characteristics to be taken into consideration. One of these concerns the

amount of data that must be transmitted and, secondly, the timing of the data. The amplifier board needs to receive commands to know what value to set the gain and little else. Currently the preset gain values are the following: 1, 5, 10, 50 and 100. However, in principle, it is possible to set and send any gain value by acting on a variable that can vary between 0 and 255, even if in reality the bits dedicated to gain alone are 7, as will see later. Obviously, the everything is limited to the amplification capacity of the component identified for the variable gain preamplifier section. A LED placed on the signal conditioning board will indicate the successful reception of a command, with different flashes (in number and color) of the received gain value or to highlight any anomalies. In addition to the gain commands, a series of accessory commands of reduced importance have also been defined, for example the one for the LED toggle in order to verify correct communication or a reset command, which sends a default gain command value, that is 1. In order to keep the HW very compact and low cost, it was decided to have the possibility to communicate only from the control board to the conditioning board (filtering and amplification), setting the first of these as the master. The type of communication adopted is therefore unidirectional, of the Simplex type, and the only feedback for the user, as mentioned, will be given by LEDs placed on both boards.

As mentioned, another aspect of fundamental importance in this protocol is the timing of the data. It was decided to adopt a scheme that provides that the signal at idle state is at a high logic level and that the decoding of the symbols takes place on the basis of their duration. As far as the signal level is concerned, at idle the power supply voltage present on the only communication line is associated. Instead, the presence of a symbol is considered as such when the signal goes below a certain predetermined threshold, which can then be managed at the software level, with respect to the idle state. *Figure 3.2* shows the scheme adopted for decoding the signals on the basis of the length of time, in the case of two different symbols.

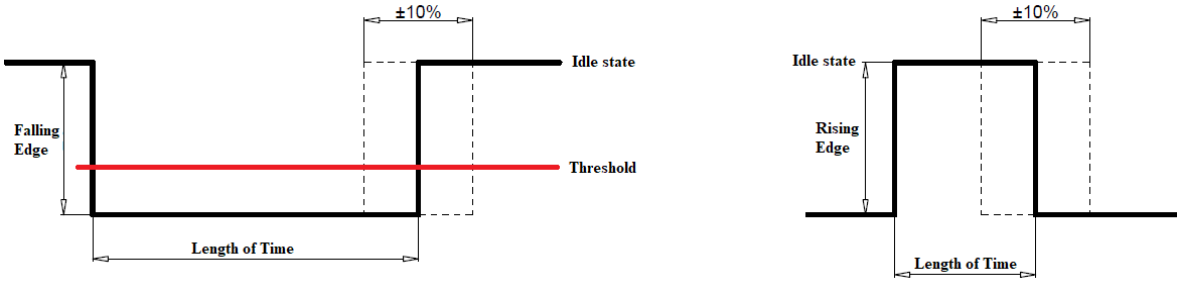

Figure 3.2: Protocol time scheme

On the left is the signal related to a symbol sent within a transmitted sequence, while on the right the guard band between one bit and the other of the sequence. Since the protocol is based on the duration of the symbol to distinguish a bit at "1" from one at "0", it is necessary to separate the bits so as not to lose synchronization in the event of a sequence of 1 or 0. To do this, between one bit and the next, a guard band with a predefined duration and in the idle state of the line has been inserted. Furthermore, since you are in a very noisy environment and this also affects the signal on the communication line, there is a possibility that the amplitude and temporal duration of a symbol are corrupted. For this, a time tolerance threshold is used, which is used by the receiver to be able to recognize a symbol even if it is corrupted or disturbed. The value of this tolerance is ±10% of total length of time for symbol. The duration of a symbol then differentiates them from each other, according to *Table 3.1* below.

Name Symbol	**Time Duration [ms]**	**Tolerance [%]**
Start Bit	250	±10
Stop Bit	150	±10
Band Guard	15	±10
Bit “0”	40	±10
Bit “1”	100	±10

Table 3.1: Time duration and tolerance of symbols

Obviously, on the basis of all the specifications indicated for communication and for what has just been defined, the appropriate choices were made in the circuit design of the devices, as will be explained later.

3.1.2 Software development of the protocol

Even if the software development of the protocol [17] did not directly concern this research activity, the principle of operation and what has been done is briefly explained below. The implementation was carried out on two Microchip microcontrollers, PIC16F1454 [18] for the control board and PIC16F1704 [19] for the filtering and amplification board. The command selected by an operator via PC, coming from the USB communication, is decoded by the microcontroller on the control board and put in "*and*" with a mask that allows you to select only the correct bits to be sent in sequence. The firmware, which has the task of sending the sequence of bits, is mainly based on a for loop that sends one bit at a time on the line, the change of state occurs by modifying the logic level of a pin of the microcontroller. The duration of the state is managed by a timer inside the microcontroller of the control board, which is set on the basis of the time duration that the symbol must have. The subsequent decoding, in reception, is performed by the microcontroller present on the packaging board. As soon as a change occurs on the line, the decoding procedure is activated and the consequent digitalization process of the voltage value present on the line. If the received packet is correct, it is interpreted and by means of a D/A conversion inside the PIC, an analog signal is sent to adjust the variable gain circuit section. The package description for the commands is given below in Table 3.2. Being 8-bit microcontrollers, each packet consists of its own 8-bit.

B0	**B1**	**B2**	**B3**	**B4**	**B5**	**B6**	**B7**
0	*Accessory Commands*						
1	*Gain Value Commands*						

Table 3.2: Packet description

In this case, it has been chosen to use the first bit to determine if the packet concerns an accessory command or refers to a gain value, while the remaining 7 bits represent the real code that the conditioning board must interpret. So, 7 bits are sufficient, as the

gain values cannot be much higher than 100, due to the nature of the component that has been chosen for the variable gain amplification section. In fact, it is limited in a certain range of amplification, as it is reasonable to expect. However, these values were considered sufficient for the developed device.

3.1.3 Communication measurements

Figure 3.3 shows the measurement carried out with an oscilloscope to display a signal containing a packet with a command for the conditioning board. To carry out the measurement and, therefore, observe the transit of the packet along the line, a "*T*" connector was placed in the middle between the two communicating boards. The oscilloscope with 1 MΩ impedance input was then connected, taking into consideration that the signal in the idle state has a value between 6V and 6.5V and the time scale has been set at 200ms, everything has been set up so as to being able to view the complete signal with a good resolution.

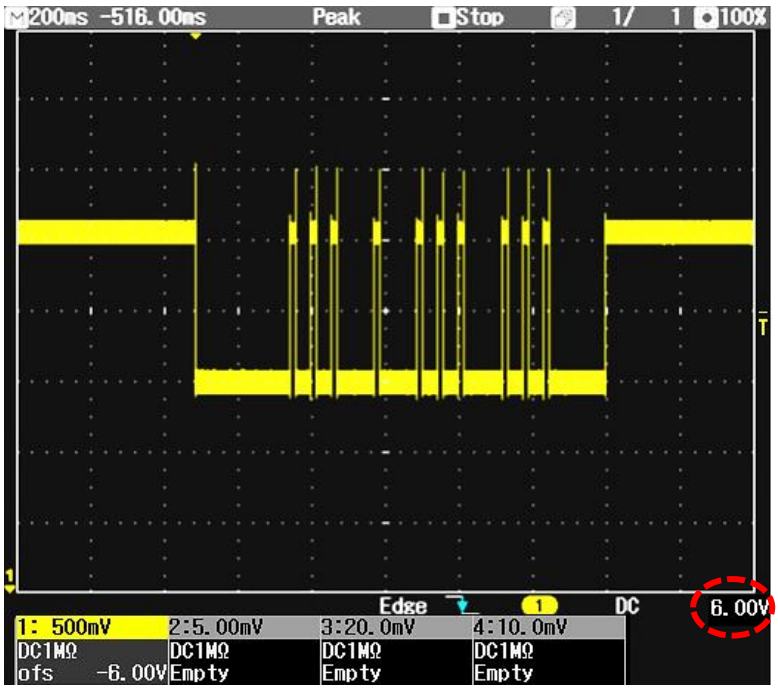

Figure 3.3: Line communication measurement

The acquisition of *Figure 3.3* shows the packet for sending the command to set the guard at 100. The bit "*0*" and bit "*1*" symbols can be clearly distinguished, thanks to the subdivision of these with of a guard band and for the clear temporal difference between them. An overshoot is also observed in the transitions from high to low, but it is not dangerous for the receiver since the signal is then appropriately managed. The images of *Figure 3.4* and *3.5* respectively show the detail of the rising and falling edges.

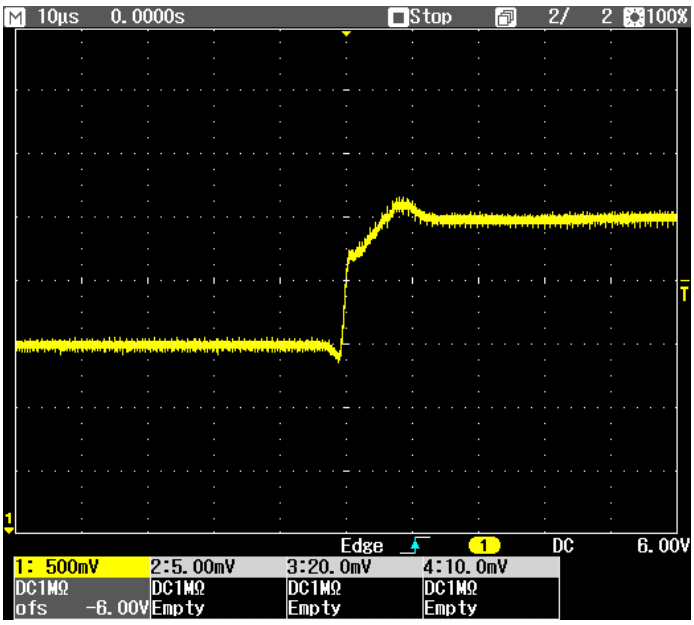

Figure 3.4: Rising edge of the communication signal

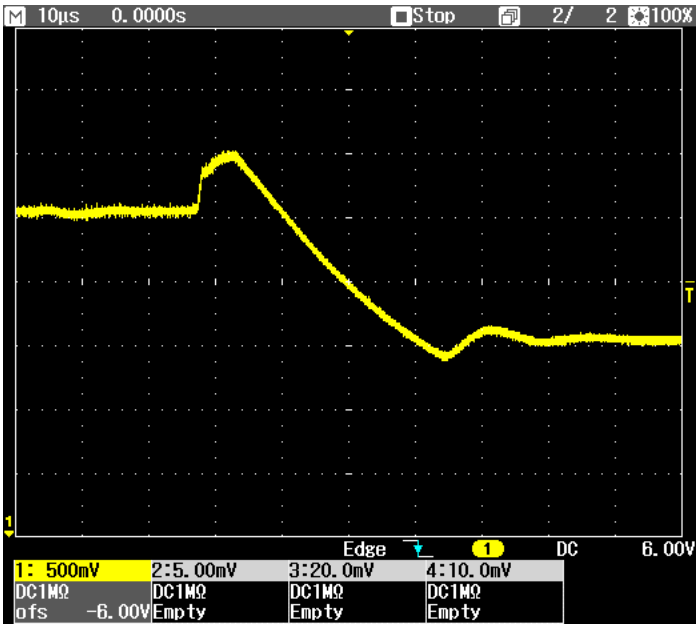

Figure 3.5: Falling edge of the communication signal

3.2 *Conditioning signal section*

The signal conditioning board (filtering and amplification) has the purpose of conditioning the signal coming from the high voltage measurement system, through the interfacing of the measurement impedance and the coupling capacitor. The signal conditioning chain is shown in the diagram of *Figure 3.6*.

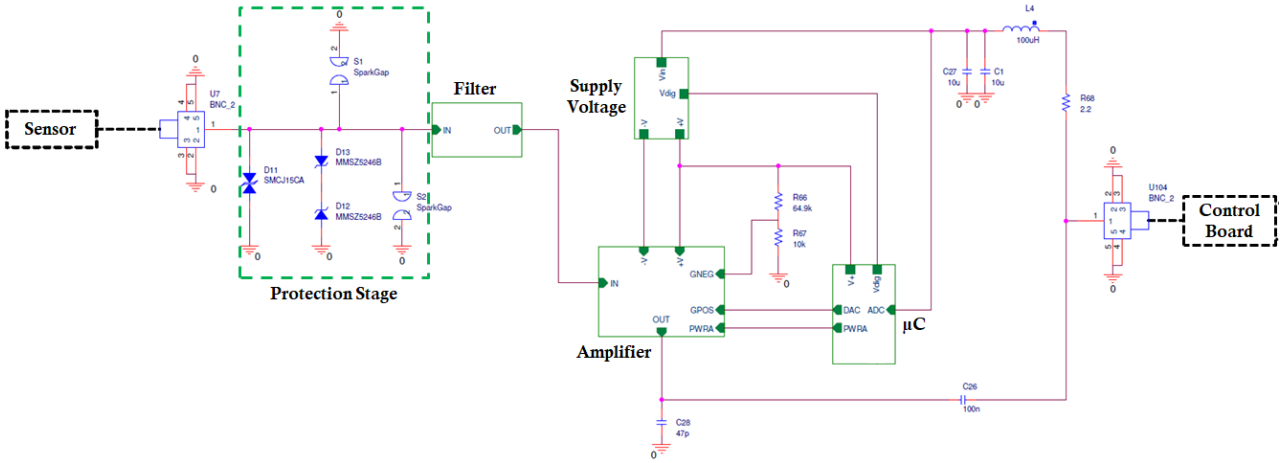

Figure 3.6: Block diagram of conditioning board

The signal is first conditioned through a filtering stage, which can be different according to the band required for the application and may or may not fall within the standard indicated by IEC-60270. Then it is processed by the amplification chain, which is essentially composed as shown in the diagram shown in *Figure 3.7*.

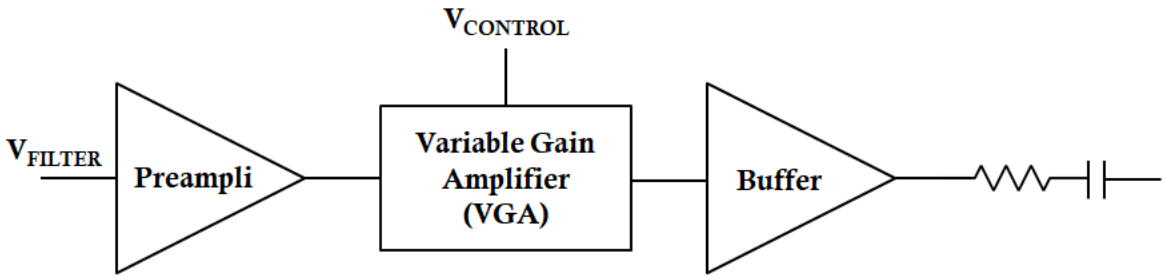

Figure 3.7: Amplifier Chain

It can be observed how the amplification stage consists of a preamplifier (with fixed gain), an adjustable gain section, through an appropriate control signal, and an output buffer (also with fixed gain), which has the task of allow the communication of measurements over distances of a few tens of meters, without having an excessive degradation of the useful signal. The usefulness of having a separate board from the control board lies in the fact that signal conditioning should take place as close as possible to the sensor. Another reason concerns the fact that, often, the device under test (D.U.T.) is located in places that are not easily accessible, therefore it is advisable to separate the two boards so that the control one, which interfaces with a PC, is in better conditions, in terms of convenience and simplicity in setting up the system.
In this context, this system that, in some parts had already been developed in the field of previous studies, has undergone a series of substantial changes that have made it a commercial device to all intents and purposes.

3.2.1 Filtering stage

The filtering stage is essential to have a good signal-to-noise ratio (S/N) and, therefore, to have a good measure. It is essential to filter the signal correctly, to have feedback on partial discharges without having excessive environmental noise, given the scope of application at an industrial level. The choice of frequency bands turns out to be a critical aspect depending on the application that you want to achieve. On the basis of this, two different filters have been developed, one in the LF band and within the scope of the IEC-60270 standard, while the other in the HF band, not standardized. These are RC type band pass filters, in the LF version the filtering band is between 40 kHz and 1 MHz, while for the HF one the range is between 3 and 20 MHz. Obviously, these bands have been chosen as the most suitable for relevant applications, but nothing precludes the creation of other custom filters, more specific for other applications. Another aspect of considerable importance concerns the input impedance that characterizes the filter, since it must be taken into consideration that the measurement impedance is also involved. The filter must be matched with the measurement impedance in order to have a correct measurement of partial discharges.

During the design stage all these aspects had to be taken into consideration in order to obtain filters with the desired characteristics. Furthermore, during previous studies, filters had been made which, after an accurate analysis, were found not to be optimized for the previously reported frequency bands. In this regard, the following *Figures 3.8* and *3.9* show the simulation of frequency response graphs of the filters designed in comparison to those developed previously, respectively for LF and HF version.

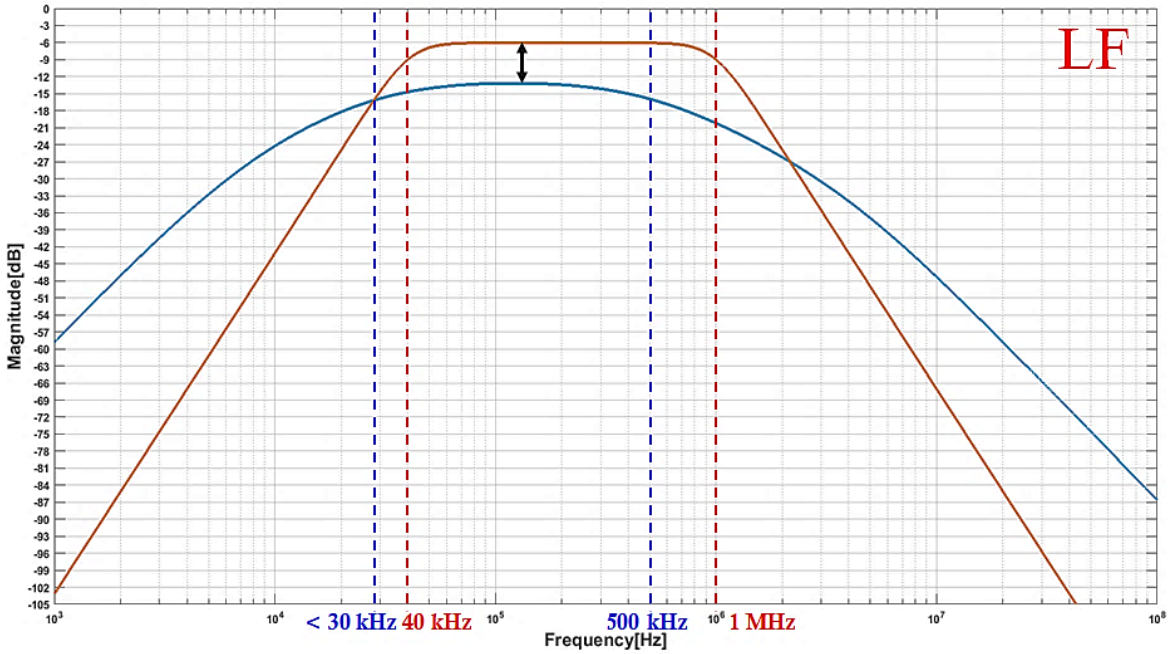

Figure 3.8: Filters comparison - LF version

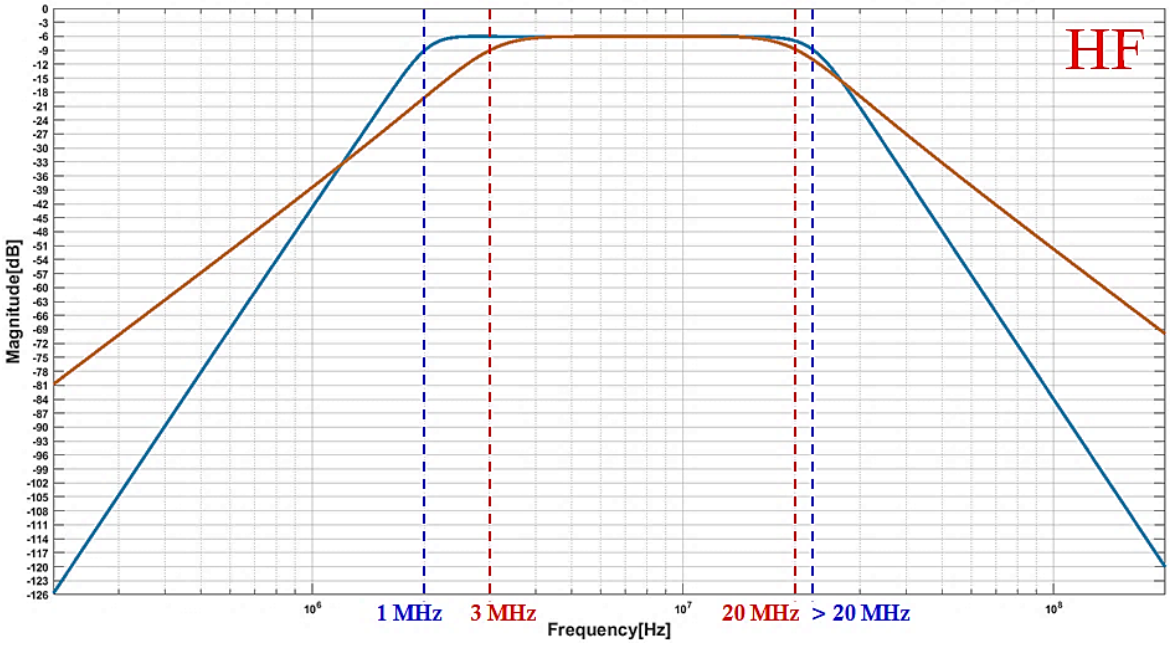

Figure 3.9: Filters comparison - HF version

To read the graphs, in both cases, must remember that the blue traces refer to the new filters, while those in orange refer to the old ones. Observing the first graph, the one for the LF version, it is evident that there were obvious deficiencies, effectively resolved in the new version. In fact, it is observed that the frequency bands were totally unbalanced, but above all also in terms of passband there is not an excellent relationship. Another noteworthy aspect is the slope assumed in the dark band. It is evident that in the new version of the filter, the dB/decade ratio is much higher, so the filter is more selective. The same can be said, in terms of passband and dark band slope, for the HF version. Both the lower and upper cut-off frequencies do not respect the band specifications.

Having observed these elements in the design stage of the filters, due to the simulations, it was decided to use the following circuit configurations, which refer to the graphs above. In *Figure 3.10* is shown in the circuit schematic for the LF filter version, while in *Figure 3.11* that for the HF.

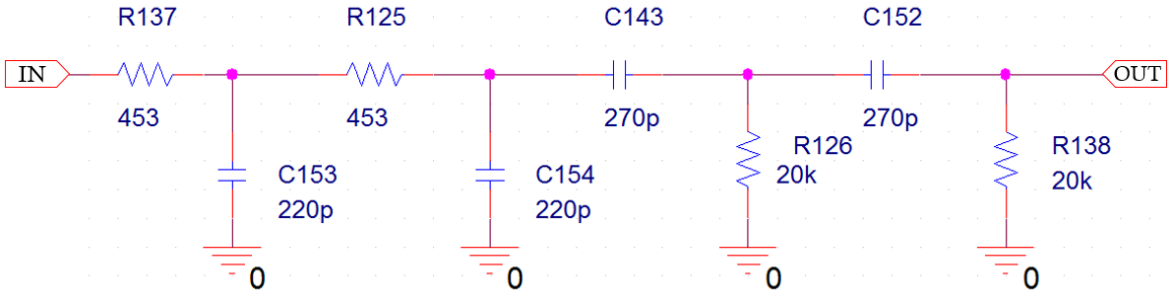

Figure 3.10: LF bandpass filter

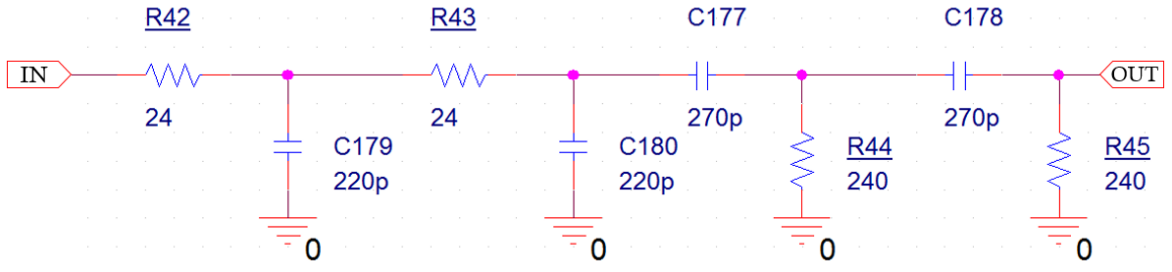

Figure 3.11: HF bandpass filter

As mentioned, another important aspect is the match between the measurement impedance and the input impedance of the filter. In the case of the LF version, reference has been made to a measurement impedance of the type shown in *Figure 3.12*, while for the HF version to a classic impedance of 50Ω. Respectively the input impedances for the filters are 10kΩ, for the LF version, and obviously 50Ω for the HF.

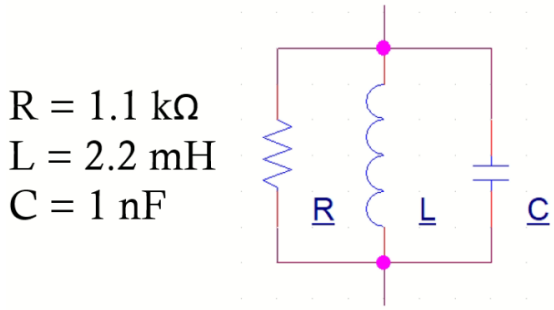

Figure 3.12: LF measurement impedance

3.2.2 Amplification Stage

The amplification stage, as mentioned, refers to the principle diagram shown in the previous *Figure 3.7*. The need to have this structure arises from the fact that:

1. Since the post-filtering signal may not be excessively high in amplitude by nature and due to the passive composition of the filter, a pre-amplification may possibly be useful to have a more considerable signal as a basis. But really, as will be explained later, in this specific case it was only necessary a unity gain preamp, but it could still be useful in other cases, so this is an important feature for the system.

2. Given that the discharge activity can be very variable and this also affects the measured amplitude values, it is extremely useful to have a variable gain amplification section that can be controlled through an analog control signal, which will then be analysed later.

3. Given the need for a connection with the control board at a distance of tens of meters, it is advisable to provide an appropriate output stage, based on the use of a fixed gain buffer. This allows there to be no excessive signal drop on the line, compromising the measurement. It must therefore be able to provide enough current to ensure good performance even with very long connections.

Other aspects of considerable importance concern the bandwidth and slew-rate of the components to be used. Obviously, it is necessary that these parameters are coherent with a classic partial discharge signal with a conducted system and the components chosen must be able to "follow" correctly the signal read on the measurement impedance. These aspects will be analysed later, during the discussion of the individual components. Before doing so, however, a further premise is necessary, linked to previous studies, during which no structural deficiencies in the amplification category were highlighted, which were then found in the analysis phases of the first prototype. In particular, reference is made to two aspects that would have totally compromised the correct measurement, namely the presence of negative oscillation peaks often greater than the main positive peak and the saturation of the positive

signal at a much lower level (well below 2V) at the level indicated on the datasheet of the reference components. Also, in this case these aspects will be analysed in detail below.

Returning to the components to be adopted for the amplification chain, the choice fell on the IC AD836 [20], whose internal scheme is shown in *Figure 3.13*.

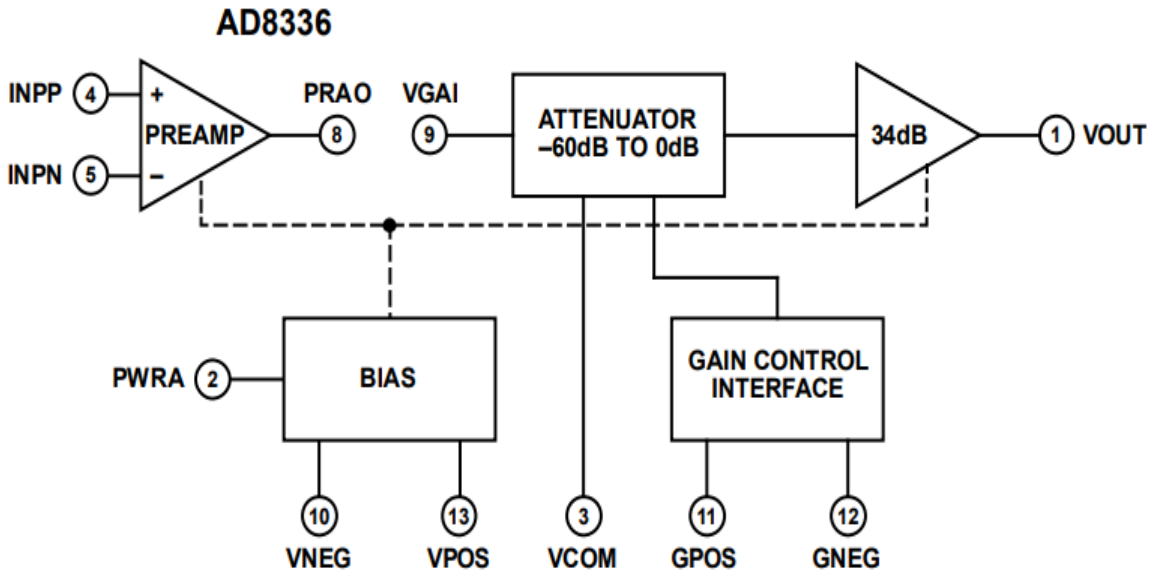

Figure 3.13: Block diagram for AD8336

It has a preamplifier inside, an attenuation network and finally an amplifier with a fixed gain of 34 dB, that is an amplification equal to about 50. Through the attenuator it is possible to vary the gain, through a control signal (GPOS-GNEG in the figure), depending on the display and scale needs. It has a sufficient bandwidth for the application relating to conducted partial discharges, since it can reach up to about 100 MHz (depending on the configurations). As regards the slew-rate, given the impulsive nature of the signals to be conditioned, a fairly high value is sufficient. Considering a typical signal, which at most has a rising edge of tens of ns, the IC in question with a slew-rate of 550V/μs, proves to be more than fast enough to follow a discharge signal. For this component it was decided to adopt a dual power supply of ± 5V, as it is sufficient for the signals of interest, but with appropriate precautions it can be powered up to ± 15V.

The tricks adopted for the configuration of the AD8336 will be analysed below. This component allows to configure the internal preamplifier, through the choice of appropriate resistors. Through the accessible inputs, the gain has been defined by means of the external resistors. Although the preamplifier is not designed to have unity gain in normal condition, but this configuration has been identified as the most suitable. Also, because for the application in question, however, it is not advisable to use higher values, as it would risk saturating the signal, amplifying it even if not necessary. Precisely for this reason, the configuration chosen and suitably tested, as it was not considered among the classic ones for the component, was the one with unit gain preamplifier. A further consideration concerns the band-gain product (GBW), which is equal to 600 MHz, which implies the choice of gains not exceeding 6, given the required passband up to about 100 MHz. Furthermore, from the datasheet it is however indicated that to obtain such performances it is necessary not to exceed the gain of 3. The disadvantage of using this type of operational amplifier with gains lower than 4 is the occurrence of an overshoot near the cut-off frequency of the system. However, by realizing an RC network, it is possible to limit this phenomenon with a sort of high-pass filtering, even if in this case this is irrelevant given the configuration. Also, the most important thing about the problem is where this overshoot occurs in frequency. In fact, from accurate simulations, it has been verified that it occurs above the frequency of 100 MHz and therefore outside the range of use for the specific application in question. Below there is a simulation graph that analyses this situation to support what has just been stated, in *Figure 3.14* it is possible to observe the comparison between the frequency response at the filter output (blue trace) and at the preamplifier output (red trace) configuration adopted for the LF version.

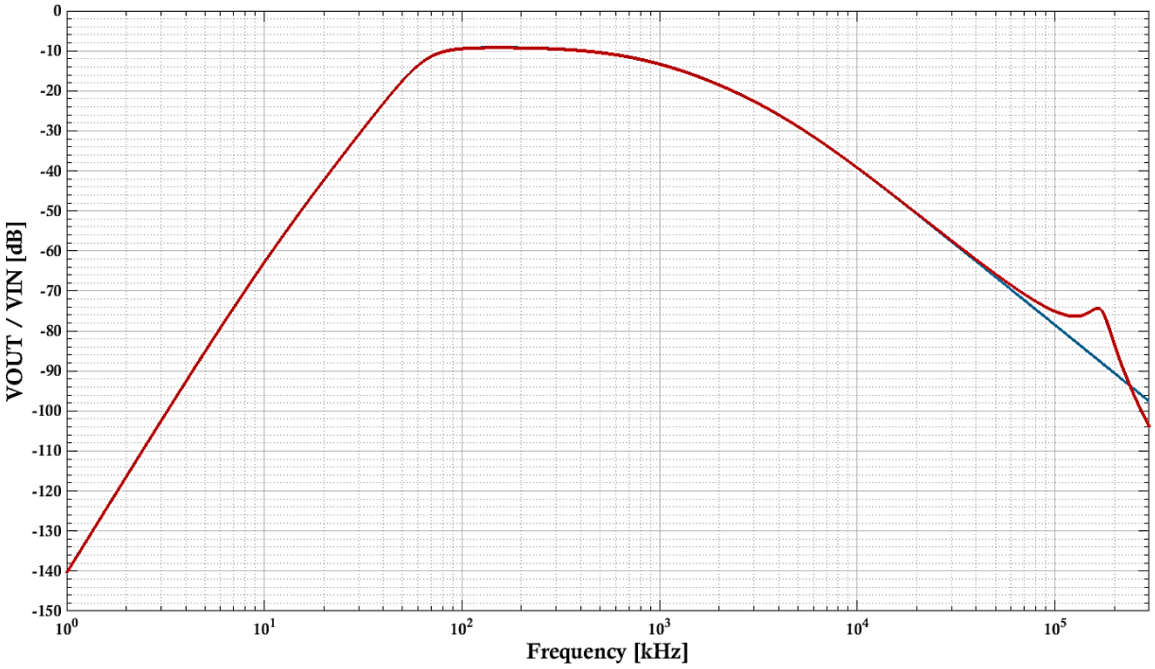

Figure 3.14: Comparison between filter and preamplifier frequency response

From the figure it is evident that the overshoot of the red trace is above 100 MHz and therefore certainly out of the band of use, in both versions (HF and LF), as well as showing how the frequency response is perfectly consistent in the range of interest. As a result of the findings, the preamplifier was used in a non-inverting configuration with unity gain. As for the output stage of the preamplifier, it can supply, with a dual power supply of ± 5V, currents up to 50mA, sufficient for the remaining circuit section, post-preamplifier. To avoid having DC offsets, it was chosen to decouple the output of the AD8336 from the next final stage using a high pass filter. This is very important, in fact, even small offset values can become considerable, in the case of amplification considering the amplification values to be achieved. Another consideration to make is related to the input, for which a high pass filter is required to eliminate the signal due to residual power supply voltage. In fact, it is possible that there is still a considerable presence of it and if this is not suitably filtered it would lead to saturation of the amplification system, with the possibility of damage.

Finally, as regards the integrated component in question, it has a PWRA input, through which it is possible to halve the power it absorbs. Due to this, the integrated component is able to operate at high temperatures and for extended periods of time,

even with high amplitude signals, but with a considerably reduced bandwidth. It goes from about 100 MHz to a band of 35 MHz. In this regard, a circuit has been set up to activate this mode, even if on the practical side this configuration has not been used, but it is still an interesting feature and that can be use if necessary, which has not been until now. This is also because, being everything powered via USB from a PC, which is then powered through the electricity network, there are no strong restrictions on the duration of the batteries or other, moreover, the measurement activity is certainly lower, in terms of time, than the duration of a laptop battery. It would however be useful in case of low frequency measurements in long monitoring and perhaps on board the machine, where temperatures can also be high. This kind of measures does not require a wide band of frequencies, allowing the use of this mode without compromising the performance of the entire system. Moreover, in this configuration, it is possible to use supply voltage up to ± 15V.

As mentioned, the last stage of the amplification chain is the output one, which has the task of providing enough power to drive even long connection sections on RG58 cable. For this purpose, the IC THS3091 [21] has been identified as a component, which allows for an output current of up to 350mA. It is a non-inverting buffer configuration amplifier with fixed gain. In this case, the gain is equal to five, in order to compensate and be able to use the AD8336 internal attenuator in a more flexible way. The integrated component provides a high slew-rate, equal to 7300V/μs, an even more critical requirement at this level, as the managed signal is greater than that of the variable gain amplifier and even in this case it is more than enough. As for all the other components, it was also chosen based on the possible supply voltage, which also in this case reaches up to ± 15V. Furthermore, a 50Ω resistor is provided at the buffer output, in order to guarantee coupling, and a capacitor to block the DC due to the simultaneous presence of power and signal on the communication line.

To conclude, in *Figure 3.15*, it is shown the schematic of the amplification chain

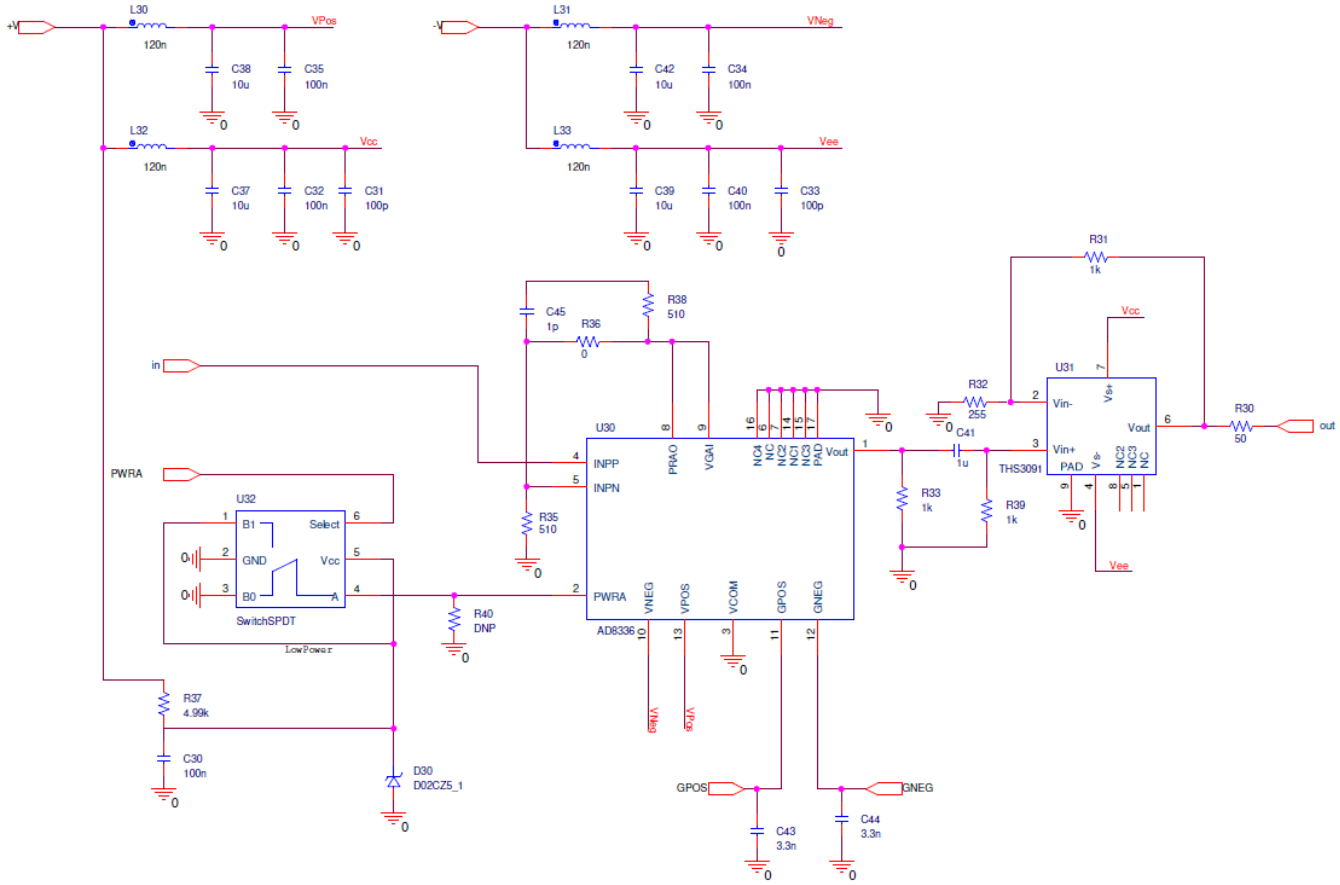

Figure 3.15: Amplification chain circuit

3.2.3 Logic stage and VGA Controlling

The gain variation is possible through the use of the PIC16F1704 microcontroller, which has an 8-bit DAC, a 10-bit ADC and a comparator on board. The microcontroller generates an analog control signal output from the internal DAC, which drives the attenuation network present inside the variable gain amplifier. In this regard, the variation of the internal gain of the AD8336 is possible due to the presence of an R/2R scale network, with a nominal value of 320Ω, a value useful for limiting noise. Furthermore, the input resistance to the network is higher than what has been said, to ensure that the preamplifier output is not overloaded. The internal attenuation network of the IC is controlled through a differential voltage input, defined below as V_{GAIN}, consisting of GPOS and GNEG. By applying a certain differential voltage between these two inputs, the gain is suitably adjusted. Consider that the applicable

voltage can vary from positive to negative values, within the nominal range of ±800mV. Since the voltage for the control is supplied through the DAC of the microcontroller, which is not able to generate negative voltages, in order to also obtain negative differential voltages, it has been chosen to clamp the voltage at the negative input with a resistive divider, so which fixes the voltage of about 668mV on GNEG, while GPOS input will be connected directly to the microcontroller DAC.
The curve relating the gain to the applied control voltage is shown in *Figure 3.16*.

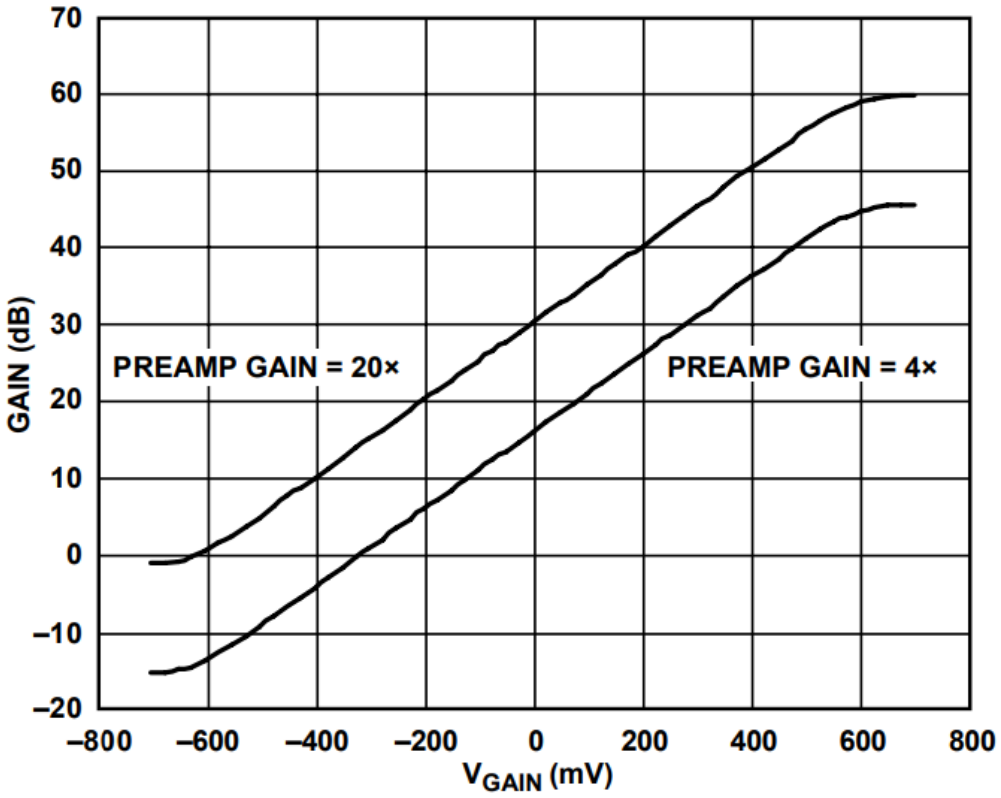

Figure 3.16: V_{GAIN} vs GAIN - Datasheet comparison

The fundamental question, however, concerns the relationship between control voltage and gain which remains unchanged except for a vertical translation, as can be seen in the red trace of *Figure 3.17*, referring to the ideal case with unity gain preamplifier.

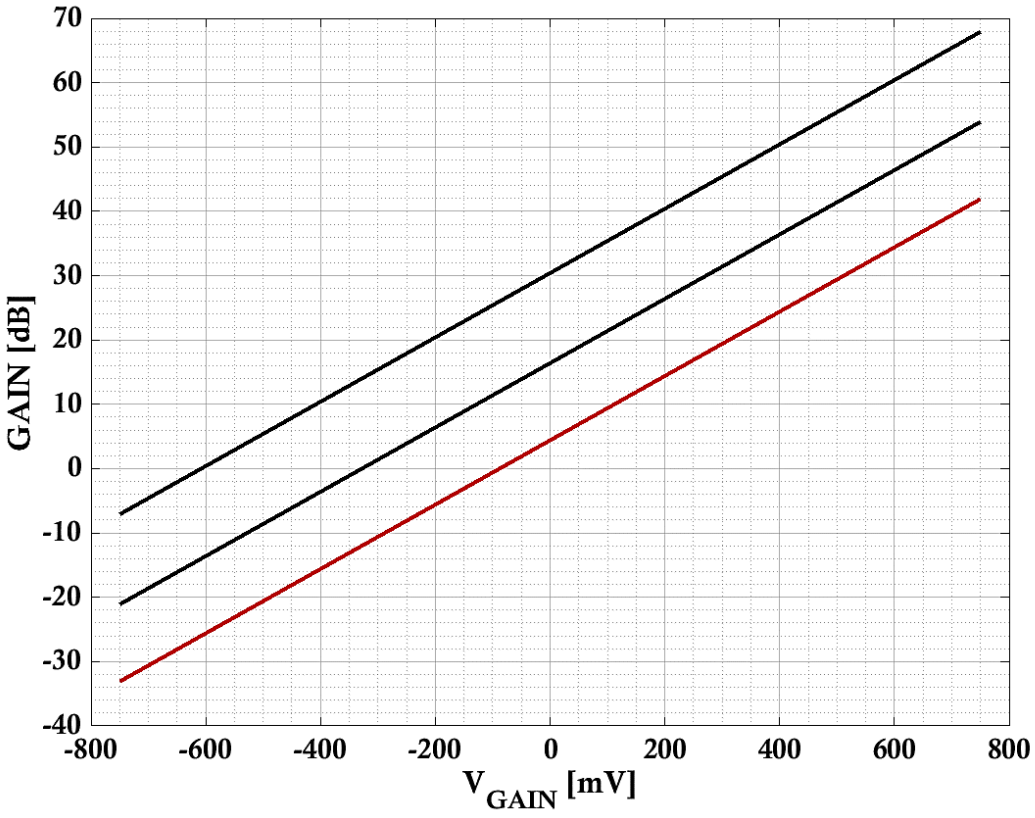

Figure 3.17: V_{GAIN} vs GAIN - Ideal comparison

It compares the two black idealized traces with respect to the real ones, shown in the previous graph, and relates them to the one with the amplifier set for unity gain (red trace). Note that the black curves in the graph show the two cases where the preamplifier gain is 4 and 20. In the unit gain configuration considered for this system the situation is to be considered different with regard to the value range for the differential voltage. In fact, the range will certainly be smaller than the nominal ±800mV and the curve will be slightly shifted below that to gain equal to 4. As said, this affects the range of differential voltages, in addition to the maximum value of gain achievable, which is still sufficient to ensure the values set during the design of the amplification chain.

The previous relationships refer only to the variable gain amplifier, while the general formula for the calculation of the total gain is the following:

$$\mathbf{GAIN_{TOT}} = (\mathbf{GPOS} - \mathbf{GNEG})\ [\mathbf{mV}] \cdot \mathbf{0.05}\ \left[\frac{\mathbf{dB}}{\mathbf{mV}}\right] + \mathbf{G_{INTERCEPT}}\ [\mathbf{dB}] + \mathbf{G_{BUFFER}}\ [\mathbf{dB}]$$

Where $G_{INTERCEPT}$ depends on the preamplifier configuration, for gain 1 it is 4.4 dB, for 4 it is 10.4 dB and for 20 it is 30.4 dB, while G_{BUFFER} is 14 dB.
Since this formula, a table can be drawn up containing the theoretical values for the gain values set in the stage design (see *Table 3.3*).

Gain Value	**$GAIN_{TOT}$ [dB]**	**G_{BUFFER} [dB]**	**$G_{INTERCEPT}$ [dB]**	**GNEG [mV]**	**Theoric GPOS [mV]**
1	0	14	4.4	668	300
5	14				580
10	20				700
50	34				980
100	40				1100

Table 3.3: Table of gain values

Considering that the PIC has an 8-bit DAC on board, it is necessary to consider that the values calculated in the table are strictly theoretical, because the output voltage is discretized in 8mV steps, given the reference voltage of 2.048V. Obviously, for what has been said, it is not certain that can arbitrarily approach the theoretical values, even if this possible deviation is not so critical for the application, committing an error of about 2.3% on the gain value. This without considering the error that normally characterizes the VGA, which is to be added to the latter and which depends on the voltage applied to its input. For values between ±0.5V there is an error which typically involves a deviation of ±0.2dB. Outside this range, however, larger values can be had, up to 3÷5dB. Even more reason it is a good thing to keep a low preamp value so as not to exceed the VGA input values. Obviously, the calculated values do not even consider the fact that the various components are subject to tolerances. For these reasons, an appropriate tuning of the voltage values that refer to the gain is envisaged, during the firmware loading and device testing step.

Focusing now on the logic circuit that controls the variable gain section and decodes the commands sent by the control board, *Figure 3.18* shows the reference logic schematic.

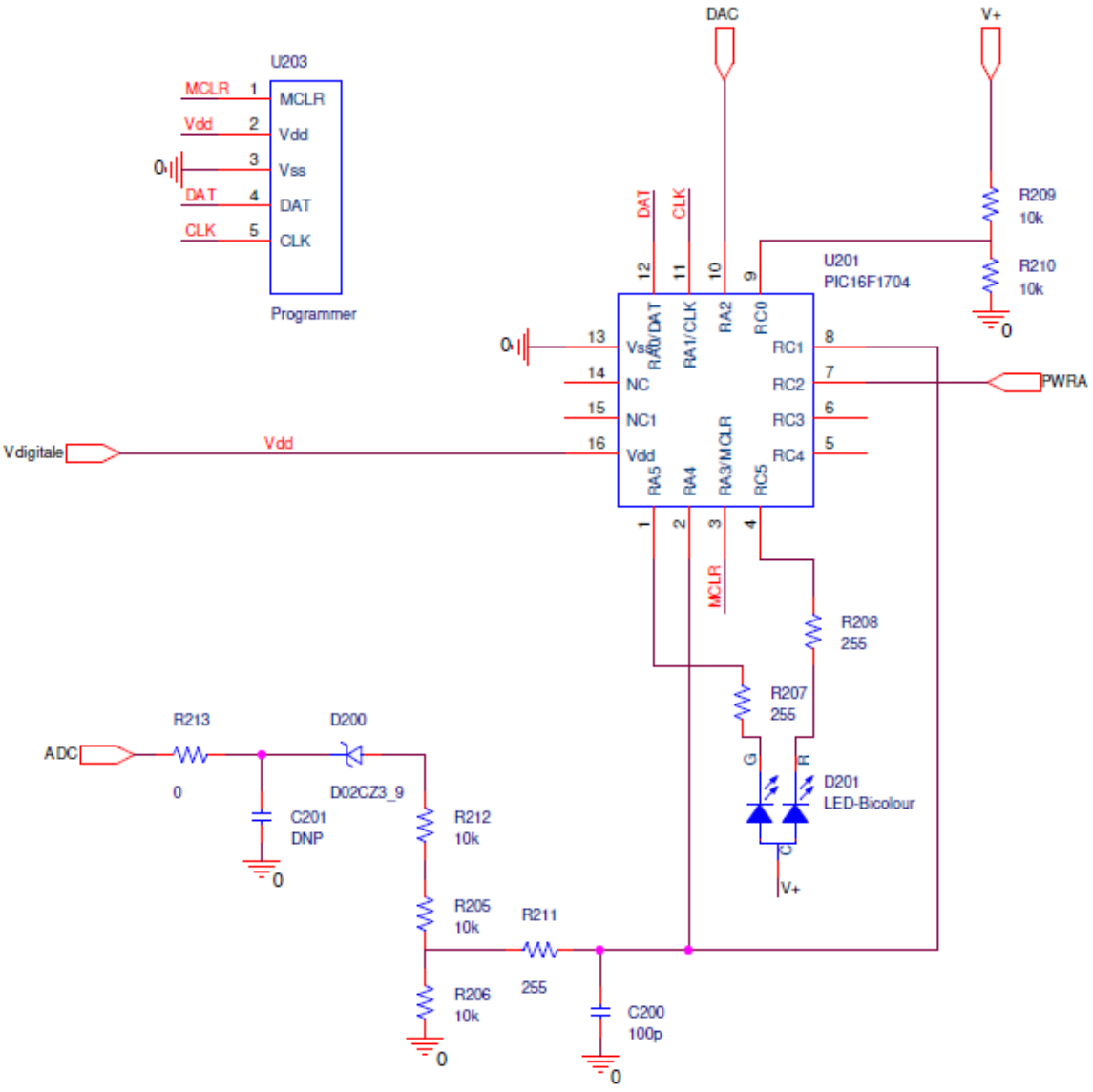

Figure 3.18: Logic circuit

Considering now the command decoding logic, we can refer to the input, called ADC. Since it is connected directly to the power line, any variation on the power supply voltage will also affect the ADC. In the circuit diagram it is possible to identify two components R213 and C201 not placed, but which can be used to make a low-pass filter to eliminate noise, although in this case, the communication seemed to be

sufficiently robust to avoid them. Then follows a resistive divider, which allows you to measure only 1/3 of the line voltage, in order to avoid overvoltage on the PIC pin and at the same time still have good discretion in the voltage variations related to the measurement. Furthermore, in order to avoid the presence of voltages higher than 5V, a Zener diode was placed in series with the voltage divider. All this makes it possible to avoid any returns on the line, but above all to guarantee a maximum voltage of 5V even with larger supply voltages. In this way a good robustness of the system is guaranteed. The diode therefore has the task of protecting the ADC without compressing the voltage variation range. Furthermore, the divider is not only connected to the ADC, but also to the inverting input of a comparator. In this way the line voltage can be compared with the voltage of another divider, formed by R209 and R210, connected to the non-inverting input. By properly writing the firmware it is possible to generate an interrupt event in the case that the line voltage exceeds the reference voltage, identifying the start of a communication, which will be decoded using the ADC to make the process more flexible and robust to noise.

For the decoding of the message it was decided to sample the signal, in order to reconstruct the durations of the various symbols simply by counting the samples that are at a high or low level. If the number of samples at a low level is between the duration of the symbol and its tolerance, it is considered correct and can be considered valid, provided it ends within the maximum time. For greater noise robustness, each sample used to make the decision is the result of the average of 4 samples, therefore, the A/D converter digitalizes the signal at a sampling rate of 4 kHz, while the useful data is obtained at 1 kHz. The communication is considered correct if all the symbols have been read correctly and, in this case, it is possible to proceed with the real decoding of the command received. In fact, the communication can be correct, but it does not necessarily contain an interpretable command. If a valid command is not found, the transmission is discarded and returned to the waiting state, otherwise the operation associated with it is performed. Moreover, the microcontroller has an internal oscillator, which can provide a sufficient frequency for the operations it is going to perform, since there is no criticality at the time level.

Also, to give feedback to the user, in cases of unrecognized commands or failed communication, as well as for the set gain values, a bicolour LED has been inserted,

whose lighting is also managed by the microcontroller in this case. Obviously, to have effective feedback, the device must be positioned so that the LED is visible to the operator, even if it is reasonable to think that on some occasions this is not possible. This is a simplification, adopted to avoid overly complicating communication. Below, in *Table 3.4*, the various light signals that can be associated with the different decoded symbols are shown.

Mode	**LED Status**
Device ON	One 2s red LED flash, when power ON
Gain 1	One 200ms green LED flash
Gain 5	One 200ms red LED flash
Gain 10	Two 200ms green flashes, interspersed with one 100ms red LED flash
Gain 50	Two 200ms red flashes, interspersed with one 100ms green LED flash
Gain 100	Three 200ms green flashes, interspersed with two 100ms red LED flashes
Default	Mode *Gain 1*

Table 3.4: Feedback light signals for conditioning board

In this way, if the appropriate sequence based on the command sent is not recognized or no signal is received (i.e. there is no flashing when a command is sent) it is possible to understand that there are problems in communication. Obviously, all this is implemented in a firmware made for the adopted microcontroller, what is treated in this paragraph, and loaded on chip with ICSP programmer.

3.2.4 Protection stage

An appropriate protection system has been set up at the device input to avoid damage caused by electrical transients such as those deriving from electrostatic discharges (ESD) or, in this case, problems related to the high voltage measurement system that can affect the measuring instrument. The circuit adopted for this purpose is shown in *Figure 3.19* and consists of:

- a TVS diode [22]
- two Zener diodes in anti-series [23]
- a spark gap

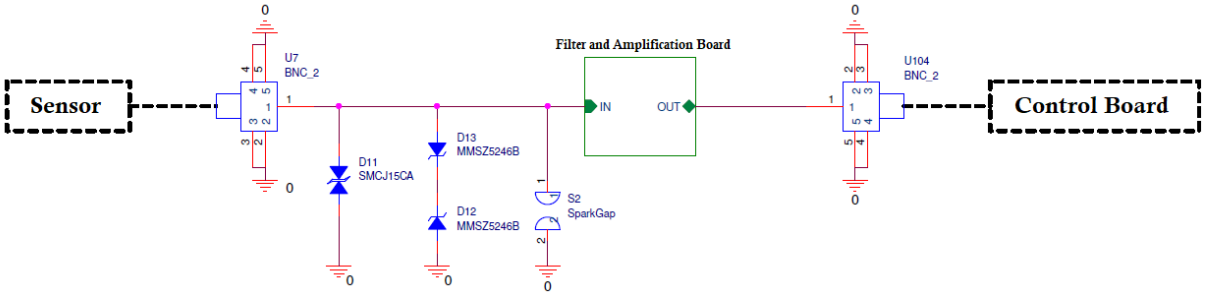

Figure 3.19: ESD protection circuit

It is known that there are several techniques for protection against transient electrical events. Mainly, three can be identified: blocking, suppression and isolation techniques. The block uses fuses and circuit breakers, blanking uses TVS devices such as TVS diodes and metal oxide varistors (MOVs), while isolation is usually relied on to optocouplers or transformers [24]. Certainly, the block is always effective and inexpensive, but once the devices have intervened, they need to be changed or reset, and this certainly makes them uncomfortable to use. As for the isolation devices, however, they are also effective and, above all, they do not need to be replaced or reset, but they are usually more voluminous, complex and expensive. TVS devices are a good compromise, turn out to be good protection devices, are small and have low to medium prices. With reference to the latter, it is a p-n device made in such a way as to be able to absorb high currents deriving from transient electrical events. They are characterized in voltage/current in a similar way to a Zener diode, but it is designed to suppress a voltage rather than to regulate it. Compared to other suppression devices, a TVS diode is characterized by an excellent and rapid intervention response to electrical transients (typically within nanoseconds, but in some cases even picoseconds), which allows the energy to be directed to ground safely while maintaining a constant impulse withstand voltage. In theory, the protection mechanism is as follows: under normal operating conditions, the TVS diode has a high impedance to the protected circuit, but when the safety operating voltage of the

circuit is exceeded, the TVS diode turns on for provide a low impedance ground path for transient current. As far as the maximum voltage to which the protected circuit is subject is concerned, it is usually limited and low levels, generally in relation to the impulse withstand voltage of the diode. The TVS device returns to the high impedance state after the transient electric current was gone down, also if in a much slower way than the intervention time, a characteristic that is irrelevant for the device in question, since there are no restrictions in this perspective. As far as the voltage, to which the circuit is subject, is usually of low and limited value, but for safety, two anti-series Zener diodes have been inserted to prevent too high voltages from being found on the filter input and then consequently on the preamplifier.
As far as the spark gap is concerned, it has been positioned before the filter, and not on the preamplifier input, to avoid altering the measurement, due to the capacitance associated with it, especially when using high frequency bands. The safety spark-gap for the user is therefore positioned where its effects in terms of measurement are less critical. Although the voltage level is not sufficient to protect the user, it is still useful for limiting the effects of electrostatic discharges, which are also managed through the other protection components.

3.2.5 Supply stage and other elements

All components used are powered with dual or single voltage of 5V, with some precautions that will be analysed below. However, given the flexibility of the power supply system, in the case of signals of amplitude greater than 5V, the system would be able to manage them without problems, it could be done without any modification to the circuit. Furthermore, it should be noted that the power supply stage was designed in the context of previous activities, so what is reported is the result of in-depth and verified studies [1].
To start the discussion, *Figure 3.20* shows the complete power supply circuit.

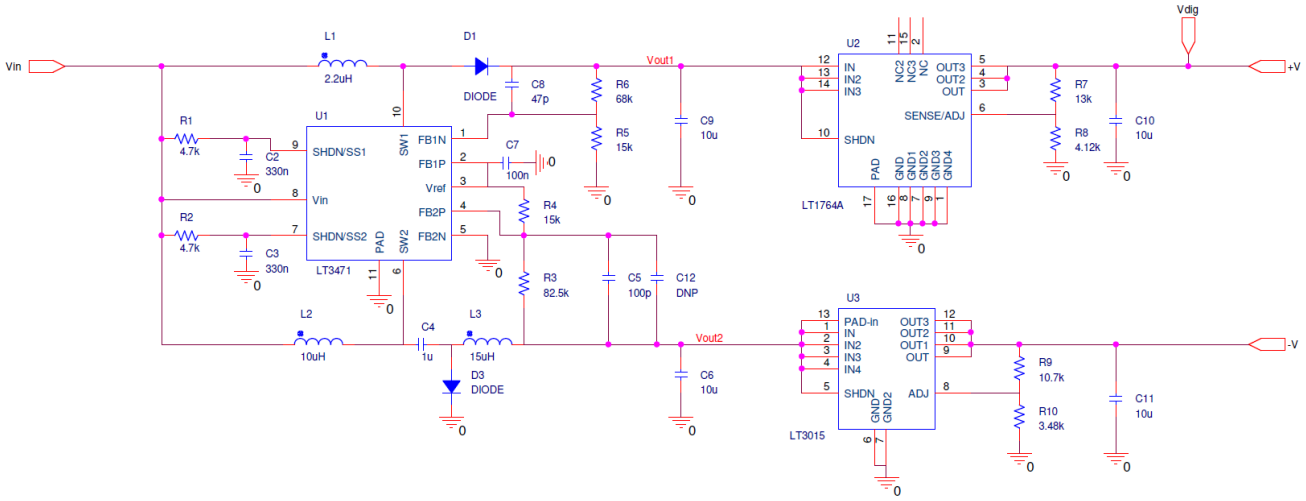

Figure 3.20: Supply voltage circuit

In this regard, the IC LT3471 [25] was chosen to create a single DC-DC conversion block, since it contains two modules that can operate independently to achieve different voltage values. Thanks to its size and high switching frequency, equal to 1.2MHz, it is possible to use low value inductors and therefore keep the circuit dimensions contained, as required. To fix the DC-DC output voltage, it was necessary to set the values of suitable external resistive dividers and the following relations were used for the calculation:

$$\mathbf{V_{OUT1pos}} = \mathbf{V_{FB1P}} \cdot \left(\mathbf{1} + \frac{\mathbf{R6}}{\mathbf{R5}}\right)$$

$$\mathbf{V_{OUT2inv}} = \mathbf{V_{REF}} \cdot \left(\frac{\mathbf{R3}}{\mathbf{R4}}\right)$$

Where, in this configuration, V_{REF}=V_{FB1P}=1V

Other important aspects concerned the choice of some components used for the realization of the power supply system diodes, capacitors and the characteristic of the positioning of the components. As for the diodes, Schottky [28] have been chosen in order to have a good conversion efficiency, low forward bias voltage and a good tolerance margin with respect to the supported forward current. As regards the capacitors, however, since the current requests are not stinging and that the absorption must be less than 500mA, given the use of USB2.0, it was possible to introduce 10 µF

decoupling capacitors on each input, as well as on the outputs to minimize DC ripple. Furthermore, again to minimize ripple, capacitors with low ESR have been chosen, SMD multilayer ceramics. Another aspect to be addressed concerns the positioning of the components associated with the power supply circuit. In fact, since it is a switching power supply, it is strictly necessary to position the components in the most suitable way in order to reduce noise phenomena as much as possible. In particular, it is important that the inductors, but in general also the other components such as capacitors and diodes, are positioned very close to the IC, which has the task of voltage control and inside which there are the two switches. This is because by reducing the area subject to the magnetic field, the effects of any disturbances are reduced. Furthermore, the chosen inductors are shielded, so as to avoid that they can influence each other by inductive coupling, and a suitable ground plane must be provided during the PCB layout, defining pre-established paths for the current during the work of the DC-DC converter.

Referring to the rest of the post DC-DC circuit, it is possible to observe, in the previous schematic, the upper part that is relative to the positive DC-DC conversion, while the lower part to the inverting converter. Since the parts of the system dedicated to signal conditioning must have a stable DC voltage with as little noise as possible. In this regard, linear regulators have been adopted, adjustable through the definition of an external resistive divider, which have the purpose of regulate the voltage and eliminating ripple and residual switching. The regulation circuit for the positive voltage was made using the IC LT1764A [26], while the one for the negative voltage with an LT3015 [27]. The adjustment relationship, for both components, is shown in the following *Figure 3.21*.

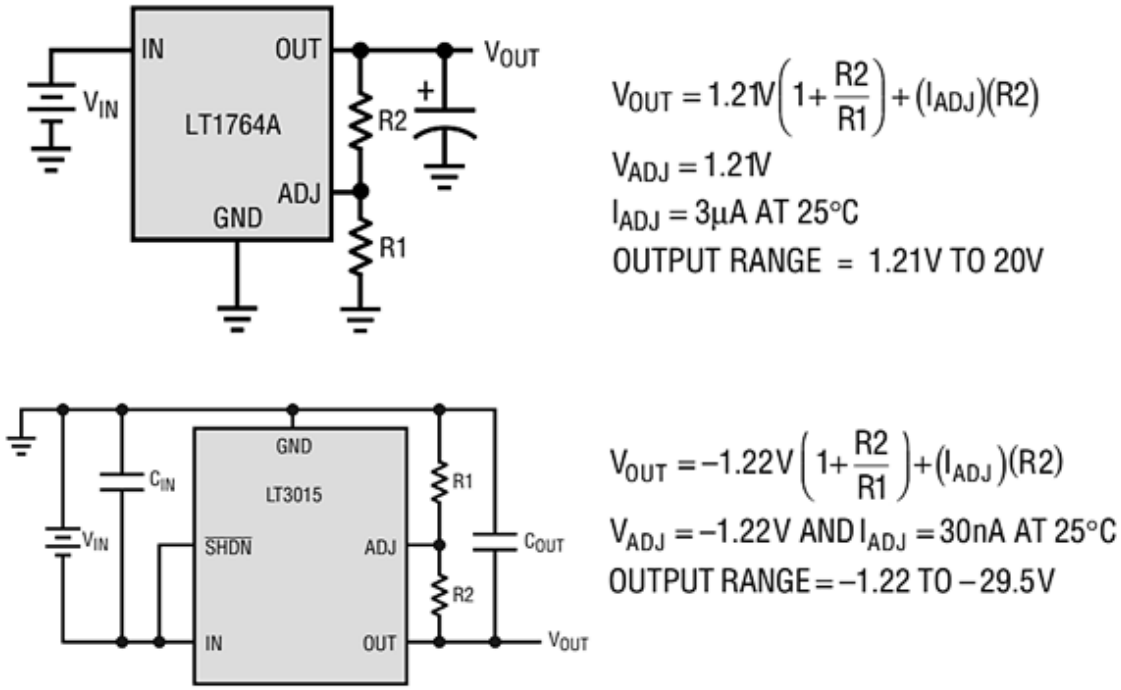

Figure 3.21: Linear regulator relations

As for the stabilization of the positive voltage, the component used is characterized by having a rapid response to variations in the load, which is compatible with the continuous variation of the voltage on the line during communication. Instead, for the regulation of the negative voltage, an integrated component was used which also requires a resistive feedback divider, as well as two Bypass capacitors, on input and output, of 10μF.

Since this system has been studied during previous activities, it is superfluous to report circuit simulations in which the operation of the circuit in its various parts is verified. For completeness, however, a representation of the power supply signal present at the output inside the system is shown. This can be seen in *Figure 3.22* below.

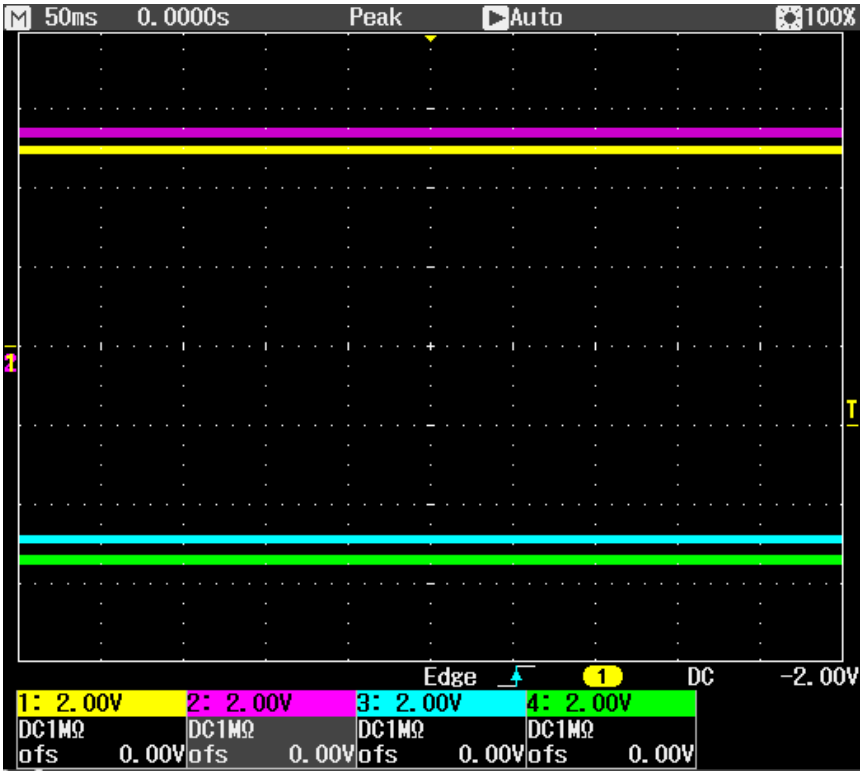

Figure 3.22: DC voltages supplied by the power supply circuit

The figure shows the acquisition of the oscilloscope relating to the measurement of the continuous voltages provided by the power supply system. The yellow trace refers to the positive output at +5V, while the light blue one refers to the negative output voltage at -5V. Both are stable and respect the desired voltage value. The same can be said for the output of the DC-DC converter at negative voltage (green trace) and for that relating to the positive voltage (purple trace). In the first case, the voltage is stable at just under -5.5V, a value for which the feedback circuit has been designed. Same thing can be said for the purple trace which turns out to be slightly lower than 5.5V. The reason for these inaccuracies is to be found in the choice of resistance tolerances. In fact, in the case of linear regulators, precision resistors were chosen to regulate the desired voltage level, while in the case of DC-DC converters the most common ones were used. This because the voltage value is not critical if it is kept within certain values, as the linear regulators chosen are able to compensate for such variations.

3.3 Control and output section

The control board is designed to have the bare minimum on board to manage the interface between the signal conditioning board, PC and acquisition system (usually a digital oscilloscope). The conditioned signals are made available on the control board output, so that they can be digitized by a digital oscilloscope or by an ad hoc acquisition board, controlled via software, and, if necessary, to obtain further data processing, such as the creation of PD pattern. The fundamental task of the control board, however, is to send the commands to the conditioning one, received from the operator through the USB connection with a PC, commands will be sent to the preamplifier, through the use of an appropriate circuit. *Figure 3.23* shows the general scheme of the control board.

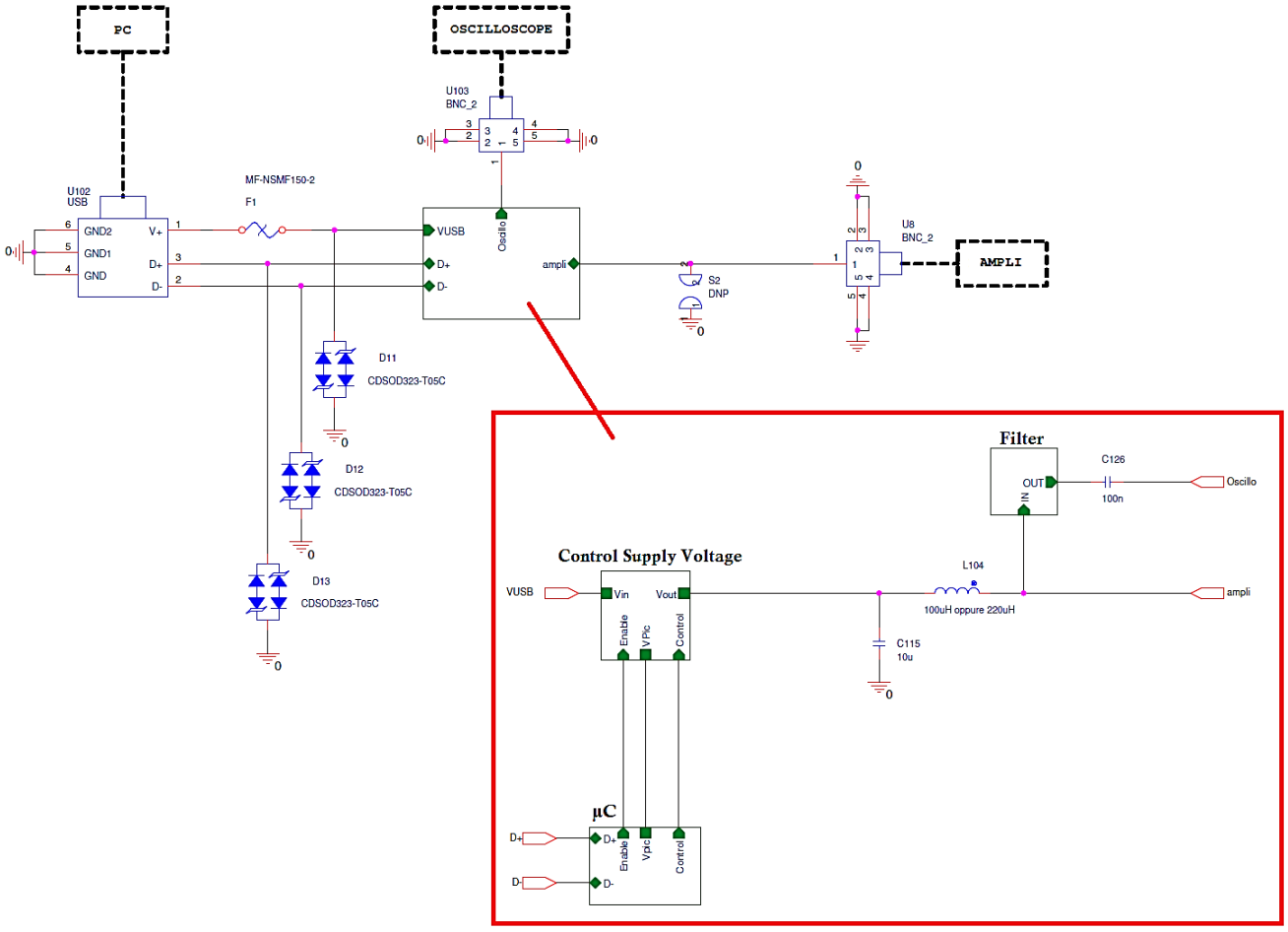

Figure 3.23: Block diagram of control board

From the figure it is possible to identify some fundamental blocks, such as the one relating to the USB connection and relative protection, the one relating to the logic that manages the interpretation of the commands received from the PC and the following sending to the conditioning board and again the section dedicated to power supply system, in addition to the part of the circuit that allows interfacing to the outside. Substantially what will be discussed below concerns the hardware implementation of the protocol previously described in *Paragraph 3.1*.

As regards the protection of the USB port, a suitable resettable fuse and TVS diodes have been inserted to make the system robust. On the other hand, for the filtering block, although foreseen for eventuality, it does not currently provide for the presence of a filtering stage, since it has not been found that it is not strictly necessary under normal conditions.

3.3.1 Control supply voltage stage

This section deals with the electronic part dedicated to the management of the various levels of DC, useful for powering the components present on this board but above all for the one dedicated to the conditional board, present on the same communication line. For this purpose, the appropriate electronics dedicated to the variation of the voltage level on the line is provided in this section, through which the commands are sent to the control board. The circuit diagram adopted is shown in *Figure 3.24*.

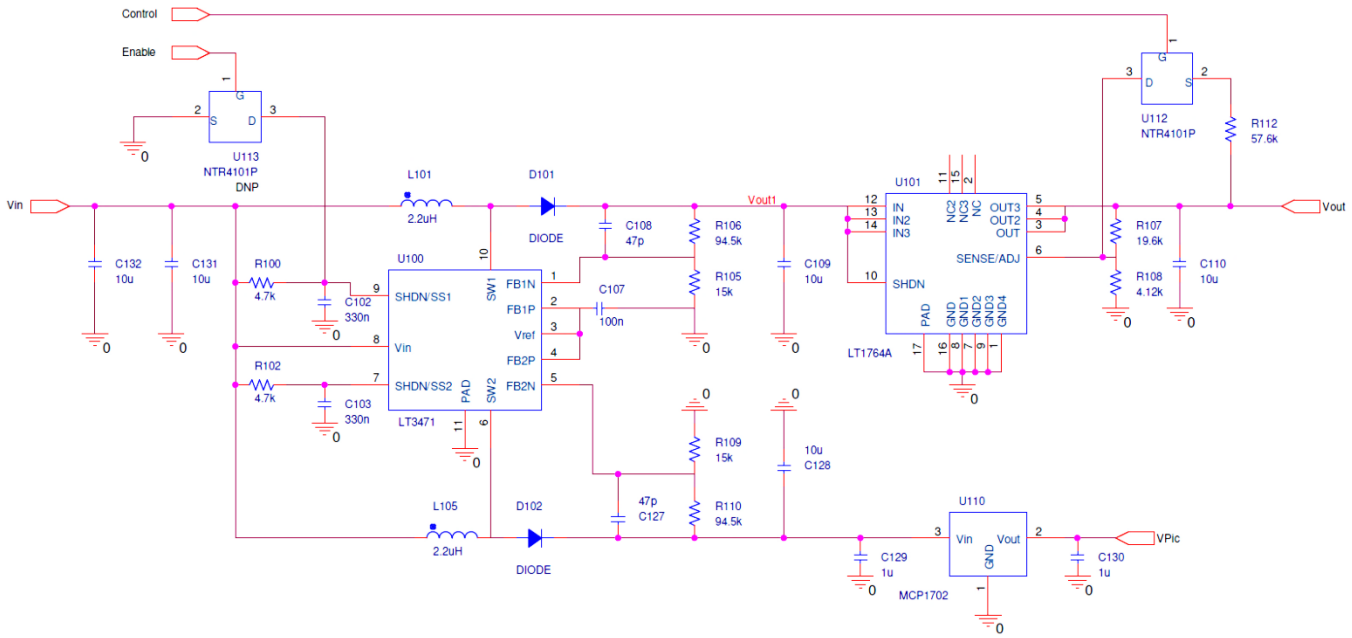

Figure 3.24: Control supply voltage circuit

The voltage level management structure is very similar to the one analysed for the analogous section of the conditioning board. In fact, there is the exact same IC for DC-DC conversion, which also in this case has two separate modules, in this case two Boosts. The first, the one that refers to the upper part of the diagram, is followed by an adjustable linear regulator, equipped with a MOS (U112) in series with a resistor, connected in parallel to the feedback divider, which allows to adjust the voltage level of the line. The MOS is controlled through the PIC microcontroller, so that the voltage level for sending commands can be varied. The other Boost, on the other hand, deals with powering the components on the control board at a constant and regulated voltage. As for the air conditioning board, for the same reasons, linear regulators have been inserted, as mentioned for the first Boost. As for the second, the integrated circuit of the Microchip MCP1702 [29] was used which sets the power supply voltage for the logic part at fixed 5V. This regulator is very compact and requires no additional components, just two 1µF Bypass capacitors. As mentioned for the part relating to the line, the same IC of the conditioning board was used, namely the integrated LT1764A. It is optimized to have a quick response to load variations, a useful feature for the continuous variation of the line voltage during communication. Obviously, the introduction of a MOS implies that the relationship for the voltage

level regulation for the linear regulator associated with it. The new relationship is shown below:

$$\mathbf{V_{OUT1boost}} = \mathbf{V_{ADJ}} \cdot \left(\mathbf{1} + \frac{\mathbf{R107 + R112}}{\mathbf{R108}}\right) + \mathbf{I_{ADJ}} \cdot (\mathbf{R107 + R112})$$

Where the resistance connected to the transistor (R112) is considered, overlooking the ON state resistance because it is much smaller than the divider resistances.

3.3.2 Logic stage

The logic stage, through the use of the PIC16f1454, takes care of managing the USB connection, interpreting the data coming from the PC, and then enabling or disabling the line control MOS once it wants to send a command to the conditioning board. The circuit adopted is shown in *Figure 3.25*.

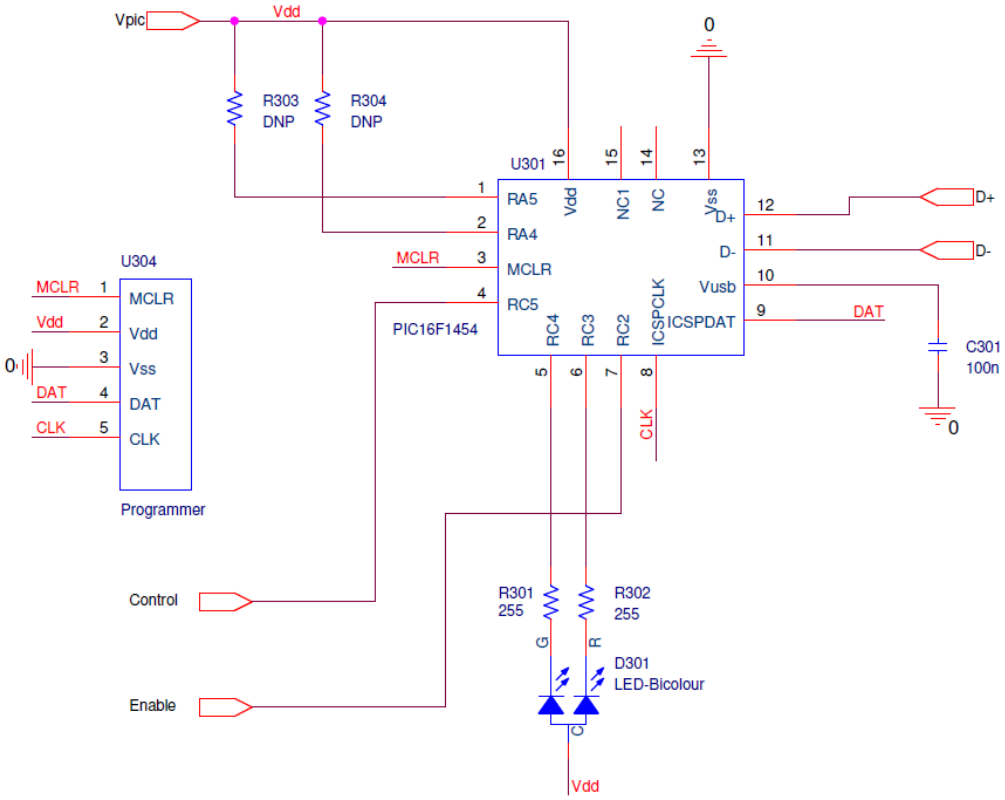

Figure 3.25: Logic control circuit

The microcontroller has an internal oscillator, which can provide a sufficient frequency for the operations it is going to perform, since there is no criticality at the time level. The data are received directly on peripherals of the microcontroller dedicated to USB (D+ and D-) and the possible data coming from the PC are summarized in the following *Table 3.5*.

Hex Code	**Command**
0x01	Gain 1 Value
0x05	Gain 5 Value
0x0A	Gain 10 Value
0x32	Gain 50 Value
0x64	Gain 100 Value
0x80	LED Toggle Check
Default	No command recognized

Table 3.5: USB commands for the control board

Once the command from USB has been interpreted, the microcontroller takes care of controlling the timed opening and closing of the transistor on the communication line, to create the symbol that you want to send to the conditioning board, according to what is specified by the custom protocol. In terms of visual feedback, also in this case a bicolour LED has been inserted which returns various information to the operator through colours and flashes. *Table 3.6* summarizes the various actions that may be followed by a change in LED status.

Mode	**LED Status**
Power ON	Green LED continuously ON
Power OFF	No light
Send Command	Green LED switch OFF briefly
No command recognized	No action, status unchanged

Table 3.6: Feedback light signals for the control board

Obviously, an appropriate firmware made for the adopted microcontroller is associated with what is treated in this paragraph, loaded on chip with ICSP programmer.

3.4 Simulation of conditioning chain

A fundamental aspect in the design concerned the simulation of the complete system, in terms of signal conditioning. This simulation provides both circuits for conditioning and control boards. It should be noted that all simulations refer to the LF version of the system, but the similar checks were performed for the HF version. Moreover, during this activity, the simulation (see the final circuit adopted in *Figure 3.26*) mainly concerns the filtering, amplification and output interface chain, since the necessary verification simulations had already been performed at the power supply system level, during previous studies.

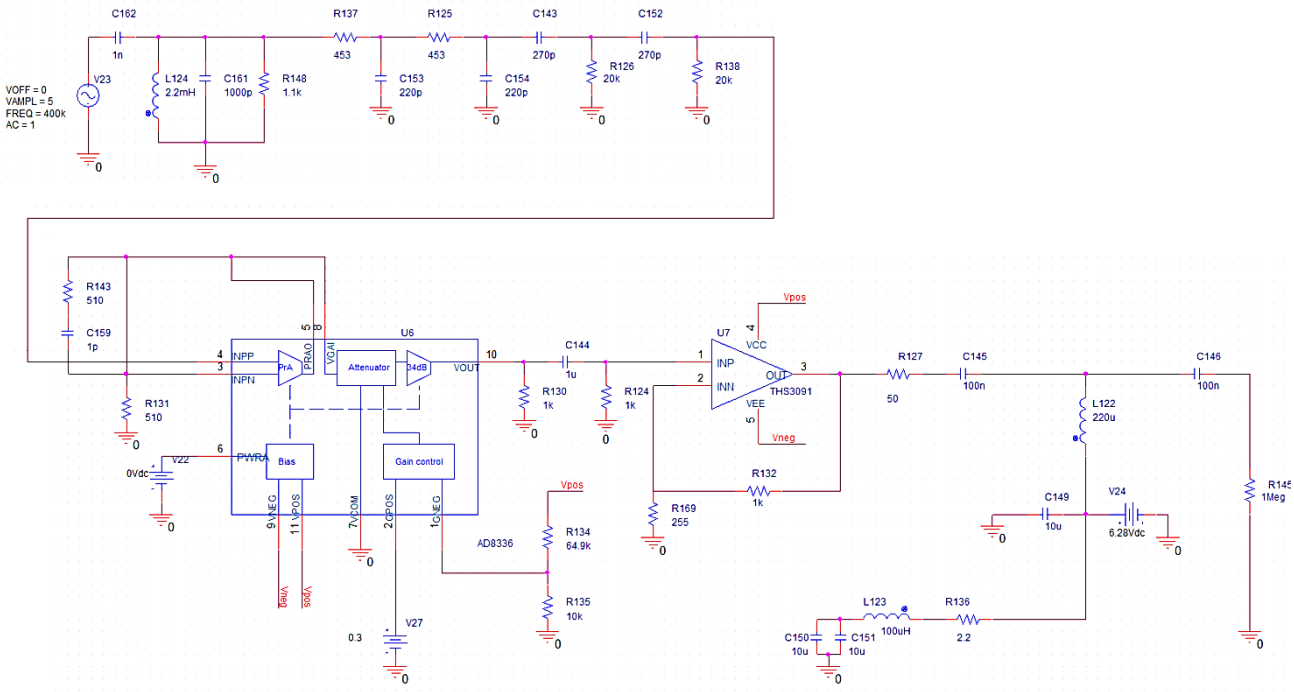

Figure 3.26: Adopted simulation circuit

In this regard, during previous studies, a possible configuration had been prepared which, by means of in-depth analysis at the beginning of the one involved in this

research activity, was found to be unsuitable. In addition to the considerations already made on the filtering stage, it included the configuration of the preamplifier with a gain equal to 3 and the buffer with fixed gain equal to 2. Below there are some traces, in *Figure 3.27*, which show how this configuration was wrong at a conceptual level.

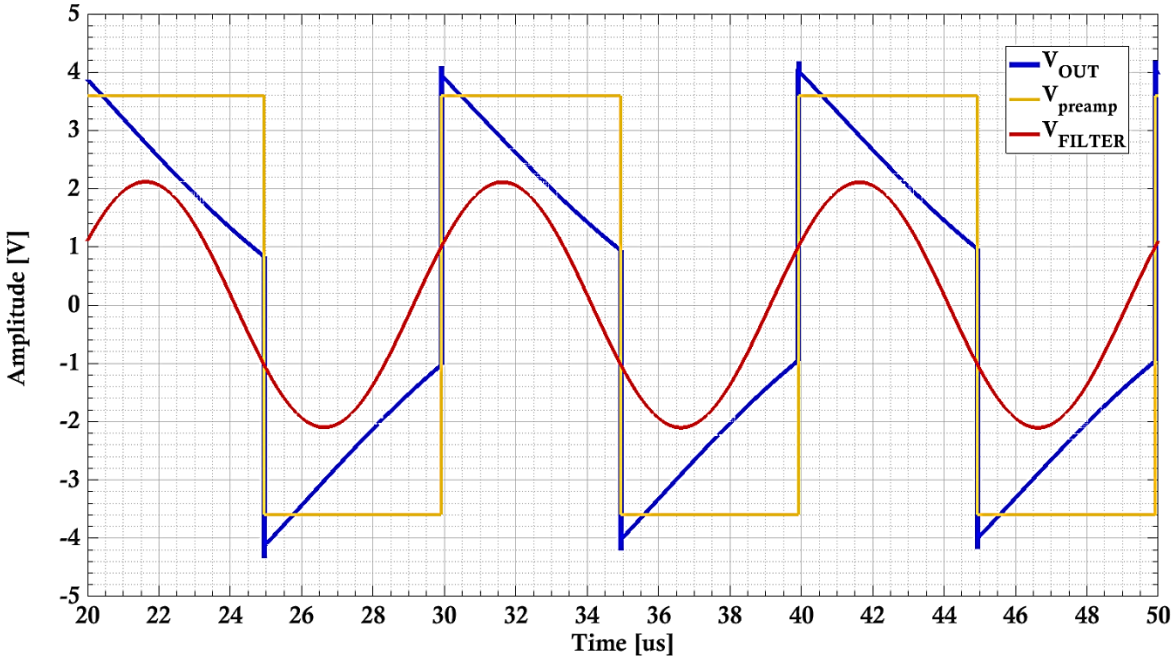

Figure 3.27: Time simulation with unsuitable configuration

In the time graph it is possible to observe the red trace which represents the signal present after the filter, in yellow the one after the preamplifier and finally in blue the one outgoing to the system, in the unity gain configuration of VGA, but the same considerations can also be made for the other gains. In this regard, it is evident that if the signal after filtering is quite high, an amplification of gain 3 by the preamplifier immediately brings the signal to saturation, which is then brought back saturated throughout the signal chain, obtaining unsuitable results to the analysis of a signal of interest. Among other things, it is not even that difficult for this situation to occur since the maximum signal that can be output from the AD8336 is equal to the supply voltage (in absolute value) minus 1.5V, therefore about 3.5V. In fact, given the preamplification value, it is sufficient that after the filter there is a signal with a maximum amplitude of about 1.2V. Furthermore, it is also evident how saturated values at the AD8336 output lead to a further distortion of the signal in the passage to

the remaining stages that make it available at the output, as can be observed in the blue trace. Nevertheless, the critical issues encountered in this configuration are not finished yet, another at a conceptual level error is shown in *Figure 3.28*.

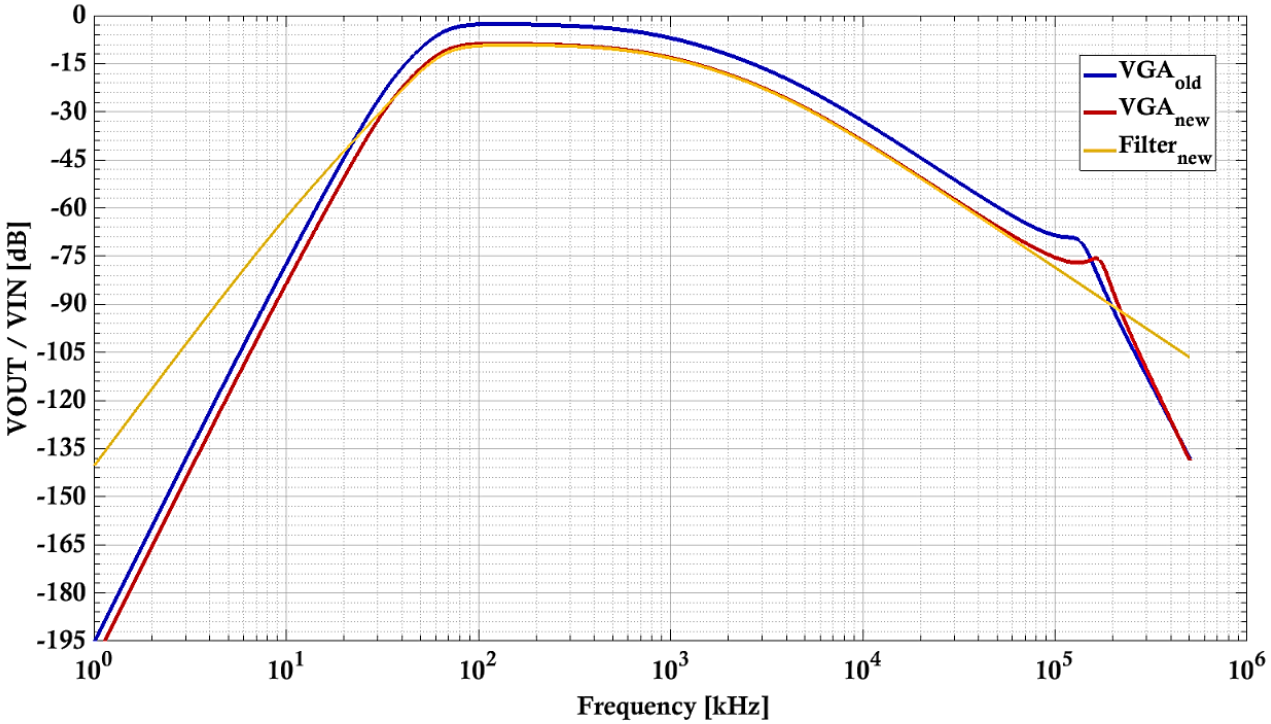

Figure 3.28: Comparison of old vs new frequency response

In fact, the graph compares the old post-VGA frequency response (in blue) and the new one (in red), always referring to the unity gain, while the yellow trace refers to the response of the new filter. It can be observed how, in the old configuration, the post filtering signal is not taken into consideration as a reference on which to calculate the gain of the stage. Conceptually this is extremely inconvenient, because a small change in the filter band or the use of a different measurement impedance is enough to completely redefine the voltage levels for the control of the variable gain amplifier (VGA). This does not occur if the signal following the filtering stage is taken as a reference, in this case variations in the filter or in the measurement impedance do not involve a new tuning of the system, a characteristic that makes it extremely flexible. From this point of view, the new circuit configuration makes the system suitable for use as a commercial tool and very flexible. Compared to the previous *Figure 3.27*, the

new situation is shown under the same conditions in the following *Figure 3.29* and, with different conditions, in *Figure 3.30*.

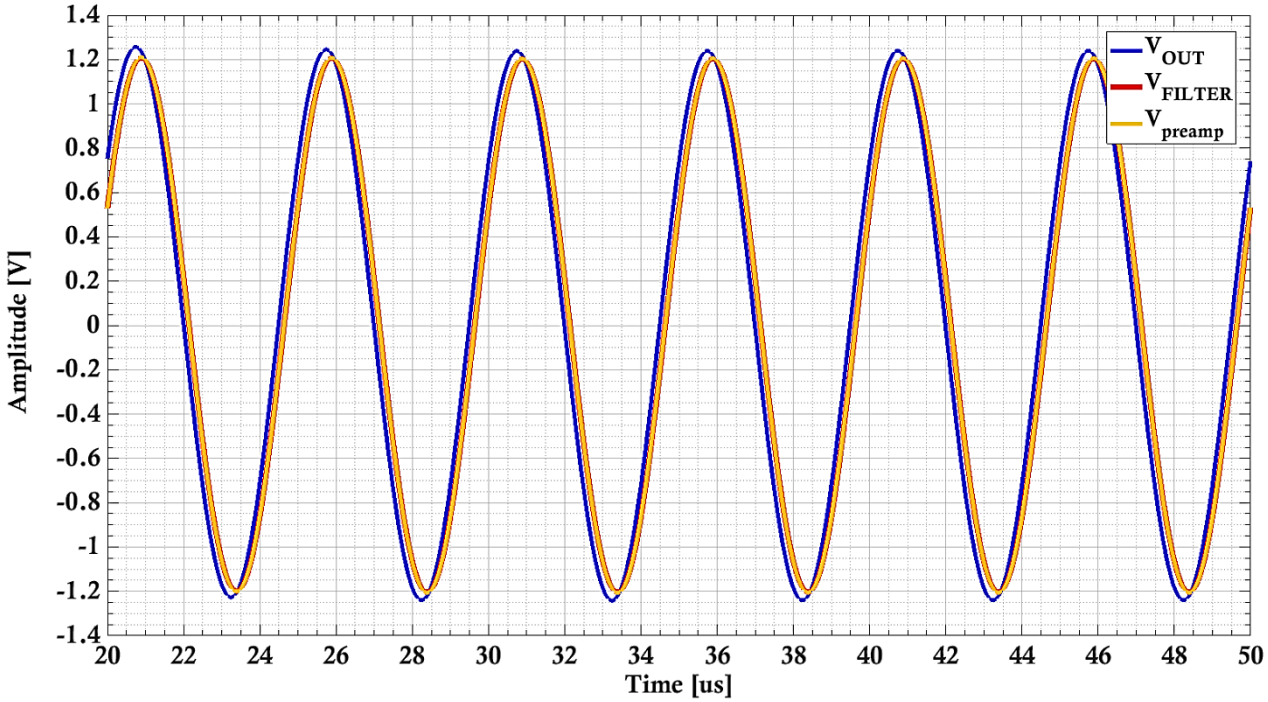

Figure 3.29: Time simulation with suitable configuration – Case I

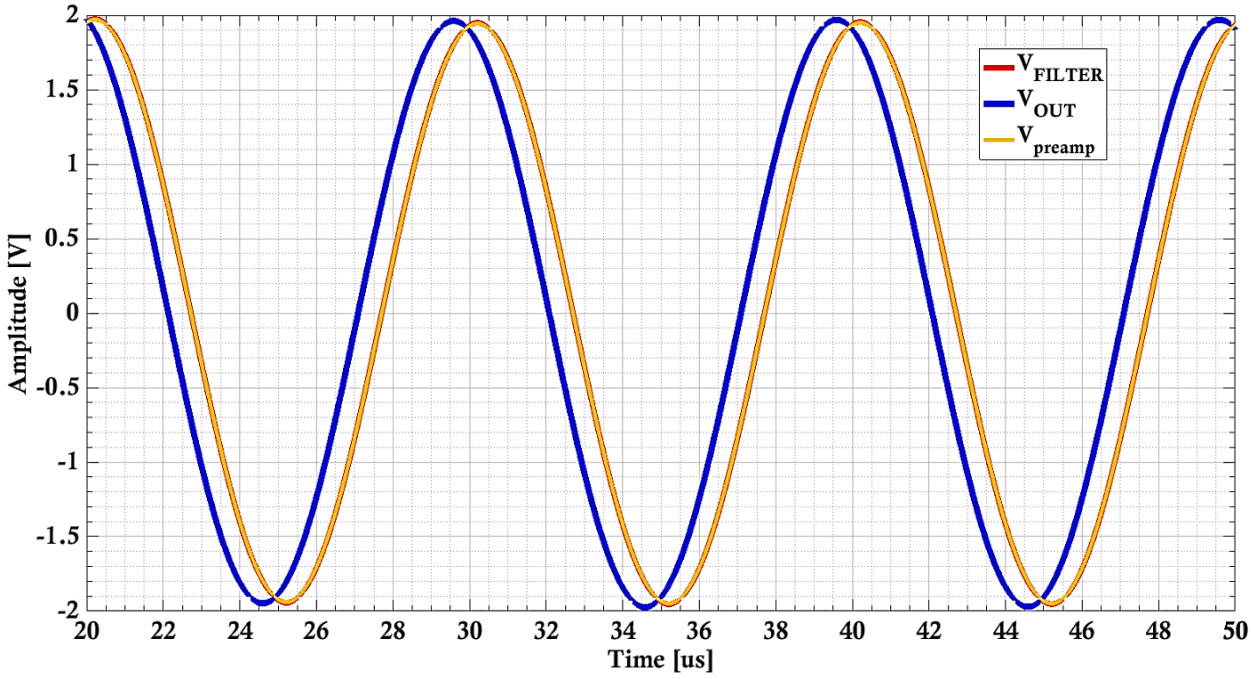

Figure 3.30: Time simulation with suitable configuration - Case II

In both graphs it can be seen that the signal relating to the preamplifier output (yellow trace) is completely overlapped on the one present after the filter (red trace). Same thing can be said for the blue trace, relative to the system output, except for a small and irrelevant temporal phase shift. Obviously, it can be seen that, under the same conditions as the previous one, no saturation and distortion of the signal occurs in this configuration, confirming what was said previously.

Following this, simulations were carried out at the time level (see *Figure 3.31*) and for the frequency response (see *Figure 3.32*) as the gain values changed, which confirmed the correct operation of the designed system.

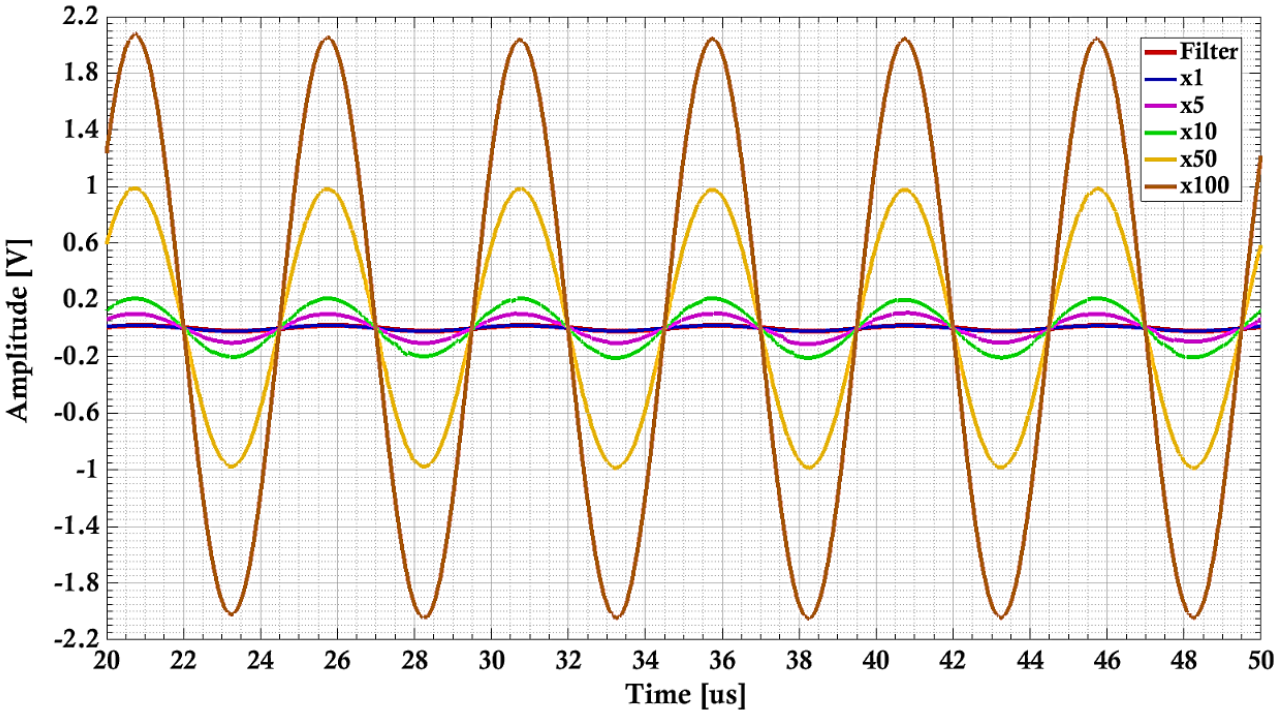

Figure 3.31: Time graph to change gain values

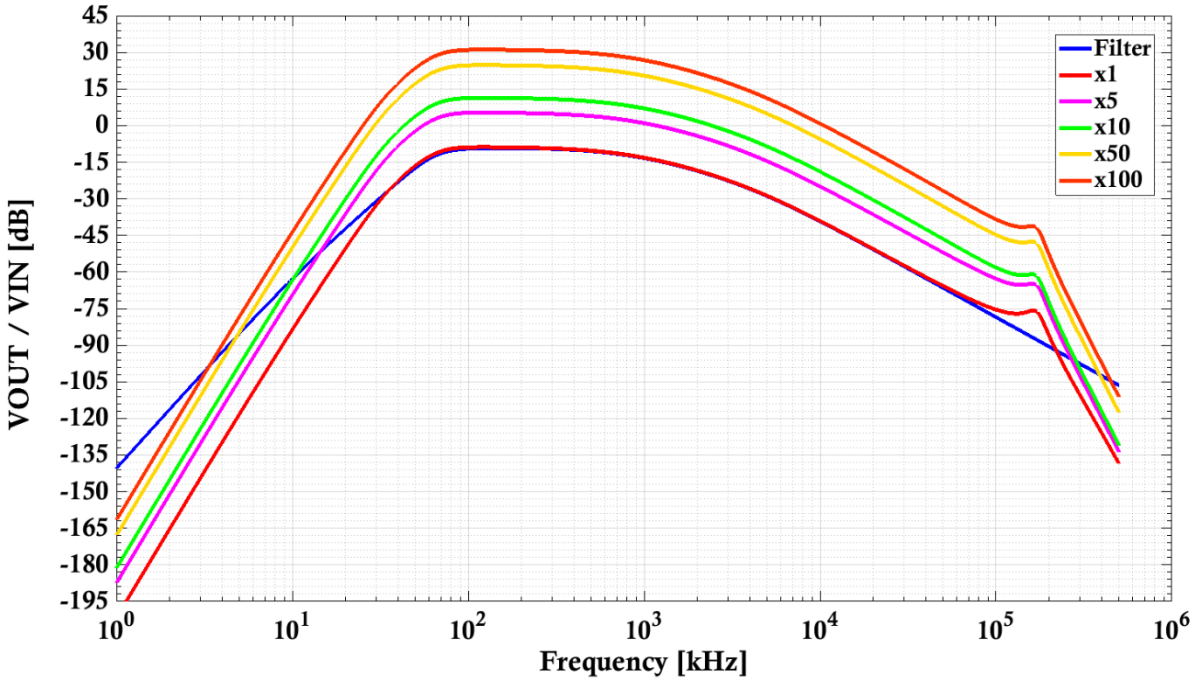

Figure 3.32: Frequency response to change gain values

From the first graph, it can be observed that at the level of gains the expected amplitude values are correctly respected, confirming the correct linearity as the gain changes. Instead, for the second graph it can be seen how the expected gain level is respected in the passband and how the desired band, set by the filtering stage, is maintained.

Finally, it is specified how similar and efficient results have been attenuated in the case of the HF band version, although they will not be reported here.

3.5 PCB: SolPre-SolCon design and realization

Having confirmed the correct working of the circuit at the simulation level, it was possible to proceed with the design of the PCB layout and the realization of the devices. As mentioned previously, the main precautions concerned the circuit section relating to the power supply, while for the other parts the main ones concerned the physical positioning of the digital electronics on the board, the definition of a flexible filtering stage (based on the type of filter to be mounted) and placement of

components, especially to achieve a compact design. The following considerations obviously refer to the two main boards made, but in general also to those attached to the system. As for the digital electronics, it has been appropriately positioned so as to remain separate from the analog parts and therefore avoid possible interference. In this regard, *Figure 3.33* shows the layout made in which the main parts of the conditioning board are highlighted, also with reference to what has been said about digital and analog electronics, referring to the Top layer.

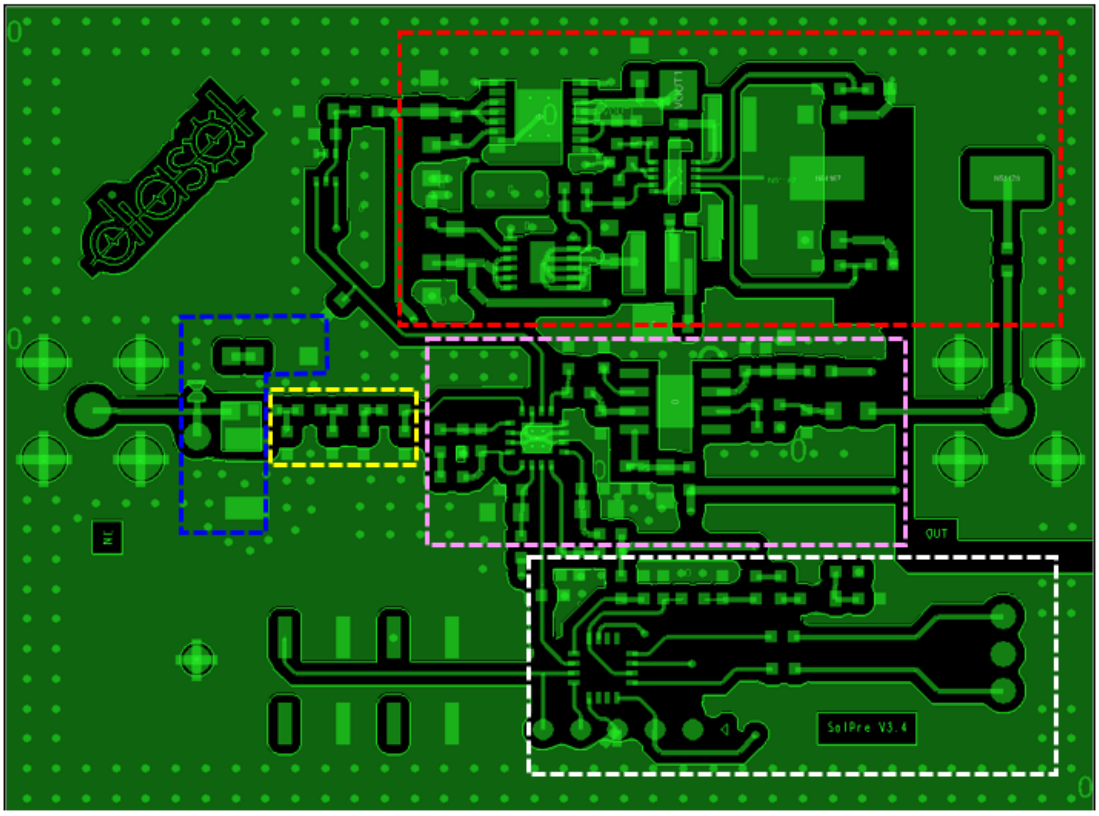

Figure 3.33: Conditioning board - Top layer

In the previous image are identified with a blue box of the protection section, the filtering in yellow, that of amplification in pink, that of power in red and finally in white that relating to digital electronics, which is the logic circuit.

As far as the filter is concerned, a flexible configuration has been prepared, which allows, if it is possible to use different passband than those mentioned, to simply mount the new designed filter, eventually reducing the number of components and therefore the order of the filter. The maximum order is obviously limited to that of the

filters adopted in this activity because it is considered the most suitable. Finally, with regard to the placement of all the components, it has tried to make boards as compact and small as possible, also to lower even if the measures reduced costs, obviously with the limitations of the case. Furthermore, it was necessary to consider the packaging of the boards and then take into consideration the placement of the connectors and the LED in order to make them available on the panel. To limit costs, prefabricated packages have been adopted, without therefore having to exceed in customizations that raise the price, which among other things turns out to be proportionally higher than that for the production and mounting of a board. *Figure 3.34* shows a detailed image of the placement of components at the layout level.

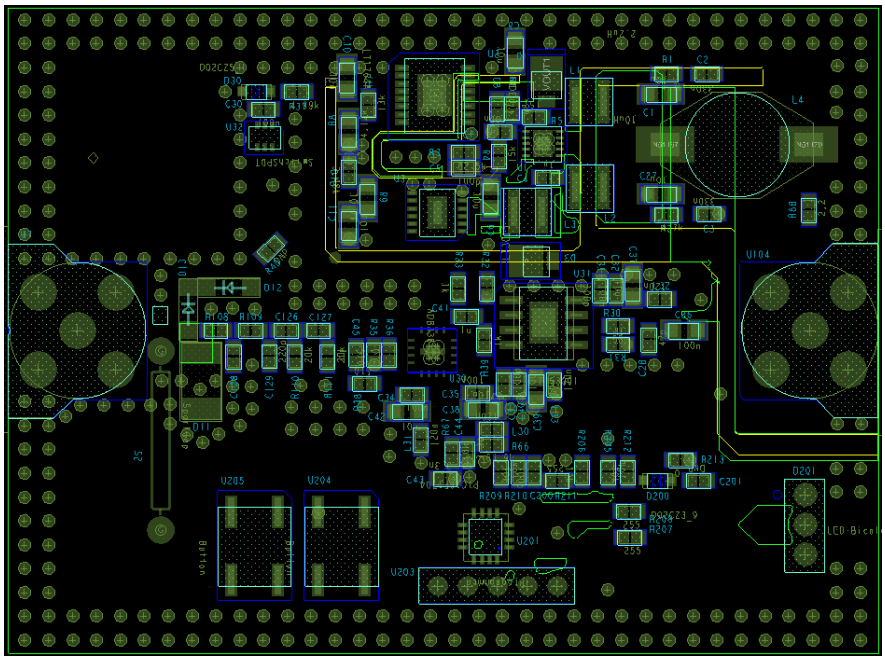

Figure 3.34: Conditioning board - Component placement

Another important aspect concerns, as also explained during the discussion of the power supply system, the creation of a suitable ground plane that allows to have correct paths for the drainage of the currents to ground, what has been achieved for the Bottom layer is shown in *Figure 3.35*.

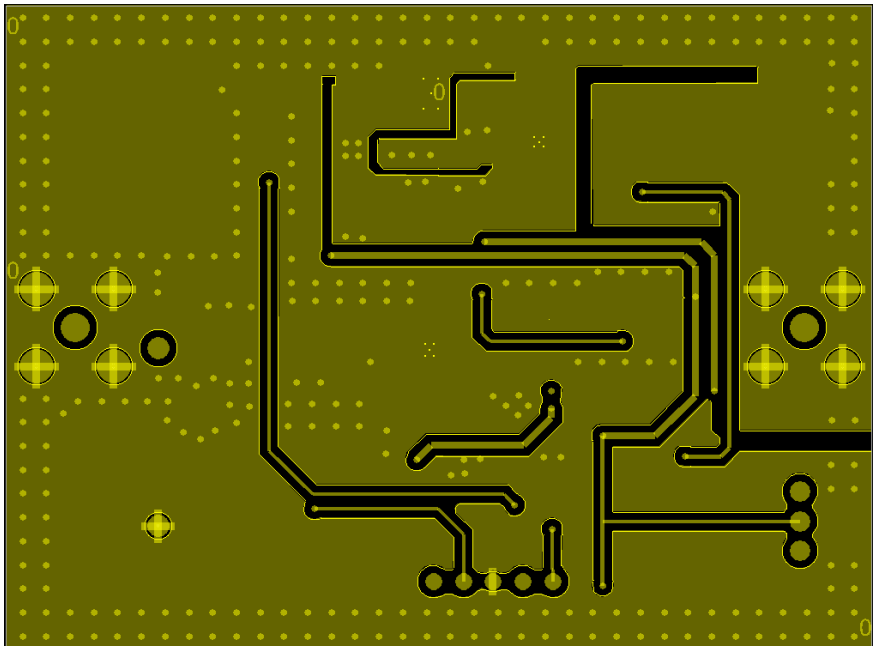

Figure 3.35: Conditioning board - Bottom layer and ground plane

Finally, *Figure 3.36* shows the complete and final layout of the conditioning board.

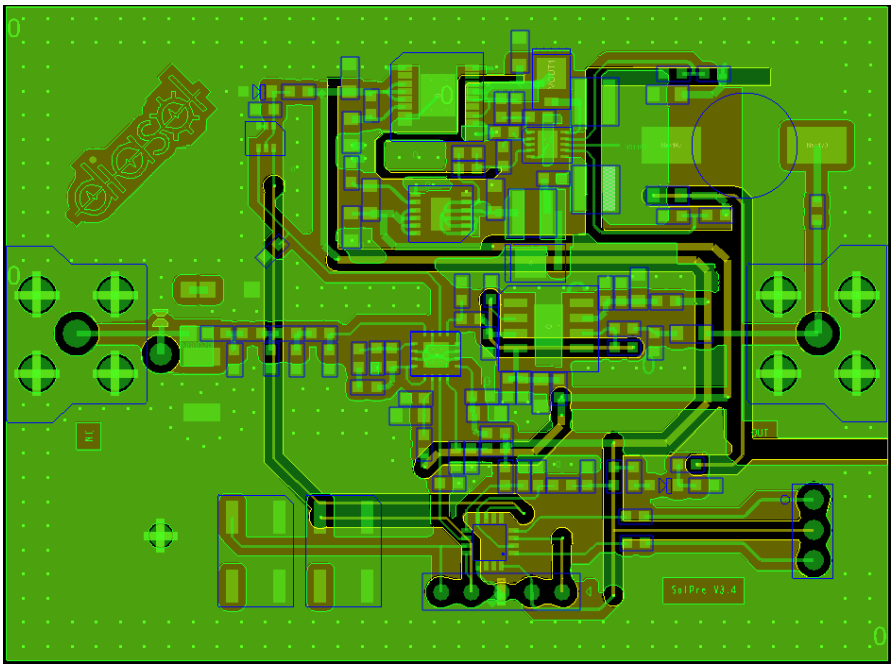

Figure 3.36: Conditioning board - Complete layout

Similarly, the same considerations can be made for the control board and the images relating to the Top layer (see *Figure 3.37*), the Bottom layer (see *Figure 3.38*) and the complete layout (see *Figure 3.39*) are shown below.

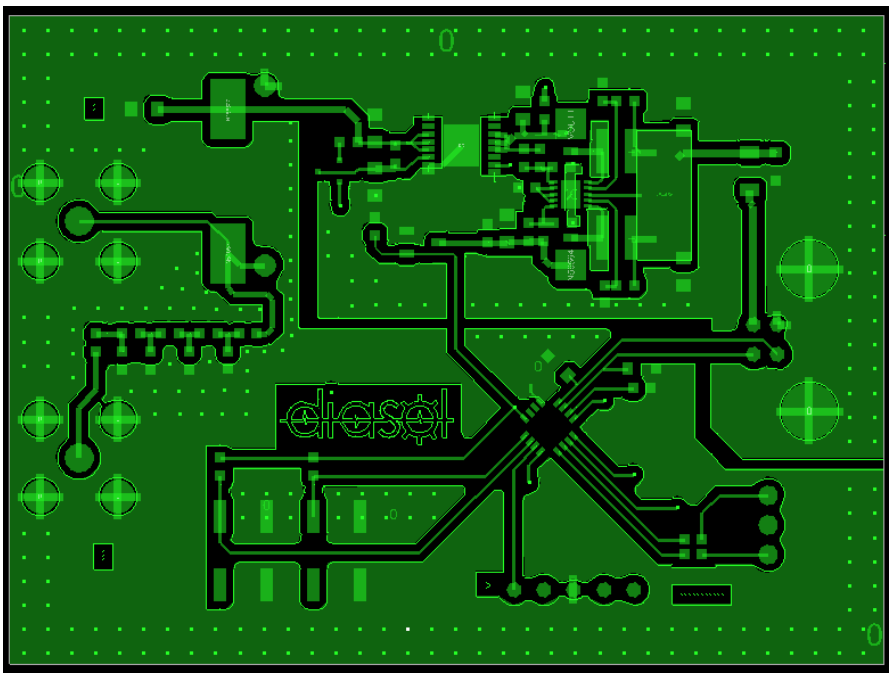

Figure 3.37: Control board - Top layer

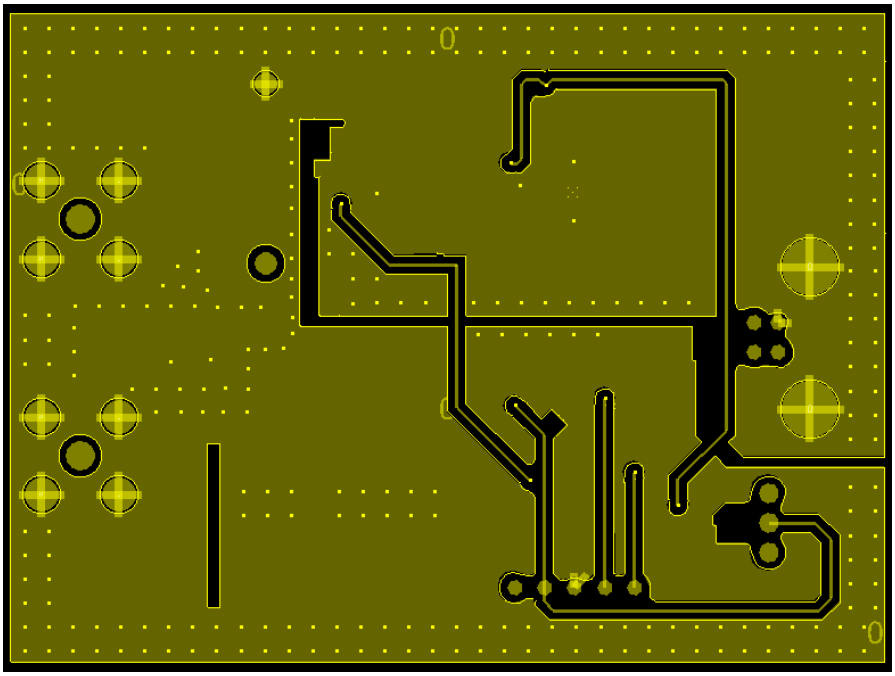

Figure 3.38: Control board - Bottom layer

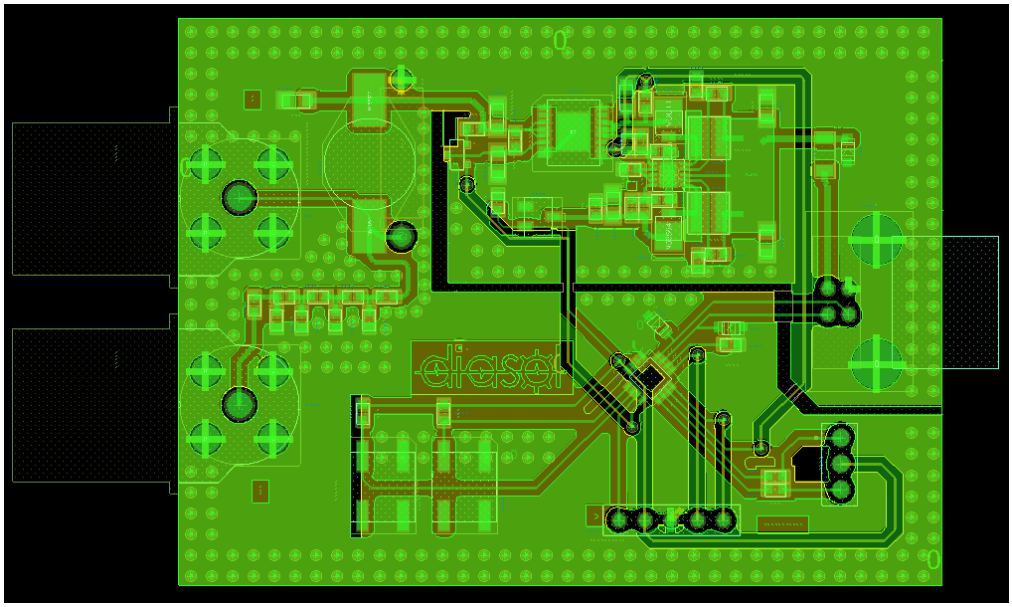

Figure 3.39: Control board - Complete layout

A further aspect of the design also involved the insertion of the silkscreen layers and those relating to the soldermask, as well as the generation of all the files useful for printing the boards and for any mounting machine. Following the design of the PCB layout, the necessary files were generated, including the Gerber, for the manufacturer of the printed boards for the realization of these. At the moment all the devices available (in the order of tens of pieces) for these boards have been mounted manually, but for the future an assembly on a larger scale using machinery is already planned. An example of a board created is shown in *Figure 3.40* for the conditioning board, defined as SolPre, and in *Figure 3.41* for the control board, defined as SolCon.

Figure 3.40: SolPre board

Figure 3.41: SolCon board

Both boards have a dimension of 74mm x 55mm, so as to be suitable to the chosen package. For the SolPre it is guaranteed the degree of protection IP65 [30] with connected connection cables, since the use in industrial area, or in any case in difficult environments, with dirt and the possible presence of water or other liquid substances. Instead the SolCon board does not have such stringent requirements as it must be used near a PC and an oscilloscope, therefore in a more controlled environment. Since packaging was also considered during design, the packaged boards are shown in *Figure 3.42*.

Figure 3.42: Packaged boards

3.6 Switch board

To complete this global vision of the system, at the circuit and PCB layout level, it can be noting the presence of an additional board which is part of the overall system. This is what is defined as Switch board in the diagram of Figure 3.1, defined ad SolSwitch. As regards the functional tests of the board, since it was developed previously and in this activity, there were only partial changes to the geometry of the board, traces and in the firmware, without changing its behaviour, those already performed are considered as such and consider as established this board. Its task is to select different measurement lines if the measure of partial discharges on different points of the same equipment or on several different machines, up to four, is required. The mechanism on which it is based is substantially simple, it has 4 relays V23079 [31] on board, controlled through a PIC microcontroller with USB interface in use combined with a relay driver MAX4896 [32]. As in the case of the control board, the commands are sent via a PC to which the switch board is connected via USB. The microcontroller in question, PIC16F1454 (the same adopted for SolCon), supports a USB interface so it is sufficient to read the data received on it and interpret it. The commands received simply concern the selection of the channel to be selected for the measurement. Also, in this case a bicolour LED returns feedback information for the user, in fact based on the number of green flashes, the corresponding channel selected among 1, 2, 3 or 4 is identified. A red flash indicates the reset of the board (and therefore the selection of the default channel number 1), instead, two red flashes indicate the receipt of an invalid command. The firmware as for the other two main boards was then loaded using a specific ICSP (In Circuit Serial Programming) programmer. During this research activity, the software was developed in the parts and changes were made in terms of layout, starting from previously designed solutions. In fact, as for the design of this board, the design was the result of previous study activities, so it will not be in-depth, but for completeness a generic schematic is shown in *Figure 3.43*, while in *Figure 3.44* it can be observed the detail of the logic section.

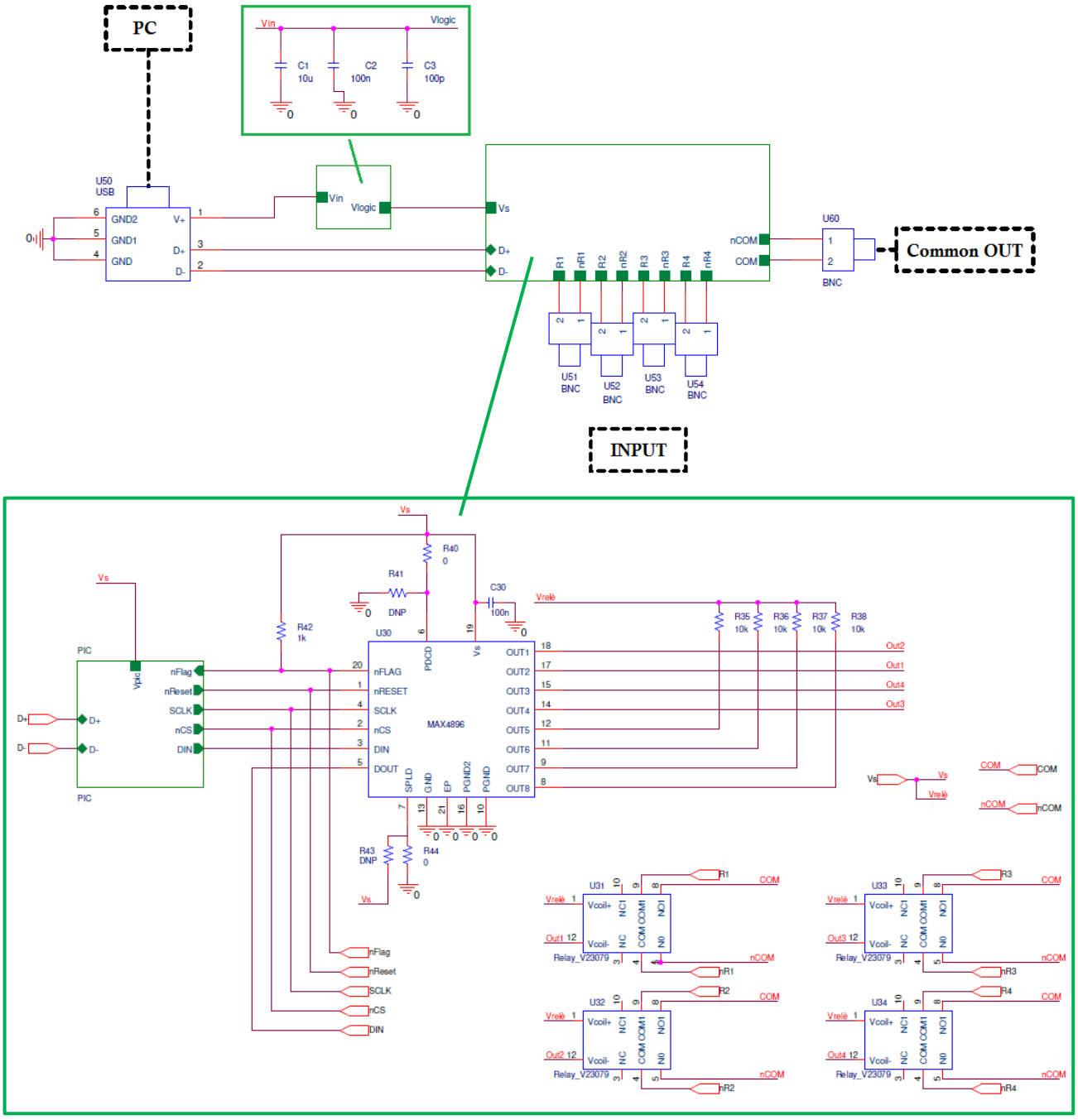

Figure 3.43: Generic SolSwitch schematic

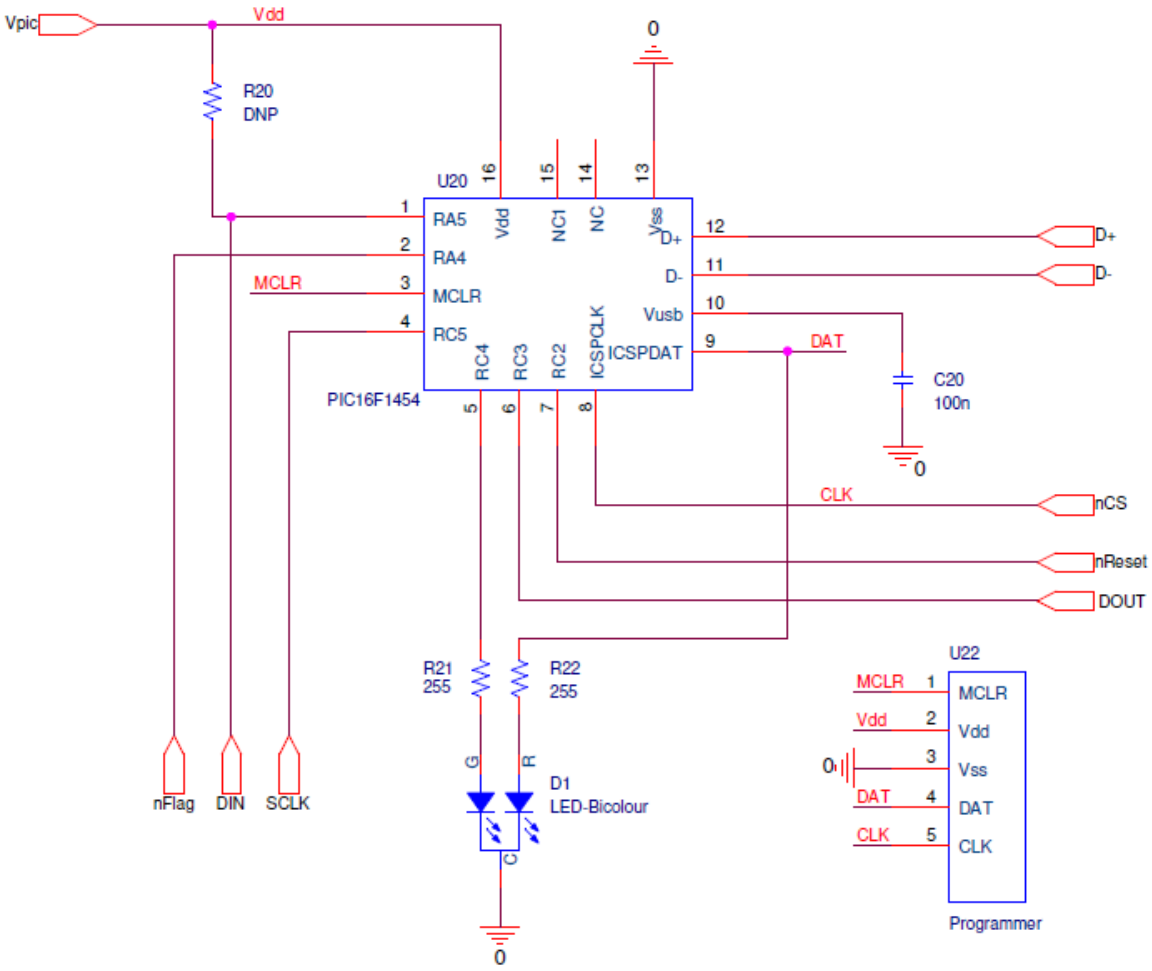

Figure 3.44: Detail of logic circuit for SolSwitch

At the PCB layout level, the main constraint concerns the size of the relay board, based on the size of the metal package. As can be seen in *Figure 3.45*, the dimensions are 80mm x 100mm. Another constraint in these terms is given by the input connectors, these are four isolated BNC connectors, which must be positioned sufficiently far apart to allow easy connection of the cable to the panel. However, with these exceptions, the positioning of the components is not critical, as the board is much larger than the number of components inserted on board. It is only necessary to have a special consideration when tracing the traces, in order to avoid crossings between signals with different characteristics, thus limiting interference phenomena between the channels. What has been said and in general the entire layout can be observed in the following *Figure 3.45*.

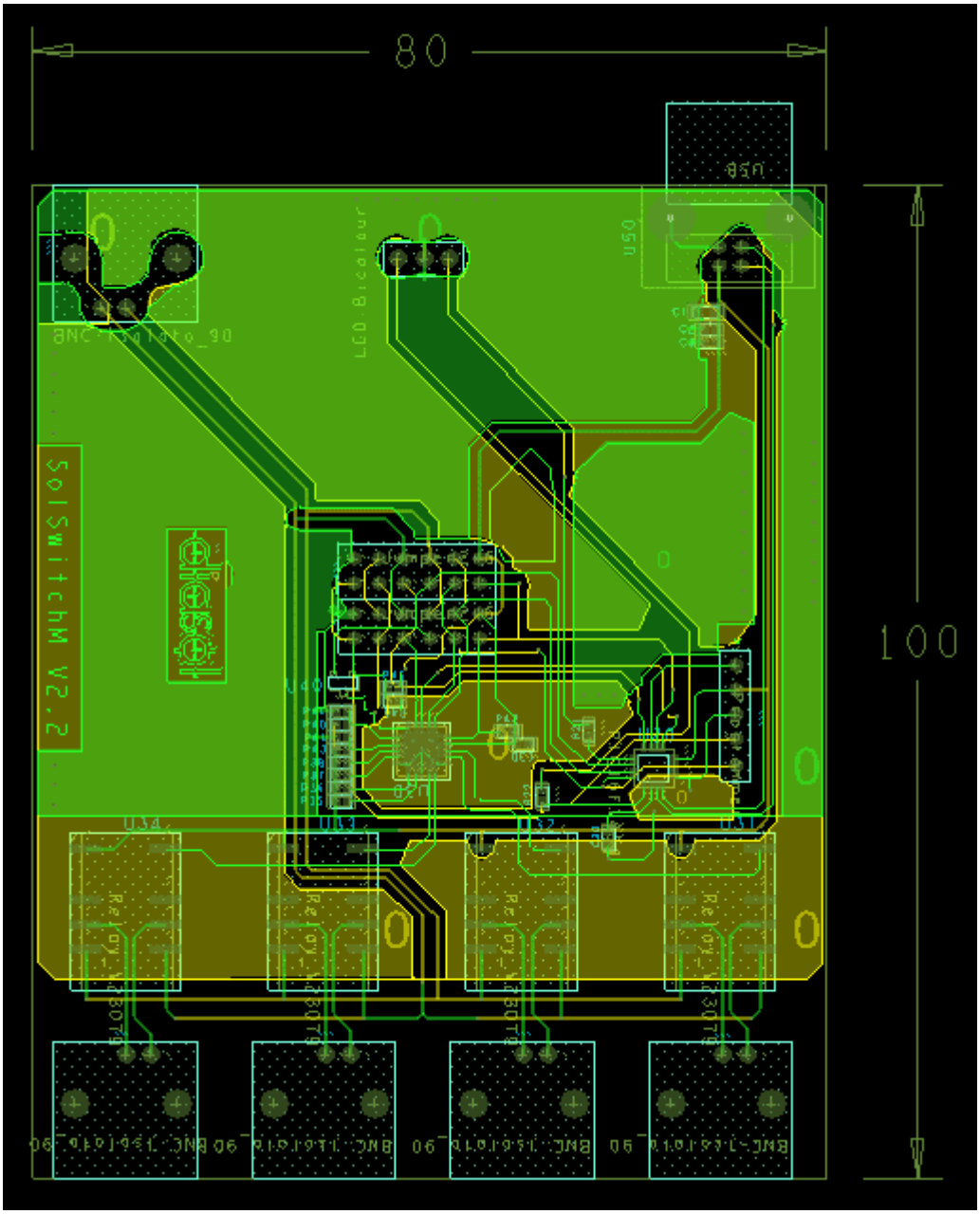

Figure 3.45: SolSwitch PCB layout

Finally, in *Figure 3.46*, the board assembled and complete with all components can be seen at the top, while the packaged version at the bottom.

Figure 3.46: SolSwitch board and package

3.7 Complete system and real measurement

In order to ensure validation of the devices created and, especially, for the tuning of the analog values for the adjustment of the variable gain values, the circuit configuration outlined in *Figure 3.47* was used.

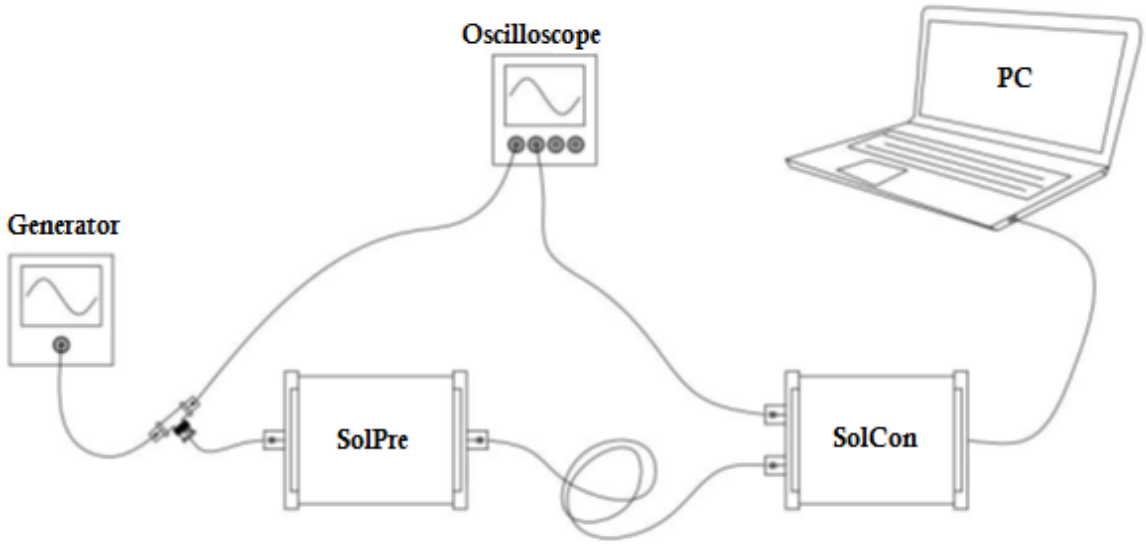

Figure 3.47: Tuning test circuit

Through a function generator a sinusoidal signal is injected with a frequency attributable to the passband and known amplitude. Through the calibration of the gain parameters via firmware, the input and output signals are displayed on an oscilloscope, verifying that the amplification level is respected. In this regard, following *Figure 3.48, 3.49, 3.50, 3.51* and *3.52* show the signal acquired by the oscilloscope, which represents the situation just described, in the different cases of gain. The oscilloscope used for these tests, but in general for each acquisition, is the LeCroy WaveJet 300A [33]. The first three graphs refer to an input with an amplitude equal to 400mVpp and a frequency of 300 kHz and report the output signal obtained to the system after the appropriate tuning phase. While the fourth and fifth graphs refer to an input with an amplitude of 40mVpp and a frequency equal to 300 kHz. The difference between them is simply due to the different set gain value, which for high values allows to amplify only small signals without obtaining system saturation effects.

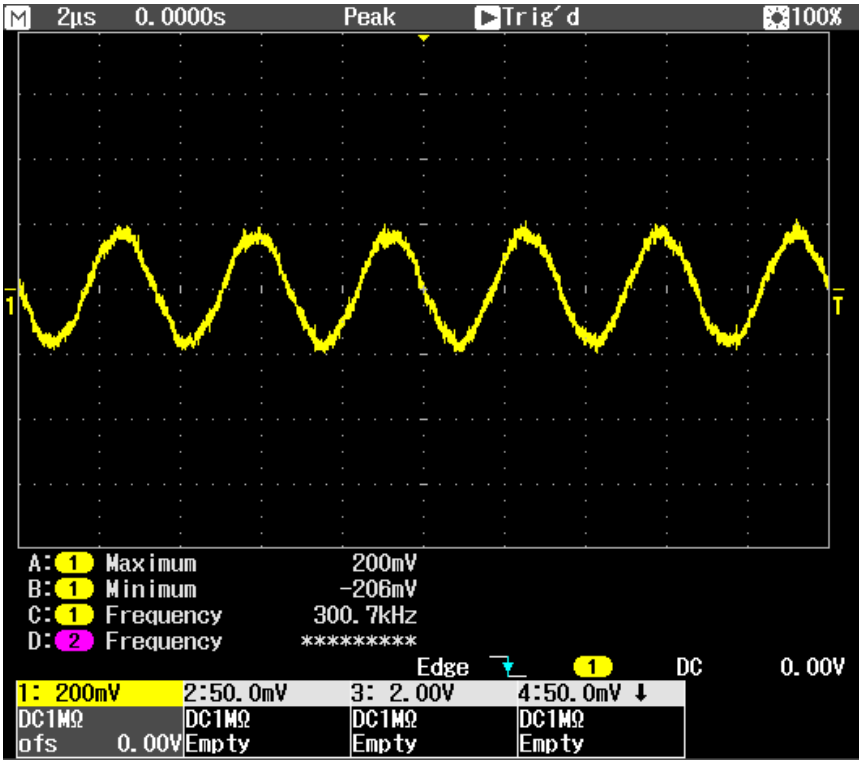

Figure 3.48: Gain = 1 - Measurement after tuning

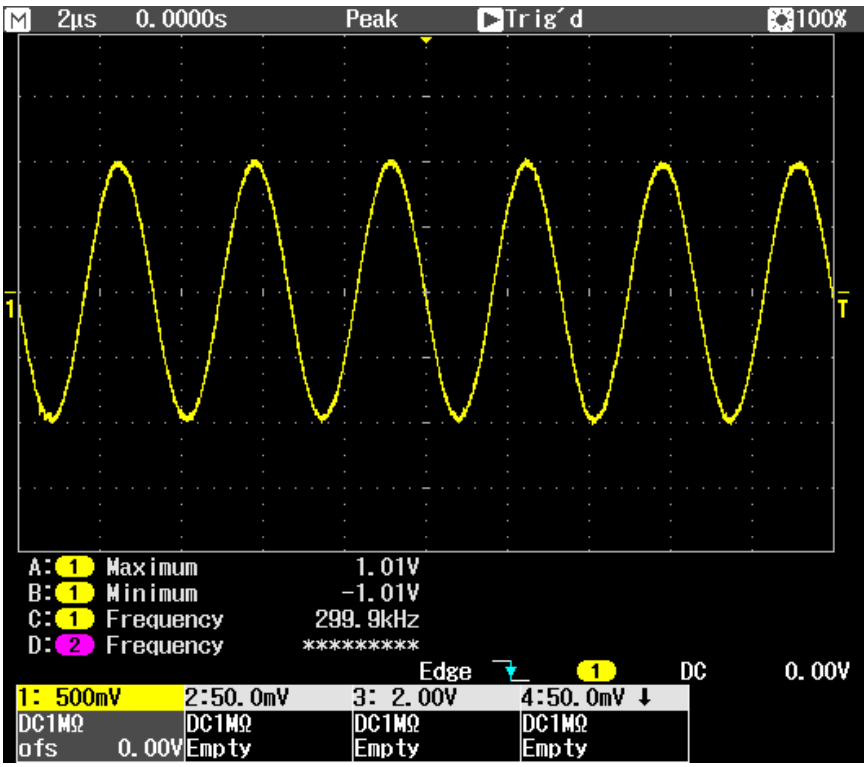

Figure 3.49: Gain = 5 - Measurement after tuning

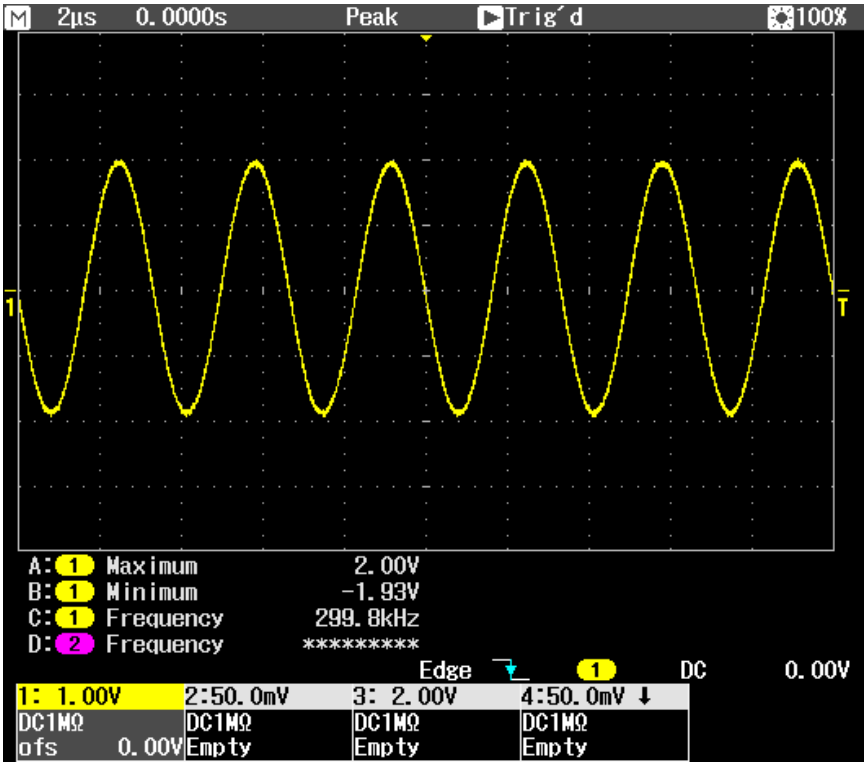

Figure 3.50: Gain = 10 - Measurement after tuning

It is observed that for the first three graphs the linearity is correctly maintained as the gain varies, as well as the signal frequency and there are no signal distortions. The same is obtained in the remaining two graphs, for gain values respectively equal to 50 and 100.

In these two cases it is necessary to pay close attention to the tuning values set, because it can be easy that by increasing too much it can risk saturating the signal, but if they are lowered too much it is possible that it is not amplified enough. At the same time for the gain 100 an incorrect tuning would risk never reaching this level of gain, since it is close to the maximum limit supported by the components combined and used together in the amplification chain.

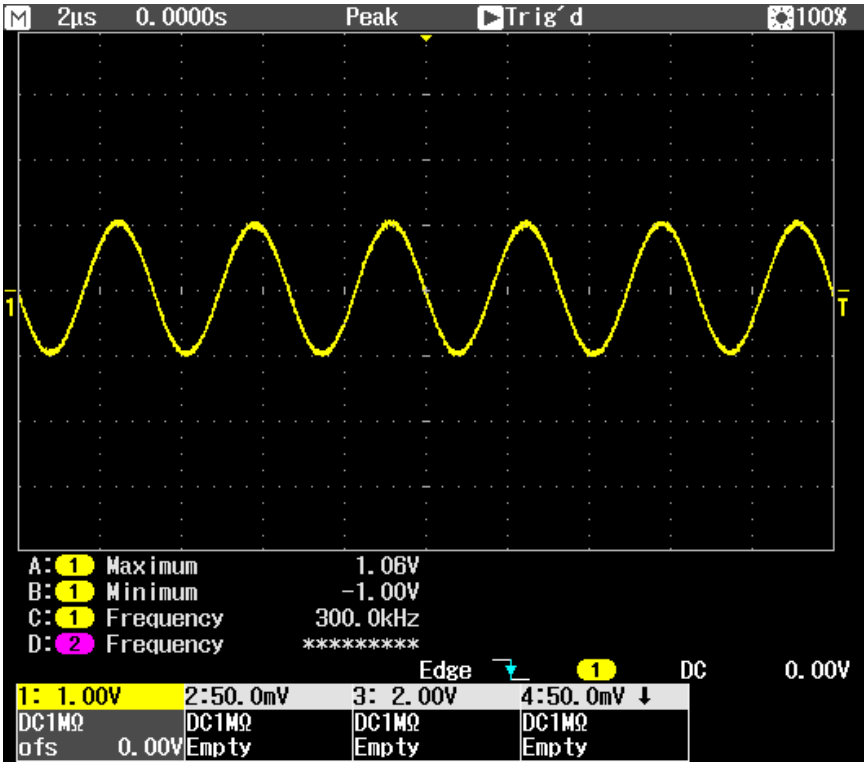

Figure 3.51: Gain = 50 - Measurement after tuning

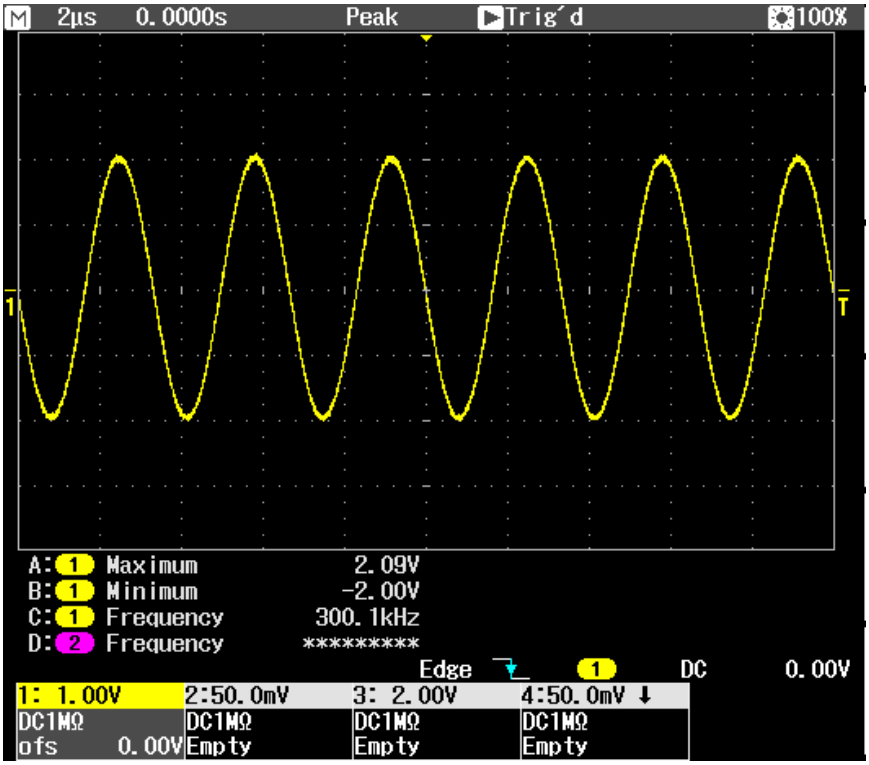

Figure 3.52: Gain = 100 - Measurement after tuning

Having verified the good linearity of the gains and the correctness of the amplification parameters, it can proceed to test the operation of the system within a classic measurement situation, which is associated with the circuit of *Figure 2.8*. Specifying that reference is always made to the LF version, even if similar results were also obtained for the HF, proceed with the verification of the operation of the system in the presence of overt discharges. Obviously, the discharge activity also depends on the voltage applied to the test object, which in this case is a twisted pair specimen like the one in *Figure 3.53*, and on type of supply voltage, in this case a 50 Hz sinusoid.

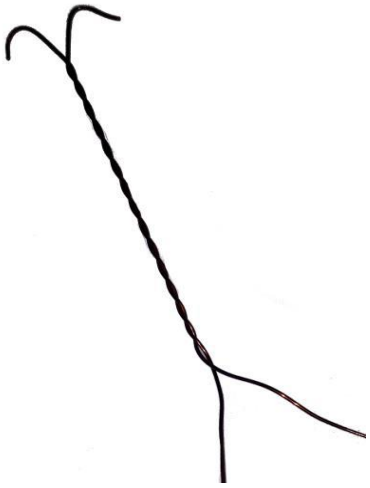

Figure 3.53: Twisted pair specimen

The tests reported below do not want to focus on aspects concerning the test voltage applied or other details in these terms, but to highlight a correct response of the system to discharge signals. Obviously, the other aspects have also been verified, such as the ignition voltage, the applied voltage levels and other relevant elements but given the discussion and the context relating to signal electronics, everything will be focused on these terms. The results obtained as the gain value increases and as the voltage level applied to the specimen decreases (the precise values in this context have no relevance). In *Figure 3.54* it is possible to observe the measurement, carried out with gain system equal to 1, in a wide time interval, while in *Figure 3.55* a detail of a single discharge.

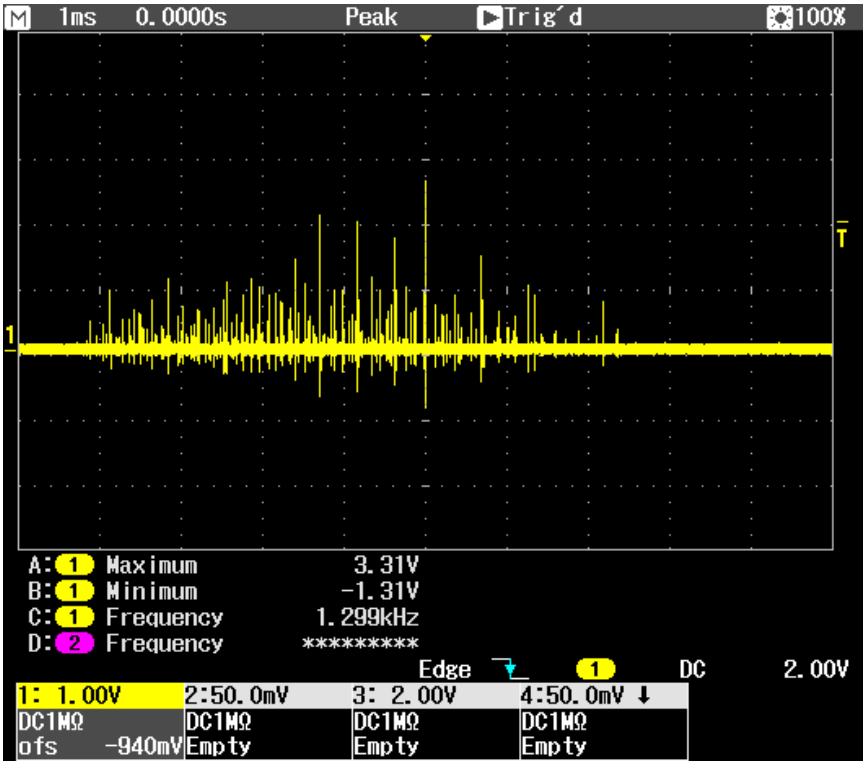

Figure 3.54: Gain = 1 - PDs measurement

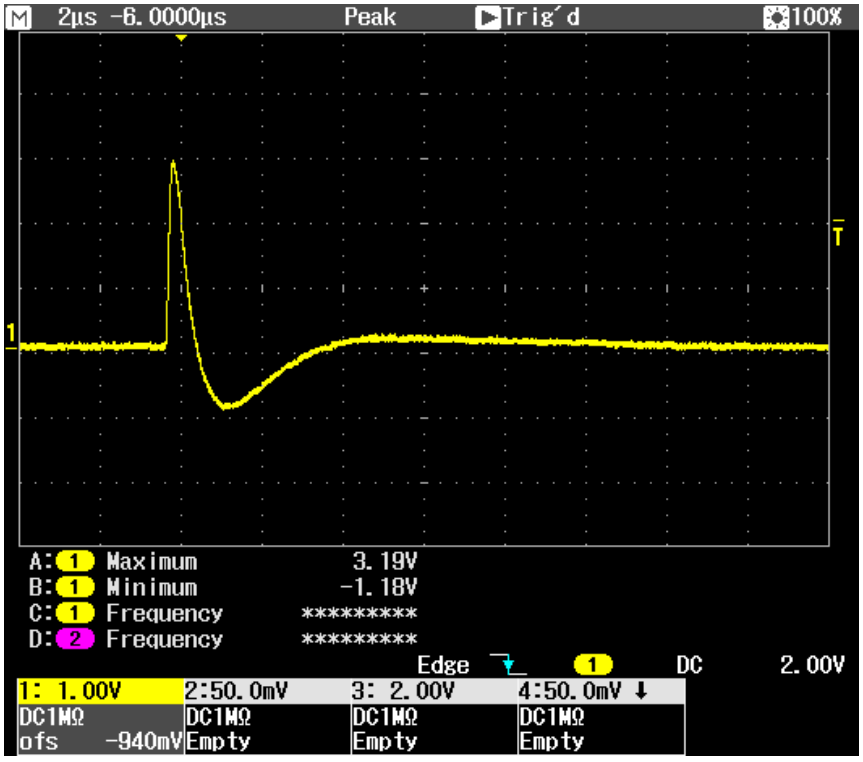

Figure 3.55: Gain = 1 - Detail of partial discharge measurement

From this last graph it can be observed that the temporal duration of the discharge is in the order of tens of microseconds, respecting the indications of the IEC-60270 standard. Furthermore, it is observed that a maximum voltage level very close to the limit of the component is reached, without distorting the signal. Returning to analyze the situation as the gain increases and the test voltage level decreases, an example useful for comparison can be observed in *Figure 3.56*.

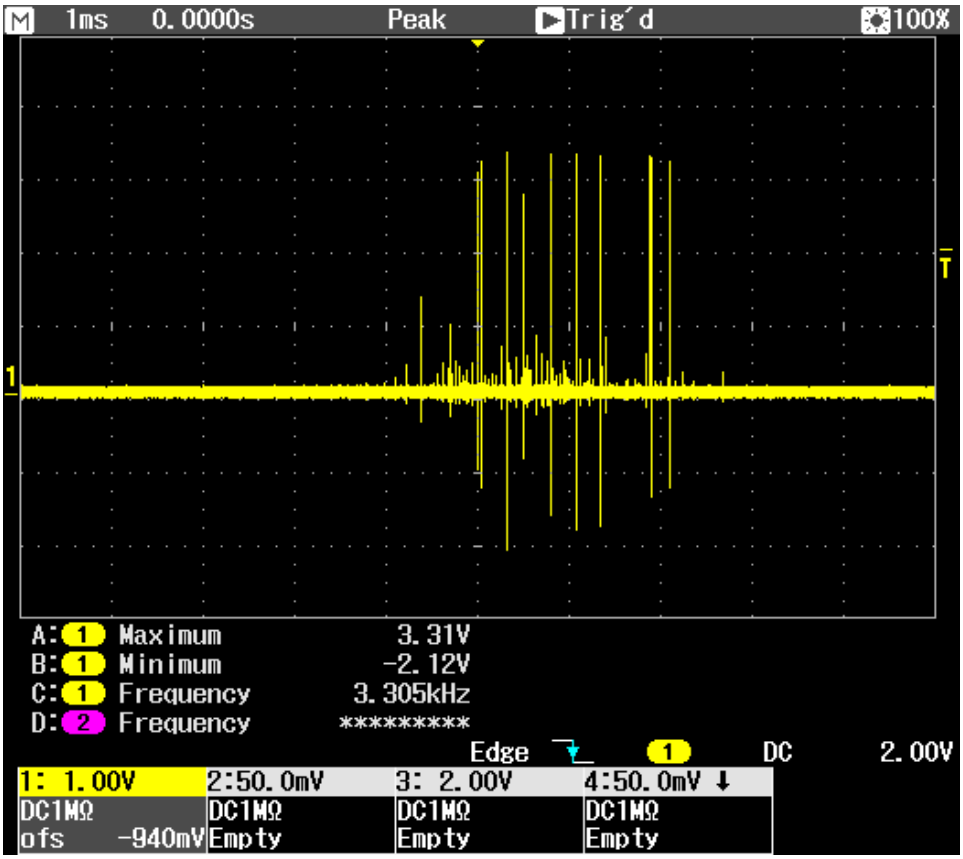

Figure 3.56: Gain = 10 - PDs measurement

For the comparison with the analogous previous wide time graph, it is necessary to take into consideration that the level of applied voltage is dimmed in the last case as a result of a gain which instead has increased tenfold. It can be observed that the number of discharges with an amplitude close to the maximum level has naturally increased, despite the fact that the applied voltage has decreased. This is obviously due to the increase in gain which allows us to have even greater discretion in the

measurement, allowing us to better visualize discharges that previously could have been "hidden" because they were too small in amplitude to have discretion.

Another aspect to consider is the possibility of having greater precision in the identification of the ignition voltage. In fact, it is possible to observe how, for the reason just mentioned, by increasing the gain level it is possible to "see" before the start of a discharge activity. A fairly explanatory example is shown in *Figure 3.57*, in which there is a gain equal to 50 and an applied voltage which is a quarter of that applied in the first case.

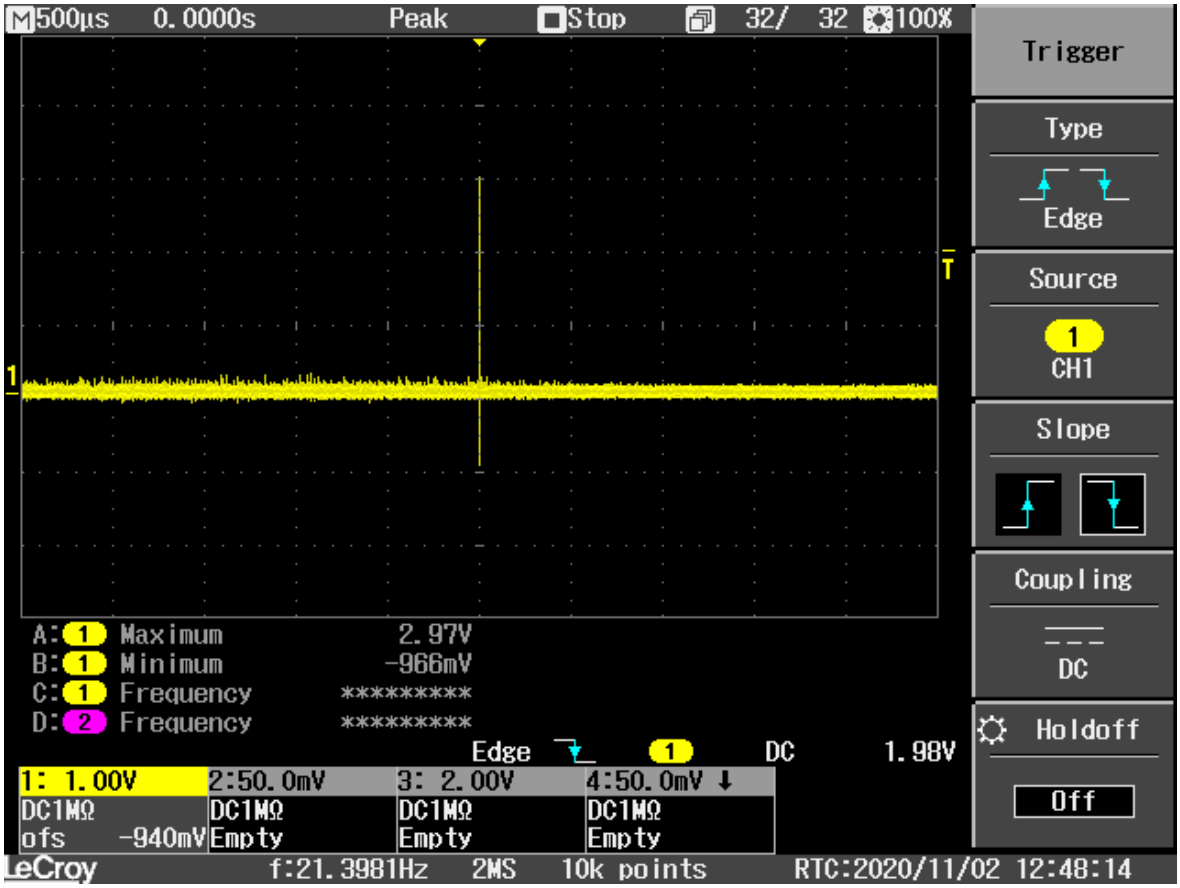

Figure 3.57: Gain = 50 - PDs measurement

From the graph it can be seen how a single discharge is detected and that it has a high amplitude value, even if the level of applied voltage is much lower. At the same time it must be specified that for a correct measurement it is necessary, on the practical side, to find a compromise of gain value, because increasing it too many risks making the system excessively saturated, which would lead to a compromise of the measurement.

It is therefore necessary to find the best compromise in the measurement to discreetly show the greatest number of discharges in a measurement window, without even a small part of them being saturated.

Finally, one last comparison can take place at the same voltage applied on the specimen, by varying the gain of the amplification stage. An overall representation of this situation is shown in *Figure 3.58*. The measurements refer to the gain values of 1, 5, 10 and 50.

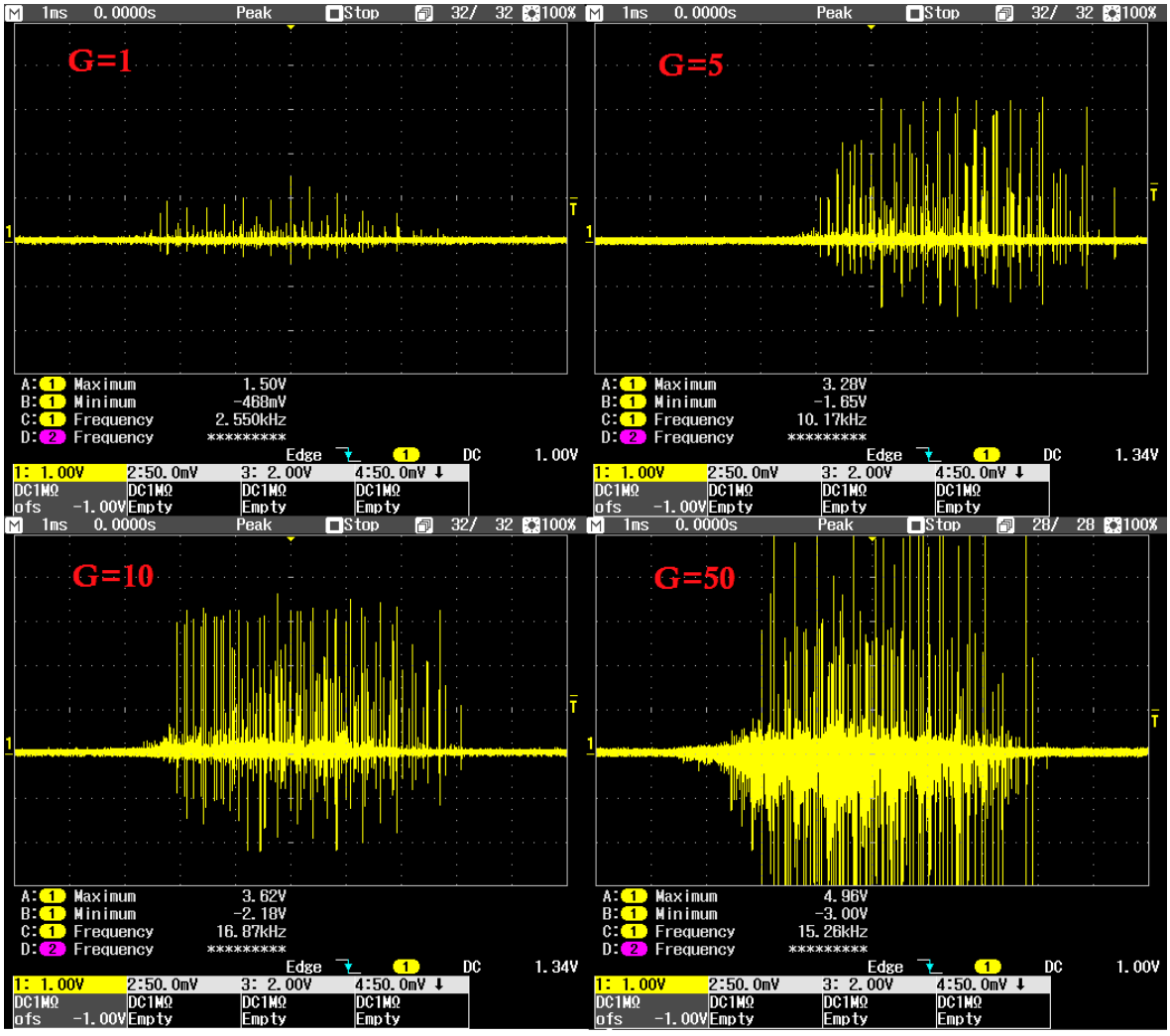

Figure 3.58: Measurement comparison with different gain values

From the comparison graphs it is even more possible to observe what has been described above.

3.8 Possible applications for the developed conducted system

The applications for which the developed system can be used are various, from the simple measurement and analysis of the temporal trend of the discharges based on the amplitude and other parameters by an expert operator, to the creation of PD patterns for identification based on the form of the type of defects always found by an operator or the insertion within a more complex intelligent system that is able, through machine learning algorithms or through statistical approaches [34–36], to obtain automatic information on the status of the machine under test and the type of defect present. Two of the possible and various uses of the system will be analyzed in the following, which in any case are always part of predictive diagnostics on electric machines, whether it is automatic or carried out by an expert technician.
Further discussions may be more related to more theoretical aspects such as the influence of DC [37] in the measurement of discharges or the different measurement situations based on the quantization [38] carried out for the digitization of the measured signal and may lead to the development of further lines of study and other types of applications related to these issues.

3.8.1 Creation of PD patterns for validation and recognition of defects

A possible application concerns the creation of PD patterns, the main characteristics of which have previously been analyzed, to validate the production of particular elements or electrical machines and eventually to recognize defects in order to intervene whenever possible. A particular application example may concern the validation of high voltage resistive divider, of the type shown in *Figure 3.59*.

Figure 3.59: High voltage resistive divider

In this case, during production, these components can incur defects in the insulation or simply dirt or conductive dust can accumulate, leading to the establishment of a discharge activity, which over time can lead to their compromise. To prevent this from happening, before putting into service the components, they are tested in advance, so as to verify that the pC level, found through the creation of the PD pattern, is below a certain threshold and in this way can validate the component. At the same time, it is possible for an expert operator, from the shape assumed by the pattern, to understand what type of defect is present and try to intervene if the problem is easily solved such as in the case of dirt on the contact terminals.

Usually for these validation tests a trend must be provided for the test voltage, in which different voltage levels are maintained for limited periods of time, in order to verify the conditions found in different situations. A generic example of trend is shown in *Figure 3.60*.

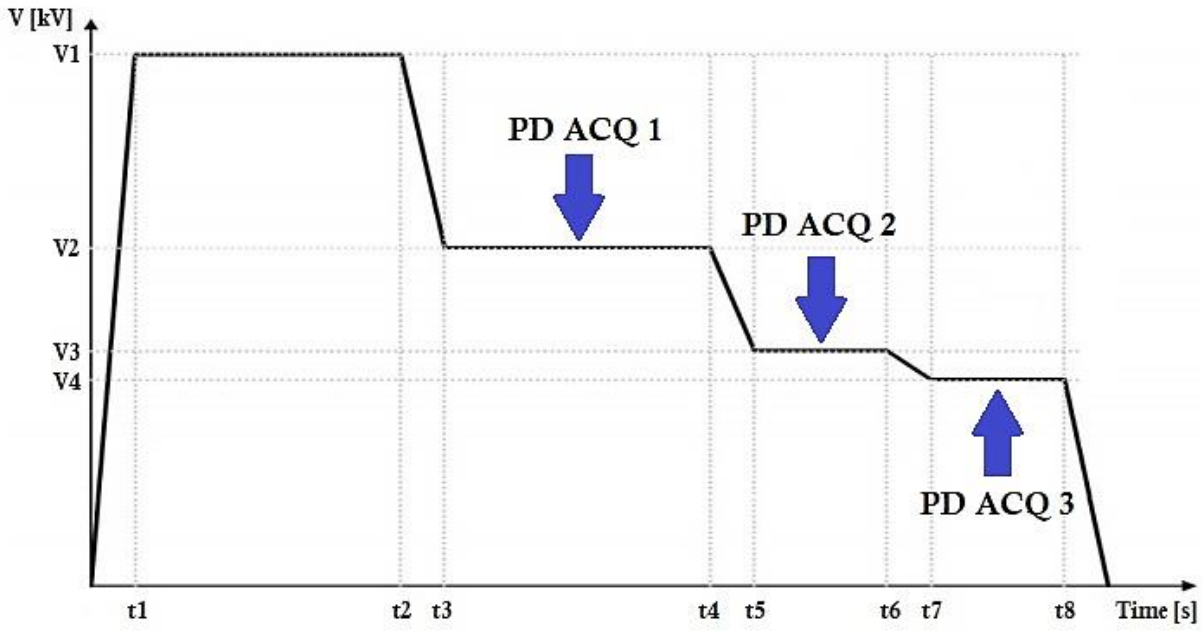

Figure 3.60: Test voltage trend

In the trend it is possible to observe the voltage levels V1, V2, V3 and V4, which are provided directly by the manufacturer's specifications and must be maintained for time intervals of the order of the minute, also in this case as indicated. It should be noted how important is also the time of variation from one voltage level to another, which usually is a few tens of seconds. Normally there is a first step in which the object is conditioned by applying V1, then at time t2 the voltage level begins to drop until reached V2 at t3. In this instant the software acquisition of the discharge signal can begin and once the data has been processed, the same software takes care of the creation of the PD pattern. From the previous graph it is verified with a PD Acquisition, that the threshold level of attention (in pC), defined a priori by the manufacturer for the validation of the component, is not exceeded at the various voltage levels reported (V1, V2, V3 and V4). All this is repeated for the other acquisition steps, depending on how many are required, obtaining as many PD patterns, which will be analyzed in the pC values and in their own shape to obtain the validation. In fact, another relevant aspect in the analysis of the patterns concerns the shape that they assume and depending on which it is, a trained user is also able to understand what the problem may be. In particular, for these specific components, they may be subject above all to partial superficial discharges due to the presence of

dirt on the contact terminals or other defects related specifically to the production, typical of the specific element analyzed, which due to confidentiality constraints (given that the real measurements are been performed on commercial products of a certain company) will not be dealt with. A PD pattern related to a situation with the presence of dirt is shown in *Figure 3.61*.

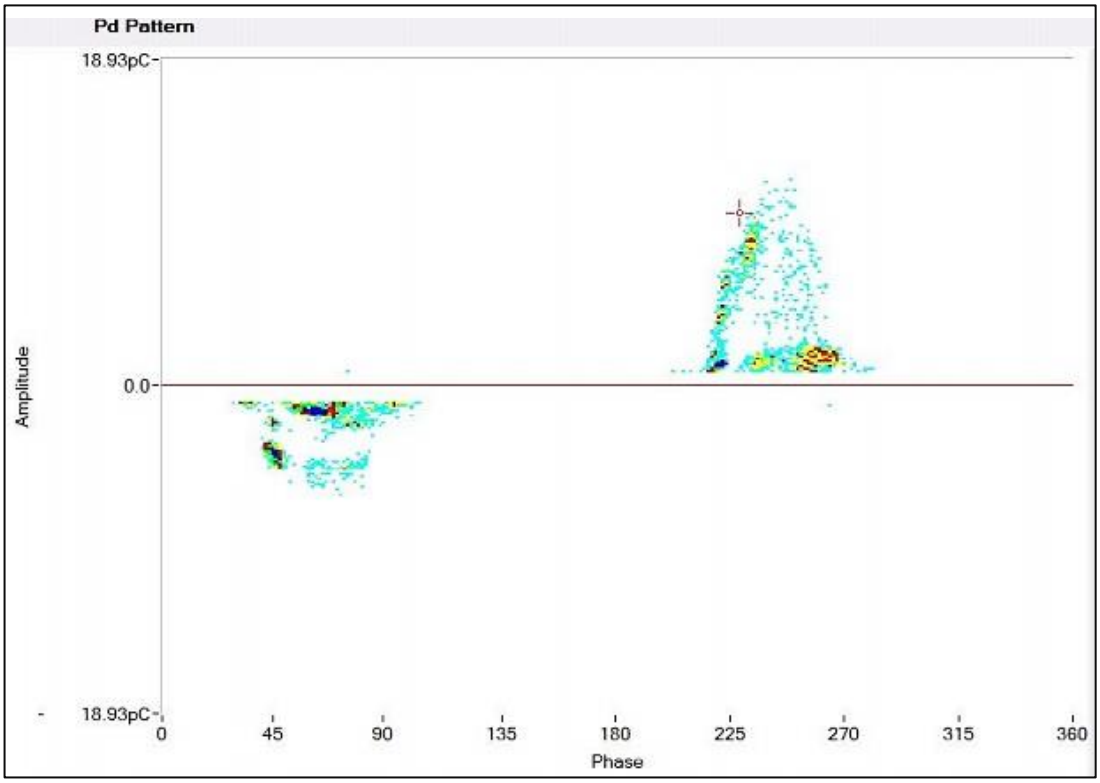

Figure 3.61: Validation application - Example of surface PD pattern

Obviously, a pattern of this type risks compromising the validation of the component, but it all depends on the constraints imposed for passing the test. However, two characteristics of the defect can be identified from the graph. The first concerns the type of discharge, which in this case, given the different densities ("clouds") that are clearly observed in the pattern, is of the surface type. The presence of clouds always indicates surface PD activity. Furthermore, if it refer to the positive half-period, the one that goes from 0° to 180°, and to the negative one, between 180° and 360°, it can be seen that there is asymmetry in the pattern, consistent with type II isolation of the observed system. At the same time, it is observed that the amplitude of charge for the positive half-period turns out to be less than the negative. This allows to identify that

most of the dirt is on a metal terminal, in particular on the ground side because in the positive half-period the electrons of the discharge move from the negative towards the positive.
One possibility, once the defect has been identified, is to try to carefully clean the contact terminal and retest the component for validation. At the same time, with the PD pattern analysis, other specific defects of the component or machine under test can be identified, making this application very useful.

3.8.2 Autonomous intelligent system for predictive diagnostics

Another possible application concerns the insertion of the conducted system within a more complex intelligent diagnostic system. In this context, it is expected a predictive maintenance apparatus continuously monitors an electrical machine to prevent a breakdown in the insulation system [39–42]. Electrical, mechanical and thermal stress sources systematically contribute to deteriorate motors. In the absence of a scheduled maintenance, this can bring about sudden breakdowns, with the consequent significant economic losses. Thus, predictive maintenance is replacing reactive maintenance, as the latter does not prevent motor failures and downtime costs. Predictive analytics relies on the ever-growing availability of reliable Internet-of-Thing (IoT) technologies, to drive the real-time scheduling of specific maintenance programs for the target machine. As a result, an effective predictive diagnostic system should prompt alerts whenever the electrical machine needs fixing to ensure operation continuity. In this regard, a possible application [34] has been studied and a monitoring system developed only relying on an unsupervised approach can support predictive maintenance effectively and the monitoring process does not require any prior knowledge about the observed apparatus. The anomaly detection paradigm drives the surveillance of aging in the insulation system. The system periodically extracts features from PD patterns and prompts an alert whenever the machine exhibits an anomalous behaviour with respect to past history. By the resulting approach one can characterize the status of the insulation system in real time and schedule maintenance operations accordingly. That monitoring approach presents some crucial features. First, it does not depend on either a knowledge base or some training process. Secondly, it is

computationally light since standard statistical tools (such as the Chi-Square test and the Kolmogorov-Smirnov test, not analysed directly in this activity) carry out anomaly detection. In this regard, it is possible to implement a low-cost embedded system. Third, the method can provide a basic module within a comprehensive IoT-based predictive maintenance apparatus. The signals acquired in real time by local monitoring apparatuses can all be collected by a remote database in a central unit, in which occurs an advanced (and computationally heavy) data analysis by means of Artificial Intelligence tools, as further improve the prediction ability of each local monitoring system. To do this, the empirical model presented in [43] has been improved. The strategy adopted is to check at any certain time whether the electrical machine presents some anomalous behaviours with respect to the past. In general, anomaly detection refers to the problem of finding patterns in data that do not conform to expected behaviour [44]. The proposed strategy uses statistical methods to implement anomaly detection [45–49]. These methods rely on the consideration that normal data instances occur in high probability regions of a stochastic model, while anomalies occur in the low probability regions of the stochastic model. Hence, hypothesis testing is exploited: a normal behaviour is fit to the data and then a statistical inference test is applied to determine if new data belongs to the normal model or not.

In this mind, for the acquisition of measurement data, connected to the local unit, the system foresees the use of HCFT sensors (non-invasive ferrites) to be interconnected to the developed conducted system then interfaced with the acquisition system or to use ferrites directly connected to the DAQ or still connect if possible the only system conducted directly to the machine under test. All these solutions make the system extremely flexible and adaptable to different situations.

Figure 3.62 shows a summary block diagram, which well illustrates the situation of the system used in this possible application. On the basis of this, it is then possible to extend the predictive control on several local systems which then interface individually with the central unit.

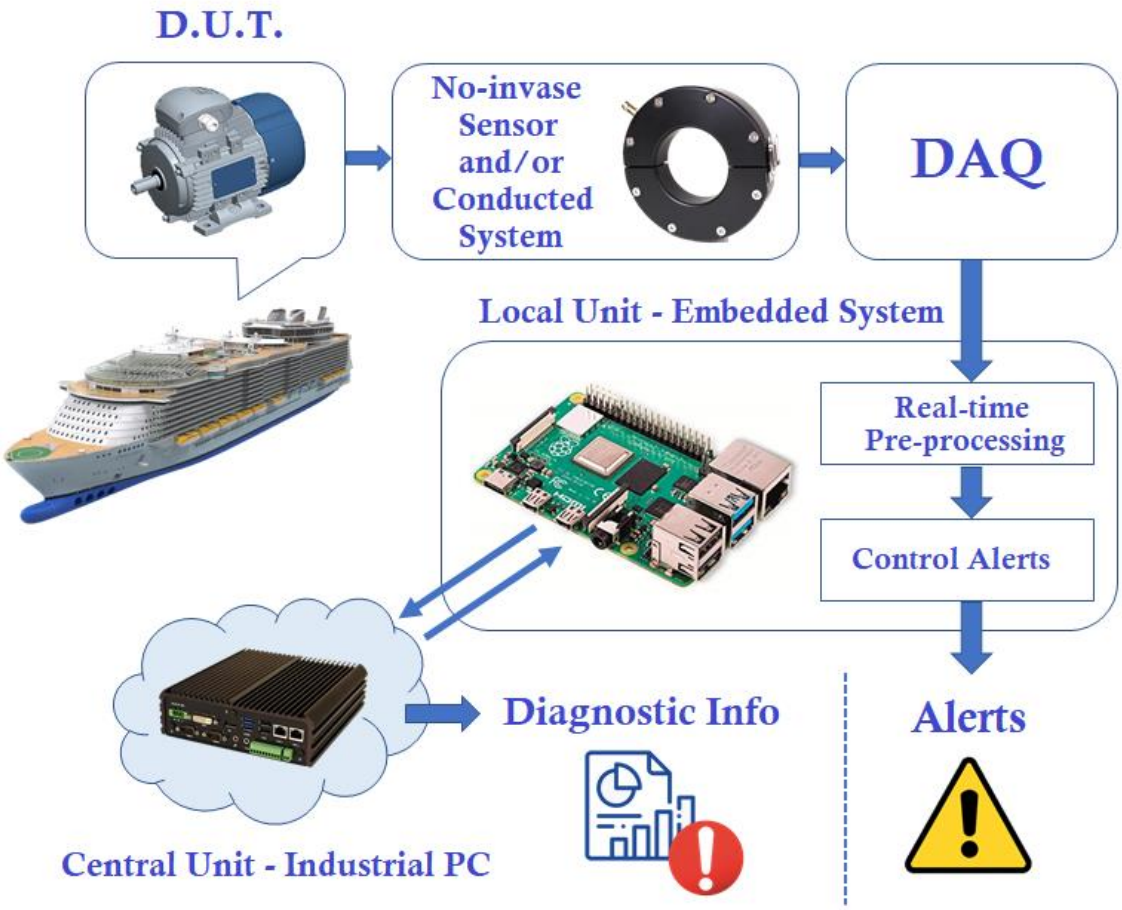

Figure 3.62: Autonomous intelligent system for predictive diagnostics

4. Irradiated PD measurement system

The irradiated partial discharge measurement system, developed during this research activity, is organized according to the scheme shown in *Figure 4.1*.

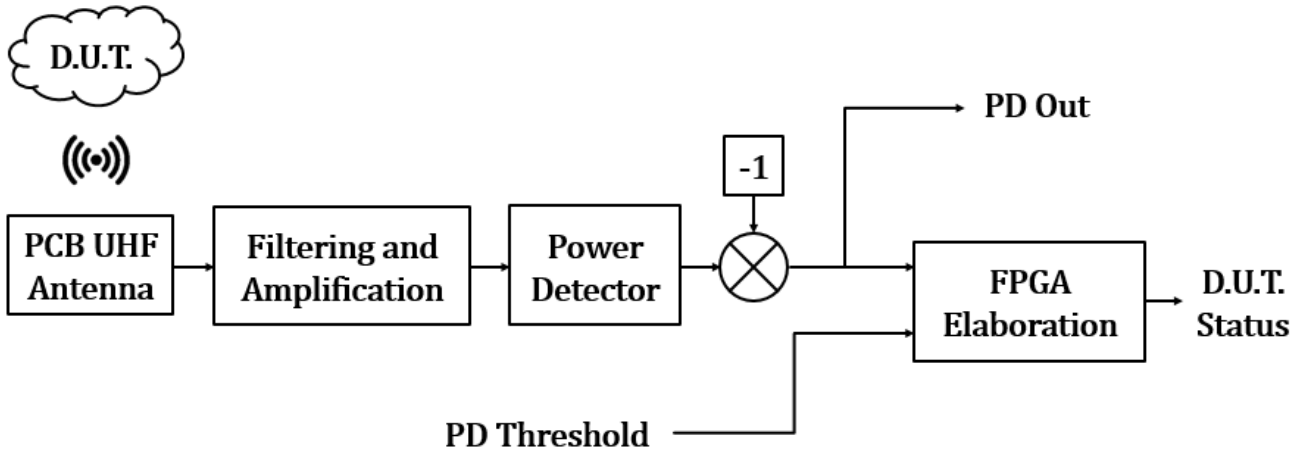

Figure 4.1: Block diagram of the irradiated PD system

Basically the system is based on the use of an Ultra High Frequency (UHF) antenna, made directly on the PCB, which can be the same one on which there is a part or the entire electronic circuit or totally separate for greater sensitivity. The signal picked up by the antenna, which during the test is pointed at a part of the machine in object, is then suitably filtered and amplified, through the use of RF amplifiers. Since this is a high frequency signal, it is advisable to carry out a sort of envelope of the signal, in order to lower the frequency range in which one works, so that it is possible to sample the signal with an instrument with more limited characteristics, with consequent advantages also at economic level. This operation takes place using a power detector, it is a demodulating logarithmic amplifier, which also allows to improve the sensitivity that occurs on signals of little importance in terms of amplitude (and consequently power). After this block, a subsequent one follows which deals with the preprocessing of the signal, adapting it in terms of voltage level and allowing it to be interpreted by a more complex logic. This signal must be processed to obtain information on the status of the device under test. In this context, it is possible for an external operator to set an external attention threshold, for which the subsequent logic must be alerted. In this

regard, the final processing is performed by an FPGA, which analysing the received signal, after sampling it, observes how many times there is a signal that has exceeded the alert threshold and, depending on the logic set, returns information on the status of the D.U.T., through the lighting of colored LEDs, according to a scale of danger.
The entire system must also be characterized by low costs, portability, and small dimensions, in order to make it an attractive product that can be placed on the market.
The study of a system for measuring discharges using antennas arises from the need to carry out diagnostics on machines and components on which it is not possible to mount a traditional duct type system or for which it is not possible to stop the system for carry out offline or otherwise invasive measurements. For example, the stoppage of small inverter-powered motors, even if they are characterized by a relatively low price compared to other components, can lead to a sudden shutdown of the plant that can bring to large economic losses. Therefore, it is also important to have a system that has a low cost compared to the machine to be tested, in order to make the owner prefer the choice to carry out diagnostics rather than buy a new device. For this reason, having an inexpensive diagnostic system that does not need to be physically connected to the power supplies is a winning solution, even on a commercial level. As mentioned above, it is sufficient to have minimal information on the status of the system, in order to give an indication of a possible and imminent failure, allowing an operator dedicated to maintenance to intervene in a scheduled action. Another different situation may concern on-board diagnostics of more complex devices in which there is no possibility of accessing the connection and in which there is little space available and in the same way such systems can be applied for the irradiated measurement, perhaps providing also an optional remote control.
The irradiated measurement by antenna is very similar to that of the conducted type, with the exception of the much higher frequency involved. At the discharge event, in addition to the pulse of current flowing inside the conductors, a signal of radiated origin is also produced, which spreads in the air. The only limitation for this measurement system concerns the loss of information on the amplitude of the discharge, since this depends on the point in which the discharge occurs and, consequently, on the point in which the antenna is pointed with respect to it, from the interposed material and the reflection phenomena of the signal. Despite this, by

observing the discharge activity, it is possible to obtain a series of information on the trend of the phenomenon and to verify if, over time, there is an increase in activity. From this perspective, two main fields of application can be identified. The first concerns type I insulation systems, for which it is sufficient to verify the presence or absence of partial discharges. The other concerns those systems where it is necessary to have more detailed information on the number and frequency of the discharge activity. In this context, the system has been developed in such a way as to guarantee operation for the first field of application, but at the same time it has already been partially prepared in order to make small changes if you want to diversify to other applications. Furthermore, given the possibility of different types of power supply for the machine under investigation, two different versions of the system have been developed:

- Version for PWM power supply with inverter
- Version for sinusoidal power supply

4.1 PCB UHF Antenna

The antenna used for the measurement of irradiated signals is of the Vivaldi type and has been patented by Diasol srl, during previous studies [50]. The geometry is that shown in *Figure 4.2* and the minimum occupation area is given by the minimum dimensions of 108.7mm x 123.3mm. Furthermore, it is optimized to work in a frequency band between 600 MHz and 1.2 GHz, but also performs very well at lower frequencies (up to hundreds of MHz). It is designed to be made directly on PCB, making the system compact and economical. It consists of a part, red in the figure, positioned on the Top layer of the printed board and a blue part on the Bottom layer, with the thickness that is given by the FR4 substrate of 1.6mm. Moreover, it is characterized by an impedance equal to 50Ω.

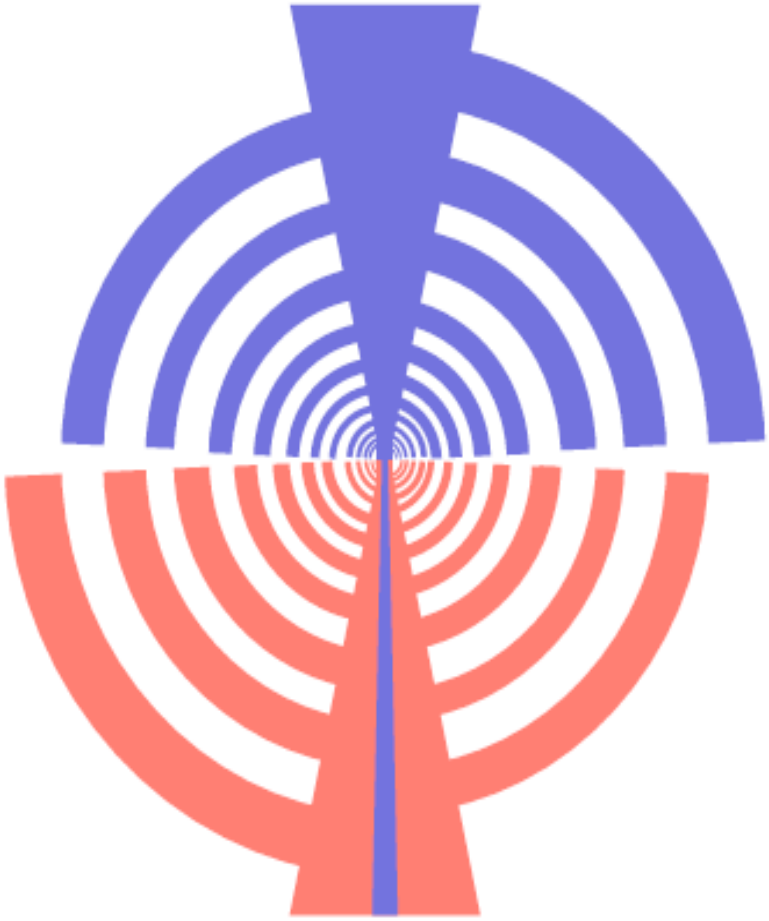

Figure 4.2: Geometry for PCB antenna

The antenna is able to pick up signals in the direction perpendicular to it, so as to detect the discharges of a single machine in an environment with multiple devices, but also to reduce the effects of environmental noise, given the industrial type of application. Obviously, a fundamental part in the removal of environmental noise will be carried out by the subsequent filtering stage, in fact, it is necessary to be able to isolate the signals of interest, extrapolating them in the best possible way from the noise, so as to be able to characterize and subsequently process them. The antenna made is the one shown in the previous *Chapter 2* in *Figure 2.15*, specifying that the geometry of the antenna on the PCB never changes, but the shape of the entire board may vary based on the version and configuration of the measurement system.

4.2 Filtering stage

The presence of an input filtering stage, after the antenna, has the purpose of defining a frequency band in which the signal with the best possible signal-to-noise ratio is present. To do this, it is certainly necessary to be clear in which band the discharge signal is most concentrated in a given application and what environmental noise may be present. As mentioned, an aspect that can diversify the concentration of discharges in different band is certainly the type of power supply adopted for the machine under test. For this reason, being the system designed for two different power supply versions, two different filters have been designed. Despite this, both have in common the characteristic of impedance compatible with the antenna and at the output with the amplifier, therefore equal to 50Ω, and the Chebyshev configuration.
Since these are signals captured in ether, it is necessary to take into consideration the irradiated signals that may already be present in the frequency bands of interest for PDs application, many considerations in this sense are the result of previous problem analysis activities. In this regard, *Table 4.1* summarizes the situation in these terms.

Subdivision of band [MHz]	**Usage**
87.5÷ 108	*FM analogue sound broadcasting*
108 ÷ 117.9	*Aeronautical radionavigation*
174 ÷ 230	*Digital television and sound broadcasting*
Different bands	*Ministry of Defence*
470 ÷ 790	*Digital television broadcasting*
791 ÷ 821	*LTE (Downlink)*
832 ÷ 862	*LTE (Uplink)*
876÷ 915	*GSM (Uplink)*
915 ÷ 921	*Ministry of Defence - Mobile*
921 ÷ 960	*GSM (Downlink)*
1800 ÷ 1900	*LTE/4G*

Table 4.1: Standard frequency bands

4.2.1 PWM version filter

At the level of measurement of partial discharges, it is necessary to consider that the frequencies in which activity occurs, in the case of PWM power supply with inverter, are usually around 1 GHz. This includes some frequencies affected by GSM, which could compromise measurement, for this reason it is necessary to find a compromise band that allows to correctly measure the discharges. Therefore, a bandpass filter was identified in the band between about 940 MHz and 1.58 GHz, having proved to be the best compromise in relation to the other frequencies of interest and the choice of components.

In addition, it is useful for the filter to be very selective, especially with regard to frequencies below the lower cutoff, for this a relatively high filter order is required. The circuit diagram relating to the filter is shown in *Figure 4.3*.

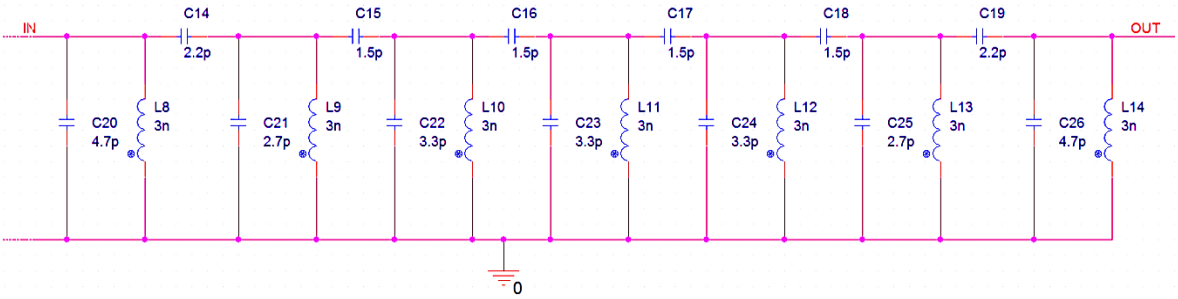

Figure 4.3: PWM version filter

As for the frequency response of the filter, it is shown in the following graph of *Figure 4.4*.

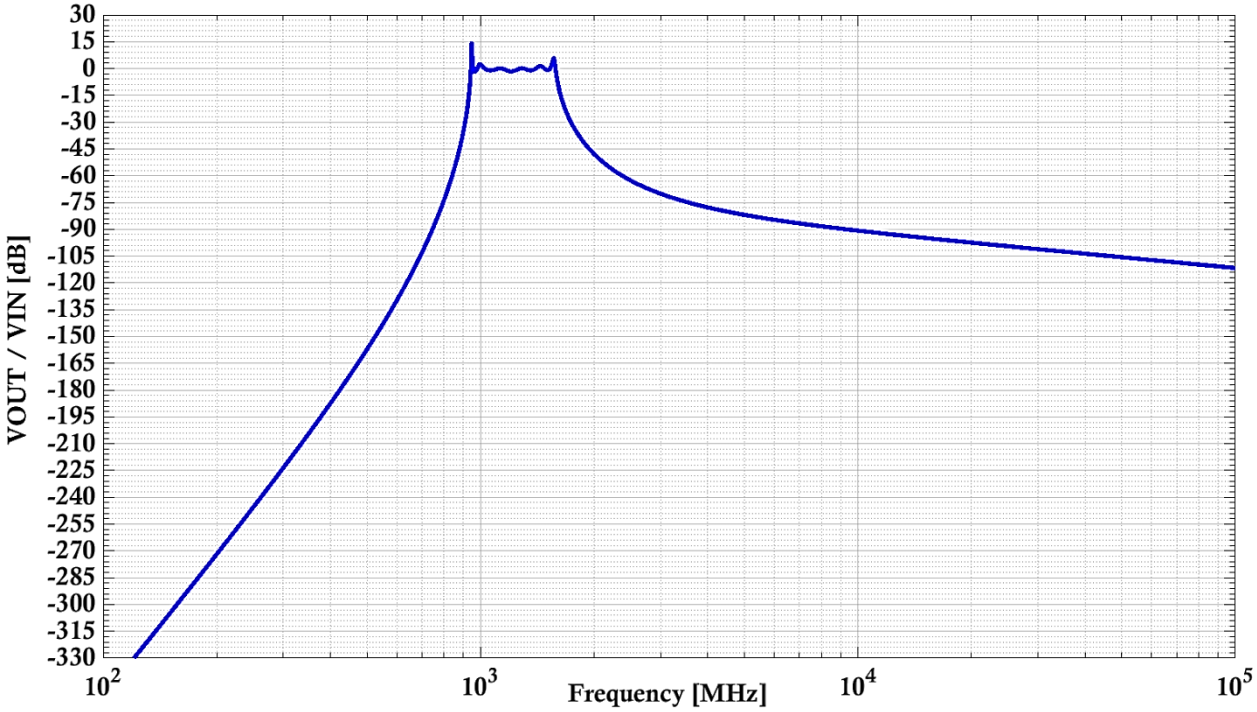

Figure 4.4: Frequency response of PWM version filter

From the graph it can be seen that the passband is included in the values previously indicated. Furthermore, it can be observed that being a Chebyshev filter there is a minimum ripple in the passband. Another important aspect concerns the previously mentioned fact on the selectivity of the filter, greater below the lower cut-off frequency, for the reasons previously explained. There are also two small overshoots, in the presence of cut-off frequencies, which should be irrelevant in terms of the specific application and above all will be dampened in the overall system configuration.

Given the higher frequencies involved, which increase the risk of undesirable effects related to RF, for this version, the input filter was replicated even after the amplification stage.

4.2.2 Sinusoidal version filter

Compared to the previous case, the situation and type of power supply lower the frequency range in which discharge activity occurs. In this regard, it was necessary to redesign a second filter suited to the required specifications. The frequency band identified is between about 200 MHz and 800 MHz. This band, although overlapped on other standard bands, appears to be the best compromise at present in order not to risk losing a useful signal and at the same time having an acceptable noise level. Another aspect to consider concerns the type of overlapping signals, given that it is the television one and that relating to communications from the Ministry of Defense, which therefore should not interfere in an industrial environment. Having made these considerations, in *Figure 4.5*, it is possible to see the circuit diagram of the filter created, which has a lower cut-off frequency of about 285 MHz and the upper one of 800 MHz.

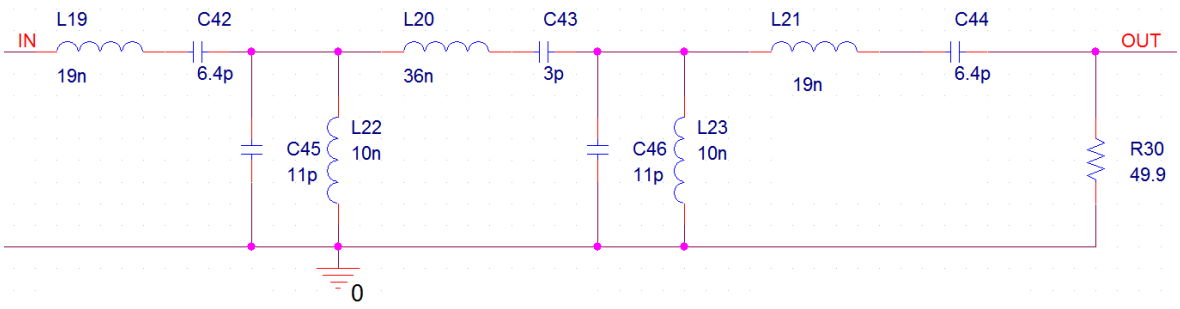

Figure 4.5: Sinusoidal version filter

About the frequency response of the filter, it is shown in the following graph of *Figure 4.6.*

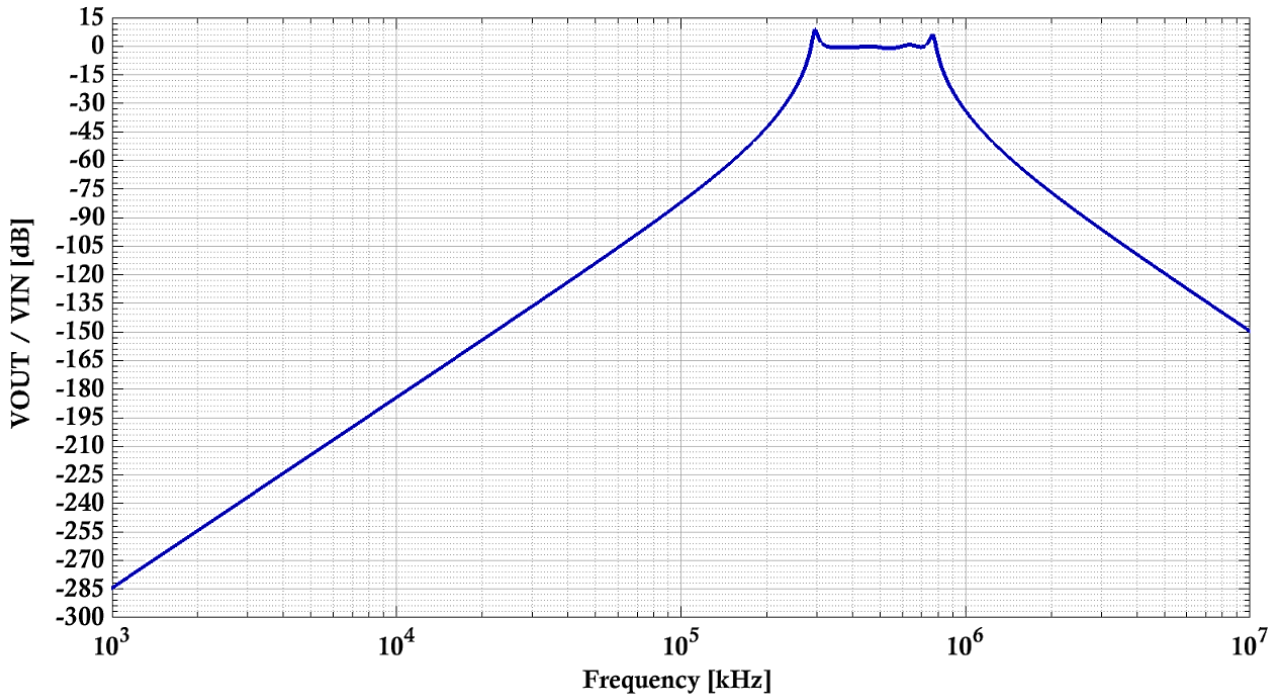

Figure 4.6: Frequency response of sinusoidal version filter

From the graph it can be seen that the passband is included in the previously indicated values. Furthermore, it can be observed that being a Chebyshev filter there is very minimal ripple in the passband, although lower than the previous case. Also, in terms of filter selectivity there is a good result and also in this case there are two small overshoots, in the presence of cut-off frequencies, but much more contained and of little relevance given what has been said previously.

4.3 Amplification stage

The signals detected with the antenna, as shown in *Figure 4.7*, can have amplitudes around 50 mV.

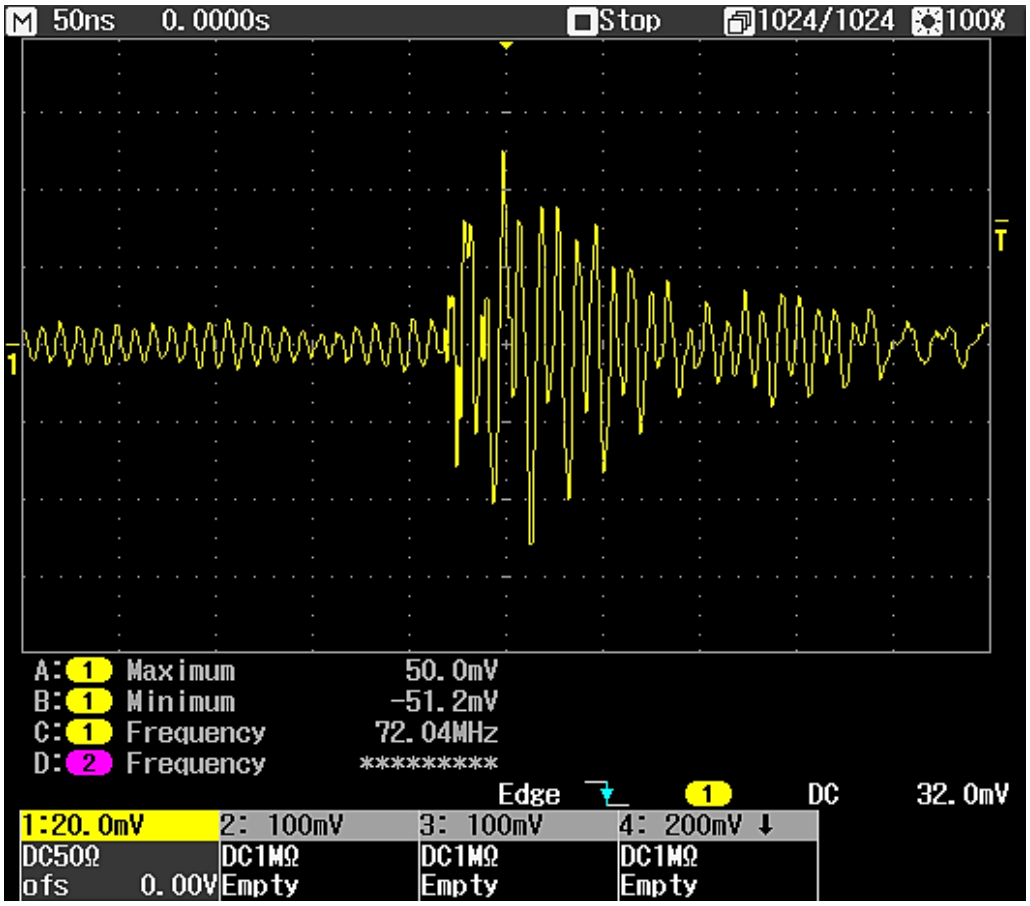

Figure 4.7: PD signal detected by the antenna

However, this depends on many factors, such as the intensity of the discharge activity, the effective band and the precise point in which it occurs, it is not uncommon for amplitudes to be on the order of or less than 10mV. In this regard it is therefore necessary to provide an amplification stage that can correctly amplify the signals detected by the antenna. To do this, it is necessary to take into consideration that the amplifier in question must be compatible in terms of passband with that of the filters adopted, as well as guaranteeing sufficient amplification. Based on these needs, it was decided to adopt the IC BGA2815 [51], a Silicon Monolitic Microwave Integrated Circuit (MMIC) wideband amplifier with internal 50Ω matching circuit in a 6-pin SOT363 plastic SMD package. This amplifier is developed for applications where it is used as a low noise wideband amplifier for frequencies between DC and 2.2 GHz, a band that is compatible with the project specifications. Furthermore, it is characterized by a typical gain between 25.3 and 25.8 dB, respectively at 950 MHz and 250 MHz.

With these values there is an amplification of about 18 and it was decided to provide for the possibility of having one or two amplifiers in cascade, in order to have flexibility in cases where more or less income is required. At the same time, given the nature of the measurement to be performed, that is to verify the presence or absence of discharges, even an excessive amplification does not involve problems. The amplitude of the discharge is not of interest, but it is sufficient to detect it. Therefore, after a certain input value it is accepted that the output always has the same value, which will coincide with the maximum voltage that the amplifier can provide, as will be seen, this feature will be appropriately managed.

The typical application circuit, taken from the component datasheet, is shown in *Figure 4.8*.

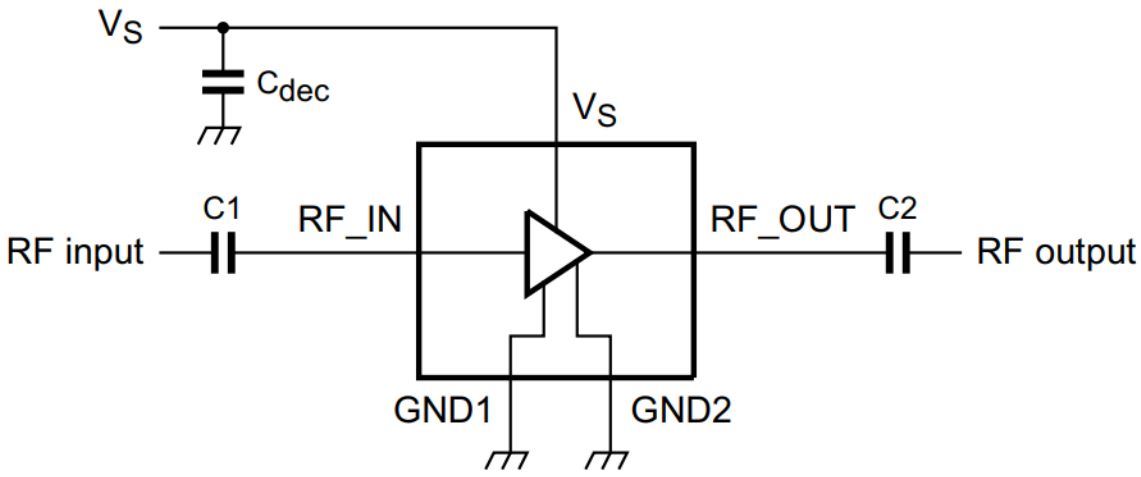

Figure 4.8: Typical BGA2815 circuit

First, from the configuration it can be seen how the amplifier has a single amplification, in this specific case with a voltage level of 3.3V. Moreover, the device is internally matched, so does not need any external matching. The value of the input and output DC blocking capacitors C1 and C2 should not be bigger than 100 pF when the device is operated above 100 MHz, otherwise the capacitor value should be increased. The placement supply decoupling capacitor (C_{dec}) can be precisely chosen for optimum performance and its value is equal to 470 pF.

On the basis of this information, the circuit diagram referring to the realized amplification stage has been drawn and shown in *Figure 4.9*.

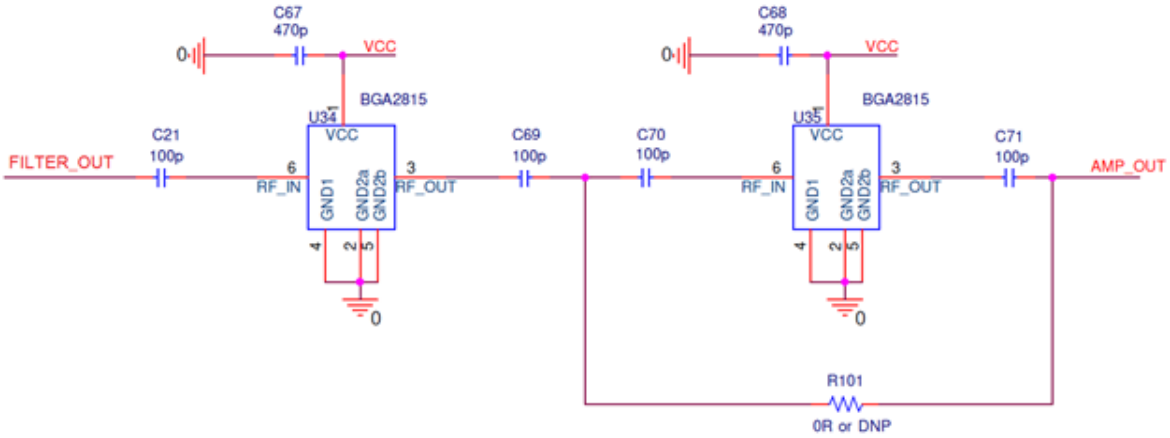

Figure 4.9: Amplification stage circuit

As mentioned, it can be seen from the circuit how it is possible to bypass (with an R0) the second amplifier so as to limit the gain to a single stage.

In *Figure 4.10*, on the other hand, you can see the frequency response graph of the selected amplifier, as the supply voltage (and working temperature) varies.

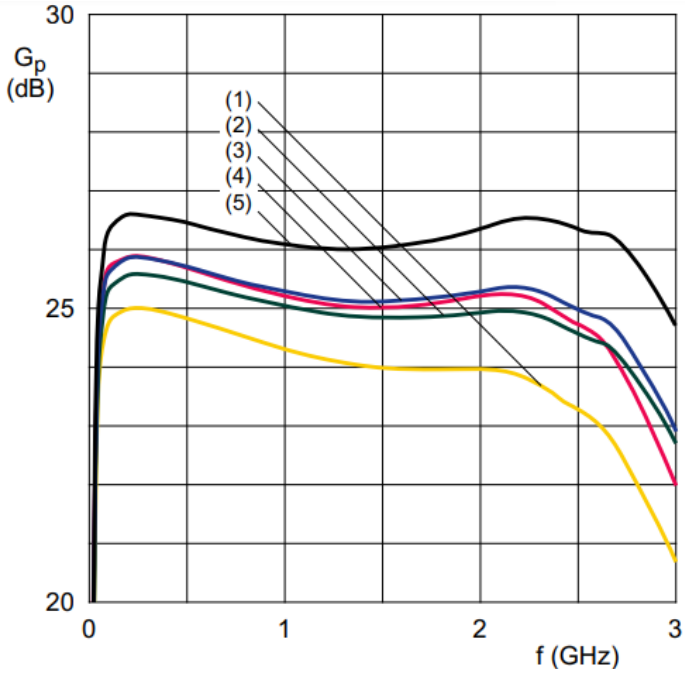

(1) V_{CC} = 3.0 V; T_{amb} = 85 °C; I_{CC} = 15.93 mA.
(2) V_{CC} = 3.0 V; T_{amb} = –40 °C; I_{CC} = 16.12 mA.
(3) V_{CC} = 3.3 V; T_{amb} = 25 °C; I_{CC} = 18.41 mA.
(4) V_{CC} = 3.6 V; T_{amb} = 85 °C; I_{CC} = 20.11 mA.
(5) V_{CC} = 3.6 V; T_{amb} = –40 °C; I_{CC} = 20.23 mA.

Figure 4.10: Typical gain power as function of frequency, supply voltage and temperature

In this graph, it can be observed how the power supply voltage (blue trace n.3), fixed in this case at 3.3V, corresponds to a gain of between 25 and 26 dB, as described above and as expected.

4.4 Frequency conversion stage

As has been anticipated, the signals picked up by the antenna can be of frequencies in the order of GHz, but especially have very fast rising and falling edges. The designed irradiated measurement system must be able to count every single discharge and ensure the signal compatible even for acquisition systems with good but still limited performance. Therefore, it is necessary to convert the signal into frequency, lowering its values in these terms. For this purpose, it was chosen to adopt the IC AD8317 [52], a logarithmic amplifier used as a power detector. The logarithmic amplifier adopted is able to measure the power associated with RF signals, very precisely, by demodulating the received signal and thus obtaining a sort of envelope. Due to the high gain of the amplification stage (which in most cases brings the signal to saturation) and in any case given the nature of the measurement activity, it is not necessary to exasperate the characteristics of the component. The power detector input is AC coupled differential type. The logic of the AD8317 is negative, in the absence of a signal the output remains at the high logic level and drops proportionally in relation to the power of the input signal. To set the setpoint it is appropriate to feedback the output on the VSET pin and to increase the dynamics it was created with a resistive divider formed by two 10kΩ resistors. In this way it is possible to obtain a slope of the input-output relationship equal to -44mV/dB. Moreover, an offset voltage of 0.35V is internally added to the detector signal. To allow a rapid response with respect to the discharge signal, which as mentioned in this case is very fast, the minimum possible resistance, equal to 150Ω, has been inserted in the output and the Loop Filter Capacitor (CLPF) has not been connected, thus obtaining a very quick falling edge. However, this can lead to slight oscillation problems, which can however be safely eliminated by subsequently using a threshold comparator, given the nature of the application. Furthermore, however, these reduced oscillations are easily recognizable. Thanks to this type of configuration it is possible to obtain a theoretical time for falling edge

equal to 7ns and similar effects, even if less evident are also observed on the rising edge. These characteristics of rapidity are fundamental in the measurement of discharges as the phenomenon can involve signals with a total duration up to 20ns, whose main content is enclosed in about 10ns. In summary, *Figure 4.11* shows the circuit diagram adopted, the result of the design, remembering that between the amplification stage and the one just described, there is the possibility of replicating the input filter, to obtain better performance in terms of S/N, if necessary.

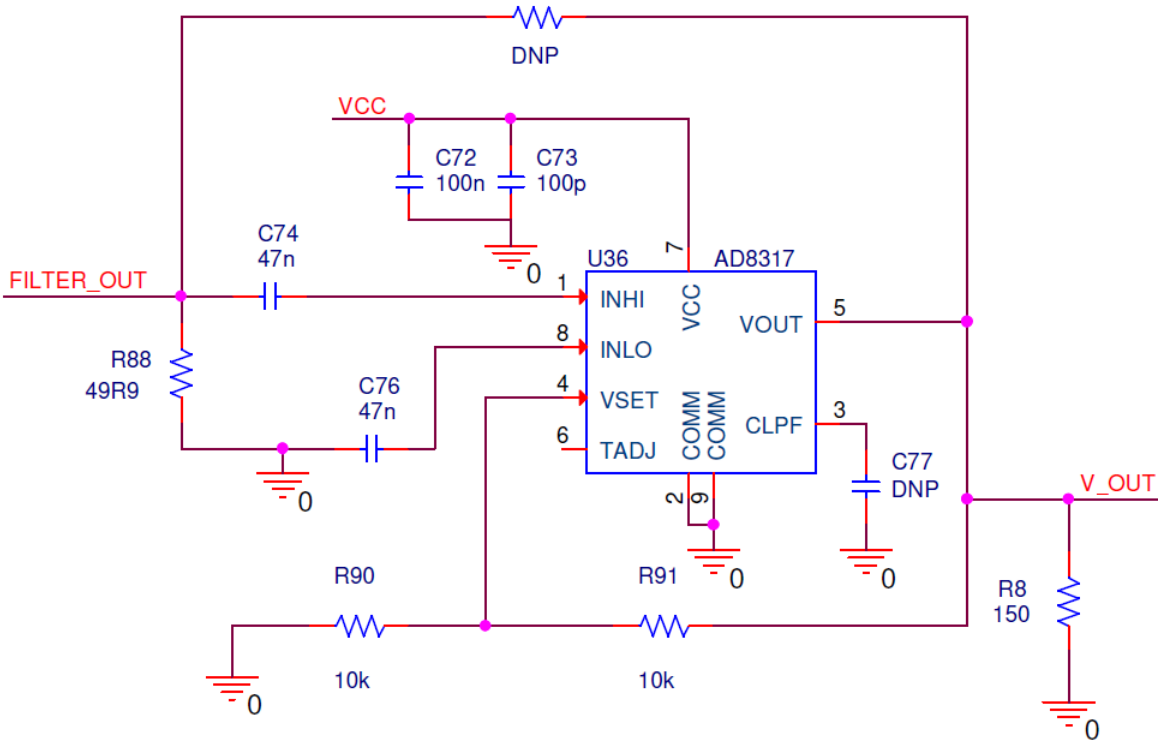

Figure 4.11: AD8317 circuit

As if observing from the circuit, there is the possibility of bypassing this stage in order to do without the frequency conversion and thus maintain the characteristics of the discharge signal and relative amplitude. In this way, the amplitude of the discharges can also be taken into consideration, adapting the system to a different type of application, than the one in object of this research activity.

In addition, *Figure 4.12* shows the graph that compares the output voltage with the power of the input signal and the following is the mathematical relationship that occurs between these:

$$V_{OUT} = X \cdot V_{SLOPE/dB} \cdot 20 \cdot \log_{10}\left(\frac{V_{IN}}{V_{INTERCEPT}}\right)$$

Where X is the feedback factor in $V_{SET} = V_{OUT}/X$, $V_{SLOPE/dB}$ is −44 mV/dB and $V_{INTERCEPT}$ is the x-axis intercept of the linear-in-dB portion of the V_{OUT} vs. P_{IN} curve (see Figure 4.12) and its value is 2 dBV, equivalent to approx. 1.25V.

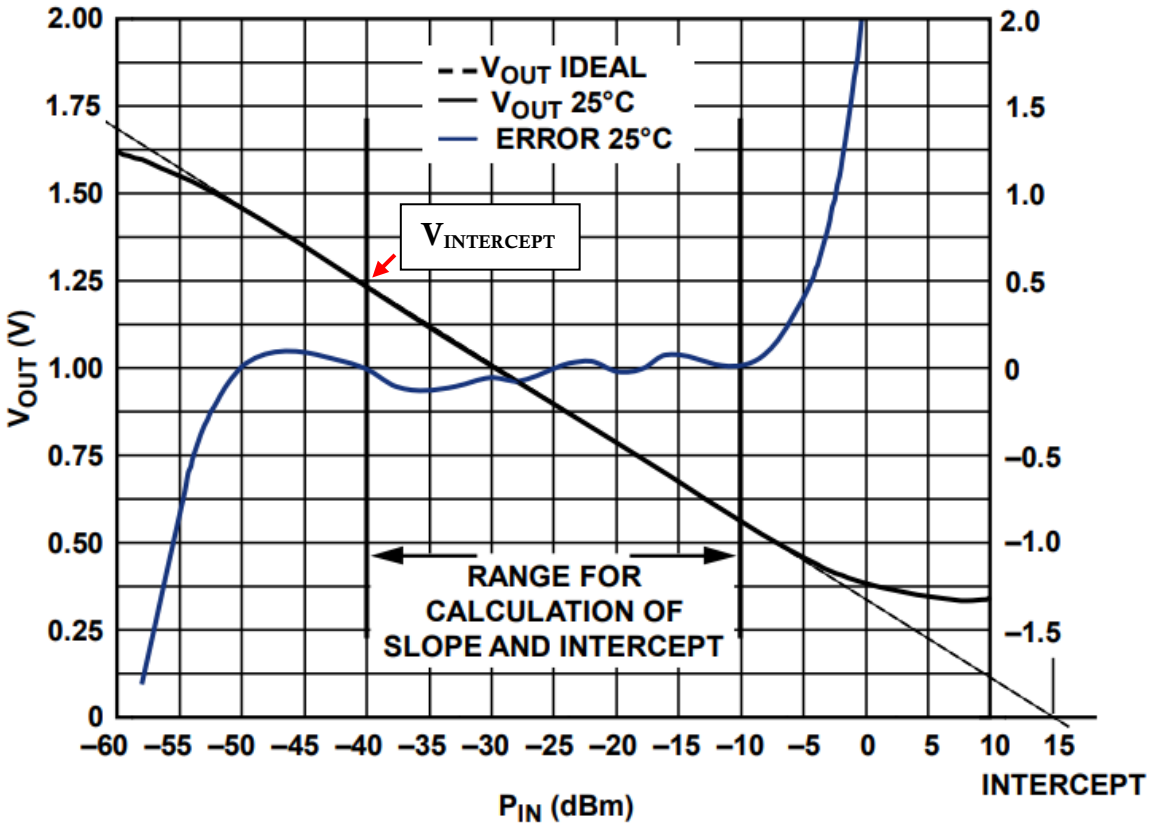

Figure 4.12: Typical output voltage vs power input signal

4.5 Pre-processing stage

Before processing the signal to the FPGA, it is necessary to suitably conditioning of the output signal from the power detector, so as to make it compatible and easier to read by logic and also to bring out the signal of the discharges and allow an operator to observe it on a digital oscilloscope. At the same time there is an interface for the

operator for which it is possible to configure a warning threshold for discharges that must be considered as such.

4.5.1 Pre-processing circuit design

The first step that needs to be addressed concerns the logic of the output signal from the power detector, it is in fact of a negative type. Therefore, it is advisable that the signal be inverted, to be interpreted in a more intuitive way. In this regard, it is also necessary to consider that a component must be chosen that has a working band compatible with what comes first in the system circuit. The IC (Integrated Circuit) in question is the OPA357 [53], a rail-to-rail operational amplifier featuring by a 250 MHz Unity-Gain Bandwidth and high slew rate, equal to 150 V/µs, which was used in a unitary inverting configuration with a single 3.3V supply voltage. For the circuit configuration adopted, refer to the following *Figure 4.13*.

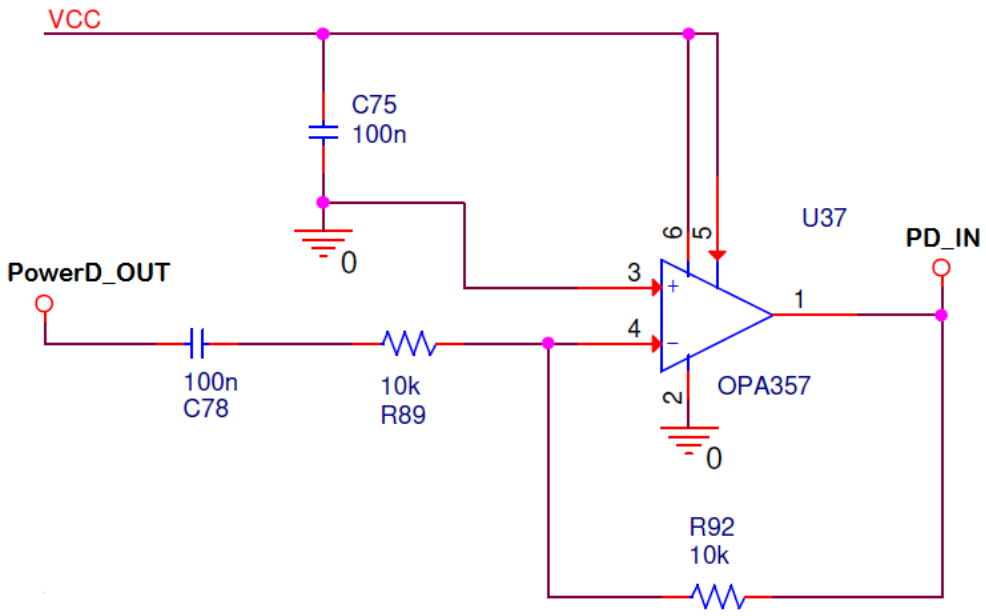

Figure 4.13: OPA357 configuration circuit

Note in the schematic the presence of the capacitor C78, which has the task of eliminating the DC and allowing a correct inversion of the signal. Considering instead the band of 250 MHz and slew rate and taking into consideration that the signals

involved are at most in the order between tens and hundreds of ns, the choice of the component in these terms can be considered as optimal.

The second aspect to consider, on the other hand, concerns the need to be able to observe the signal of interest processed up to now on an oscilloscope. To do this it is necessary to provide a buffer and the choice fell on the integrated component MAX4212 [54]. It is a rail-to-rail operational amplifier, featuring by only 5.5mA of quiescent supply current, a 300 MHz bandwidth and a 600 V/µs slew rate. Again, these characteristics are compatible with what is before the component. The insertion of a buffer is useful to avoid signal drops on the line if cables of considerable length are inserted between the diagnostic device and the oscilloscope.

The configuration adopted is the typical one recommended on the datasheet to have unitary gain, which includes the circuit in *Figure 4.14* and respects the values of the components shown in *Table 4.2*.

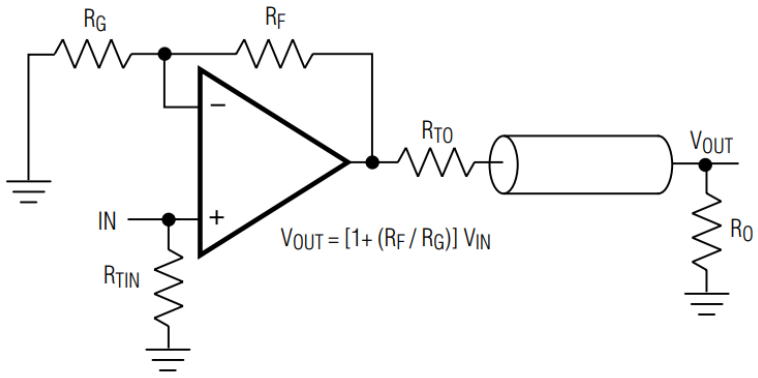

Figure 4.14: MAX4212 configuration circuit

COMPONENT	GAIN (V/V)									
	+1	-1	+2	-2	+5	-5	+10	-10	+25	-25
R_F (Ω)	24	500	500	500	500	500	500	500	500	1200
R_G (Ω)	∞	500	500	250	124	100	56	50	20	50
R_S (Ω)	—	0	—	0	—	0	—	0	—	0
R_{TIN} (Ω)	49.9	56	49.9	62	49.9	100	49.9	∞	49.9	∞
R_{TO} (Ω)	49.9	49.9	49.9	49.9	49.9	49.9	49.9	49.9	49.9	49.9
Small-Signal -3dB Bandwidth (MHz)	300	90	105	60	25	33	11	25	6	10

Table 4.2: Recommended component values

Finally, the last aspect concerns the signal that must be sent to the logic to be processed. Given the need to count all the partial discharges that are above a certain threshold of attention, but also to avoid confusing the noise with a discharge, it was chosen to insert a comparator that deals with managing this situation. The attention threshold is adjustable through a small potentiometer, accessible externally by an operator, while the component chosen as a comparator is the same one adopted previously, the MAX4212. Obviously, in this case, it has been suitably configured as a comparator, so that when the threshold level is exceeded, the component output is brought to saturation at the power supply voltage level. The adopted configuration is shown in the diagram of *Figure 4.15*, in which the buffer circuit described above can also be observed.

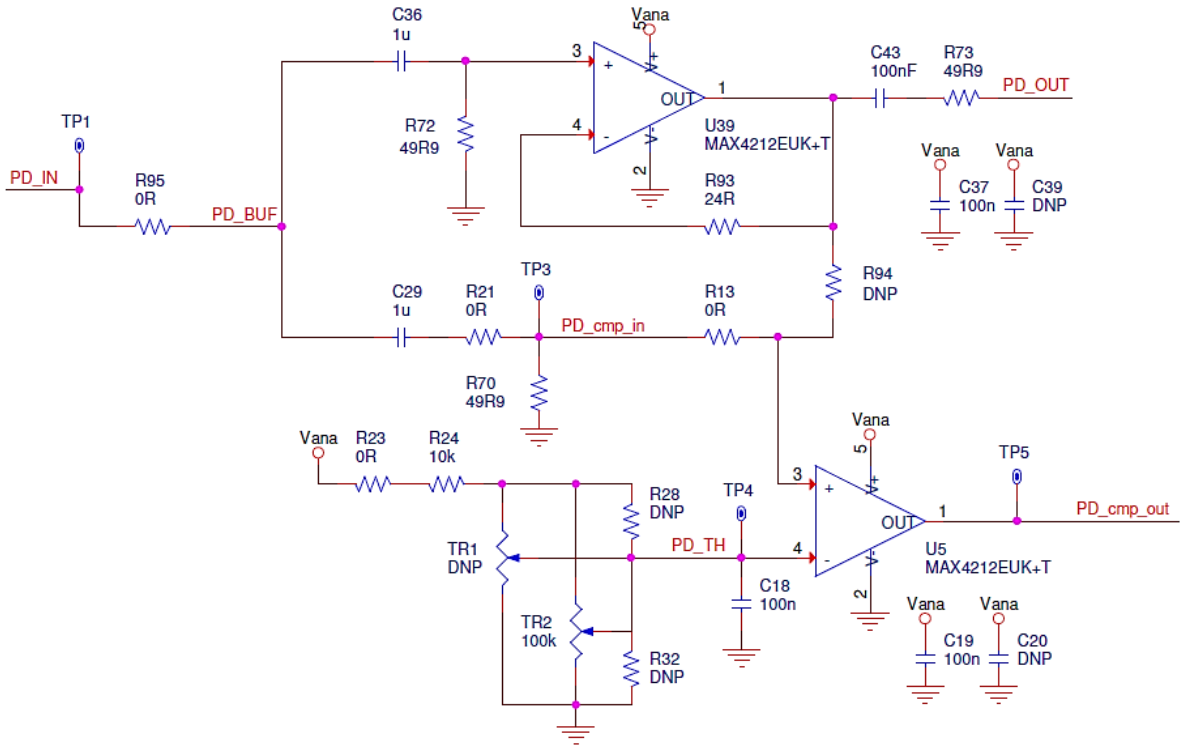

Figure 4.15: Pre-processing circuit

It can be observed that the two sections have the same input signal in common, which is parallelized in order to be suitable for the configuration. In both branches there is a DC blocking capacitor, coupled with a suitable resistance to form a high pass filter at about 3.2 kHz. On the other hand, an RC configuration can be noted for filtering the continuous level for the threshold, which can vary between the supply voltage (or

portions of it, depending on the value set for R24) and zero, on the negative input of the comparator U5. Both the MAX4212 are powered through a single 3.3V supply.

4.5.2 Pre-processing simulations

To validate the functional behavior of the circuit section described a series of simulations with relevant signals were performed. Also, in this case, the behaviors were analyzed separately for the two main components used. The first simulation refers to the OPA357 and provides an input signal compatible with the real one that could be output from the power detector. *Figure 4.16* shows the circuit simulation graph.

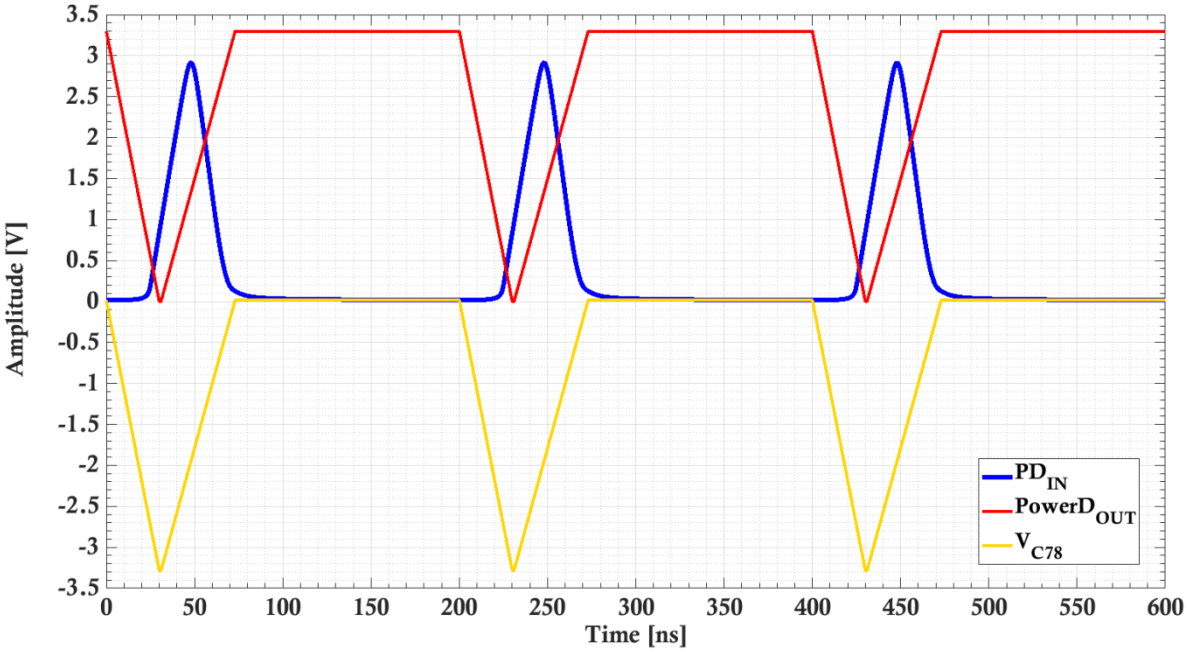

Figure 4.16: OPA357 simulation

In the graph it can observed in red the trace relating to the output signal from the power detector, in yellow the one present after the capacitor C78 and in blue the one in output to the inverting. The input signal is characterized by a falling edge of tens of ns, while the rising one is always in that order but less fast, as per specifications. It is observed that following an input signal, which represents a possible generic output signal from the power detector, the signal after the OPA357 (red trace) is correctly inverted, unless there is a small difference in voltage, due to limitations of the

characteristics of the component. It is in fact characterized by a voltage output swing between 0.1 and 0.4V, therefore perfectly compatible with what was obtained in the simulation.

Likewise, using a signal compatible with the one obtained at the output of the section just described, it has been returned to the input of the next stage, the one which envisages the use of the two MAX4212, respectively in buffer and comparator configuration. In this case the following graph, shown in *Figure 4.17*, shows what has just been mentioned and described previously.

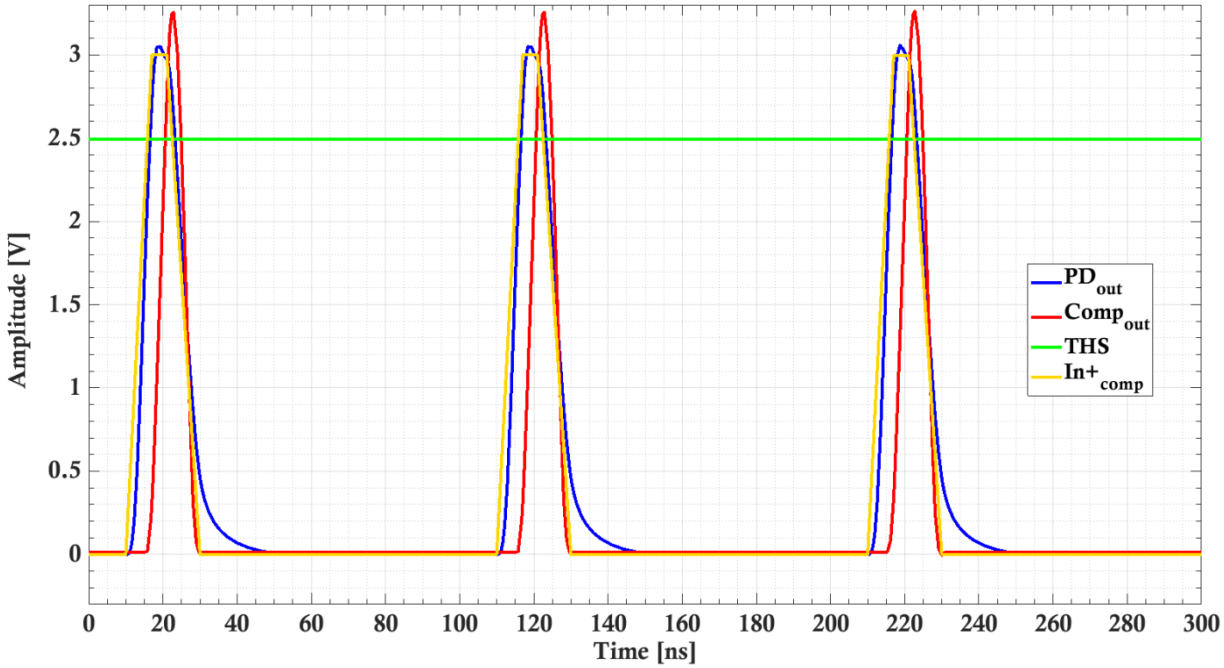

Figure 4.17: Buffer and comparator simulation

From the graph it is possible to observe in yellow the signal present on the positive input of the comparator, which substantially is also the one in input also to the buffer, whose output is shown in the blue trace, the DC signal relating to the attention threshold set is shown in green and the comparator output in red. It can be seen how fundamentally the buffer signal reflects what is present at the input to it, while in the presence of a signal above the threshold it is observed how the comparator brings its output to a high logic level, after a small delay of a few ns. In addition, it is specified that the signals in question are extreme to verify the behavior of the component in the

worst conditions, in which it is more difficult to follow the signal due to excessive speed and despite this the result can be considered excellent.

4.6 Supply voltage stage

Before proceeding with the last stage of the signal chain, it is advisable to analyze the power supply circuit so as to define the various voltage levels present. The device provides two main types of power supply to be used alternatively, depending on the need. Therefore, it is possible to power through an external 24V supply or with four 1.5V C batteries in series, for a total of 6V nominal. Both power supplies are protected by an anti-reverse current diode, the model chosen is the PMEG3010EH [55]. It is a 1 A, very low drop voltage, Schottky diode. As for the 24V voltage, it is regulated at the 5V level by means of a suitable adjustable linear regulator. The integrated chip chosen in this case is the LM1085IS-ADJ [56], it is a 3-A, low-dropout, positive regulator, which only needs two SMD tantalum bypass capacitors (on input and output) and a resistive regulator divider to set the output voltage level to 5V. As for the battery power supply, it is initially used simply in parallel with the one just described, without any regulation (even if a 5V regulation is possibly provided), thus forming a single power supply branch, to be used alternatively, with the previous one. Subsequently, other specific and smaller linear regulators follow, which deal with supplying power to the various parts of the circuit. One is used to supply the 3V voltage for the timing control section, the other 1.5V for the FPGA power supply and finally one to manage the power of the part of the circuit relating to the analog electronics dedicated to the signal chain. In all three cases the IC TPS71701 [57] was used, a low-noise, low-dropout, 150-mA linear regulator, whose regulation ratio is fixed through resistive feedback dividers.

To complete this description of the power supply circuit, the final schematic is shown in *Figure 4.18*.

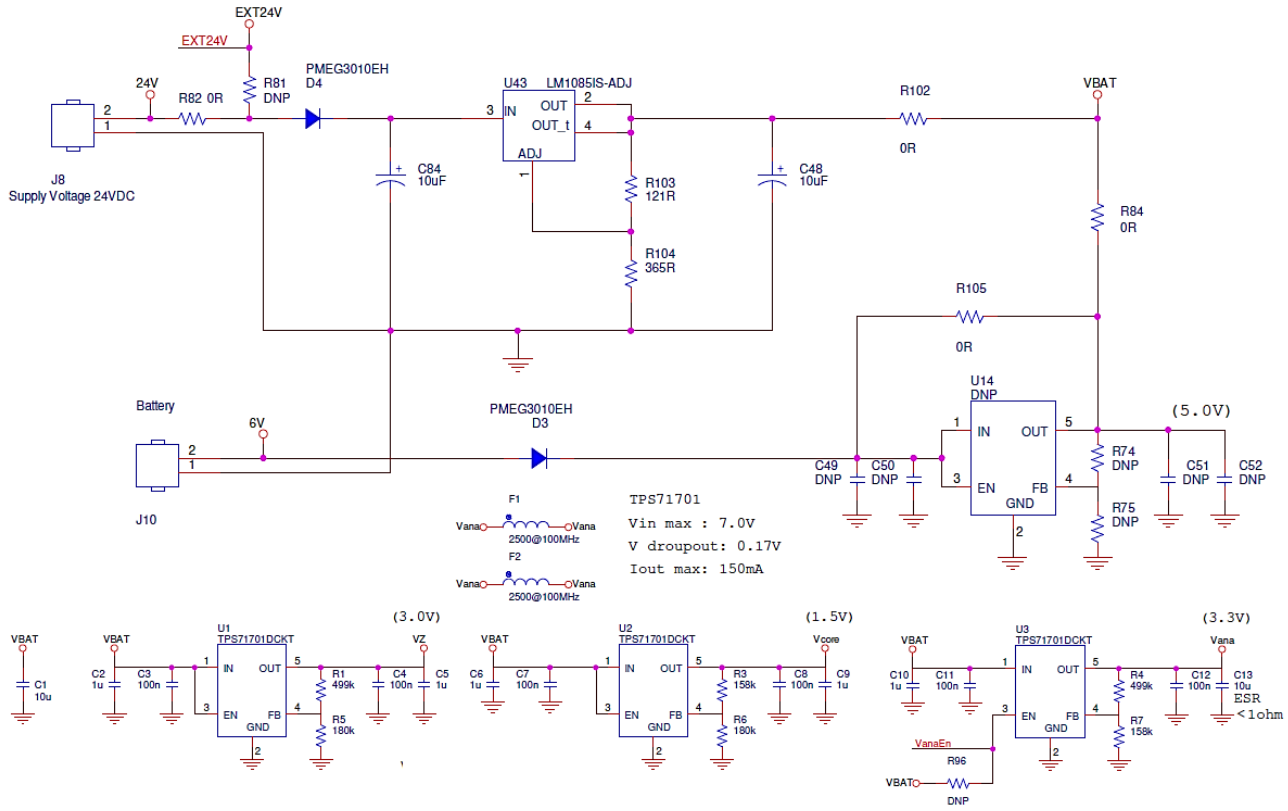

Figure 4.18: Supply voltage system

4.7 Logic and processing stage

Returning to the signal chain, for the last stage there is a logic, based on FPGA, which deals with managing and processing the received signal to provide information on the status of the machine under test and control a series of additional features, prepared with appropriate electronic circuits. In this research activity, circuit design was the fundamental point to focus on, knowing that there was an appropriate firmware whose characteristics and peculiarities were known.

4.7.1 Operating principle

The basic idea for the operation of the developed logic is the following: the device to be built must have three buttons and five bright LEDs. The buttons refer to three operating modes, the first concerns the start of a single measurement of a certain duration defined via firmware, the second when the device is reset and the third when a continuous measurement is started, which is interrupted at the next click of the above button. In parallel to this, an automatic measurement is provided which allows, once the device is installed, to keep under test machines with a measurement, of duration defined via software and therefore variable according to the needs, every 6 hours (for a total of 4 daily measurements). The idea is to monitor periodically the D.U.T. throughout the day, but also to be able to carry out specific and timely measurements by an operator, which can be single or continuous, if necessary, to observe a phenomenon for a longer time. The measurement, whether automatic or manual, consists in the acquisition by a logic device, in this case an FPGA, of the signal conditioned by the previous electronic circuit described and in the count of the number of pulses, present in the observed time interval, which exceed a certain threshold of attention arranged externally via the potentiometer. Based on the number of pulses counted in this interval, further alarm thresholds are generated via software, in particular two. These can vary according to the frequency of power supplies, but an example at 50 Hz, for an interval of 30 s, can identify these thresholds as greater than 50 discharges (hence pulses) for the first level and 300 for the second. Obviously, the appropriate elaborations via software for the management of measurement times and discharge count will follow. Regarding this processing, the luminous LEDs must light up with a certain logic. In fact, a red LED is dedicated to the warning of a dangerous measurement and this must happen during the measurement itself. Instead, at the end of the measurement, two other LEDs light up, one green and one yellow, to indicate the exceeding of the two danger thresholds. When the first is passed, the green LED lights up, both of them on the second. Obviously, it will be the task of an expert user to indicate the intervention times but given the nature of the tested systems it is reasonable to intervene promptly, in particular when the second threshold is exceeded. The remaining two LEDs, on the other hand, are responsible for indicating that the

device is on or off (with another green LED) or if the batteries are about to discharge (with another yellow LED), in the case of battery power. Furthermore, these LEDs must continuously flash once turned on, so as to limit energy consumption and save battery, only during the measurement, to identify it, the LEDs are fixed, starting to flash again once finished. Finally, if you want to provide the possibility to remotely control the diagnostic device created, by setting up the connection with a relay board which in turn interfaces with a PLC. In this way it will be possible to control the device, even if positioned in places where it becomes difficult to go and click the buttons for the various manual modes. To do this, appropriate electronics have also been set up on board the standard device, so as to make the same layout uniform and reusable. *Figure 4.19* summarizes what has just been explained, as well as indicating the actual placement of the elements described.

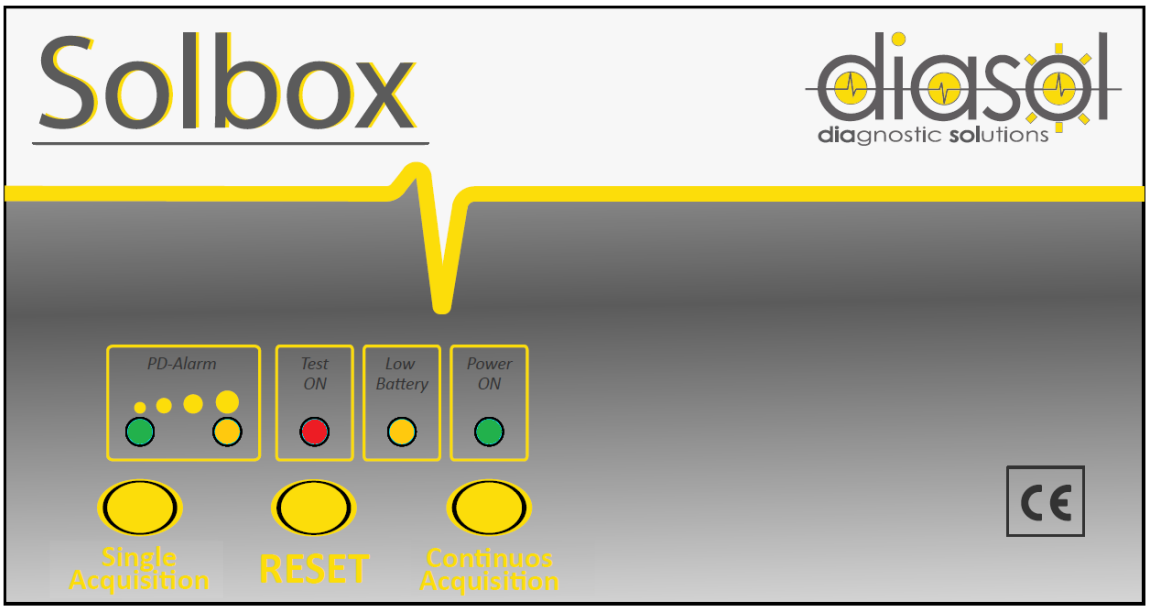

Figure 4.19: Configuration for buttons and LEDs

4.7.2 Control electronics for the logic stage

On the basis of this described in terms of operating principle, what observed in *Figure 4.20* has been designed at the circuit level.

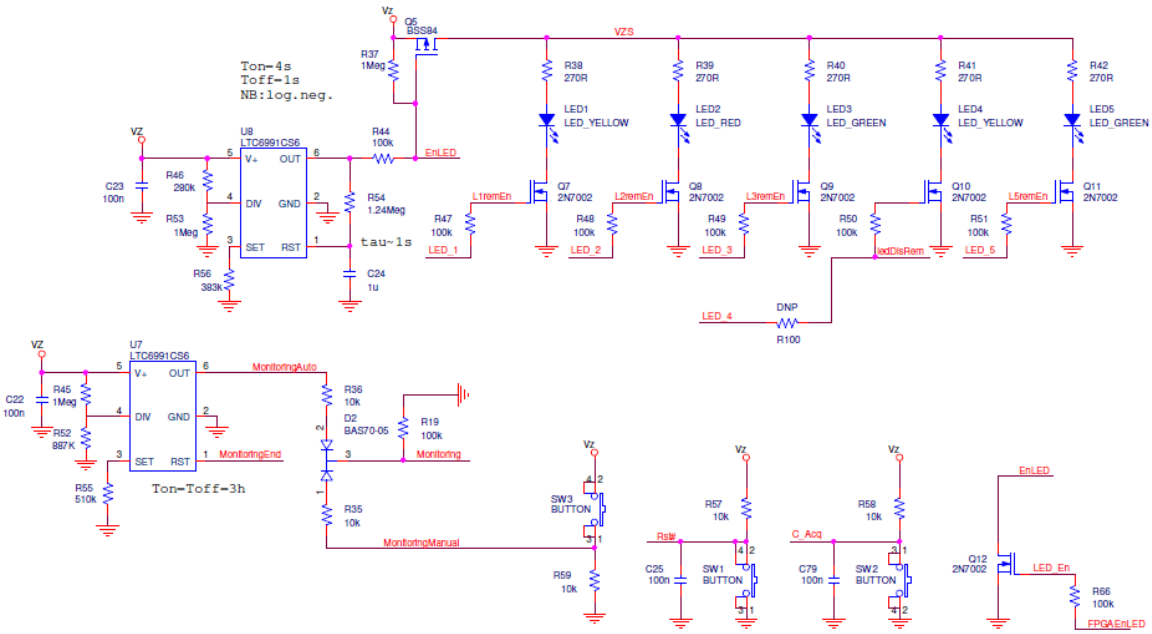

Figure 4.20: Logic stage - Control electronic circuit

From the circuit it is possible to observe the three buttons and the 5 LEDs previously described, as well as two integrated timers LTC6991CS6 [58] which in this case have the task of setting the flashing interval of the LEDs (U8) and the automatic measurement interval (U7). Observe how the LED control is managed with 2N7002 [59] transistors, driven through the logic device. At the same time, the fixing of the LEDs during the measurement is also managed identically, with the FPGAEnLED signal.

4.7.3 FPGA connections

Based on the above, it was necessary to identify a suitable FPGA for what was required. In this case the choice fell on the AGL030V5VQG100 [60], an IGLOO Low Power Flash FPGA. As mentioned, this research activity has developed on circuit design at the level of signal conditioning and for this reason the inclusion of this component has been indicated on the basis of further studies, which have also elaborated and produced the relative firmware on the basis of the operating idea previously reported. Therefore, we have limited ourselves to making the necessary

connections regarding input/output signals and the necessary power supplies, as well as defining a printed connector through which to interface with the programmer tool. *Figure 4.21* shows the circuit diagram that describes the connections relating to the FPGA.

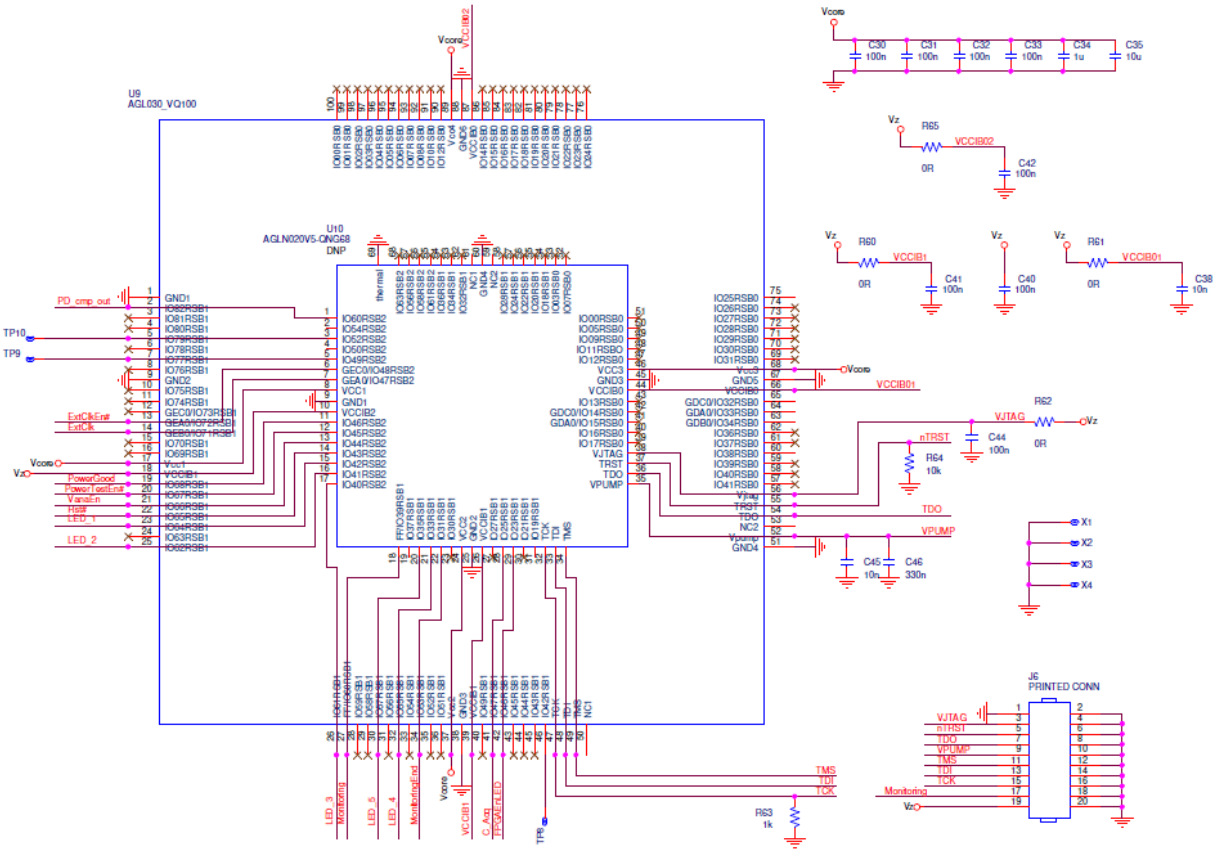

Figure 4.21: FPGA connections

4.7.4 Remote control stage

Lastly, a stage dedicated to remote control was designed with control through a relay board that can be interfaced with a generic PLC. In this case, what has been designed deals with signalling the disabling of the remote station if a manually intervention occurs on the local station, disabling, following a click of one of the buttons, the remote control for a time equal to 5 minutes. At the same time, the externalization of the signals useful to be exchanged with the interface board (which will be discussed later) was also envisaged. Since it is possible that there are connection cables between

the local station and the remote station with a length that can reach 50 meters, the possible voltage drop on the line has been evaluated as not considerable and therefore irrelevant in practice, given the small voltages and currents what it is for these signals. Eventually an external 24V power supply from the remote station to the local one is also provided. What has just been described briefly is shown in the circuit of *Figure 4.22*.

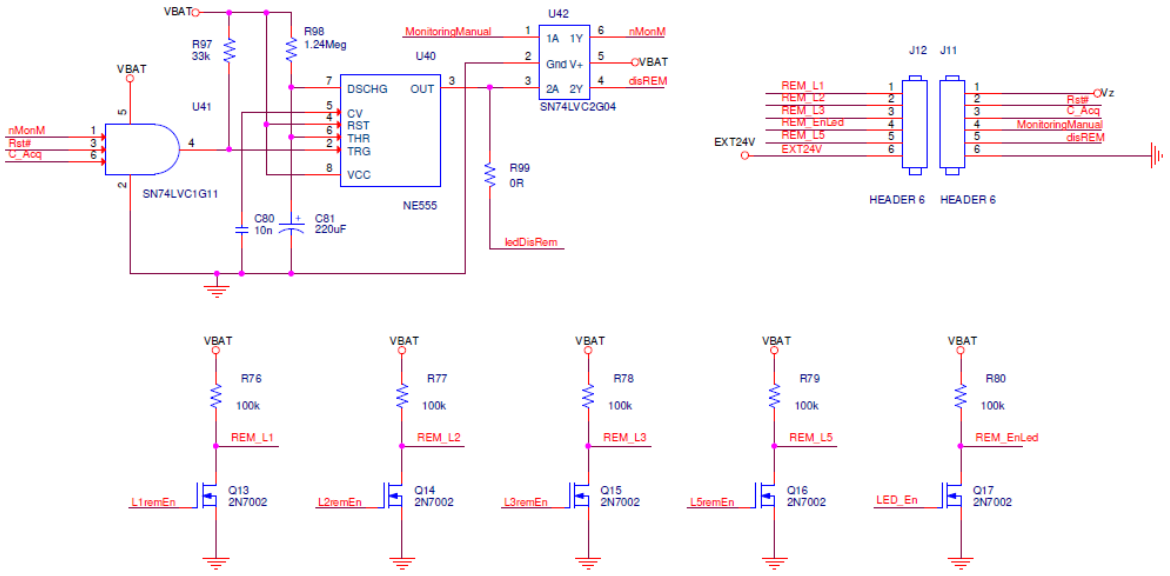

Figure 4.22: Remote control stage circuit

The figure shows remote LED signals, whose control is always managed through 2N7002 transistors, pull-upped to the supply voltage VBAT, and remote connectors. However, the fundamental part concerns the timing circuit for disabling the remote control. Through the use of a NE555 [61] and some logic gates it was possible to adjust the disabling time, obtaining a signal that is sent to the remote station informing it not to act in any way on the local station, because someone on site has already clicked a button. The components shown in the figure are those sized in such a way as to obtain a disabling signal with a duration of 300s, or 5 min. Furthermore, it is also possible to observe locally that the disabling of the remote control has been activated, through the lighting of an appropriate LED. For signal compatibility with the interface board, the NE555 output signal is negated with a NOT gate, while an OR gate, in which inputs refer to the signals relating to the buttons, is placed on the trigger pin of

the timer, in order to detect the click of one of these. The result of a simulation of the circuit relating to the NE555 only, is however shown in *Figure 4.23*. The simulation refers to the case in which one of the three buttons is pressed during remote control. This event consequently activates the NE555 output, which remains high for 300s, as requested. Everything is defined through the appropriate choice of the passing components and easy and simple to eventually redefine different time intervals according to the needs.

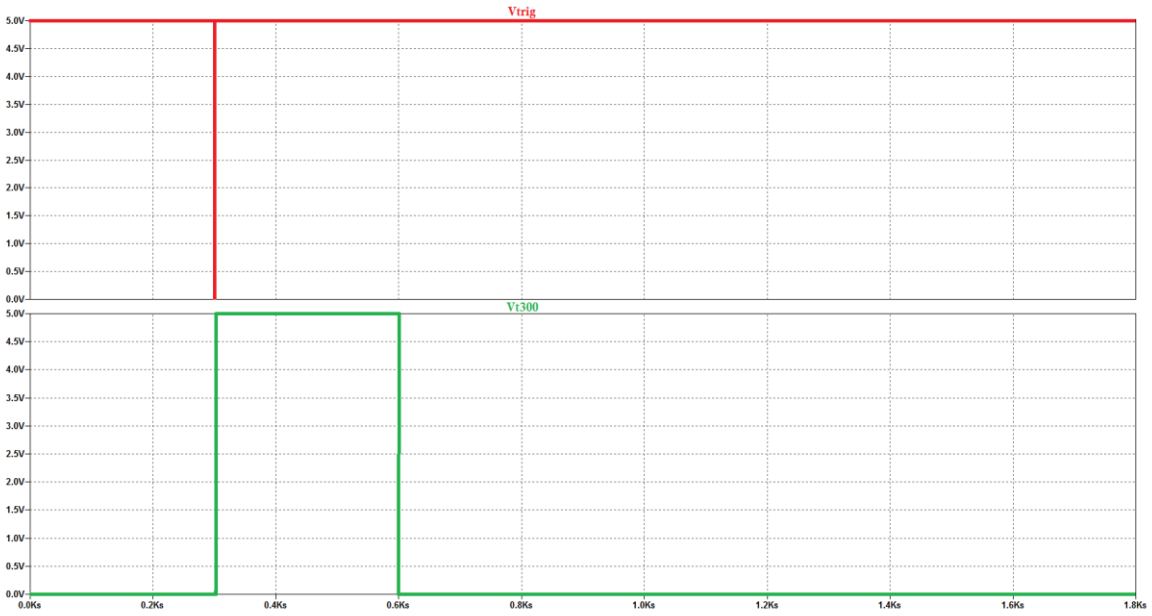

Figure 4.23: Simulation for the disable remote control signal

The red trace therefore refers to the output signal ideally from the OR logic gate. While the green trace is relative to the output of the NE555 and from which it is evident that the signal is actually high for the duration of 300s and is activated right at the click of one of the buttons.

4.8 PCB: SolBox® design and realization

Having concluded the circuit design, it was possible to proceed with the design of the PCB layout and the realization of the devices.

4.8.1 Main board

As has been said, it was decided to create a single flexible board, which can be used in a common way for different versions and applications, without having to print a different board each time. In this way, a single board is suitable for different uses and packages. Roughly the tricks used in the layout design are the same as those adopted for the previous conducted devices, for this reason they will not be further mentioned and the results obtained from the PCB design at the layout level will be briefly reported. The board obtained has the dimensions of 103 mm x 92 mm and has four fixing holes. As can be better observed from *Figure 4.24*, which shows the shapes of the components placed on the top and bottom layer, the quantity of components adopted in this board is substantial.

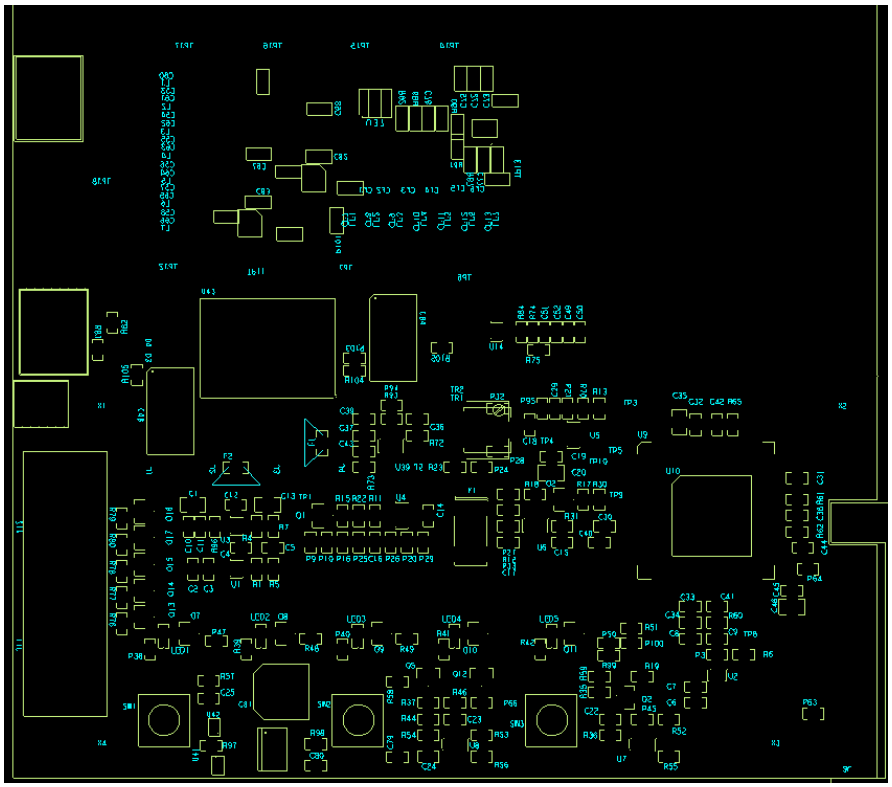

Figure 4.24: Placement - PCB design view

To better clarify the differences between Top and Bottom layers, the images relating to them are shown respectively in *Figure 4.25* and *4.26*.

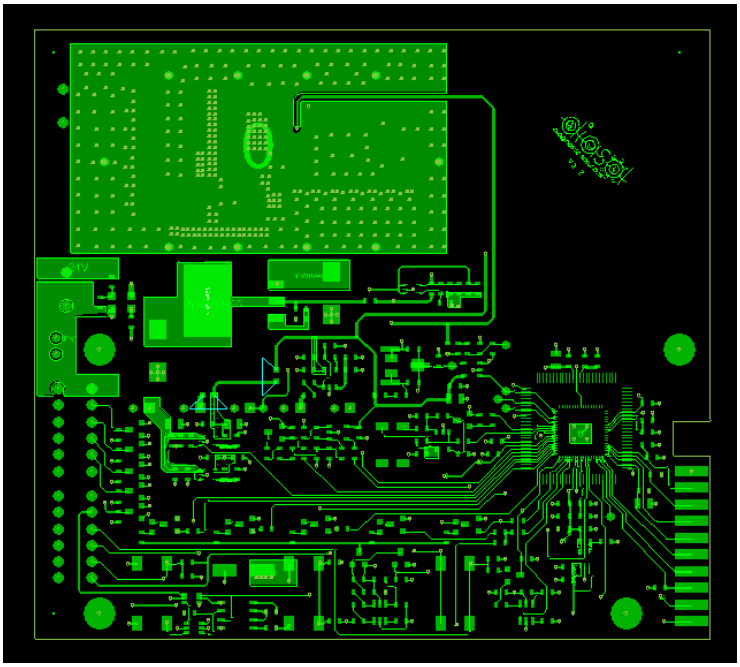

Figure 4.25: Top layer - PCB design view

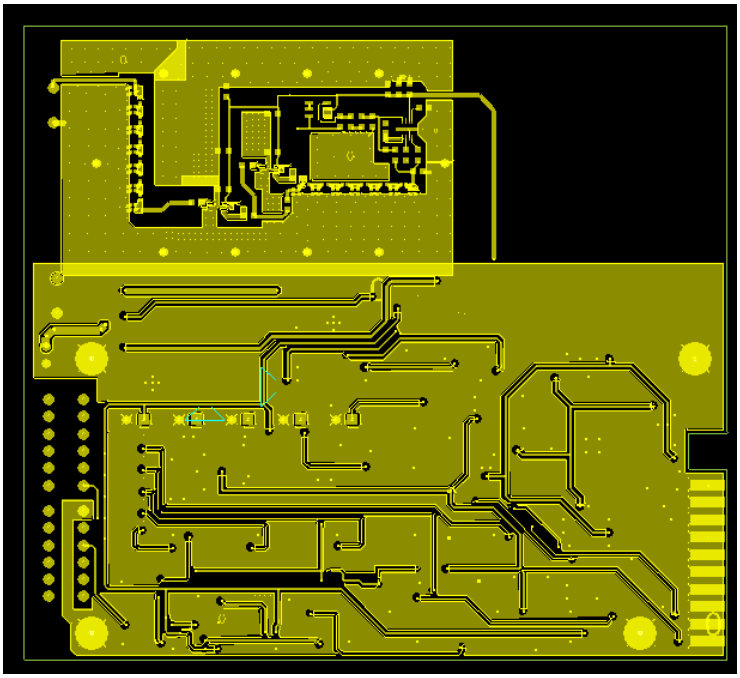

Figure 4.26: Bottom layer - PCB design view

Finally, a global view of the layout created is shown in *Figure 4.27*.

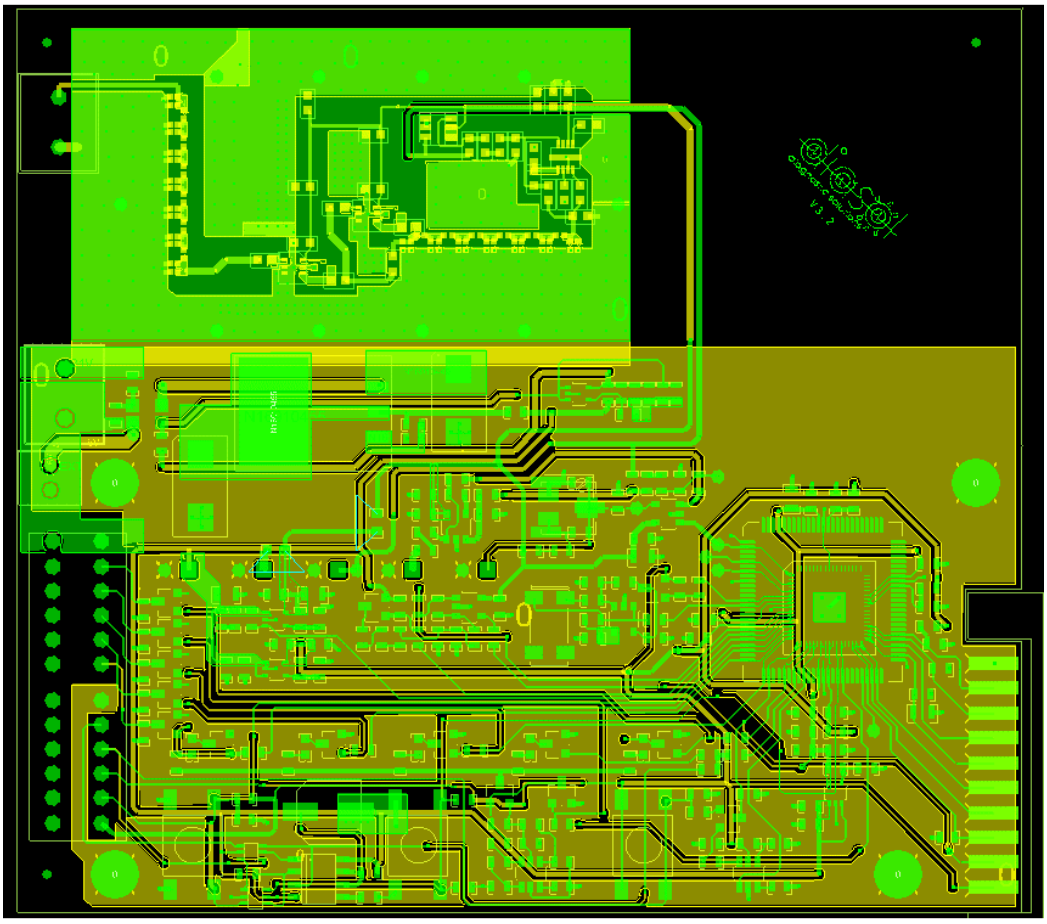

Figure 4.27: Complete PCB design view

From the figure, in particular, it is possible to identify at the top, on the bottom layer, the section relating to the conditioning (filtering, amplification and frequency conversion) of the signal captured with the antenna, while just below, but on the top, the relative section to the power supply. Moving further below, on the top layer you can identify on the left the analog pre-processing section and immediately on the right the digital part dedicated to the FPGA. Finally, at the bottom, on the top layer, there are the circuit sections relating to the interface with the user (LEDs and buttons), together with the optional circuit for disabling the remote control. Numerous connectors can also be observed, useful for connections to the outside and suitably provided with panel connections in the board package.

A further aspect of the design also involved the insertion of the silkscreen layers and those relating to the soldermask, as well as the generation of all the files useful for printing the boards and for any mounting machine. Following the design of the PCB

layout, the necessary files were generated, including the Gerber, for the manufacturer of the printed boards for the realization of these. These boards, in the last version have been mounted with ad hoc automatic machines. An example of a board created is shown in *Figure 4.28*.

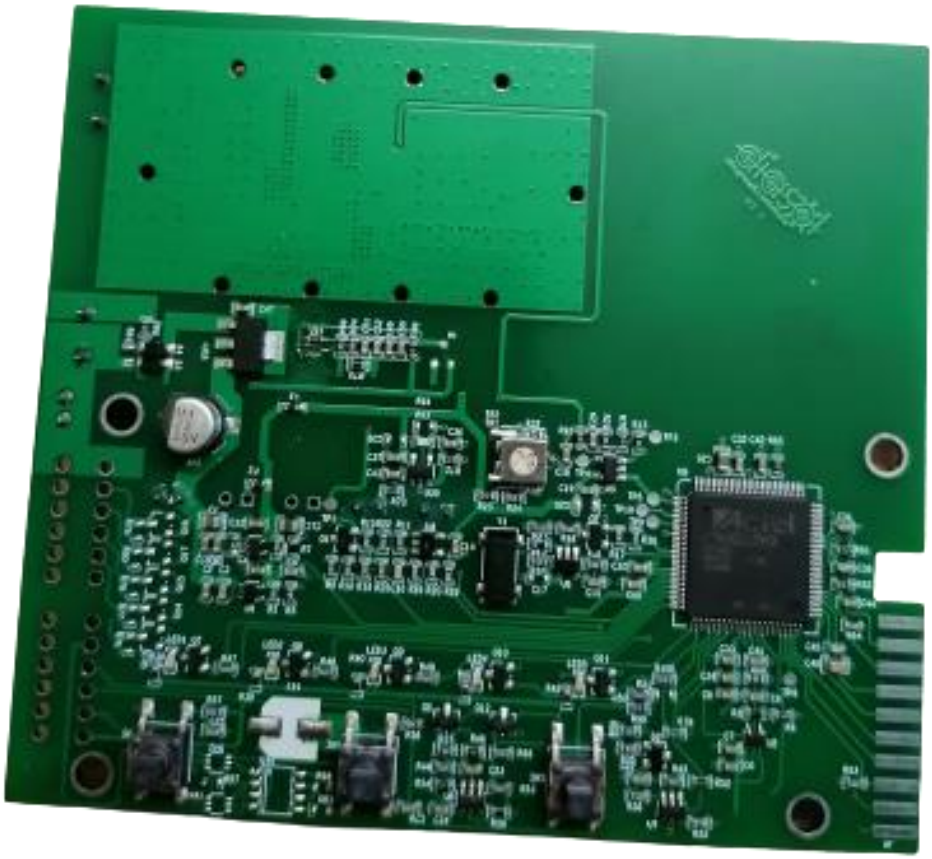

Figure 4.28: Example of SolBox® board

At the packaging level, as will be seen in the next chapters, different packages have been provided according to the version adopted, but as an example one of those available in *Figure 4.29* is shown.

Figure 4.29: An example of packaged board

4.8.2 Optional board: SolREM

As mentioned, an interface board has also been developed that can be connected to the local station with the main board to implement remote control via PLC. The board in question has been named as SolREM and basically has a series of inputs and outputs controllable through relays driven by the local station or the PLC, depending on the direction of the signals. This was designed at the circuit and layout level, printed and assembled manually, but due to lack of time, it was not possible to perform functional tests in this research activity. The basic idea is to control relays with a PLC to emulate the click of the buttons with a remote command, while in the same way you want to inform the PLC of the LEDs lit on the local station, if this is not accessible. In this way, all possible feedbacks have been externalized and remoted for a user, who for various reasons cannot easily access the local station and therefore relies on a remote station interfaced with a PLC or in any case other programmable embedded devices that are compatible with such logic. As for the choice of relays, it fell on the HE721A0500 [62] component, as it has voltage levels compatible with most PLCs and embedded devices. Other elements of concern are the power supply circuit, based on the LM2940IMP-5.0 IC [63], which allows a linear regulation of 5V, in

correspondence with a 24VDC input. Furthermore, the connection with the local station is provided through a 12-pole connector at panel and a respective shielded multipolar cable, on which the power supply is also reported, in addition to the remote signals, while the connection with the PLC through multi-way screw connectors.
In *Figure 4.30* one can observe the result of the circuit design.

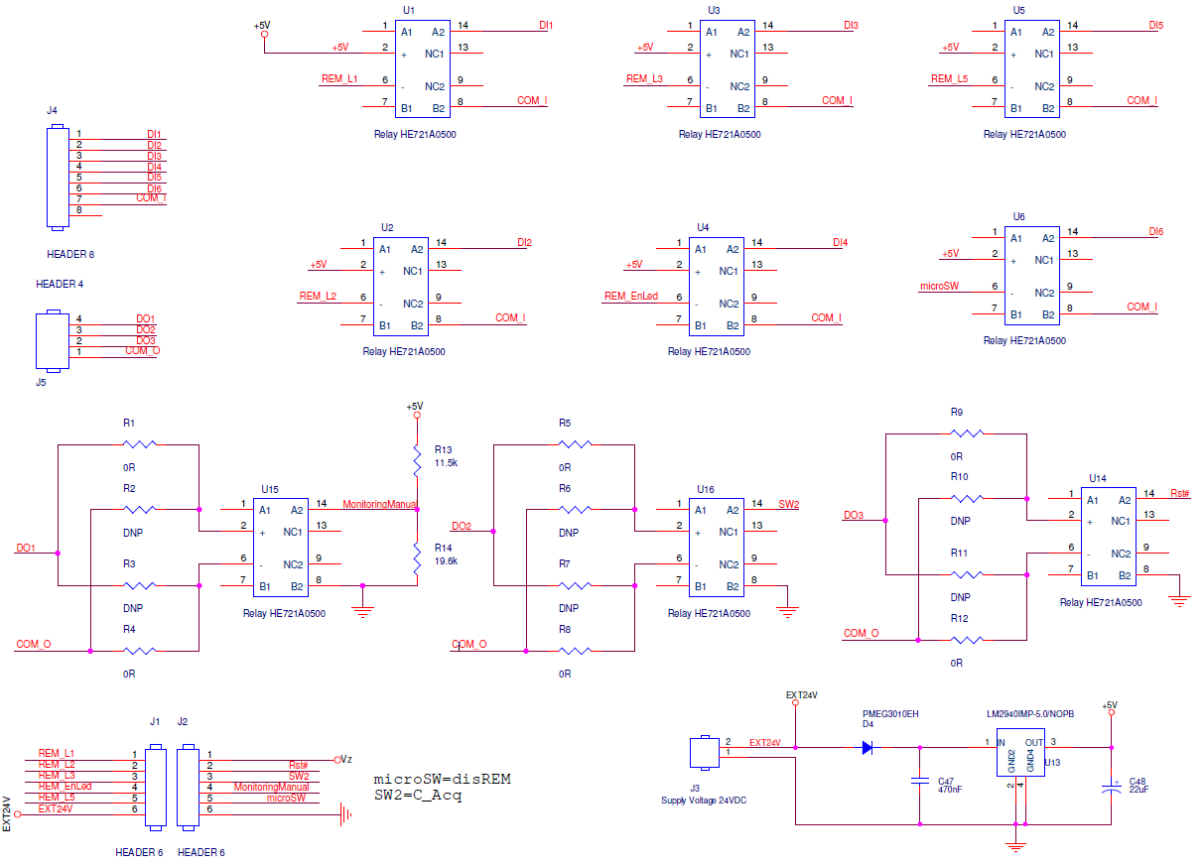

Figure 4.30: SolREM circuit

At simulation level, a series of tests were performed, with a generic model for the relay, which highlighted the effectiveness of the designed circuit correctness, but for brevity will be omitted because of little importance, just know that they gave expected results. At the end of this inspection phase, it was possible to proceed with the PCB layout, in which no particular precautions were necessary, except for the placement of the connectors at the ends of the board to then provide for the panel connection in order to correctly package the board. In this regard, *Figure 4.31* shows the layout generated with CAD, which is then followed by the generation of files useful for

printing. Instead, in *Figure 4.32* it is shown the image of the assembled board, while in *Figure 4.33* it can be seen the board packaged in the full version.

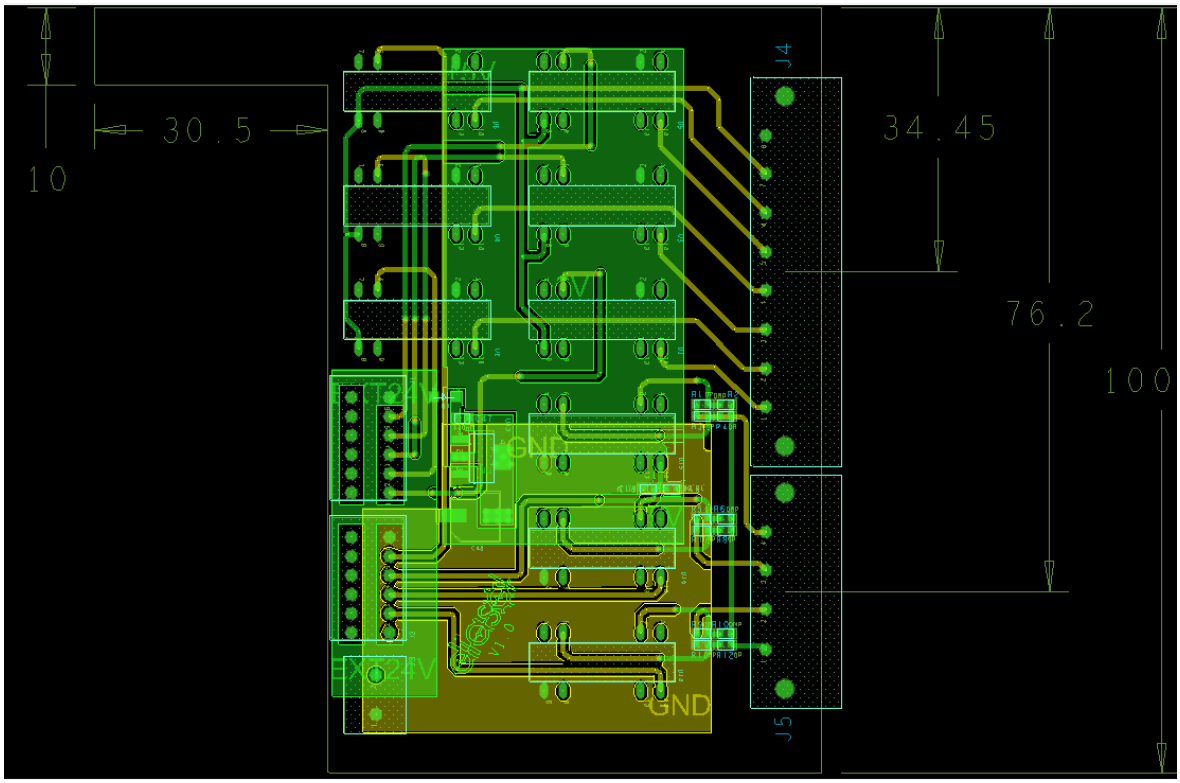

Figure 4.31: SolREM - PCB layout view

Figure 4.32: SolREM - Complete mounted board

Figure 4.33: SolREM - Packaged board

4.9 SolBox® versions and real measurement

As discussed above, given the flexibility of the board, different versions of the device described have been predisposed, which at the same time can be differentiated according to the type of power supply used for the machine, apparatus or component under test and the category of the same. The different versions and the measurements made on the basis of different supply voltage will then be analysed.

4.9.1 SolBox® versions: FE, HS and RSC

Based on the different needs, three different versions of the device have been developed, each of which makes use of the same identical board with only some variations on some components and circuit parts, defined as follows:

- *Full Embedded (FE)*, in which antenna and board are enclosed within the same package, so as to be able to apply the device externally near the machine or

equipment that needs to be controlled, without having connection cables given the battery powered.

- *High Sensitivity (HS)*, in which the antenna is separated from the board, which is packaged independently. In this way it is possible to position the antenna itself inside the terminal box, if possible, and in any case in places where it is difficult to position a packaged board. For this reason, the antenna is only resin-coated without having its own package, but there is also a version that includes the package, if more space is available or for other needs.

- *Remote Signalling and Controlling (RSC),* is a variant of the HS version, which involves the use of the remote control station to manage the local one, which may not be easily accessible on site, for the reasons already mentioned.

Depending on the needs, each of these versions can be adapted to be powered by batteries or through an external power supply, but much depends on the characteristics of the application and the use to be made of it, which is why this customization is provided.

The different versions and their configurations are summarized below in *Figures 4.34*, *4.35* and *4.36*.

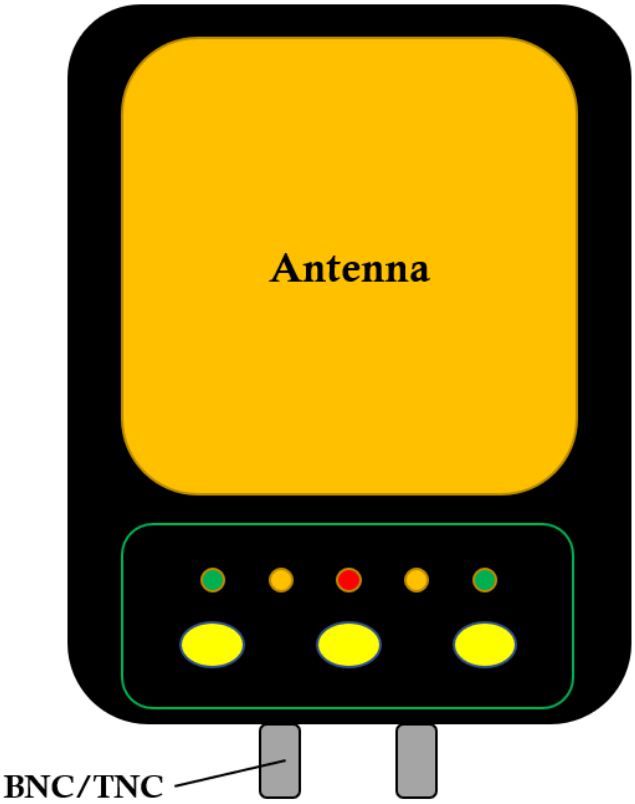

Figure 4.34: FE version representation

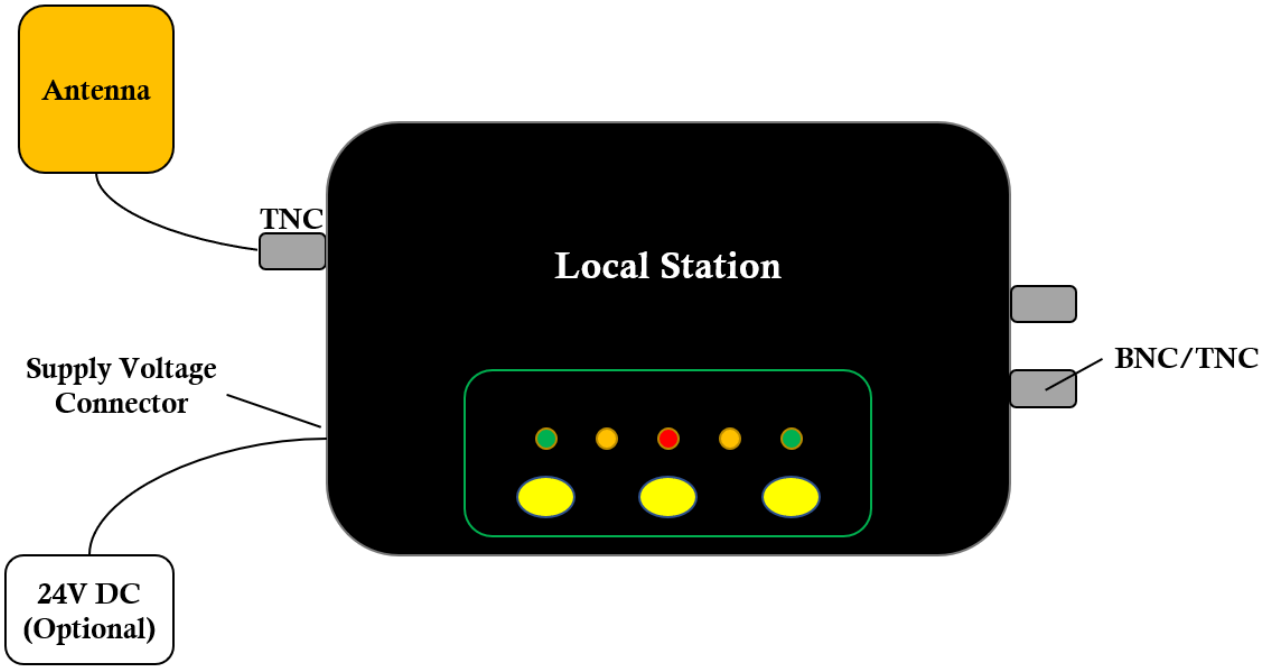

Figure 4.35: HS version representation

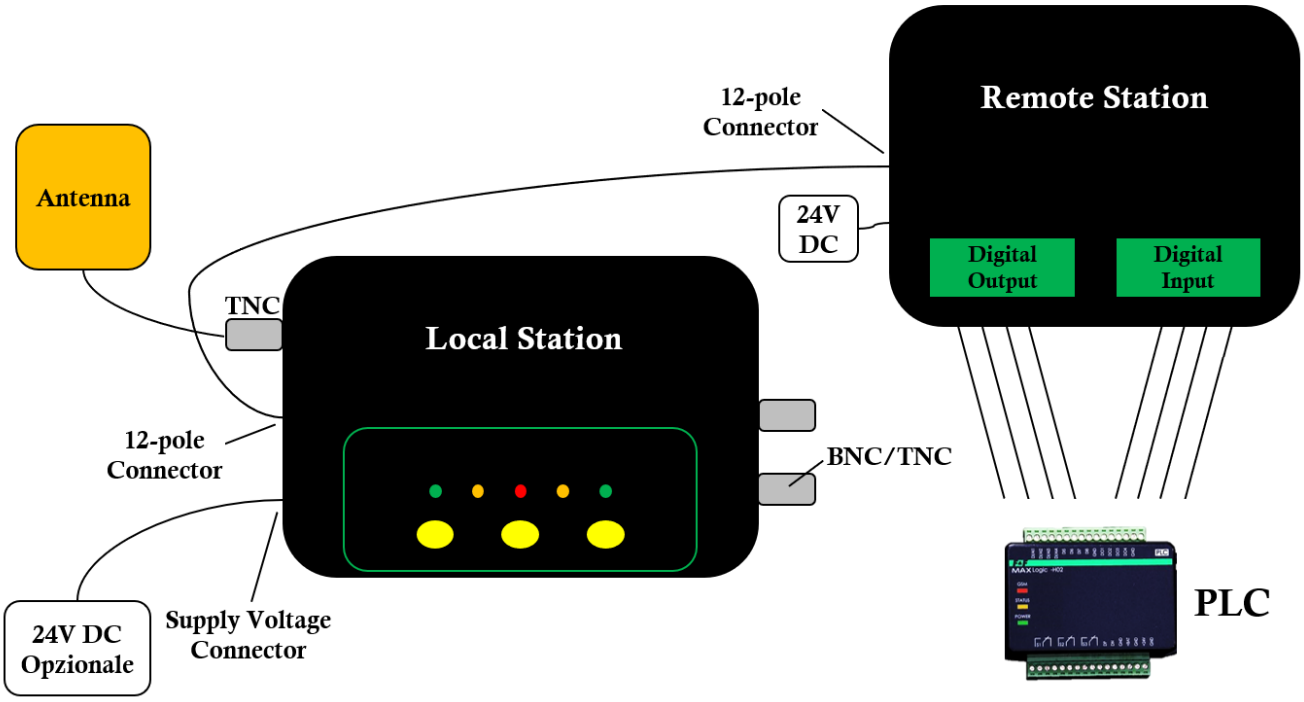

Figure 4.36: RSC version representation

Each of the packages is structured to fix the board to one of the walls, so that the buttons can be clicked and the LEDs can be seen when they light up. In addition, there are connectors that guarantee at least, in part or totally, the IP55 degree of protection. If BNCs are mounted, instead of TNCs, this is partly true because the connection cables must be present to guarantee the required degree of protection. from this point of view, the TNC solution is the best, but a lot depends on the specifications required by a potential customer. However, two solutions are totally interchangeable. To complete what is described in this context, the 3D drawings of the packages of the various versions are shown below, as can be seen in *Figure 4.37*, *4.38* and *4.39*.

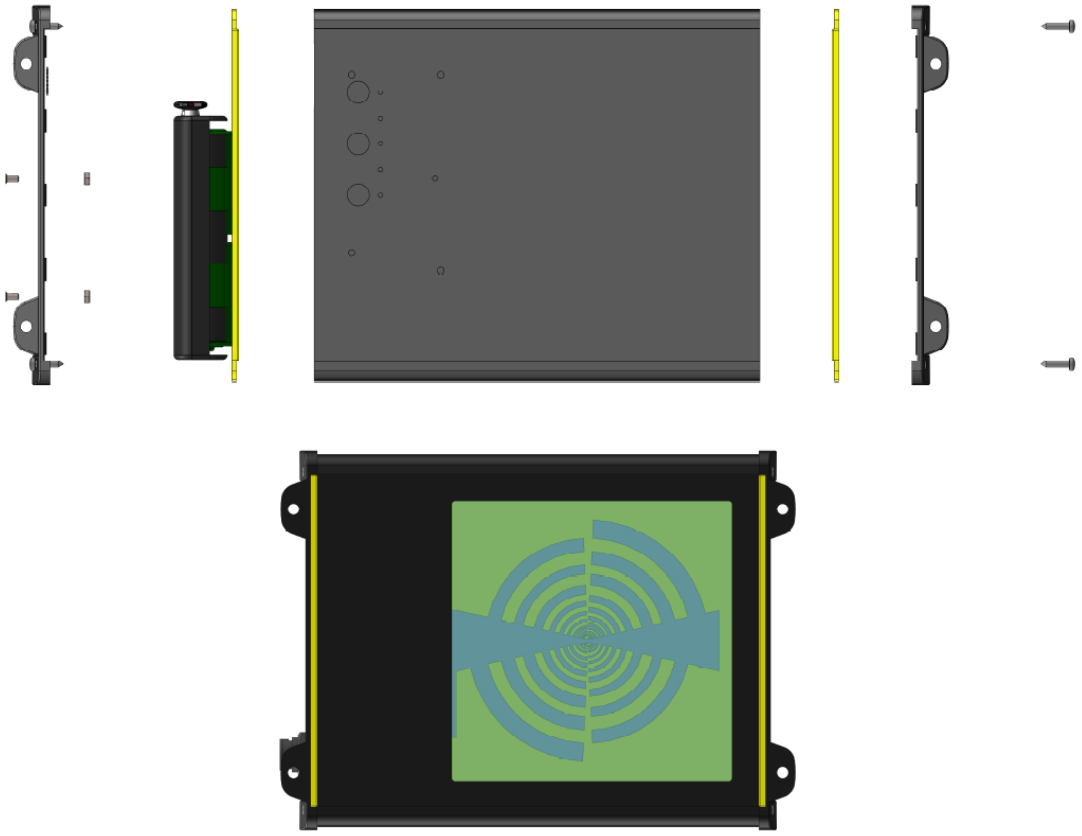

Figure 4.37: Full embedded packaging

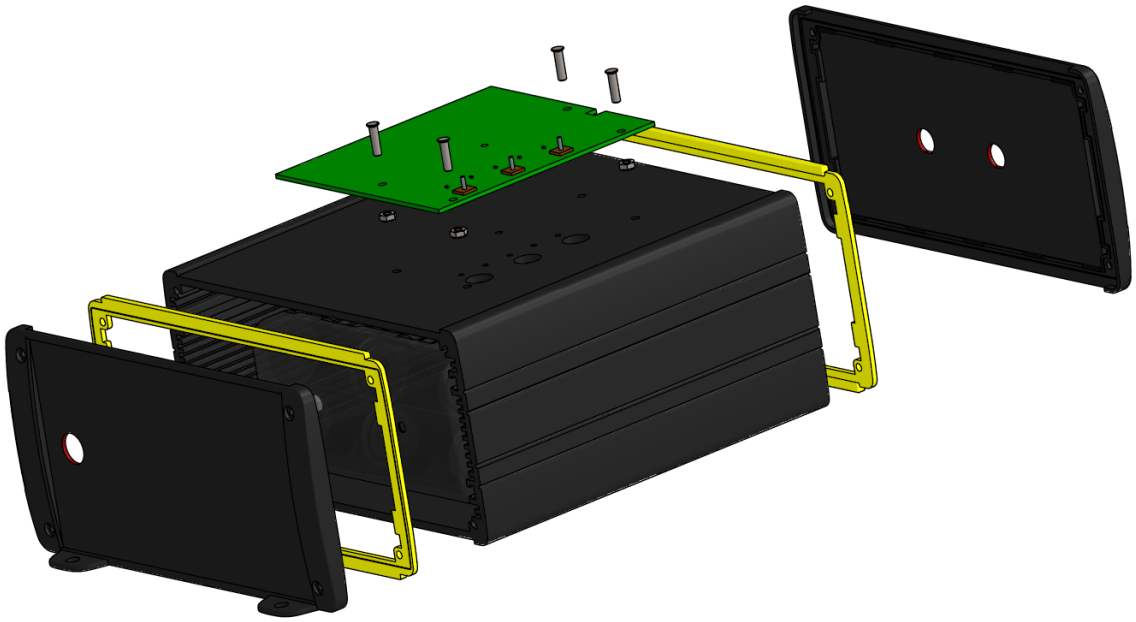

Figure 4.38: Local station packaging

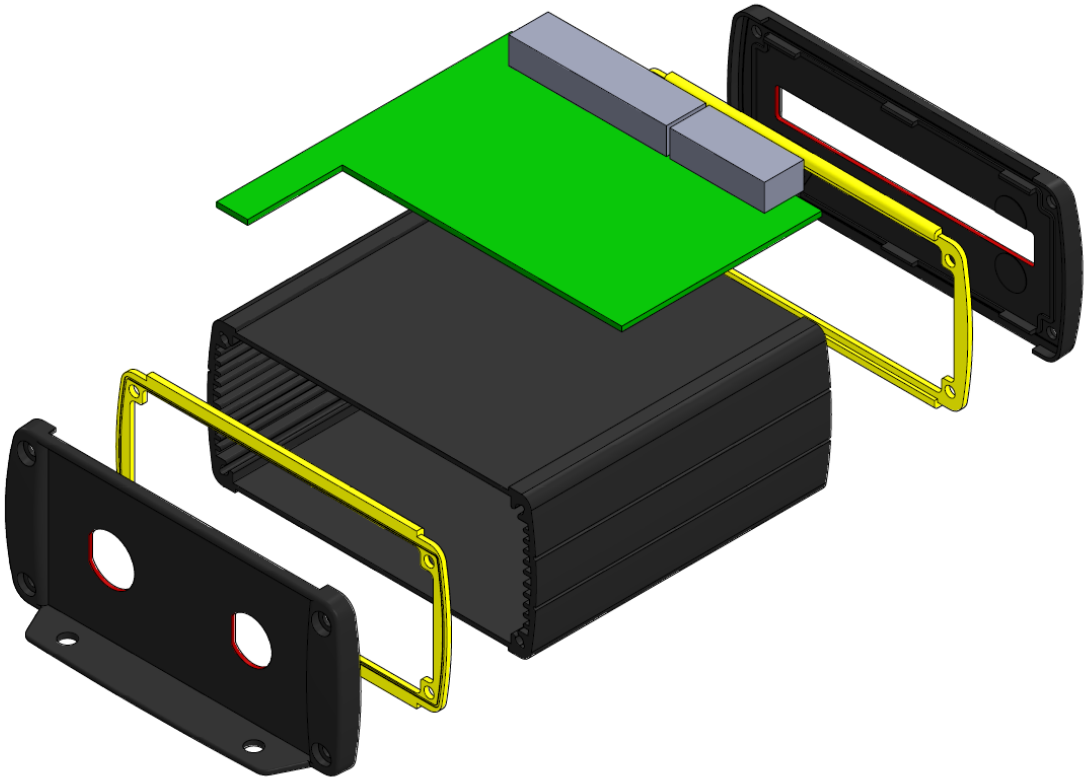

Figure 4.39: Remote station packaging

4.9.2 SolBox® real measurement

As previously said, a further distinction must be made for the device developed on the basis of the type of power supply adapted by the electrical machine or apparatus under test. Based on this, two different filters have been identified to adapt the device to the measurement of discharges according to the PWM or sinusoidal power supply. Therefore, a real case of measurement with PWM power supply will be analysed first and then the one with a classic sinusoidal one.

The first case refers to a power supply whose waveform is shown in *Figure 4.40*.

Figure 4.40: PWM power supply

It is a signal with a fundamental frequency of 3kHz and a switching frequency equal to 24kHz. The rising and falling edges have a dV/dt slope of 1.5kV/µs, while the maximum peak value reaches 3kV. The waveform was generated using the Tektronix AWG2005 function generator [64], whose signal was then amplified through AWADIT, which is nothing more than a gauge tube amplifier with gain equal to 1000, made for the University of Genoa in previous years to this activity.
The block diagram of the scheme adopted in this case is the one shown in *Figure 4.41*.

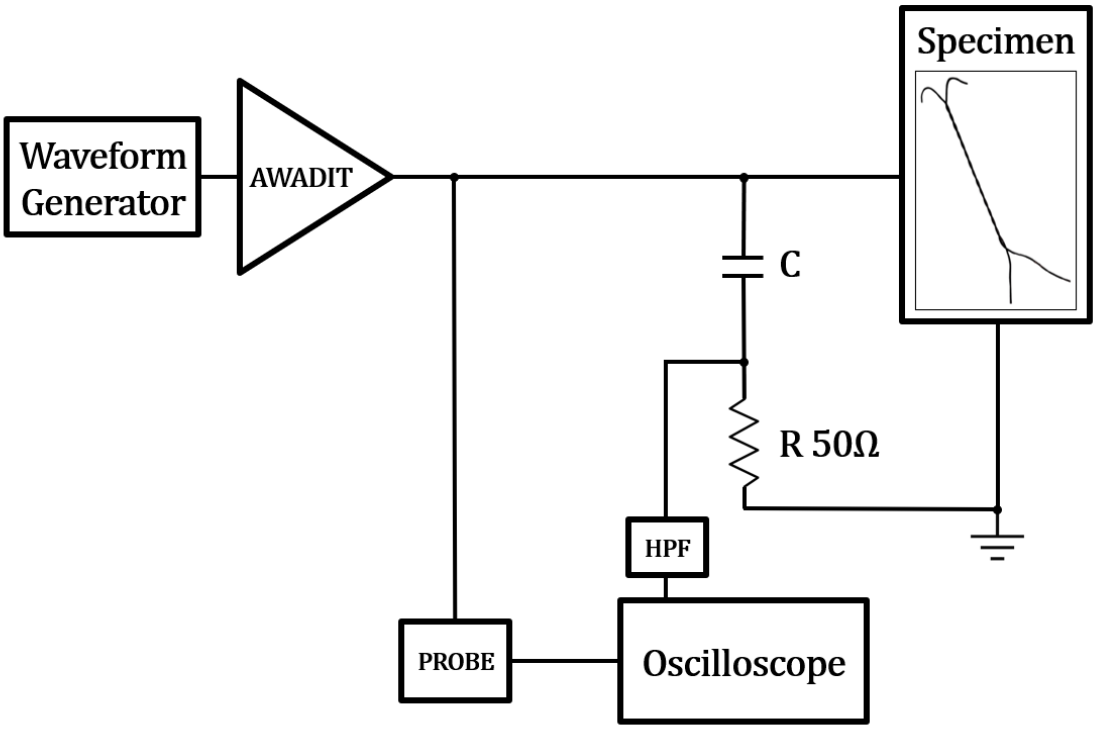

Figure 4.41: System for measuring discharges with PWM power supply

The system adopted foresees the positioning of a twisted pair specimen, made according to CEI EN 60851-5, inside a temperature-controlled oven. This specimen-based system simulates the behaviour of a low voltage motor where the windings are made by means of enameled wires and powered by an inverter. For the irradiated measurement it will be sufficient to place the SolBox® (in this case, FE version) near the oven wall and connect it to an oscilloscope if it is necessary to observe the discharge signal or otherwise simply observe the activity of the luminous LEDs and possibly intervene to deepen. Obviously in this case the direct signals on the oscilloscope will be observed, so as to observe the correct functioning of the device in terms of conditioned signal, which is the core issue relating to this activity. At the same time, however, it is also possible to observe the conducted signal suitably filtered with an HF high pass.

Once the structure of the tests has been defined, the results obtained can be analysed to validate and verify the correct functioning of the device for irradiated discharge. The first situation to check is the actual and correct detection of discharge, to be sure of this it is necessary to refer to the conducted signal. In particular, see what is reported in

Figure 4.42, in which an example of oscilloscope acquisitions (with the usual instruments adopted in this activity) is reported for what has been mentioned.

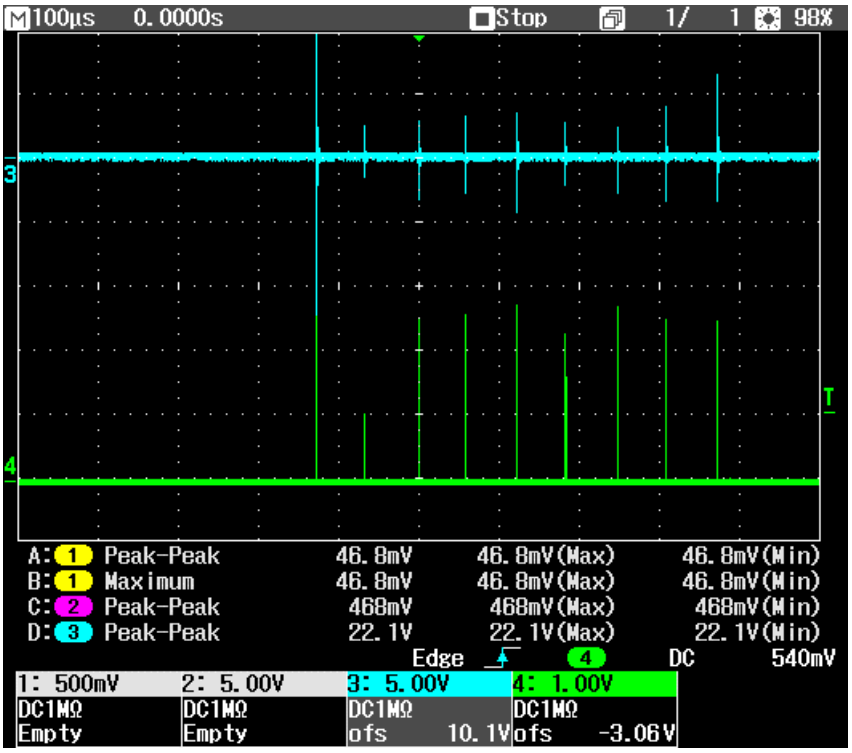

Figure 4.42: PWM - Conducted vs irradiated measurement in a 1ms interval

In the graph it is possible to observe a light blue trace relating to the conducted discharge signal, while the green one refers to the signal received by the SolBox® (on output buffer). It can be clearly observed that following a discharge in the conducted system, a discharge is also detected in the irradiated system, remembering that, due to the nature of the problem, there is no need for information on the amplitude of the signal, because this system simulates the behaviour of a low voltage motor where the windings are made by enameled wires. Furthermore, there is an excellent signal to noise ratio, given that the background signal is very clean, as can be seen from the figure. Once the goodness of detection of the discharge has been ascertained, it is possible to observe it is possible to observe PDs phenomena, obtained over a wider time interval which, as can be seen in *Figure 4.43*, in this case is equal to 10ms.

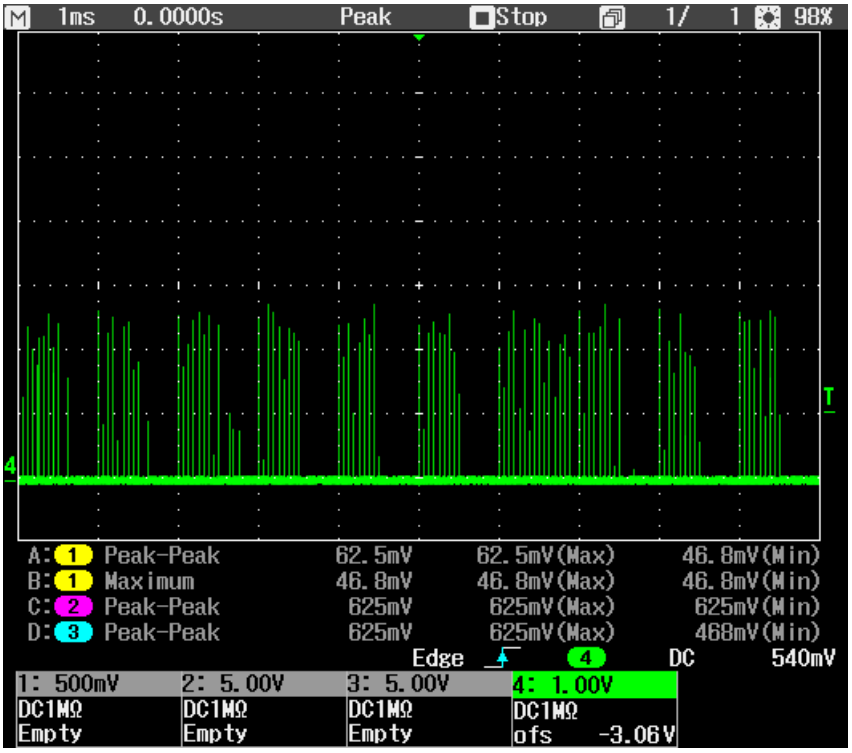

Figure 4.43: PWM - Irradiated measurement in a 10ms interval

From this graph it can be seen how the maximum voltage level reached is compatible with the supply voltage value that can be reached with the components used, i.e. 3.3V. Furthermore, considering that for the pulse number count, the signal will be further processed by an operational amplifier, configured as comparator, that will bring it into saturation if the defined attention threshold is exceeded, but this topic will be addressed following. Another aspect to note is the repetition of pulse signal patterns which are very similar. This characteristic is due to the measure of the type of power supply since the discharges occur in correspondence with the PWM impulsive peaks. All this shows that the circuit is actually working correctly, given that the amplitude and distribution of the detected discharge pulses are consistent with what is expected.
Obviously, following a discharge of this type, the activation of the alarm levels is indicated by the lighting of the LEDs, but since this research activity is not focused on verifying the goodness of the firmware, this topic will not be dealt with, neither now nor later, but it will limit only to saying that the logical operation of the firmware has been validated, through the appropriate tests.

Other elements that guarantee the expected results can be addressed by analysing the case of measurement with a system powered with a sinusoidal waveform. Other elements that guarantee expected results can be addressed by analysing the case of measurement with system powered with a sinusoidal waveform. In this case, the system adopted is based on the block diagram shown in *Figure 4.44*.

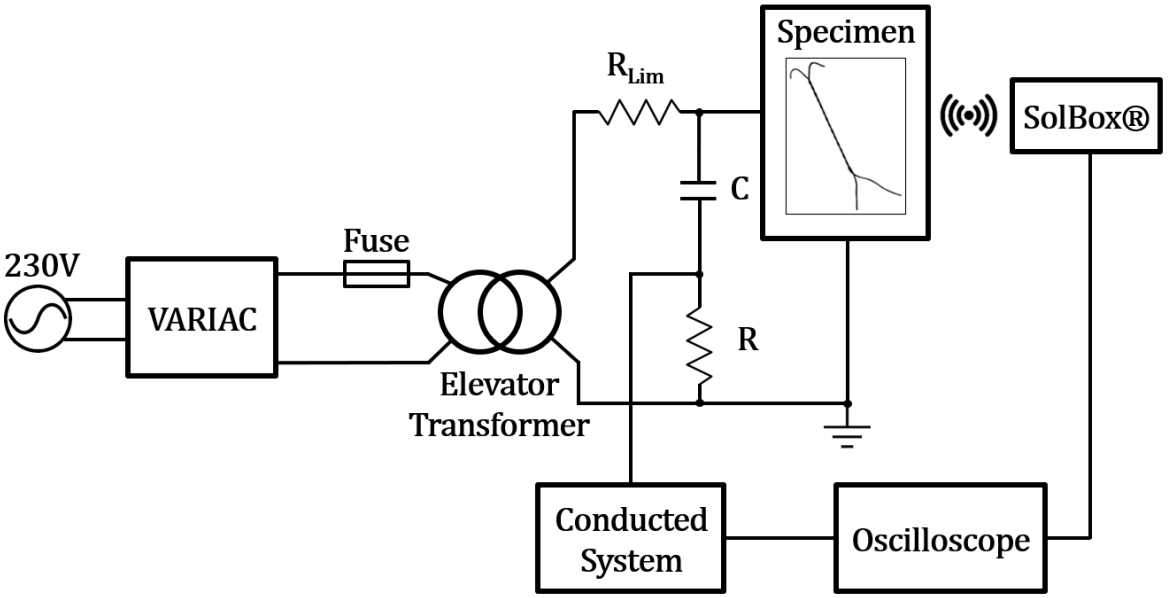

Figure 4.44: System for measuring discharges with sinusoidal power supply

The waveform used is a classic 50 Hz, supplied by the electrical network, followed by a variac and an elevator transformer. Also in this case, a twisted pair specimen is used to emulate the winding of an electric machine and the possibility of acquiring, with a digital oscilloscope, the conducted signal is also provided. At the same time, the irradiated measurement takes place with the SolBox®, this time in the HS version, positioned near the object under test. Also in this different situation, the comparison with the conducted system found the actual goodness of detection of the discharges, as can be seen from *Figure 4.45*. Take into consideration that, given how the problem is structured, the representation of discharges in the conducted system will be with alternating polarity.

Figure 4.45: Sinusoidal - Conducted vs irradiated measurement in a 20 ms interval

In the graph, the yellow trace refers to the radiated signal, while the green trace refers to the conducted signal and, as mentioned, the correspondence between conducted and irradiated discharges (on output buffer) is verified. Furthermore, it can be observed that, as in the previous case, also here the maximum voltage level reached is compatible with the supply voltage in compliance with the components used. For the same reasons as in the previous case, it can be concluded that the operation of the system is the desired and expected one. A further observation can be made regarding the zoom of a single discharge phenomenon, as can be seen in *Figure 4.46*.

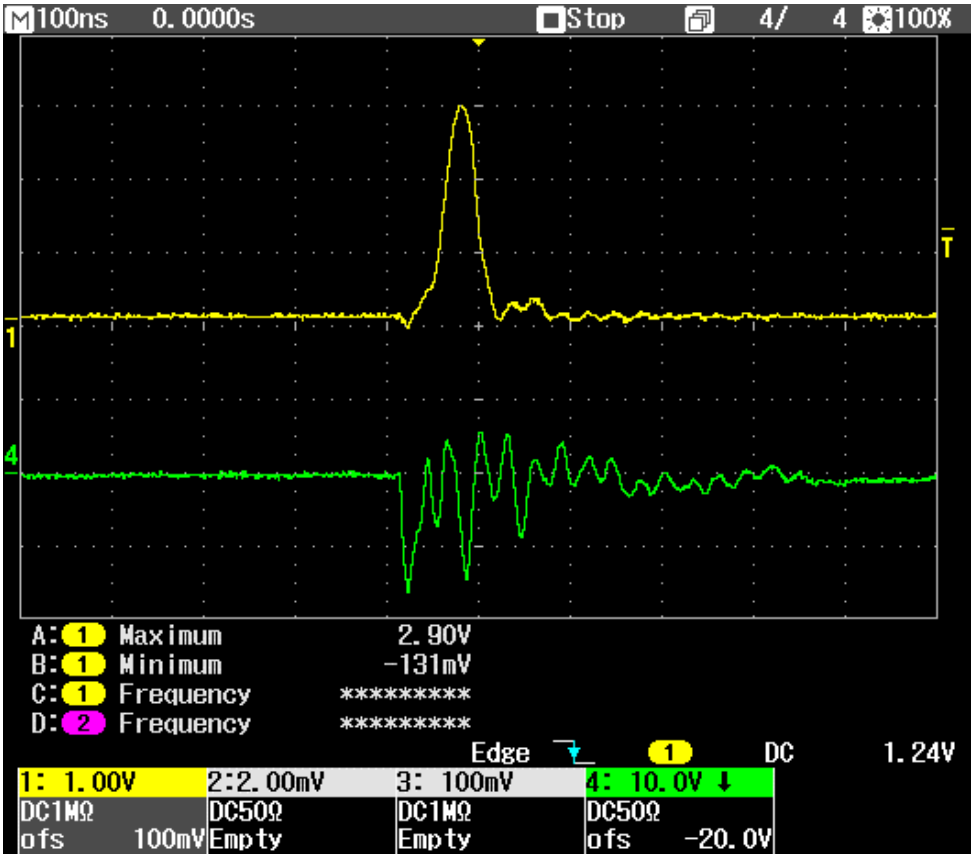

Figure 4.46: Sinusoidal - Single discharge zoom

In this graph, the signal of a single discharge measured with the conducted system is shown in green, compared with the signal picked up by the SolBox® (yellow trace). It is observed that, as expected, only one discharge impulse is shown in the yellow trace, given the processing carried out by the power detector. Furthermore, even in the condition of a signal conducted at negative values, a respective completely positive signal is returned to the irradiated, so as to facilitate comparison with the comparator and to be able to provide a signal compatible with the acquisition with programmable logic. Also in terms of voltage level, reasonable values are reported, while with regard to the rising and falling times, they amounted to tens of nanoseconds, as well as expected in this case. Another observation may concern the background noise, which, as can be seen in the yellow trace of *Figure 4.46*, appears to be of reduced value compared to the useful signal, attested in about 250mV of maximum peak amplitude, and visible with small and really limited impulses close to the discharge phenomenon. Thus it is evident that the signal-to-noise ratio is excellent and, in the presence of a

signal with an amplitude of about 3V, approximately equal to 12. In addition to this, it is sufficient to set the threshold level of attention for the comparator just at above the maximum background noise values so as to discard even these small peaks, avoiding that they are counted as discharges. The aspects addressed with regarding the use of the comparator can be better observed in the oscilloscope acquisition graph of *Figure 4.47*.

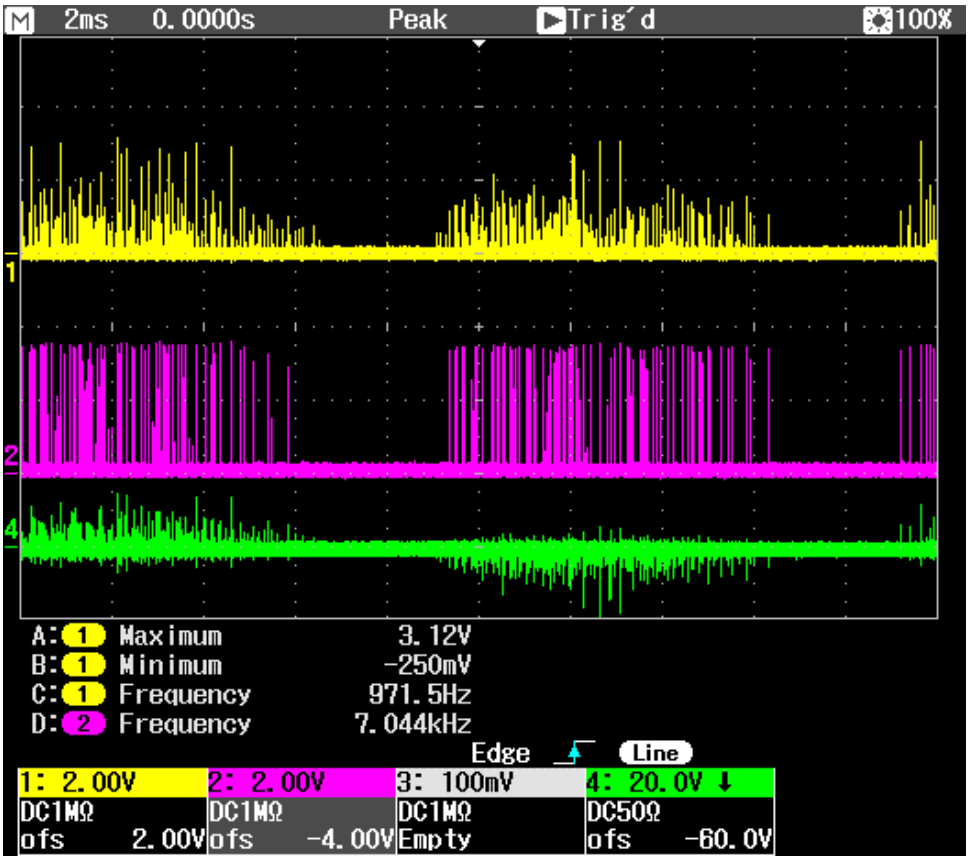

Figure 4.47: Comparator signal

Compared to the yellow and green traces, which are analogous to those shown in the previous figure, the signal relating to the comparator output can be observed in fuchsia. From this it can be observed that, in addition to respecting the detection of the discharges, the signal of the discharges that exceed the threshold is actually saturated in value at the power supply voltage level, levelling at about 3.3V.

Finally, a consideration may concern the behaviour of the power detector. Remembering that it is a logarithmic amplifier that takes care of obtaining a sort of

envelope of the signal it receives at the input on the basis of the power associated with it, in *Figure 4.48* the signal relating to this is reported in comparison to that of the conducted signal and the irradiated one.

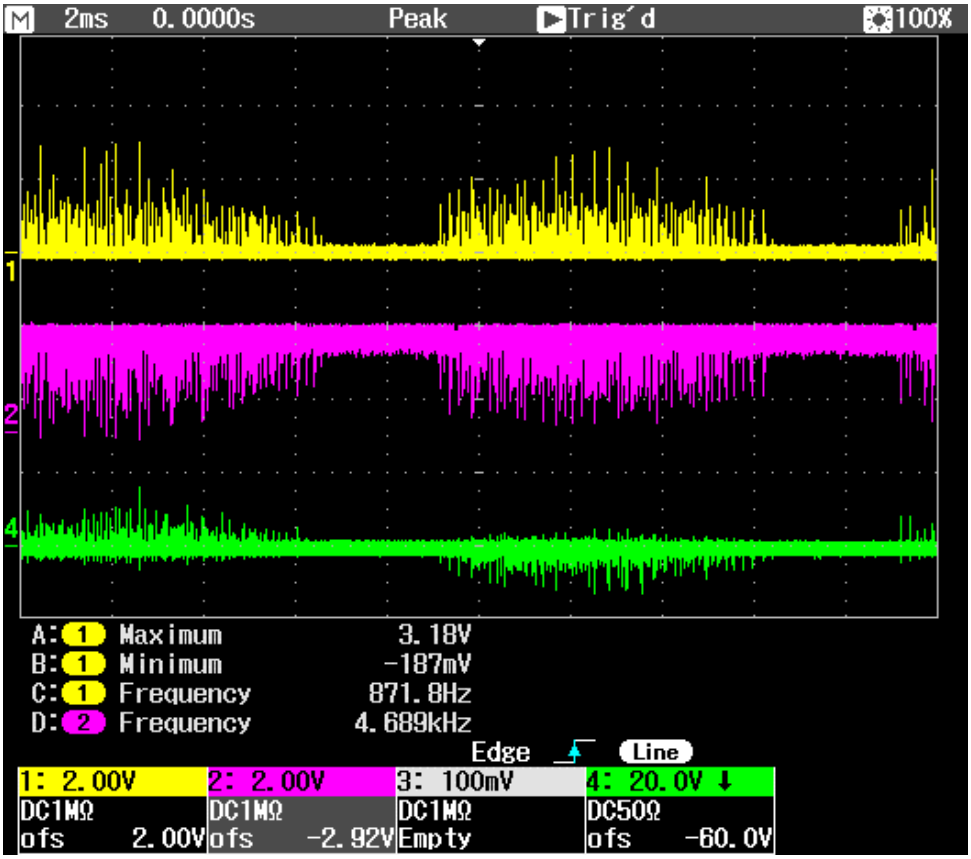

Figure 4.48: Power detector signal

From the graph it is evident how the fuchsia signal, referring to the power detector signal, remains at 3.3V when in idle state, i.e. there is no detected signal. On the other hand, when a signal is present at the input to the power detector, then the output is lowered in relation to the power associated with it, until it reaches almost zero in the case in which it is greater. This trend, as observed from the traces, is then also reflected in the yellow one which refers to the conducted system and an analogy can also be observed with the amplitudes of the green conducted signal. When the power detector signal lowers around zero, the higher amplitude levels are also denoted in the yellow trace, relative to the irradiated measurement. This behaviour appears to be fully expected as planned in the design. This is consistent with the operation of the chosen power detector, in fact, it varies its output according to the power of the signal it sees

at its input. Having negative logic, in the absence of a signal its output is kept at the power supply level, while what is of the signal, it decreases in proportion to the power of the same. This allows to obtain this sort of envelope of the measured signal which allows a "lowering" in terms of frequency value. Since the system in the real case behaves in this way (referring to the fuchsia trace) and considering that in cascade to the power detector there is an operation amplifier in inverting configuration, which only has the task of making the logic positive for ease of management on the part of the FPGA, it can be said that the expected behaviour (highlighted in yellow trace) by the system is to be considered optimal. Therefore, the devices made for the irradiated measurement can be considered validated.

4.10 Possible applications for the developed irradiated system

The possible applications of the SolBox® as already anticipated can be of the most varied as regards the object under test, but what matters is the ability to provide diagnostic information on each of those tested, whether through the analysis of the output signal to the instrument by an operator or the evaluation of alarm levels by means of luminous LEDs and subsequent intervention by an expert user. In the following two possible applications concerning the enforcement in the wind power sector and the test of a real electric motor will be analyzed.

4.10.1 Wind power application

The diagnostics on wind turbines can be limited by the difficult conditions related to the environment on board the nacelles and due to the need to limit machine downtime as much as possible, it is advisable to use measurement systems for partial discharges, which must be as least invasive as possible, such as the one created within this activity. In fact, the shutdown of a wind power plant is obviously a very significant source of economic loss, so it is clear that those who managed them tend to want to stop them as little as possible and a preventive type of diagnostics certainly goes in this direction. It would be possible to intervene only on the machines that really need it as signaled by SolBox® through LEDs or through the analysis of the output signal to the system, which in this case can be remoted using particular industrial PCs connected to the

network, via Wi-Fi or ethernet, so to be checked directly by machine online and without being on site. In economic terms, a wind turbine can generally generate only 25-50% of its nominal capacity, so if the minimum percentage value is taken into consideration, in a working day a turbine, for example of 3 MW, would produce: 3 MW x 0.25 x 24h = 18 MWh = 18000 kWh. In terms of costs, considering an average selling price of energy alone on the open trade is 0.0625 €/kWh, the shutdown of just one wind turbine for a day costs at least 1125€ of lost profit. Considering that the shutdown could involve more machines for several days, the numbers could be higher, in addition to the fact that if no action was taken, there would be a risk of totally compromising the machine, with much more substantial replacement costs.

A possible intervention scheme in the most critical points [65], related to an example of eolic nacelle, for the observation of partial discharge phenomena can be schematized with what can be seen in *Figure 4.49*.

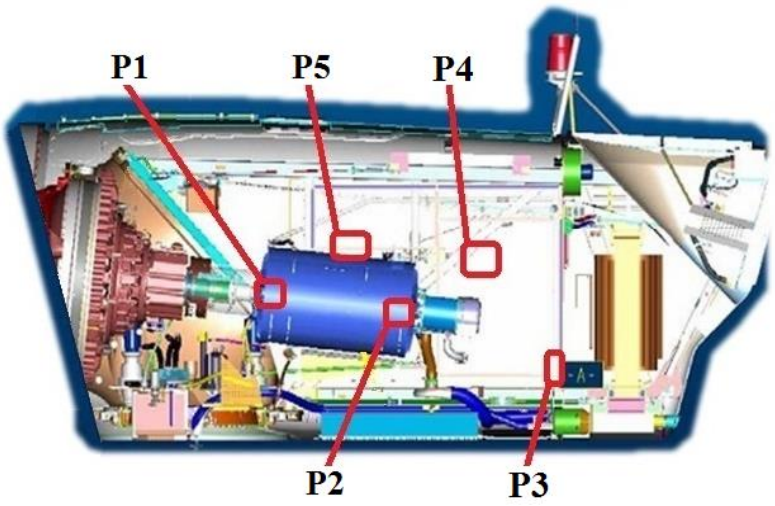

Figure 4.49: Sites of measurement on board of an example nacelle

Referring to figure, two sites, P1 and P2, can be chosen to be place the SolBox® in front of and close to the two generator shields. Other measurements sites can be positioned: one in front of the power transformer named P3, one near the inverter in P4 and one close to the stator connection cables in P5. Depending on the needs, an instrument could be positioned in any of the predisposed versions in configuration for PWM power supply, even if perhaps in terms of temperature on board the nacelle, the

best could be the Full Embedded. A possible placement of the instrument in sites is shown in *Figure 4.50*.

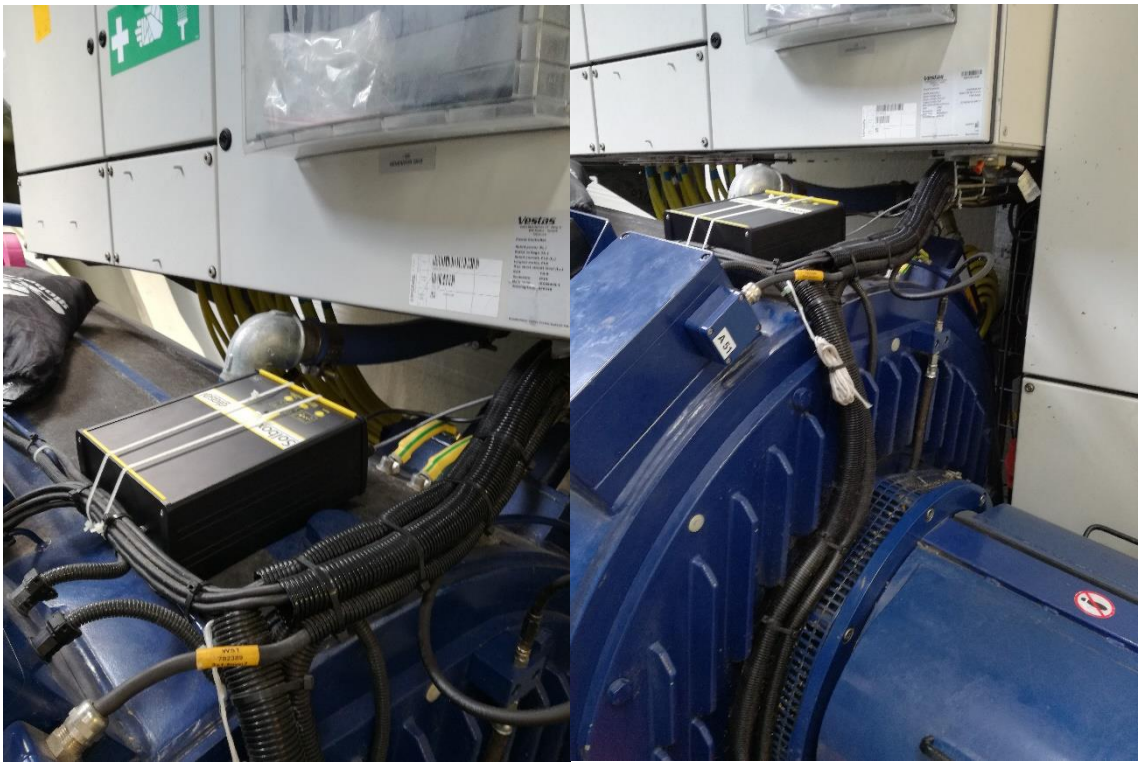

Figure 4.50: Possible placement of the instrument in sites

As explained, it is clear that the introduction of one of these systems would clearly be effective in terms of savings in maintenance/replacement costs, losses due to machine downtime and targeted maintenance scheduling. For this reason, the application of SolBox® in this area can be considered more than favourable and useful, as well as advantageous in all terms (mainly costs and size).

4.10.2 Real electric motor application

Another possible application concerns real electric motors with sinusoidal power supply. It is a 160 kW three-phase motor with nominal supply voltage 380-400V and current 290-279A. The motor working frequency is 50 Hz, the power factor is 0.87-0.86. Finally, it is capable of spinning at 2980 revolutions per minute and therefore

only two poles (pp=60*f/rpm, where pp is the number of pole-pair and rpm is the revolutions per minute).
A possible configuration for positioning the SolBox® in the case of the FE version can be the one shown in *Figure 4.51*.

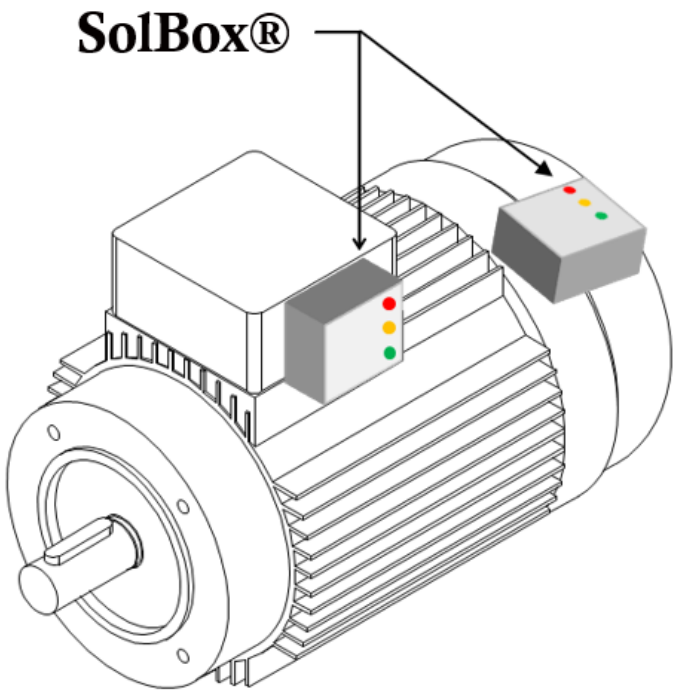

Figure 4.51: Possible SolBox® FE placement on electric motor

However, if you have the possibility to do so and you want to have more sensitivity, you can set up the use of the HS version, in order to position the antenna directly in the connection box. For this application it is possible to use the basic circuit diagram already shown in *Figure 4.44*. The real situation of the case just described is instead shown in the photos of *Figure 4.52*, in which all the components belonging to the overall test system are observed.

Figure 4.52: System setup for real electric motor application

From the photos it can be seen the device without package positioned on the table (to carry out measurements also on the circuit), the black cable that comes out of the

connection box is that of the antenna, while in the background the conducted devices and general all the elements that make up the entire power supply system. The specific motor tested is used for control of large cold storage and in this case, as mentioned, fed in sinusoidal, in particular only one electrical phase of this was powered. It is about a low voltage motor and it has been used to demonstrate the performances of the measurement system. The voltage amplitude has been risen up to and over the PDIV (Partial discharge inception voltage) so that PD activity incepted to be measured. The aim was to validate the measurement method and not to characterize the insulating system, for this reason only a phase has been considered. Also in this case, the tests showed an effective confirmation of the presence of discharges during the test compared to the measurement conducted, as can be seen in *Figure 4.53*.

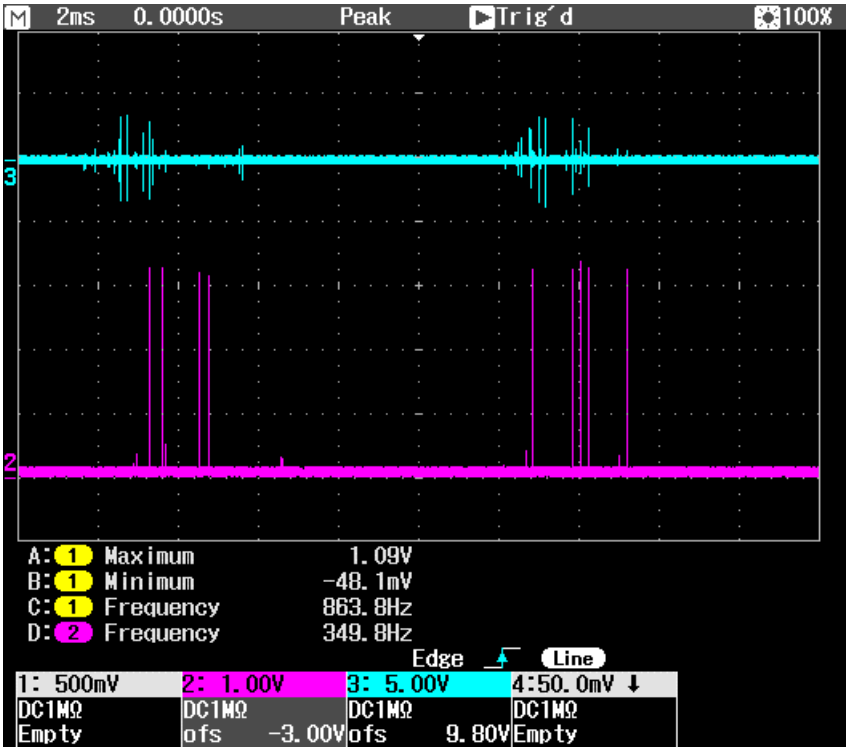

Figure 4.53: Real electric motor application - Conducted vs comparator signal

The figure shows how in the presence of discharges in the conducted (light blue trace), induced not far above the inception voltage, there is an effective confirmation of the activity of the phenomenon on the output of the comparator (fuchsia trace), in condition of a threshold voltage set at about 500mV. Obviously, it is not said that there is a complete correspondence between the peaks that are seen in the conducted

and those of the comparator because it depends on the point in which the discharges occur with respect to the positioning of the antenna (which affects the detected amplitude), which, although it is excellent, it is not said that it is able to pick up a signal in any condition, coupled with the fact that exceeding the threshold can be influenced in these terms. However, *Figure 4.54* further clarifies the correct operation of the device.

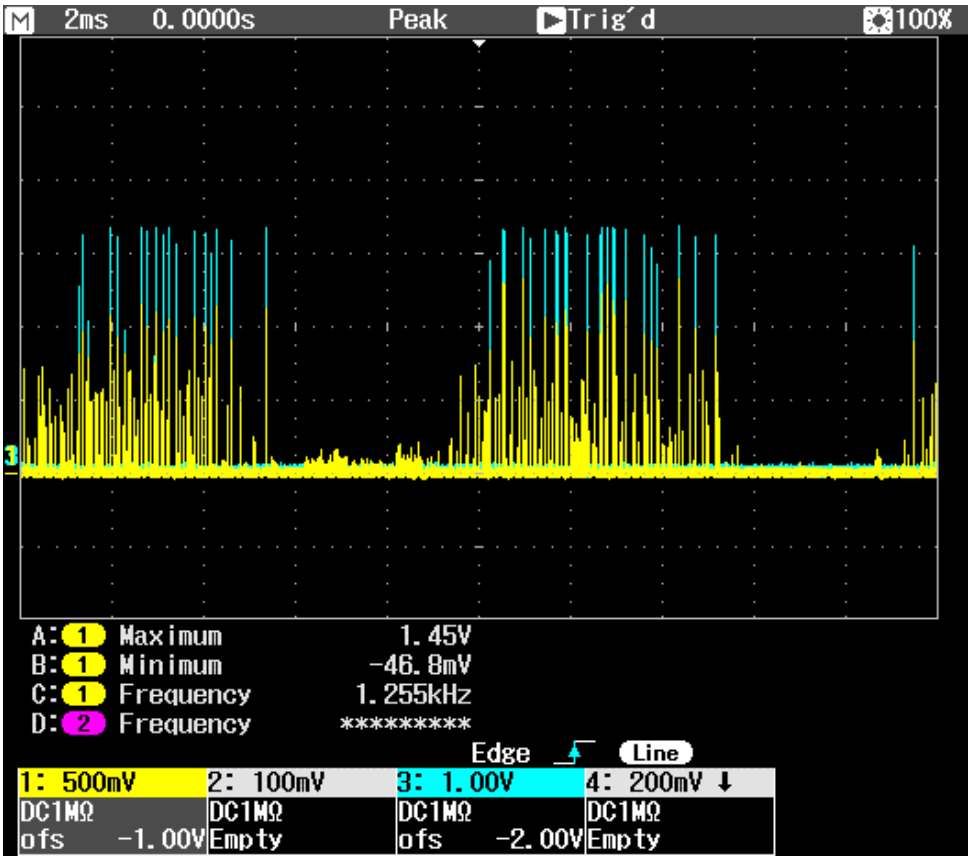

Figure 4.54: Real electric motor application - PD out vs comparator signal

The representation refers to the signal of the discharges in output from the buffer, with the yellow trace, and at the output of the comparator with the light blue one. In this case, the attention threshold has been set at around 750mV so as to have some evidence also at a visual level, with respect to the discharges that are considered by the comparator as of interest to be counted by the logic. It can therefore be observed that the discharges that are above the threshold are saturated by the comparator at the

supply level of about 3.3V, as required, highlighting once again the correct functioning of the SolBox®.

5 *Final conclusions*

The main objective of the research activity was the realization of two systems for the measurement of partial discharges, one through the measurement of conducted and irradiated signals. Both have been developed in such a way as to make them commercial devices to be placed on the market and therefore, in addition to the circuit aspect, issues such as the economic impact, the choice of packages, the reduction of size, in order to obtain minimally invasive instruments, in terms of occupied area, and much more have been evaluated.

5.1 Conclusions relating to the conducted system

The strength characteristics that make the system developed, for the measurement of conducted partial discharges, different and innovative compared to other competing systems are mainly:

- the small size, which makes it easy to apply even if there is not much space in the test sites and easily transportable (in this regard, refer to *Figure 5.1*)
- the possibility of having the conditioning board near the sensor (facilitated by the minimum size), increasing the sensitivity of the measurement
- the possibility of supplying power directly and only from a USB port on the PC, without to have dedicated power supplies
- having a degree of protection at least equal to IP65, it is possible to use this system even in inaccessible places and in unfavourable environmental conditions
- thanks to the possibility to control the gain level of the amplification stage online, it is possible to carry out measurements of a few pC up to very high signals without any saturation
- The system is already integrated with an ad hoc software created by the spin-off Diasol srl, which allows to directly create and view the PD patterns and thus perform an analysis of the measurements, acquired through a specific DAQ, also powered by PC USB port

- the system is very versatile; in fact, it is sufficient to adjust the filtering parameters and it can be used both for measurements with ferrites and for measurements with impedance
- Thanks to the relay board (SolSwitch) it is possible to perform monitoring on multiple systems, at least on four measuring points, using a single acquisition system

Figure 5.1: Comparison between a traditional system and developed SolPre & SolCon

At the end of this, it is specified that the devices made for the conducted system are already on the market and some units have already been sold.

5.2 Conclusions relating to the irradiated system

The developed system appears to be different from what can be found on the market, so much so that it is difficult to identify a similar instrument among those developed by the main companies that have established themselves on the market in the field of partial discharge measurement. The strength characteristics that make the system developed, for the measurement of irradiated partial discharges, different and innovative are mainly:

- the small size and compact design make it easy to apply even if there is not much space in the test sites and easily transportable
- the possibility of having different versions characterized according to the configuration and application according to the type of power supply used
- the possibility of having the antenna in the HS version near the measurement point identified for greater sensitivity
- the possibility of battery power supply that does not imply the need for connection cables and at the same time is calibrated so as to have an operation of about 1 year without having to replace them
- parallel to the batteries, there is the possibility of an external power supply between 10 and 24VDC
- having a degree of protection at least equal to IP65, it is possible to use this system even in inaccessible places and unfavourable environmental conditions, in addition to the fact that the packages are also prepared with appropriate supports and holes for functional fixing
- thanks to the possibility of remoting the system, there is the possibility of carrying out maintenance checks even without being physically on site
- the system does not necessarily have to be interfaced with high performance acquisition devices
- the system is very flexible as regards the extension to other types of testable machines based on the type of insulation that compose them, with small precautions already provided it would be possible to obtain a further version of the device for other applications
- the user interface is very intuitive and clear, through the well-defined lighting of alarm LEDs

In this case, following some latest functional tests, the device is close to being placed on the market.

6 *Future development*

Since these are instruments that have the purpose of being on market, it is obvious that the aim is to optimize their performance even more, making them strong on the market and able to be increasingly competitive with the products of more listed companies and possibly add new features that make it even more interesting and innovative.
As regards the duct system, which is the one developed and established for the longest time, we want to focus on marketing on a larger scale, increasing production and also some additional features can be provided such as:

- the introduction of circuitry that allows the hardware reset of the device, both locally and remotely, if there are problems on the USB connection
- possibly the implementation of a communication error management protocol, which still appears very robust, but in the case of environments really saturated with background noise, this could be an interesting feature
- further developments regarding shielding and additional elements of protection and security

As regards the irradiated system that is about to be placed on the market, we want to:

- complete the latest functional tests on inverter systems, so as to validate this last application as well
- focus on the marketing of the product in its various versions, also focusing on identifying the best monitoring solutions for the customer based on the desired application
- check what has already been prepared for a discharge measurement solution for insulation systems in which it is also necessary to check the amplitude of the discharges and not just the presence, evaluating whether what has been devised is sufficient or it is necessary to intervene by creating a new ad hoc board

Bibliography

- [1] Fabio Rossi. *Progettazione e ottimizzazione di sistemi di misura delle scariche parziali per segnali condotti ed irradiati.* PhD Thesis, University of Genoa, 2018.
- [2] Guastavino, F.; Dardano, A.; Torello, E.; Massa, G.F. *PD activity inside random wire wound motor stator insulation and early failures: A case study analysis.* IEEE International Symposium on Diagnostic for Electric Machines, Power Electronics & Drivers (SDEMPED), Page(s): 283-287, 2001.
- [3] C. Gianoglio, F. Guastavino, E. Ragusa, A. Bruzzone, E. Torello. *Hardware Friendly Neural Network for the PD Classification.* Conference on Electrical Insulation and Dielectric Phenomena (CEIDP), 2018 IEEE Conference. Cancun, Mexico, October 21-24, 2018.
- [4] Christian Gianoglio, Andrea Bruzzone, Edoardo Ragusa, and Paolo Gastaldo. *Unsupervised Monitoring System for Predictive Maintenance of High Voltage Apparatus.* ApplePies 2019 International Conference on Applications in Electronics Pervading Industry, Environment and Society. Pisa, September 11-13, 2019.
- [5] Guastavino, F.; Torello, E.; Squarcia, S.; Dardano, A.; Secci, M.; Ferraro, F.; Pistone, D. *Morphologic Analysis and Diagnosis of Defects Inside Cast Resin Medium Voltage Current Transformers Insulation by Digital Partial Discharges Acquisitions.* Annual Report Conference on Electrical Insulation and Dielectric Phenomena (CEIDP), Page(s): 493-496, 2011.
- [6] K.L. Chrzan. *Concentrated Discharges and Dry Bands on Polluted Outdoor Insulators*. IEEE Transactions on Power Delivery, Volume: 22, Issue: 1

- [7] P. Mraz, P. Treyer, U. Hammer. *Evaluation and Limitations of Corona Discharge Measurements-An Application Point of View.* International Conference on Condition Monitoring and Diagnosis – Xi'an – China
- [8] Stone, G.C; *Partial Discharge - Part VII: Practical Techniques for Measuring PD in Operating Equipment.* IEEE Electrical Insulation Magazine, Vol. 7, No. 4, July/August 1991
- [9] Bishop, Christopher M. *Pattern recognition and machine learning*. Vol. 4. No. 4., *New York: springer*, 2006.
- [10] AVO International. *Ultrasonic Corona and Leak Detector Instructional Manual.* Instruction Manual AVTM56-9J Rev. A.
- [11] Y.Tian, P.L.Lewin, D.Pommerenke, J.S.Wilkinson, S.J.Sutton. *Partial discharge on-line monitoring for HV cable systems using electro-optic modulators.* IEEE Transaction on Dielectrics and Electrical Insulation, Volume 11 Issue 5.
- [12] Luca Bottega. *Sistema digitale per il rilievo delle scariche parziali in banda ultra larga in trasformatori isolati in resina epossidica*. University of Padua, 2009/2010.
- [13] F. Guastavino, D. Cordano, E. Torello, F. Rossi, V.C. Garzone. *UHF Sensor for PD Detection on Wind Turbin.* Conference on Electrical Insulation and Dielectric Phenomena (CEIDP), 2018 IEEE Conference.
- [14] IEC 60034-18-41 *TS Ed. 1: Rotating electrical machines - Part 18-41: Qualification and type tests for Type I electrical insulation systems used in rotating electrical machines fed from voltage converters*. Ed. 2006.

- [15] IEC 60034-18-42 *TS Ed. 1: Rotating electrical machines - Part 18-42: Qualification and acceptance tests for partial discharge resistant electrical insulation systems (type II), used in rotating electrical machines fed from voltage converters.* Ed. 2008.
- [16] IEC 60270. *High-voltage test techniques – Partial discharge measurements*
- [17] Fabio Rossi. Chapter 3 - *Progettazione e ottimizzazione di sistemi di misura delle scariche parziali per segnali condotti ed irradiati.* PhD Thesis, University of Genoa, 2018.
- [18] Microchip Technology. *PIC16(L)F1454/5/9 - 14/20-Pin, 8-Bit Flash USB Microcontroller with XLP Technology*. Datasheet.
- [19] Microchip Technology. *PIC16(L)F1704/8 - 14/20-Pin 8-Bit Advanced Analog Flash Microcontrollers.* Datasheet.
- [20] Analog Devices. *General-Purpose, -55°C to +125°C Wide Bandwidth, DC-Coupled VGA AD8336*. Datasheet.
- [21] Texas Instrument. *High-voltage, Low-distortion, Current-feedback Operational Amplifier THS309x*. Datasheet.
- [22] BOURNS. *Transient Voltage Suppressor Diode Series SMCJ15CA*. Datasheet.
- [23] Diodes Inc. *500mW Surface Mount Diode Zener MMSZ5246B*. Datasheet.
- [24] Steven Keeping. *L'integrazione di diodi TVS per la protezione del progetto migliora l'affidabilità del bus CAN.* Digi-key Electronics, 2019.
- [25] Linear Technology. *Dual 1.3A, 1.2MHz Boost/Inverter in 3mm x 3mm DFN LT3471.* Datasheet.

- [26] Linear Technology. *3A, Fast Transient Response, Low Noise, LDO Regulators LT1764A Series*. Datasheet.
- [27] Linear Technology. *1.5A, Low Noise, Negative Linear Regulator with Precision Current Limit LT3015 Series*. Datasheet.
- [28] ON Semiconductor. *Surface Mount Schottky Power Rectifier, POWERMITE MBRM120LT1G*. Datasheet.
- [29] Microchip. *250 mA Low Quiescent Current LDO Regulator MCP1702*. Datasheet.
- [30] CEI 70-1. *Gradi di protezione degli involucri (Codice IP)*
- [31] TE Connectivity. *Signal Relay P2 Relay V23079*. Datasheet.
- [32] Maxim Integrated. *Space-Saving, 8-Channel Relay/Load Driver MAX4896*. Datasheet.
- [33] LeCroy. *WaveJet 300A Oscilloscope*. Manual.
- [34] Gianoglio, C., Ragusa, E., Bruzzone, A., Gastaldo, P., Zunino, R., Guastavino, F. *Unsupervised Monitoring System for Predictive Maintenance of High Voltage Apparatus*. Energies, MDPI, 2 March 2020.
- [35] Gianoglio, C., Ragusa, E., Bruzzone, A., Gastaldo, P., Guastavino, F., Torello, E. *Tensor Based Algorithm for Automatic Partial Discharges Pattern Classification*. In European Conference on Power Electronics and Applications (EPE'19 ECCE Europe). Genova, September 2-5, 2019.
- [36] Guastavino, Gianoglio, C., Torello, E., Bruzzone, A. *Hardware friendly Neural Network for the PD classification*. In Conference on Electrical Insulation

and Dielectric Phenomena (CEIDP), 2018 IEEE Conference. Cancun, Mexico, October 21-24, 2018.

- [37] Guastavino, Gianoglio, C., Torello, E., Bruzzone, A. *Influence of DC component on Partial Discharge activity*. In Conference on Electrical Insulation and Dielectric Phenomena (CEIDP), 2018 IEEE Conference. Cancun, Mexico, October 21-24, 2018

- [38] Guastavino, F., Gianoglio, C., Torello, E., Bruzzone, A., & Cordano, D. *Comparison Between PD Acquisition System Measurements Using Different Number of Bits for the Quantization*. In International Conference on Dielectrics (ICD), 2018 IEEE Conference. Budapest, July 1-5, 2018.
- [39] De Faria, H., Jr.; Costa, J.G.S.; Olivas, J.L.M. *A review of monitoring methods for predictive maintenance of electric power transformers based on dissolved gas analysis*. Renew. Sustain. Energy Rev. 2015, 46, 201–209.
- [40] Selcuk, S. Predictive maintenance, its implementation and latest trends. Proc. Inst. Mech. Eng. Part J. Eng. Manuf. 2017, 231, 1670–1679.
- [41] Stone, G.C. *A perspective on online partial discharge monitoring for assessment of the condition of rotating machine stator winding insulation*. IEEE Electr. Insul. Mag. 2012, 28, 8–13.
- [42] Luo, Y.; Li, Z.; Wang, H. *A review of online partial discharge measurement of large generators*. Energies 2017, 10, 1694.
- [43] Guastavino, F.; Gianoglio, C.; Torello, E.; Ferraris, M.; Gianelli, W. *Electrical Aging Tests on Conventional and Nanofilled Impregnation Resins.* In Proceedings of the 2018 IEEE Conference on Electrical Insulation and

Dielectric Phenomena (CEIDP), Cancun, Mexico, 21–24 October 2018; pp. 156–158.

- [44] Chandola, V.; Banerjee, A.; Kumar, V. *Anomaly detection: A survey*. ACM Comput. Surv. (CSUR) 2009, 41, 1–58.
- [45] Aissa, N.B.; Guerroumi, M. *Semi-supervised statistical approach for network anomaly detection.* Procedia Comput. Sci. 2016, 83, 1090–1095.
- [46] Ye, N.; Chen, Q. *An anomaly detection technique based on a chi-square statistic for detecting intrusions into information systems*. Qual. Reliab. Eng. Int. 2001, 17, 105–112.
- [47] Yu, M. *A nonparametric adaptive CUSUM method and its application in network anomaly detection*. Int. Adv. Comput. Technol. 2012, 4, 280–288.
- [48] Manikopoulos, C.; Papavassiliou, S. *Network intrusion and fault detection: A statistical anomaly approach*. IEEE Commun. Mag. 2002, 40, 76–82.
- [49] Goldstein, M.; Dengel, A. Histogram-Based Outlier Score (Hbos): *A Fast Unsupervised Anomaly Detection Algorithm*. German Research Center for Artificial Intelligence (DFKI): Kaiserslautern, Germany, 2012; pp. 59–63.
- [50] Davide Cordano. *Analisi comparativa di antenne per la misurazione delle scariche parziali in trasformatori di media e alta tensione*. Thesis, University of Genoa.
- [51] NXP Semiconductors. *BGA2815*. Datasheet.
- [52] Analog Devices. *AD8317*. Datasheet.
- [53] Texas Instruments. *OPA357*. Datasheet.
- [54] Maxim Integrated. *MAX4212*. Datasheet.
- [55] Nexperia. *PMEG3010EH*. Datasheet.

- [56] Texas Instruments. *LM1085IS-ADJ*. Datasheet.
- [57] Texas Instruments. *TPS71701*. Datasheet.
- [58] Analog Devices. *LTC6991CS6*. Datasheet.
- [59] Diodes Inc. *2N7002*. Datasheet.
- [60] Actel. *AGL030V5VQG100*. Datasheet.
- [61] Texas Instruments. *NE555*. Datasheet.
- [62] Littelfuse. *Reed Relays HE721A0500*. Datasheet.
- [63] Texas Instruments. *LM2940IMP-5.0*. Datasheet
- [64] Tektronix. Arbitrary Waveform Generator AWG2005. Manual
- [65] Guastavino, Gianoglio, C., Torello, E., Bruzzone, A., & Cordano, D. *A Predictive Maintenance Remote System based on Partial Discharges Measurements on Wind Turbines*. In International Conference on Dielectrics (ICD), 2018 IEEE Conference. Budapest, July 1-5, 2018.